Alma Mater Studiorum - Università di Bologna

DOTTORATO DI RICERCA IN

IL FUTURO DELLA TERRA, CAMBIAMENTI CLIMATICI E SFIDE SOCIALI

Ciclo 35

Settore Concorsuale: 09/B2 - IMPIANTI INDUSTRIALI MECCANICI

Settore Scientifico Disciplinare: ING-IND/17 - IMPIANTI INDUSTRIALI MECCANICI

LOW CARBON SYSTEMS FOR CLIMATE CHANGE MITIGATION AND ADAPTATION

Presentata da: Arash Aghakhani

Coordinatore Dottorato	**Supervisore**
Silvana Di Sabatino	Cesare Saccani

Esame finale anno 2023

Acknowledgment

First and foremost, I would like to express my sincere gratitude to my supervisor, Prof. Cesare Saccani for the continuous support of my PhD study and related research, for his patience, motivation, and immense knowledge. His guidance helped me in all the time of research and writing of this thesis. I could not have imagined having a better supervisor and mentor for my PhD study. Besides, I would like to thank my co-supervisors, Dr. Marco Pellegrini and Dr. Alessandro Guzzini for their support, insightful comments, and encouragement.

My sincere thanks also go to the University of Bologna and Prof. Nadia Pinardi, who started “Future Earth, Climate Change and Societal Challenges” (Frontiers) PhD program and provided me an opportunity to experience research abroad in Australia at CSIRO research institute.

I would also like to thank my esteemed research abroad supervisor, Dr. Nawshad Haque for his invaluable supervision and support. His immense knowledge and plentiful experience have encouraged me in all the time of my academic research at CSIRO.

Last but not the least, my appreciation goes out to my family and friends for their encouragement and support throughout my studies.

Dedication

I dedicate my PhD thesis to my family and friends who have supported me throughout my PhD studies.

I also dedicate this work to anyone struggling for freedom and their basic rights, especially Iranians who are fighting for the same reason and those who are no longer with us.

“Woman, Life, Freedom”

“Donna, Vita, Libertà”

Abstract

Global warming and climate change have been among the most controversial topics after the industrial revolution. The main contributor to global warming is carbon dioxide (CO_2), which increases the temperature by trapping heat in the atmosphere. Atmospheric CO_2 concentration before the industrial era was around 280 ppm for a long period, while it has increased dramatically since the industrial revolution up to approximately 420 ppm. According to the Paris agreement it is needed to keep the temperature increase up to 2°C, preferably 1.5° C, to prevent reaching the tipping point of climate change. To keep the temperature increase below the range, it is required to find solutions to reduce CO_2 emissions. The solutions can be low-carbon systems and transition from fossil fuels to renewable energy sources (RES). This thesis is allocated to the assessment of low-carbon systems and the reduction of CO_2 by using RES instead of fossil fuels. One of the most important aspects to define the location and capacity of low-carbon systems is CO_2 mass estimation. As mentioned, high-emission systems can be substituted by low-carbon systems. An example of high-emission systems is dredging. The global CO_2 emission from dredging is relatively high which is associated with the growth of marine transport in addition to its high emission. Thus, ejectors system as alternative for dredging is investigated in chapter 2. For the transition from fossil fuels to RES, it is required to provide solutions for the RES storage problem. A solution could be zero-emission fuels such as hydrogen. However, the production of hydrogen requires electricity, and electricity production emits a large amount of CO_2. Therefore, the last three chapters are allocated to hydrogen generation via electrolysis, at the current condition and scenarios of RES and variation of cell characteristics and stack materials, and its delivery.

INDEX

***List of tables* ....iii**

***List of figures* .... iv**

***Abbreviation list* .... vii**

***Introduction to PhD thesis*..1**

***CHAPTER 1: Modification of Fraser's Method for the Atmospheric CO_2 Mass Estimation by Using Satellite Data*……………………………………………………………………………………….5**

***CHAPTER 2: Assessment of an Innovative Ejector Plant for Port Sediment Management*…………. 78**

***CHAPTER 3: CO_2 emission of hydrogen generation via PEM and Alkaline electrolysers, and sensitivity analysis regarding cell characteristics and energy source*………………………………………….. 111**

***Chapter4: Life Cycle Assessment of hydrogen generation via PEM electrolyser regarding stack component weight and energy source variation*……………………………………………………. 162**

***CHAPTER 5: Hydrogen delivery*……………………………………………………………………… 240**

***Conclusion*..278**

List of tables

Table 1. 1 KPI table of the means of observations. 21
Table 1. 2 Comparison of the global atmospheric carbon dioxide mass using NOAA data and OCO2 data, 2019–2020. 24

Table 1.A. 1 Stations data adapted with permission from Fraser et al. [8] for 1980. Copyright 1983 by the American Geophysical Union.flask is sampling and in-situ is the measurement performed in the site. 29
Table 1.A. 2 Effective parameters on carbon dioxide concentration. 32
Table 1.A. 3 Sites that are currently included in the global gas reference network [136]. 35
Table 1.A. 4 Comparison of satellite data and TCCON stations. 50
Table 1.A. 5 worldwide ground-based station. 56
Table 1.A. 6 Tall towers in the NOAA Earth System Research Laboratory’s Global Greenhouse Gas Reference Network [171]. 65

Table 2. 1 Bathymetries considered in the analysis for the period June 2017–April 2020. 86
Table 2. 2 Energy-based classification of the sea storm. 88
Table 2. 3 Sea storm events in the period 2017–2020, together with the list of bathymetry surveys and sediment movimentation at the port entrance: peak wave significant height (H_S), mean (T_M), and peak (T_P) wave period, mean wave direction (MWD), compass sector, storm duration (dur), storm energy (E), energetic class, sea level at the H_S instant, and maximum sea level during storm. [A] Sea level data not available; [B] Nausicaa data not available. [29] 89
Table 2. 4 Summary of number of storms, related energy in periods under analysis, and the mean energy per day. [29] 91

Table 2.A. 1 Frequency table of significant wave heights H_S and mean direction MWD for the year 2017–2018 [29]. 102
Table 2.A. 2 Frequency table of significant wave height H_S and mean direction MWD for the year 2018–2019 [29]. 103
Table 2.A. 3 Frequency table of significant wave height H_S and mean direction MWD for the year 2019–2020 [29]. 104

Table 3. 1 Prediction of CO_2 emission for electricity generation in 2030 127
Table 3. 2 Contribution of energy sources and average emission of sources 133

Table 3.A. 1 PEM electrolyser characteristics in literature 146
Table 3.A. 2 PEM electrolyser theoretical and experimental energy consumption for hydrogen production in literature 148
Table 3.A. 3 Alkaline electrolyser energy consumption in literature 150

Table 3.B. 1 PEM and alkaline manufacturers based on publicly available information, in case of several models from a company an example is represented, only some leading manufacturers are included 151

Table 3.C. 1 Fuel combustion emission factors [43] 154

Table 4. 1 Main materials and assumed masses of the PEM plant stack, divided by stack components and materials. 170
Table 4. 2 Main materials and assumed masses of the PEM plant stack, based on material separation. 171
Table 4. 3 Main materials and assumed masses of the PEM plant without stack, based on unit separation. Modification of the results from Bareiß et al. [18] and Niklas Gerlof [28]. 173
Table 4. 4 Main materials and assumed masses of the PEM plant without stack, based on material separation 174
Table 4. 5 Stack and BOP assembly energy 174
Table 4. 6 Operational energy consumption and Water consumption 175
Table 4. 7 LCIA for scenario Sc2, Sc4, and Sc5 in Australia, the whole world, and Italy 182
Table 4. 8 Summary of the indices' values for 9 scenarios and SMR (2 tables to cover all indices) 188

Table 4.A. 1 literature list 193

Table 5. 1 Cost analysis of pipeline delivery [11], total cost includes production, terminal, delivery, and retail. 257
Table 5. 2 Tube trailer (vehicle) cost based on Lahnaoui et al. [33] study, 2021. 258
Table 5. 3 Cost analysis of liquid trucks delivery [11], total cost includes production, liquefaction, terminal, delivery, and retail. Total distance is considered 2*61.15 km for roundtrip 259
Table 5. 4 Hydrogen delivery cost comparison via different pathways in case “A”, numbers are extracted from diagrams in the European Union report [26]. All deliveries are considered via shipping except pipeline. 261
Table 5. 5 Hydrogen delivery cost comparison via different pathways in case “B”, numbers are extracted from diagrams in the European Union report [26]. 262

List of figures

Figure 1. 1 Building blocks for the global atmospheric carbon dioxide content calculation. Letters a-g are used to label the blocks to simplify mentioning the steps in the text. 10
Figure 1. 2 Building blocks for the proposed methodology to reach a higher accuracy of the results for global atmospheric carbon content. Letters a-j are used to label the blocks to simplify mentioning the steps in the text. 17
Figure 1. 3 OCO2 global 4-day carbon dioxide mass estimation in the period 2019–2021. The orange is 4-day global atmospheric carbon dioxide mass estimation, the black curve is related to NOAA data, and the blue is the fitting curve. The red dashed line is the prediction of global carbon dioxide mass since the data was not available for OCO2. 23

Figure 1.A. 1 The number of active observation sites at the beginning of each year. Data elaborated from the information reported in Table 1.A. 3 in the Appendix. 26
Figure 1.A. 2 Comparison of satellite observations and TCCON stations (References detail are provided in the Table 1.A. 4 in the Appendix.). The different studies are labelled based on references. 27
Figure 1.A. 3 OCO2 4-day observation, 22.04.2019–25.04.2019. 27
Figure 1.A. 4 Global atmospheric carbon dioxide mass 1980–2021. 28

Figure 2. 1 (**a**) Sketch of the ejector [14] and (**b**) underwater picture of the ejector in operation. 81
Figure 2. 2 Cervia position (**a**) and harbour aerial picture of the study area (**b**). 82
Figure 2. 3 Wave rose from the Nausicaa buoy in the period 2010–2020: polar distribution of the significant wave height (**a**) and peak period (**b**) [29].. 83
Figure 2. 4 Location of ejectors in the demo plant of Cervia. 84
Figure 2. 5 Classification by phases of the ejector demo plant operation in Cervia. 85
Figure 2. 6 Grids in the common area of the analysed bathymetries. The box identifies the area primarily impacted by ejector operation. The black dots represent the mooring points of inlet (north) and outlet (south) ejectors’ pipes. 86
Figure 2. 7 Annual number of sea storm events in the period 2017–2020. [29] 91
Figure 2. 8 Seasonal distribution of the sea storm energy in the period 2017–2020: winter (DJF), spring (MAM), summer (JJA), and autumn (SON). [29] 91
Figure 2. 9 Maps of water depth at the port entrance after dredging and propeller operation on 13 June 2017. The positions of the mooring points of the ejectors’ inlet and outlet pipelines are also reported as black dots. 92
Figure 2. 10 Water depth changes in the period: (**a**) 13 June 2017–28 December 2017 and (**b**) 28 December 2017–7 April 2018. The positions of the mooring points of the ejectors’ inlet and outlet pipelines are also reported as black dots for reference purposes. 93
Figure 2. 11 Maps of water depth at the port entrance after propeller operation on 11 May 2018. The positions of the mooring points of the ejectors’ inlet and outlet pipelines are also reported as black dots. 94
Figure 2. 12 Water depth change in the period 11 May 2018–10 October 2018. The positions of the mooring points of the ejectors’ inlet and outlet pipelines are also reported in black dots. 94
Figure 2. 13 Maps of water depth at the port entrance after dredging and propeller operation on 10 April 2019. The positions of the mooring points of the ejectors’ inlet and outlet pipelines are also reported as black dots. 95
Figure 2. 14 (**a**) Water depth change in the period 10 April 2019–12 June 2019, and (**b**) water depth measured on 12 June 2019. The positions of the mooring points of the ejectors’ inlet and outlet pipelines are also reported as black dots. 96

Figure 2. 15 Critical areas (i.e., water depth < 2.5 m) during the ejector operation (12 June 2019–30 April 2020). The positions of the mooring points of the ejectors' inlet and outlet pipelines are also reported as black dots. 97
Figure 2. 16 Mean water depth variation per day (in mm/day) between two consecutive bathymetries in the common area and in the ejector area before and after ejector demo plant operation 98
Figure 2. 17 Mean water depth variation per energy of storms in the period (in mm/m^2 h) between two consecutive bathymetries in the common area and in the ejector area before and after ejector demo plant operation. 99

Figure 2.B. 1 Bathymetry of 28 December 2017. 105
Figure 2.B. 2 Bathymetry of 7 April 2018. 105
Figure 2.B. 3 Bathymetry of 10 October 2018. 106
Figure 2.B. 4 Bathymetry of 6 September 2019. 106
Figure 2.B. 5 Bathymetry of 9 January 2020. 107
Figure 2.B. 6 Bathymetry of 30 April 2020. 107

Figure 3. 1 Electricity production by source, World (data from [2]) 112
Figure 3. 2 Specific energy consumption kWh per kilogram of hydrogen production using PEM electrolyser 122
Figure 3. 3 Specific energy consumption kWh per kilogram of hydrogen production using Alkaline electrolyser 123
Figure 3. 4 Experimental energy consumption for 1 kg hydrogen production by means of PEM electrolyser versus cell voltage, cell efficiency and current density 128
Figure 3. 5 Experimental energy consumption for 1 kg hydrogen production by means of PEM electrolyser versus cell faradaic efficiency 129
Figure 3. 6 correlation between experimental and estimated energy consumption for 1 kg hydrogen production by means of PEM electrolyser 130
Figure 3. 7 Minimum required fuel to generate 1 kg hydrogen (based on experimental energy values) by means of PEM technology, numbers in the x axis is the fuel row number in Table 3.A. 1. Highlighted part is related to zero emission fuels 134
Figure 3. 8 Minimum required fuel to produce 1 kg hydrogen (based on experimental energy values) by means of Alkaline technology, numbers in the x axis is the fuel row number in Table 3.A. 1. Highlighted part is related to zero emission fuels 134
Figure 3. 9 CO_2 emission of 1 kg hydrogen generation only from fuel burning (based on experimental energy values) by means of PEM technology, numbers in the x axis is the fuel row number in Table 3.A. 1. 135
Figure 3. 10 CO_2 emission of 1 kg hydrogen generation only from fuel burning (based on experimental energy values) by means of Alkaline technology, numbers in the x axis is the fuel row number in Table 3.A. 1. 136
Figure 3. 11 Scope 2 and Scope 3 combination CO2 emission of 1 kg hydrogen generation in Australia and its states based on studies provided in Table 3.A. 2 (last estimate after 2019), PEM technology 137
Figure 3. 12 Scope 2 and Scope 3 combination CO2 emission of 1 kg hydrogen generation in Australia and its states based on studies provided in Table 3.A. 3 (last estimate after 2019), Alkaline technology 138
Figure 3. 13 CO_2 emission of the generation of 1 kg hydrogen in Europe and Australia based on studies provided in Table 3.A. 2, PEM technology. 138
Figure 3. 14 CO_2 emission of the production of 1 kg hydrogen in Europe and Australia based on studies represented in Table 3.A. 3, Alkaline technology 139
Figure 3. 15 Emission for 1 kg hydrogen generation using PEM technology (based on experimental energy values)-2030 prediction, Australia states 140
Figure 3. 16 Emission for 1 kg hydrogen generation using alkaline technology (based on experimental energy values)-2030 prediction, Australia states 140
Figure 3. 17 Emission for 1 kg hydrogen generation using PEM technology (based on experimental energy values)-2030 prediction, European countries and Australia 141
Figure 3. 18 Emission for 1 kg hydrogen generation using PEM technology (based on experimental energy values)-2030 prediction, European countries and Australia 141
Figure 3. 19 variation of parameters (-30 to 30%) and variation of estimated energy consumption for 1 kg hydrogen generation through PEM electrolyser 142
Figure 3. 20 variation of energy source contribution and impact on CO_2 emission for 1 kg hydrogen production by means of PEM and alkaline electrolyser in Italy 143
Figure 3. 21 variation of energy source contribution and impact on CO_2 emission for 1 kg hydrogen generation by means of PEM and alkaline electrolyser in Australia. 144

Figure 4. 1 Scheme of PEM system boundary, based on K. Bareiß et al. [18] with modification 167

Figure 4. 2 Scaled relative LCIA of Global warming, stratospheric ozone depletion, ionizing radiation, Ozone formation, Human health, Fine particulate matter formation, Ozone formation, Terrestrial ecosystems, Terrestrial acidification, Freshwater eutrophication, Marine eutrophication indices. 177
Figure 4. 3 Scaled relative LCIA of Terrestrial ecotoxicity, Freshwater ecotoxicity, Marine ecotoxicity, Human carcinogenic toxicity, Human non-carcinogenic toxicity, Land use, Mineral resource scarcity, Fossil resource scarcity, Water consumption indices. 177
Figure 4. 4 Global warming (kg CO2 eq per kg of hydrogen) index 178
Figure 4. 5 Ionizing radiation (kBq Co-60 eq per kg of hydrogen) index 179
Figure 4. 6 freshwater eutrophication (kg P eq per kg of hydrogen) index 179
Figure 4. 7 Human carcinogenic toxicity (kg 1,4-DCB per kg of hydrogen) index 180
Figure 4. 8 Fine particulate matter formation (kg PM2.5 eq per kg of hydrogen) index 180
Figure 4. 9 Indices variation range regarding sc2 182
Figure 4. 10 Global warming index variation in Sc6, Sc7, Sc8, and Sc9 scenarios regarding sc2..........................183
Figure 4. 11 Freshwater ecotoxicity index variation in Sc6, Sc7, Sc8, and Sc9 scenarios regarding sc2 184
Figure 4. 12 Marine ecotoxicity index variation in Sc6, Sc7, Sc8, and Sc9 scenarios regarding sc2.......................184
Figure 4. 13 Human non-carcinogenic toxicity index variation in Sc6, Sc7, Sc8, and Sc9 scenarios regarding sc2 185
Figure 4. 14 Mineral resource scarcity index variation in Sc6, Sc7, Sc8, and Sc9 scenarios regarding sc2 186
Figure 4. 15 Human carcinogenic toxicity index variation in Sc6, Sc7, Sc8, and Sc9 scenarios regarding sc2........186
Figure 4. 16 Water consumption index variation in Sc6, Sc7, Sc8, and Sc9 scenarios regarding sc2......................187
Figure 4. 17 Stack and BOP materials' contribution in global warming index 190
Figure 4. 18 contribution comparison of materials, electricity, water consumption, and heat to global warming, in global region 191

Figure 4.A. 1 LCIA results for the current condition (remaining indices), units are provided in Table 4. 7 per kg of hydrogen...196
Figure 4.A. 2 Indices variation in Sc6, Sc7, Sc8, and Sc9 scenarios regarding sc2 (remaining indices) 200

Figure 5. 1 Existing hydrogen pipelines length, 2016 248
Figure 5. 2 Life-cycle GHG emissions for delivery by tube trailer for gaseous H2, by tanker for liquid H2, or by pipelines in various delivery distances (Modified figure from Frank et al. [27]) 253
Figure 5. 3 Mass of delivered hydrogen in 1 m^3 of delivered material. H100 refers to 100% hydrogen. 260
Figure 5. 4 Pathway choice regarding distance and demand...262
Figure 5. 5 network representation of the total hydrogen production, delivery, and carbon tax model 271

Abbreviation list

Abbreviation	Meaning	Chapter
a.s.l	Above the sea level	1
ACE	Atmospheric Chemistry Experiment	1
ADEOS	Advanced Earth Observing Satellite	1
AEM	Anion exchange membrane	3, 4
AIRS	Atmospheric InfraRed Sounder-Aqua satellite	1
BCE	Before Common Era	1
BOP	Balance of plant	4
CARVE	Carbon in Arctic Reservoirs Vulnerability Experiment	1
COAG	Council of Australian government	3
CONTRAIL	Comprehensive Observation Network for Trace Gases by Airliner	1
CRS	Coordinate Reference System	2
EHB	European Hydrogen Backbone	5
ENVISAT	Environmental Satellite	1
ESRL	Earth System Research Laboratory	1
FRP	Fibre-reinforced polymer	5
GFRP	Glass fibre reinforced polymer	5
GGGRN	Global Greenhouse Gas Reference Network	1
GHG	Green House Gases	1, 3, 5
GOSAT	Greenhouse Gases Observing Satellite	1
GWP	Global warming potential	3, 4
Hi	High price	5
HIPPO	High-performance Instrumented Airborne Platform for Environmental Research Pole-to-Pole Observations	1
HRS	Hydrogen refuelling stations	5
IAGOS	In-Service Aircraft for a Global Observing System	1
IASI	Infrared Atmospheric Sounding Interferometer	1
IMG	Interferometric Monitor for Greenhouse Gases	1

INTEX-NA	Intercontinental Chemical Transport Experiment-North America	1
KPI	Key Performance Indicators	1
LCA	Life cycle assessment	4
LCIA	Life cycle impact assessment	4
LCOTH	Levelized cost of transporting hydrogen	5
LDEO	Global Surface pCO_2	1
LH	liquid hydrogen	5
LHV	Lower heating value	3
Lo	Low price	5
LOHC	Liquid organic hydrogen carriers	5
MWD	Mean wave direction	2
NCEI	National Centers for Environmental Information	1
NG	Natural gas	5
NOAA	National Oceanic and Atmospheric Administration	1
OCADS	Ocean Carbon Data System	1
OCO-2	Orbiting Carbon Observatory-2	1
OCO-3	Orbiting Carbon Observatory-3	1
PEM	Proton exchange membrane	3, 4
ppm	Parts per million	1
RES	Renewable energy sources	3, 4
SCIAMACHY	Scanning imaging absorption spectrometer for atmospheric cartography	1
SMR	Steam methane reforming	3, 4
SOEC	Solid oxide electrolysis cells	3, 4
SOOP	Ships Of Opportunity Program	1
TCCON	Total Carbon Column Observing Network	1
TES	Thermal Emission Sounder	1
UCTE	Union for the Coordination of Transmission of Electricity (Europe)	4
XCO_2	Column average carbon dioxide concentration	1

Introduction to PhD thesis

Climate change can be due to natural and anthropogenic activities. Since the industrial revolution, anthropogenic activities have dramatically increased which has resulted in the release of large quantities of green house gases (GHG) and other forms of pollutants. GHG trap heat in the atmosphere and cause global warming. The main contributor to global warming and climate change is carbon dioxide (CO_2) which is a long-lasting GHG. Currently, the atmospheric CO_2 concentration is around 420 ppm while the records show the concentration at around 281 ppm before the industrial revolution era. According to the Paris agreement, the temperature rise is limited to 2° C compared to the pre-industrial level, however, it is pursued to keep the level less than 1.5° C. Greater values of temperature increase could lead to the tipping point of climate change which is an irreversible condition. Therefore, carbon neutrality targets have attracted more attention in previous years. The main question is “How is it possible to reduce carbon dioxide emissions and mitigate climate change? “. Low carbon systems and the transition from fossil fuels to renewable energies could be the solutions for climate change mitigation and adaptation. Thus, the focus of this PhD thesis is systems with low carbon emissions and transition from fossil fuels to renewable energy sources (RES). There are various low-carbon technologies and fossil fuel alternatives. Considering the defined scope of this PhD course, a low-carbon system (ejectors system), and an alternative to fossil fuels (hydrogen) are investigated in this thesis.

The activities performed in the PhD course and summarized in the thesis have been financed both by the UNIBO central budget and by the Department of Industrial Engineering.

This thesis is divided into five chapters as follows:

- Chapter 1: Modification of Fraser’s Method for the Atmospheric CO_2 Mass Estimation by Using Satellite Data.
  The available method for the estimation of atmospheric carbon dioxide mass based on observation and measurement was proposed by Fraser in 1980. In Fraser’s method only 21 ground stations were used to estimate the atmospheric CO_2 mass. In addition, no stations were in Europe, Asia, Africa, and South America, resulting in unbalanced earth surface coverage. Furthermore, it is not possible to calculate the CO_2 mass geographical distribution by Fraser’s method, because average concentration and not local concentration is used by the model. To propose practical solutions for climate change mitigation and adaptation such as low carbon systems, the transition from fossil fuels to RES, and carbon capture systems, CO_2 concentration is required but not enough. Concentration can be used to determine the capability of a system for a specific concentration, but for scale and capacity determination of a system, it is necessary to know the amount of carbon dioxide mass. Moreover, high concentrations in a

measurement station might be due to a local anthropogenic activity in which the CO_2 mass could be very low or high depending on the area of the region. In addition, concentrations slightly below the average global concentration seem to be acceptable, while, considering the area of the study, the total amount of carbon dioxide could be significant. Therefore, there are uncertainties in defining the significance of carbon dioxide in a location based on its concentration. These uncertainties can be addressed by using carbon dioxide mass. In this chapter, the amount of carbon dioxide mass is estimated for the whole world by using the information extracted from satellite data, OCO2 satellite. In this study the whole world is divided into small cells compatible with the spatial resolution of the OCO2 satellite, the CO_2 is estimated for each cell and finally, the total global carbon dioxide mass is reported. OCO2 satellite observations are from the Earth's surface up to the satellite altitude, around 700 km. Carbon dioxide mass decreases considering that the air mass is decreasing by increasing altitude from the Earth's surface. The main air mass is in the troposphere layer and a small portion of the stratosphere, approximately less than 20 km in total, however, higher air density is related to the lower altitudes of the troposphere. Therefore, the result of the proposed method in this study is mostly related to the carbon dioxide mass at the troposphere layer. Since the calculation are done for various cells, it is possible to use this method to define the regions with high carbon dioxide mass to plan for carbon capturing or installation of the systems with low carbon emissions.

- Chapter 2: Assessment of an Innovative Ejector Plant for Port Sediment Management.

  Dredging is one of the high-emission and hard-to-abate anthropogenic activities. Considering the necessity of removing sediment from the port entrance and navigation path of ships and boats, and the growth of marine transportation, overall global CO_2 emission from dredging is significant. Reducing the emissions of traditional technologies such as dredging is very challenging. Therefore, innovative technologies, e.g., the ejectors, are necessary for this purpose. Therefore, in this chapter, the effectiveness of the first demo plant of ejectors is investigated. The ejectors system was designed in 2002 at the University of Bologna. The location of the demo plant is port Cervia, in Italy, and the project name is STIMARE project. To check the effectiveness, temporal sediment volume variation is assessed based on the bathymetries data. The acceptable performance of this technology, which consumes a low amount of electricity and has low CO_2 emission, can be the proof to be used in other ports all around the world.

- Chapter 3: CO_2 emission of hydrogen generation via PEM and Alkaline electrolysers, and sensitivity analysis regarding cell characteristics and energy source.

  Hydrogen as a zero-emission fuel can be a suitable alternative to fossil fuels. In addition, hydrogen can support the energy system in the decarbonization process by acting as storage for RES. Hydrogen generation carbon dioxide emission, which is currently mostly based on the steam methane reforming

(SMR) method, is not low. Therefore, other hydrogen production methods such as water electrolysis should be considered. PEM and alkaline, as the most mature water electrolysis technologies, are compared in this chapter to assess the carbon dioxide emission of hydrogen generation at the stack operational level. This comparison is made to choose the technology with lower operational emission to investigate the whole life cycle in the other part of this study. Since the electricity for water electrolysis can be supplied by the grid, the environmental impact depends on the energy mix existing in the specific country. Therefore, carbon dioxide emission for the current condition, i.e., using the electricity from the current grid, and prediction of 2030 for several countries are estimated in this study. In addition, sensitivity analysis is performed regarding the source of electricity to evaluate the impact of the transition from fossil fuels to RES. Furthermore, sensitivity analysis is performed regarding cell characteristics, such as cell voltage, and current density to define the most effective parameter to be focused on in future studies.

- Chapter 4: Life Cycle Assessment (LCA) of hydrogen generation via PEM electrolyser.

  In chapter 3 it will be shown that the PEM technology has lower carbon dioxide emission in comparison to the alkaline technology. Therefore, the LCA is applied on a 1 MW PEM plant for hydrogen production in 3 regions, Italy, Australia, and the whole world. In this chapter, in addition to carbon dioxide emission (global warming potential), other environmental indices are considered. It is important to estimate the other pollutant emissions because it is likely, in some methods, that carbon dioxide emission is reduced while the other pollutant emissions increase which is undesirable. Several scenarios regarding the variation of stack materials mass and variation in electrical energy source, including the transition from fossil fuels to solar, wind, or hydro, and their combination, are provided and assessed in this chapter. Furthermore, the comparison with SMR method emissions is provided to define the best alternative of the SMR method for hydrogen generation.

- Chapter 5: Hydrogen delivery.

  Hydrogen delivery is an integral part of hydrogen technology regarding its cost and environmental emissions. In this chapter, a general overview of hydrogen delivery pathways is provided. Based on the collected information a comparison is made to define the highest hydrogen content of the same volume of hydrogen carriers among mature and immature delivery methods. In addition, a general guide for pathway choice regarding the demand and distance of delivery is provided. Low-cost hydrogen is usually obtained in remote areas; thus, its delivery affects the end users' final costs. Optimization is, therefore, necessary to ensure competitiveness concerning traditional fuels.

  A transportation model is recommended in this chapter which considers carbon tax for hydrogen generation and hydrogen delivery. The result of this model is the determination of the amount of hydrogen which is delivered from each hydrogen generation plant to each end-user in the network by the optimization of the cost. Therefore, the carbon tax which is included in the cost is also optimized, and as a result, the amount of carbon dioxide emission could be optimized.

It should be noted that, despite the positive results of investigations in this PhD thesis regarding carbon dioxide emission reduction, a lot of research is still needed in order to reach the Paris agreement objectives.

1 CHAPTER 1: Modification of Fraser’s Method for the Atmospheric CO_2 Mass Estimation by Using Satellite Data

ABSTRACT

Carbon dioxide (CO_2) is one of the most important greenhouse gases (GHG) in the atmosphere, which plays an important role in global warming, because of its long-lasting and negative impact on climate change. The global atmospheric monthly mean CO2 concentration is currently greater than 410 ppm, around 419 ppm, which has varied dramatically since the industrial era. To define suitable climate change mitigation and adaptation strategies it is required to determine the CO_2 mass distribution and global atmospheric carbon dioxide mass. The available method, without using the transportation models, to estimate the global atmospheric CO2 mass was proposed in 1980. In this chapter, to improve the accuracy of the available method, comparison of various observation platforms such as ground-based stations, ground-based tall towers, aircrafts, balloons, ships, and satellites is provided to choose the best available observations dataset, regarding the temporal and spatial resolution. In the method proposed in this study, satellite observations (OCO2 data), from January 2019 to December 2021, are used to calculate the atmospheric CO2 mass. The global atmospheric CO2 mass is estimated around 3.24 × 1015 kg in 2021. In addition, Global atmospheric CO2 mass is estimated by applying Fraser’s method to NOAA data for the mentioned study period. The proposed methodology in this study estimated slightly higher amounts of CO2 compared to Fraser’s method. This comparison resulted in 1.23% and 0.15% maximum and average difference, respectively, between the proposed method and Fraser’s method. The proposed method provides the opportunity to estimate the required capacity of the plant for carbon capturing. In addition, it can be applied to smaller districts to determine the most critical locations in the world for climate change mitigation and adaptation planning.

Keywords:

climate change; CO2 concentration; climate change mitigation and adaptation; global atmospheric CO2 mass; satellite data; OCO2

1.1 Introduction

Greenhouse gases (GHGs) in the atmosphere trap heat and lead to global warming. One of the most important GHGs is carbon dioxide (CO_2) which has attracted more attention for researchers than other GHGs because of its long-lasting presence in the atmosphere and negative impact on climate change. In addition, carbon dioxide concentration is increasing each year. In 6000 Before Common Era (BCE), based on high-accuracy Antarctic ice-core records, the concentration of CO_2 is assumed 20 parts per million (ppm) [1]. During the Industrial Revolution, between the 17th and 18th centuries, more than fourteen times greater concentrations, i.e., up to around 281 ppm, were recorded [2, 3]. The global monthly mean CO_2 concentration is currently greater than 410 ppm, approximately 419 ppm, based on the information provided by the National Oceanic and Atmospheric Administration (NOAA) website [4]. However, a simple correlation cannot be recognized between global warming and available CO_2 concentration data. Therefore, new carbon dioxide indices should be introduced for the global warming issue investigation. Carbon dioxide concentration is a complex balance of sources and sinks, such as, e.g., natural phenomena and anthropogenic activities [5, 6, 7]. Thus, several parameters must be taken into account, as shown in Table 1.A. 2 in the Appendix section.

Considering the current atmospheric CO_2 concentration some questions arise as follow:
- Is CO_2 concentration the best representative parameter for climate change planning?
- If CO_2 concentration is not the best choice, what could be a better parameter for climate change planning regarding carbon dioxide?
- Is the methodology to use alternative parameter accurate?

Despite considerable efforts for CO_2 concentration measurement, limited studies have been done regarding CO_2 mass calculation. For example, a preliminary estimation of approximately 7.15×10^{11} tons was reported in 1980 by Fraser et al. [8], while a more recent publication of the Global Carbon Budget in 2019 estimates this amount up to 8.60×10^{11} tons [9]. Thus, around 1.45×10^{11} tons of carbon dioxide seems to be the balance of carbon dioxide sinks and sources in approximately 39 years. It results in a mean annual net positive flux to the atmosphere of 3.7 Gton/year ($= 1.45 \times 10^{11}/39$). The annual growth rate in the atmospheric carbon dioxide mass was calculated and reported based on the concentration data reported by Dlugokencky and Tans [4], i.e., from the Global Greenhouse Gas Reference Network (GGGRN) (including 84 active sites in 37 countries). The GGGRN sites' list is reported in Table 1.A. 3 in the Appendix section. Despite the number of GGGRN sites increasing through the years with a maximum number of active sites up to 116 in 2011 (Figure

1.A. 1 in the appendix), the currently active 85 observatory sites seem insufficient to evaluate the global carbon dioxide mass.

Using data from more datasets and not limited to the one currently used could be the first improvement step in carbon dioxide mass estimation. According to Jiang and Yung [10], various CO_2 databases exist even if not included in the algorithms used for mass calculation. The list of existing surface-based and aircraft-based CO_2 concentration databases is reported below:

Ground-based CO_2 concentration observations:

- The Earth System Research Laboratory of the National Oceanic and Atmospheric Administration (NOAA ESRL) [11];
- Total Carbon Column Observing Network (TCCON) [12].
- Airborne based CO_2 concentration observations:
- The Earth System Research Laboratory of the National Oceanic and Atmospheric Administration (NOAA ESRL) [11];
- Comprehensive Observation Network for Trace Gases by Airliner (CONTRAIL) [13];
- Intercontinental Chemical Transport Experiment-North America (INTEX-NA) [14];
- High-performance Instrumented Airborne Platform for Environmental Research Pole-to-Pole Observations (HIPPO) [15];
- In-Service Aircraft for a Global Observing System (IAGOS) [16];
- Carbon in Arctic Reservoirs Vulnerability Experiment (CARVE) [17].

Data sets from ships can be acquired by means of research ships or commercial ones. As an example, the NOAA National Centers for Environmental Information (NCEI) hosts a data management project, the Ocean Carbon Data System (OCADS), in this project data from deep and shallow waters are recorded to analyse carbon dioxide fluxes between the oceans and atmosphere. The following list includes ship-based observation under the OCADS project:

- Ships Of Opportunity Program (SOOP) Data [18];
- Global Surface pCO_2 (LDEO) [19].

Moreover, there are atmospheric carbon dioxide concentration data sets produced in the open ocean sites via a moored autonomous system [20].

Providing an accurate and reliable estimation and location of carbon dioxide mass quantity through simple algorithms is a research gap that needs to be filled. For the application of simple algorithms avoiding the use of state-of-the-art algorithms, big data for CO_2 is needed. It is not economically feasible to construct new measuring sites around the world, therefore, the elaboration of the datasets from satellites is the best alternative. The benefits and the challenges of carbon dioxide observation satellites for climate governance and applications at national/regional, megacity, and point source levels were already reviewed by Pan et al. [21]. To define the best satellite choice various satellites are checked, the list of satellites is provided as follow:

- The Orbiting Carbon Observatory-3 (OCO-3) [22];
- The Orbiting Carbon Observatory-2 (OCO-2) [23];
- The Greenhouse Gases Observing Satellite (GOSAT) [24];
- Thermal Emission Sounder (TES), measurement instrument installed on Aura satellite by NASA [25];
- Atmospheric InfraRed Sounder-Aqua satellite (AIRS) [26];
- The Infrared Atmospheric Sounding Interferometer (IASI) is an instrument flown on METOP satellite [27];
- The Atmospheric Chemistry Experiment (ACE) SciSat [28];
- The scanning imaging absorption spectrometer for atmospheric cartography (SCIAMACHY) onboard the Environmental Satellite (ENVISAT) [29];
- Other satellite missions are launched or will be launched in the future, such as Tansat, Carbonsat, MERLIN, Sentinel-5p, MicroCarb, and ASCENDS [3], which would increase the amount of available information.

More data would be available in the future from satellites' observations, thus, a new methodology for atmospheric carbon dioxide mass estimation is described in this chapter. To the best knowledge of the author, there has not been any study that uses only satellite data to estimate global atmospheric

CO_2 mass. It should be noted that there are some studies based on satellite data and simulation such as the atmospheric chemical transport model, but transport models are not in the scope of this study. The proposed method in this study provides the opportunity to perform a comparative analysis of the atmospheric CO_2 mass for different locations and periods. In addition, the proposed method results could be used for the evaluation of the required capacity for systems to capture carbon dioxide based on the CO_2 mass. Furthermore, since the methodology is based on the division of the Earth's surface into smaller cells proportional to satellite resolution, there is a possibility to apply the method to smaller districts to recognize the most critical locations in the world for proper planning regarding climate change mitigation and adaptation.

The purpose of this chapter is the proposed model validation using the most suitable observation platforms considering the resolution, coverage, and accuracy of the data to define the global atmospheric CO_2 mass, which considers the mass distribution on the Earth with higher precision compared to Fraser's method. Satellites' observations are considered as input for the methodology, therefore, the validation of satellite data with respect to other platforms introduced in the Materials and Method section, i.e., ground-based stations, airborne and ships observations, is provided in the Results and Discussion sections. In the last section, the new methodology for atmospheric carbon dioxide mass described in the Materials and Method section is validated with state-of-the-art quantities.

1.2 Materials and Method

1.2.1 Simplified Fraser's Method for the Calculation of CO_2 Atmospheric Mass

The global atmospheric carbon content was estimated at around 7.15×10^{14} kg in 1980 by Fraser et al. [8]. Figure 1. 1 is suggested as a schematic representation of the procedure which was used in [8] to estimate the global atmospheric carbon dioxide mass in Fraser's study. The estimated value is checked based on the following steps. The first step is the calculation of the number of dry air moles (block c) in the atmosphere by dividing the global atmospheric mass of dry air (block a) by dry air mean molecular weight (block b), which is shown in Eq 1. 1:

$$\mathrm{Air}_{\mathrm{dry,mol}} = \frac{\mathrm{Air}_{\mathrm{dry,mass}}}{\mathrm{Air}_{\mathrm{dry,mw}}} \qquad \text{Eq 1. 1}$$

where:

$\mathrm{Air}_{dry,mol}$ = Dry air moles (mol)

$\mathrm{Air}_{dry,mass}$ = Global atmospheric mass of dry air (kg), that is 5.12×10^{18} kg;

$\mathrm{Air}_{dry,mw}$ = Dry air mean molecular weight (kg/mol), that is 0.02897 kg/mol.

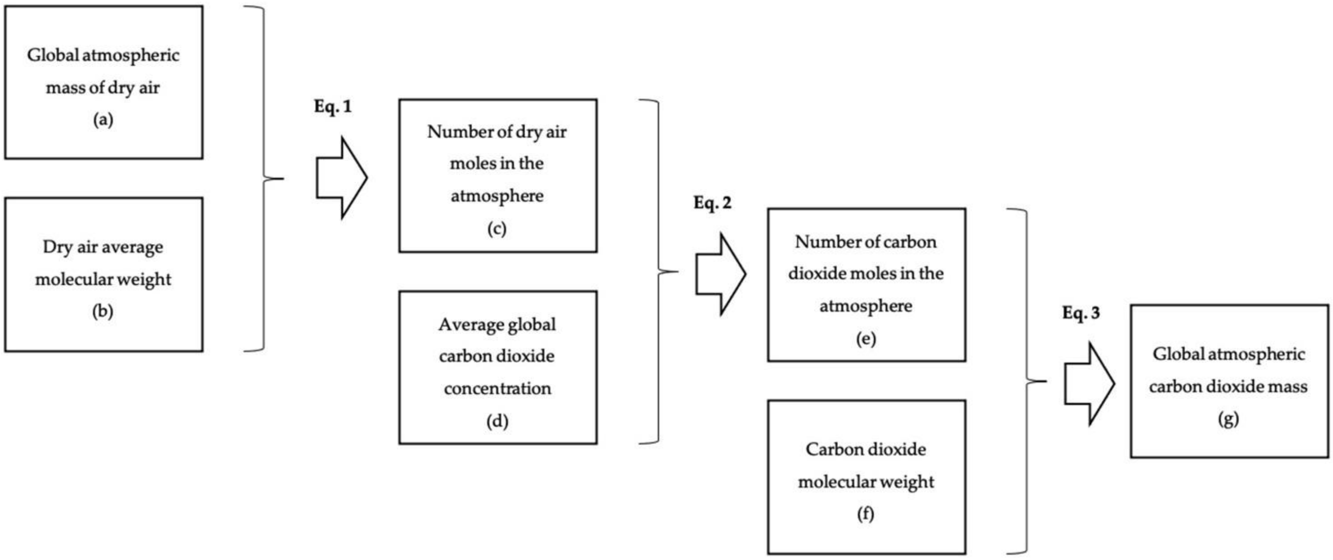

Figure 1. 1 Building blocks for the global atmospheric carbon dioxide content calculation. Letters a-g are used to label the blocks to simplify mentioning the steps in the text.

The number of carbon dioxide moles in the atmosphere is calculated (block e) in the second step. This number is the product of the average global carbon dioxide concentration (block d) and the number of dry air moles (block c), Eq 1. 2:

$$\mathrm{CO}_{2,\mathrm{mol}} = \mathrm{CO}_{2,\mathrm{con,avg,vol}} \times \mathrm{Air}_{\mathrm{dry,mol}} \times 10^{-6} \qquad \text{Eq 1. 2}$$

where:

$\mathrm{CO}_{2,mol}$ = CO_2 moles (mol)

$\mathrm{CO}_{2,con,avg,mol}$ = Average global CO_2 concentration (ppm_V—part per million by volume)

The average global CO_2 concentration is calculated as the ratio between the CO_2 and the dry air as follow:

$$CO_{2,con,avg,vol} = \frac{CO_{2,vol}}{Air_{dry,vol}} \times 10^{6} \qquad \text{Eq 1. 3}$$

where:

$CO_{2,vol}$ = The volume of carbon dioxide (m^3)

$Air_{dry,vol}$ = The volume of dry air (m^3)

The desired parameter is the number of CO_2 moles, therefore, Eq 1. 3 is manipulated by using the ideal gas law to obtain Eq 1. 4, then Eq 1. 2 is obtained by manipulating Eq 1. 4:

$$CO_{2,con,avg,vol} = \frac{CO_{2,mol}}{Air_{dry,mol}} \times 10^{6} \qquad \text{Eq 1. 4}$$

The final step is the calculation of the global atmospheric carbon dioxide mass (block g). It is calculated by Eq 1. 5 as the product of the number of CO_2 moles in the atmosphere (block e) and the CO_2 molecular weight (block f).

$$CO_{2,gac} = CO_{2,mol} \times CO_{2,mw} \qquad \text{Eq 1. 5}$$

where:

$CO_{2,gac}$ = The global atmospheric carbon dioxide content (kg)

$CO_{2,mw}$ = CO_2 molecular weight (kg), that is 44.01×10^{-3} kg/kmol.

By substitution of Eq 1. 2 and Eq 1. 1 in Eq 1. 5, Eq 1. 6 is obtained:

$$CO_{2,gac} = CO_{2,con,avg,vol} \times \frac{Air_{dry,mass}}{Air_{dry,mw}} \times CO_{2,mw} \times 10^{-6} \qquad \text{Eq 1. 6}$$

1.2.2 Data Sources for the Comparison of Existing Platforms for CO_2 Concentration’s Measurement

Fraser’s study used only 21 sites for the calibration of their proposed model for CO_2 atmospheric concentration. After their study, more observation platforms have been established to measure CO_2

concentration, such as ground-based platforms (including ground-based stations and tall towers), aircraft, balloons, ships, and satellite-based observations.

Ground-based measurement is a fixed platform for the observation and measurement of carbon dioxide in a specific location on the earth. Depending on the location of the instrument in these kinds of platforms, the earth coordinates (latitude and longitude), and the elevation of the sampling vessel, i.e., the height regarding the level of the sea, are fixed. Ground-based stations are research stations mostly located at remote sites such as islands, mountains, and coasts. However, several stations have been constructed within a short distance from cities for urban greenhouse gas emission monitoring. The first station where the carbon dioxide concentration was measured is the Mauna Loa observatory site. Mauna Loa site is located on the north flank of Mauna Loa Volcano on the main island of Hawaii (19.54° N, 155.58° W, 3397 m above the sea level (a.s.l)) [26]. Mauna Loa is one of the so-called "Baseline Observatories" of the NOAA network. In other words, Mauna Loa is representative of the background air for a large region that is not affected by local sources of pollution. Other baseline stations are observatories located at Barrow (Alaska), American Samoa, and the South Pole. Other ground-based stations are currently monitoring and measuring carbon dioxide concentration. Among the ground-based stations, the abovementioned baseline stations and TCCON stations seem to be more reliable according to the literature [30]. The list of the worldwide ground-based stations is provided in Table 1.A. 5 in the appendix. Tall towers are used since the 1990s to assess the vertical carbon dioxide concentration gradient in continental areas and to minimize the impact of local sources and sinks [31]. It is possible to consider the impact of remote and local emission sources by means of tall towers [32]. It should be noted that the construction of a new tall tower costs millions of dollars [33], thus, investment in new towers to increase existing spatial resolution is not economically feasible. The list of the worldwide ground-based tall towers in the NOAA Earth System Research Laboratory's Global Greenhouse Gas Reference Network is provided in Table 1.A. 6 in the Appendix.

Airborne measurement is assessed in several studies as a method for CO_2 concentration data collection and validation of satellite and ground-based observations due to its high precision. Airborne measurement means of transport could be aircraft, helicopters, and balloons. The measurement can be performed by flask sampling and/or in-situ methods. As reported by Bischof [34], the measurement of carbon dioxide concentration in air samples from aircraft began in 1957 at the Institute of Meteorology in Stockholm. A specific program was performed until 1961 to take air samples at 1000 m a.s.l. Airborne measurement by means of aircraft has limitations such as the height of flight and the path, while the measurement by means of helicopter and balloons can provide samples at the various desired elevations (vertical profile), and times, due to their ability to fly vertically; however, it will be influenced by the capability of the helicopter and balloon. Another issue related to aircraft observation is related to the limited number of measurements, only one measurement for each set of spatial coordinates is allowed in aircraft observation. Thus, more than one flight is needed to take different measurements in a desired location. In addition, the sampling time interval is related to the type of observation, such as in-situ or flask sampling, and also the travel duration. In some cases, to prevent the effect of time on the accuracy of the result, sampling with a flask is performed on the return path to minimize the time between measurements and the analysis.

Ships are another way for sample collection which covers relatively wide regions. The issue with this measurement is the necessity of many ships to cover the whole world's water; moreover, long times are needed to cover all the world's water surfaces. The advantage of this method is its relatively low cost. The sampling time interval and the sampling location depend on the ship and the program, e.g., some sampling flasks or analysers are attached onboard the commercial ships, and the path and times of the observation are the same as the defined path and timetable of the journey. In some cases, research ships can be used which makes it possible to plan to sample. Because of the issues regarding the limitation in the time intervals and sampling path of this platform, a detailed assessment of this platform will not be carried out in this study.

Because of the low coverage of the airborne and ground observation platforms, it is difficult to measure the carbon dioxide concentration globally; thus, the use of satellite retrieval was recommended by several authors, especially for the regions with a low density of observing stations. Yanfang Hou et al. [35] stated that the first satellite instrument with the aim of CO_2 measurement in the lowest atmospheric layers, i.e., up to 50 km a.s.l is the Scanning Imaging Absorption Spectrometer for Atmospheric Cartography (SCIAMACHY) on board ENVISAT, which was launched in 2002. The first carbon dioxide concentration in the upper troposphere (less than 20 km), using satellite, was obtained by the Advanced Earth Observing Satellite (ADEOS) in 1996, by using the Interferometric Monitor for Greenhouse Gases (IMG)) [36]. Satellite observations have several benefits compared to other means of observation, such as high coverage. Despite its advantages, there are several challenges such as the accuracy of the data, data filtration (e.g., in case of the presence of clouds), and the satellite life span (e.g., the mission duration of the ADEOS satellite was less than a year). Furthermore, the data observation in the satellite is relatively fast due to the method which is used in satellites, e.g., it is not necessary to have flask samples.

The most usual method to validate the data retrieved by means of satellites is the comparison with calibrated ground-based data. Comparison of OCO2 satellite and ground-based was made by Wunch et al. [37], Bi et al. [38], Timofeyev et al. [39], Wu et al. [40], O'Dell et al. [41], Liang et al. [42], Liang A. [43], considering various parameters such as modes of observation, satellite data version and different bands, i.e., the channel which the OCO2 satellite measures the sunlight backscattered by the Earth's surface and atmosphere. Comparison of GOSAT satellite and ground-based observations was done by Qin et al. [44], Dan-dan et al. [45], Velazco et al. [46], Eguchi et al. [47], Ohyama et al. [48], Rokotyan et al. [49], Yates et al. [50], Qu et al. [51], Zeng et al. [52], Wunch et al. [53]. In several papers, the observation of several satellites was simultaneously compared with the ground-based data. Yuan et al. [54] compared the data of in-situ measurement and satellite ones, SCIAMACHY on ENVISAT, TANSO-FTS on GOSAT, and OCO2. Buchwitz et al. [55, 56], in the GHG-CCI project (Climate Change Initiative (CCI)), compared TCCON data with the observation from SCIAMACHY/ENVISAT and TANSO/GOSAT satellites. Miao et al. [57] compared GOSAT, SCIAMACHY, and AIRS with TCCON. They found that the AIRS data perform better in coverage and accuracy compared to the two others, in the case of the monthly mean. The validation of data from AIRS and GOSAT at mid-atmosphere with ground stations was performed by Avelino and Arellano [58]. Zhang et al. [59, 60] compared the data from ground stations with AIRS, SCIAMACHY, and GOSAT. Jiang et al. [61] compared GOSAT, TES, AIRS, and TCCON. Reuter et al. [62] and Michael Buchwitz et al. [63] researched the difference between SCIAMACHY/ENVISAT, TANSO-FTS/GOSAT, and TCCON. Dils et al. [64] compared various algorithms in different satellites with TCCON data and found a precision of approximately 2.4–2.5 ppm for almost all algorithms. Various algorithms in GOSAT were assessed by Kim et al. [65], Wunch et al. [30], Dongxu Yang et al. [66], and Lindqvist et al. [67]. The available information on concentration differences of satellites and TCCON stations in these studies is provided in Section 3.

Several studies compared data obtained from satellites with airborne measurements. It is not possible to measure the concentration of carbon dioxide with aircraft at altitudes higher than 15 km a.s.l., therefore, stratospheric balloons are used in the range of 15–35 km a.s.l. [68]**.** Tadic and Michalak [69] compared the data from aircraft, GOSAT, and OCO2 satellites and concluded that the difference could be above 0.5 ppm_v between aircraft and satellites. Maddy et al. [70] made a comparison among all available data from NOAA ESRL/GMD aircraft and AIRS during 2005, they found an agreement of approximately 0.5%. The annual cycle from AIRS and CONTRAIL over the western Pacific is done by Chahine et al. (2005) [71], they found a good agreement with AIRS in both hemispheres. Uspensky et al. [72] applied an improved scheme for XCO_2 on AIRS data in Siberia and cloud-cleared

IASI data, comparing it with the YAK-AEROSIB aircraft campaign; they found an error of around 2.2 $\mathrm{ppm_v}$. In another study, Kukharskii and Uspenskii [73] worked on a numerical solution for the XCO_2 data retrieved from AIRS and compared it with airborne data over the areas of boreal forests (the Novosibirsk region) and ecosystems (the region of Surgut); they reached an error not worse than 1%. Data from HIPPO flights with GOSAT, TES, and AIRS is compared by Frankenberg et al. [74]; they concluded that over the remote Pacific Ocean the GOSAT satellite, with about 0.5 ppm accuracy, shows the best performance among the three mentioned satellites.

To define the difference between the measurement of carbon dioxide concentration by satellites and other platforms, i.e., the error of the data, the average value, and the standard deviation reported by each study were taken into account. The average mean and the pooled standard deviation are used to combine all data sets because the number of samples in each of the referenced studies is different.

The average mean of CO_2 concentration difference between satellites and other platforms is calculated according to Eq 1. 7:

$$\mu_p = \frac{\sum_{i=1}^{N} n_i . \mu_i}{N} \qquad \text{Eq 1. 7}$$

where:

μ_p = The average mean difference between satellites and other platforms CO_2 concentration

μ_i = Mean difference between satellites and other platforms CO_2 concentration in each data set

n_i = Number of measurements (samples) per data set

N = Total number of measurements

The pooled standard deviation value is calculated by Eq 1. 8 as suggested by [75]:

$$\sigma_p = \sqrt{\frac{1}{N-K} \sum_{i=1}^{N} (n_i - 1) . \sigma_i^2} \qquad \text{Eq 1. 8}$$

where:

σ_p = Pooled standard deviation

σ_i = Standard deviation in each data set

K = Number of data sets

1.2.3 The New Proposed Model for Atmospheric CO_2 Mass Calculation

The main objective of this study is to validate the proposed method for the calculation of the atmospheric CO_2 mass; thus, the whole Earth's surface is considered as the area of study. The main parameters to define the global atmospheric mass of CO_2 are (i) its concentration, (ii) total dry air mass, and (iii) air molecular weight. Because of the limitation in the number of stations and observations in Fraser et al. [8] and the uncertainties in the listed factors, a new approach which is a modification of Fraser's method to calculate CO_2 mass is designed in this study. The methodology is illustrated as a block diagram in Figure 1. 2. The main difference with Fraser's methodology is that the proposed method uses higher resolution data for CO_2 concentration. Therefore, estimation is not limited to values calculated by elaborating the data coming from a few stations located around the world (block a).

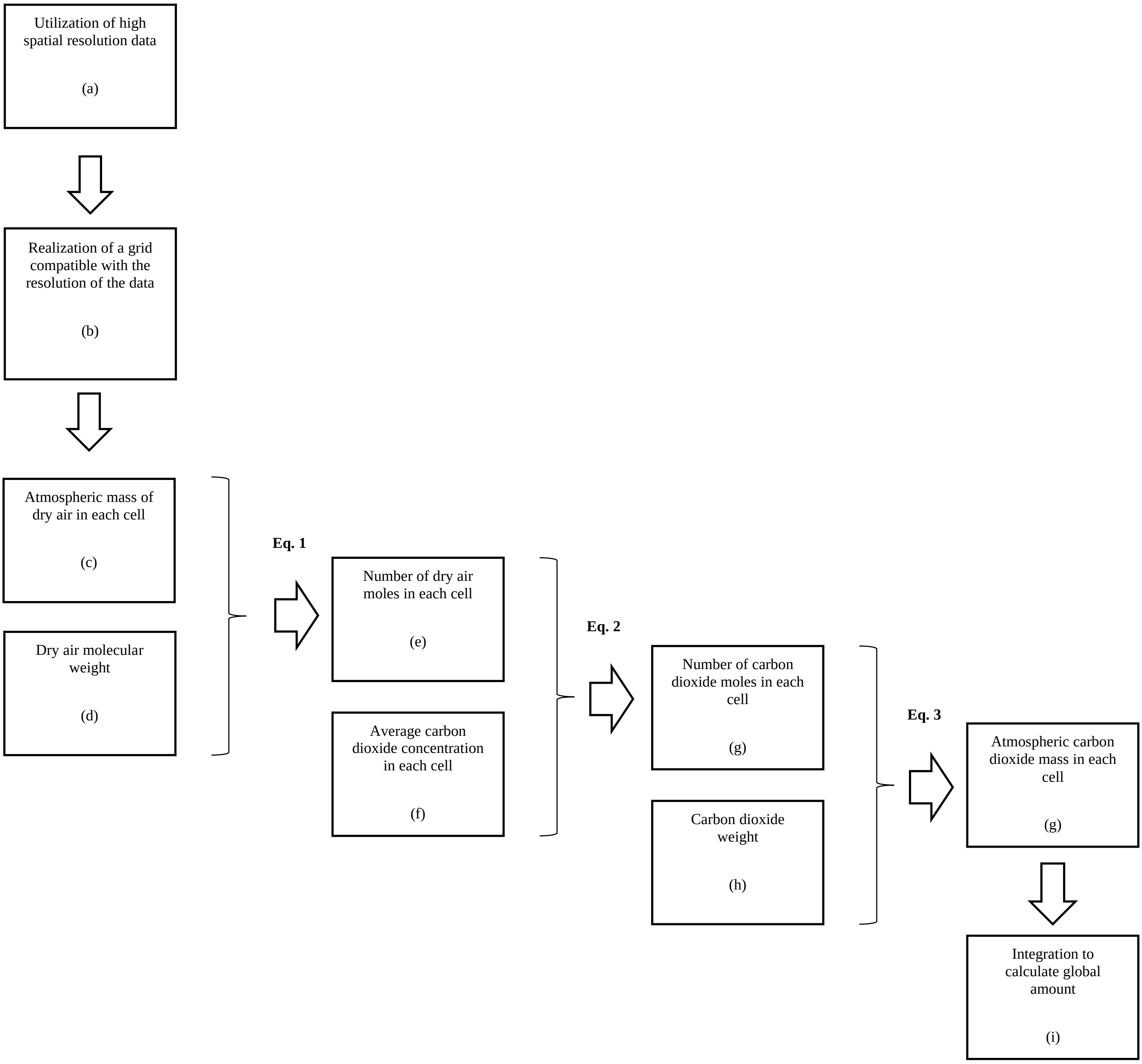

Figure 1. 2 Building blocks for the proposed methodology to reach a higher accuracy of the results for global atmospheric carbon content. Letters a-j are used to label the blocks to simplify mentioning the steps in the text.

Desired information from satellite observation was selected to allocate to each cell. For this purpose, OCO2 and OCO3 satellites were investigated because they are the latest satellites launched for the CO_2 observation goal. instead of direct measurement, OCO2 measures atmospheric CO_2 [76] from the Earth’s surface up to the satellite elevation [77] by means of spectrometers using the reflected sunlight intensity from CO_2 in a column of air. Wavelength bands that are measured by OCO2 are 0.765 µm, related to oxygen, and two CO_2 bands at 1.61 µm and 2.06 µm. For the separation of the reflected light energy into a spectrum of multiple component colours diffraction grating is used [78].

OCO2 was launched on 2 July 2014, and it orbits at 705 km; it captures around 1 million soundings each day. Among the soundings, approximately 10% are aerosols-/cloud-free which can be used to measure XCO_2 [77]. The spatial resolution of OCO2 is 2.25 km × 1.29 km and the temporal resolution is 16 days [76].

It was decided to use 4-day data as the complete Earth's surface coverage, based on the coverage of the satellite daily observation. OCO2 requires almost four days to cover the entire Earth's surface (Figure 1.A. 3, in the appendix). It is assumed that the global CO_2 atmospheric mass change is negligible in four days. Thus, the 4-day observation was chosen as a representative to calculate the CO_2 global atmospheric mass. The observation related to the 5th day has overlap with the 1st day.

Bias-corrected data from both OCO2 and OCO3 satellites were assessed to investigate the applicability of the data. OCO2 and OCO3 satellites' bias-corrected files, version 9r, were downloaded from the NASA website [76]. The downloaded data were in the netCDF format. R programming language was used for data extraction. The desired parameters are the longitude, latitude, quality flag, XCO_2 (that is the column average carbon dioxide concentration in each cell), total water vapor column, and surface pressure. For data cleaning the quality flag is used, it defines if the data are acceptable or not. Only data with a quality flag equal to zero was acceptable in accordance with OCO2 and OCO3 documentation [79] and considered in the following calculations. Based on an initial analysis, it was decided to use only data from OCO2. The main reason is the low number of observations that passed the quality flag filtration Approximately 40,000 observations on average for each day of 4-day observation are used for OCO2 for the calculations. In addition, OCO3 data were available since August 2019, and there were considerable missing data.

A grid compatible with the data's resolution was designed to divide the Earth's surface into cells (block b) for computational purpose. Approximately 177,500,000 cells (514,720,000/2.90) are considered. The Earth's surface is 514,720,000 km^2 and each cell has an area of 2.90 km^2 (=2.25 km × 1.29 km, the spatial resolution of the satellites)

The following steps (from block c to block i) are almost the same as Fraser's methodology. Instead of applying the calculations to the whole Earth's surface, they are applied to each cell. Codes were written in MATLAB for data elaboration while the available "curve fitting" was applied for regression. To calculate the atmospheric mass of dry air in each cell (block c), data about the total surface pressure and the column of water vapor was taken from the NASA website [76]. The dry air pressure in each cell was calculated according to Dalton's Law. Therefore, the dry air mass, which can be used in Eq 1. 1, is calculated, considering the cell area and gravity.

The final step is the integration of the cell values to calculate the global CO_2 atmospheric mass by Eq 1. 9:

$$CO_{2,gac} = \frac{\sum_{i=1}^{N_c}\left(\frac{CO_{2,cac,i}}{2.25 \times 1.29}\right)}{N_c} \times S_{earth} \qquad \text{Eq 1. 9}$$

where:

$CO_{2,cac,I}$ = CO_2 mass in the i-th cell

N_c = number of cells

S_{earth} = Earth surface, i.e., 510.1×10^6 km^2

For the validation of the proposed model, Fraser's model [8] was applied by using data from NOAA. CO_2 concentration data from NOAA is used and the global CO_2 atmospheric mass was estimated for the period between 1980 and 2021. However, the global carbon dioxide atmospheric mass from OCO2 was calculated for 2019 and 2020 because the elaboration of the model is time-consuming.

1.3 Results and Discussion

1.3.1 Validation of the Simplified Fraser's Method for the Calculation of CO_2 Atmospheric Mass

The global amount of CO_2 mass in Fraser's study is calculated by assuming an average CO_2 atmospheric concentration of 337.04 ppm_v, based on a two-dimensional global atmospheric CO_2 transport model calibrated through the data from 21 stations [80].

Based on Eq 1. 6, and the average global concentration calculated by Fraser et al., the global CO_2 mass was calculated as in Eq 1. 10.

$$CO_{2,gac} = 337.04 \times \frac{5.12 \times 10^{18}}{0.02897} \times 10^{-6} \times 44.01 \times 10^{-3} = 2.62 \times 10^{15} kg \qquad \text{Eq 1. 10}$$

The global carbon mass is calculated also equal to 7.15 × 10^{14} kg, by the substitution of the CO_2 molecular weight with carbon molecular weight in Eq 1. 6.

According to Eq 1. 6, the effective parameters on CO_2 mass estimation are the average global carbon dioxide concentration, the global atmospheric mass of dry air, and dry air mean molecular weight. Fraser et al. [8] stated a probable uncertainty of 0.5 to 1% relating to carbon mass calculation as follows:

- 0.4–0.9% related to carbon dioxide concentration. Only 21 stations were used to design and calibrate the model. In addition, there was not any station in Europe, Asia, Africa, and South America, resulting in unbalanced earth surface coverage. Furthermore, the number of observations in which the annual mean CO_2 concentration is estimated is not mentioned in Fraser's study. Therefore, it is not possible to check if the reported values cover all diurnal, daily, weekly, monthly, and seasonal variations or not.

- 0.1% is the contribution of the air's global atmospheric mass and the air mean molecular weight in the uncertainty. Concerning the global atmospheric mass of dry air, 5.12 × 10^{18} kg was used in the model. However, in 1994, Trenberth and Guillemot [81] estimated the mass of dry air in a more accurate way and stated its amount as around 5.132 × 10^{18} kg. However, in 2005, Trenberth and Smith [82] estimated the dry air mass equal to $5.1352 \pm 0.0003 \times 10^{18}$ kg. The difference with respect to Fraser's model is around 0.29%. It should be noted that concerning the dry air average molecular weight, the effect of boundary conditions such as temperature and humidity is not taken into account.

- By comparing the result of global atmospheric carbon dioxide mass in Fraser's study and the result achieved by applying the information from this study in Eq 1. 6, it is assumed that the procedure used in Fraser's study is as depicted in Figure 1. 1.

1.3.2 Assessment and Comparison of Existing Platforms

The comparison of existing platforms through the definition of suitable Key Performance Indicators (KPI) is provided in Table 1. 1. In this table, "ground-based stations", "aircraft, helicopter and balloon", "satellites" and "ships" are compared based on the available literature at the state of the art, including measurement accuracy, precision, coverage, and time. Based on the information provided in the literature, as shown in Table 1. 1, the accuracy of the data is almost the same, less than 0.5 ppm, except for ships. It is worth mentioning that due to utilizing different instruments in ships by researchers the result is a wide interval of accuracy.

Table 1. 1 KPI table of the means of observations.

Means of Observation	**Accuracy** [(a)]	**Precision**	**Cost** [(b)]	**Coverage**	**Time Scale**
Ground-based stations	Could be ± 0.5 ppm	Better than 0.25% for TCCON	low-high [(c)]	local-regional [(d)]	Sampling and Analysing duration
Aircraft, Helicopters and Balloons	Could be less than ± 0.25 ppm (± 0.1, ± 0.05 ppm are also obtained)	Could be ± 0.1 ppm	low-high [(c)]	regional	Flight and Analysing duration [(e)]
Ships	N/A [(a)]	Could be better than 0.6%	low	regional	Travel duration + Analysing duration [(c)]
Satellites	−0.08 ppm regarding TCCON according to the calculations	Less than 2 ppm is needed	high	global	OCO2 & OCO3-16 days GOSAT-3 days

Notes: (a) It depends on the utilized instrument. (b) The satellite cost is assumed to be the comparison base. (c) In case of network it is expensive. (d) Regarding the elevation of the sampling vessel and filtering approach, this can be representative of local or regional. In case of combination of the stations in a network with models it is possible to have the global coverage. (e) It can be only sampling and analysing duration if the analysing instruments are installed in the means of observation.

It is seen that almost all platforms can have high accuracy and precision, and the distinctive indices which make a difference between the platforms seem to be the coverage and the time scale required for observation. According to the objective of this chapter which is the global mass calculation satellite coverage is the best choice. However, other platforms and global atmospheric transport models can be used to calculate the global atmospheric carbon dioxide concentration, which is not in the scope of this study.

The temporal resolution of satellites, shown in this table, is related to the operating satellites, in which the data are available. The temporal resolution of the satellites is higher in comparison to other platforms if global coverage is desired. Other platforms can provide global observation, but it takes more time to integrate regions.

Approximately 1–2 ppm precision is required for satellite retrievals because the variation in the CO_2 concentration related to the surface sinks and sources are typically less than 1 ppm, and seasonal and annual XCO_2 variation are smaller compared to the mean atmospheric concentration [83].

1.3.3 Comparison of CO_2 Concentration Measured by Satellites with TCCON

Figure 1.A. 2 shows the satellite observations and TCCON stations comparison based on the data provided in Table 1.A. 4. Since satellites' observations are compared in Table 1. 1 to indicate the accuracy and reliability, several satellites are compared with TCCON in this figure. By using the mentioned formulas in the previous sections, and the data represented in Table 1.A. 4 in the appendix, it is possible to calculate the average mean and pooled standard deviation of the datasets. It is seen in this figure that the mean difference ranges between −2 and 2 ppm and the mean ± standard deviation ranges between −5 and 4 ppm. According to Eq 1. 7 and Eq 1. 8, the mean average of the comparison between satellites and TCCON is −0.08 ppm and the pooled standard deviation is ±1.66 ppm.

1.3.4 Global Atmospheric CO_2 Mass Calculation

The result of the application of Fraser's methodology to the NOAA data is shown in Figure 1.A. 4 in the appendix. As shown, a continuously upward trend occurs in the period. The atmospheric carbon dioxide mass increased up to 3.22×10^{15} kg in 2021, the estimated yearly increase is around 1.44×10^{10} tons per year between 1980 and 2021.

The result of the proposed model application to OCO2 data is shown in Figure 1. 3 for the period 1 January 2019 to 31 November 2020. The yellow curve is the global CO_2 atmospheric mass calculated using the data from the satellite based on the methodology proposed in this chapter. The blue curve is a 12th polynomial regression curve for the global atmospheric carbon dioxide mass calculated by using satellite data ($R^2 = 0.71$). The black line is the curve obtained from the elaboration of data from NOAA after applying Fraser's methodology ($R^2 = 0.86$). The last part is neglected because the polyline regression with high degrees results in huge anomalies in the boundary of data. For the end of the blue curve, a trend is assumed, which is shown in the dashed red line. The available carbon dioxide average concentrations, provided in the NOAA database are weekly and monthly, of which the monthly one is used for the calculation in this study. It is seen that there is less fluctuation in the NOAA database curve which is related to the difference between the time frames.

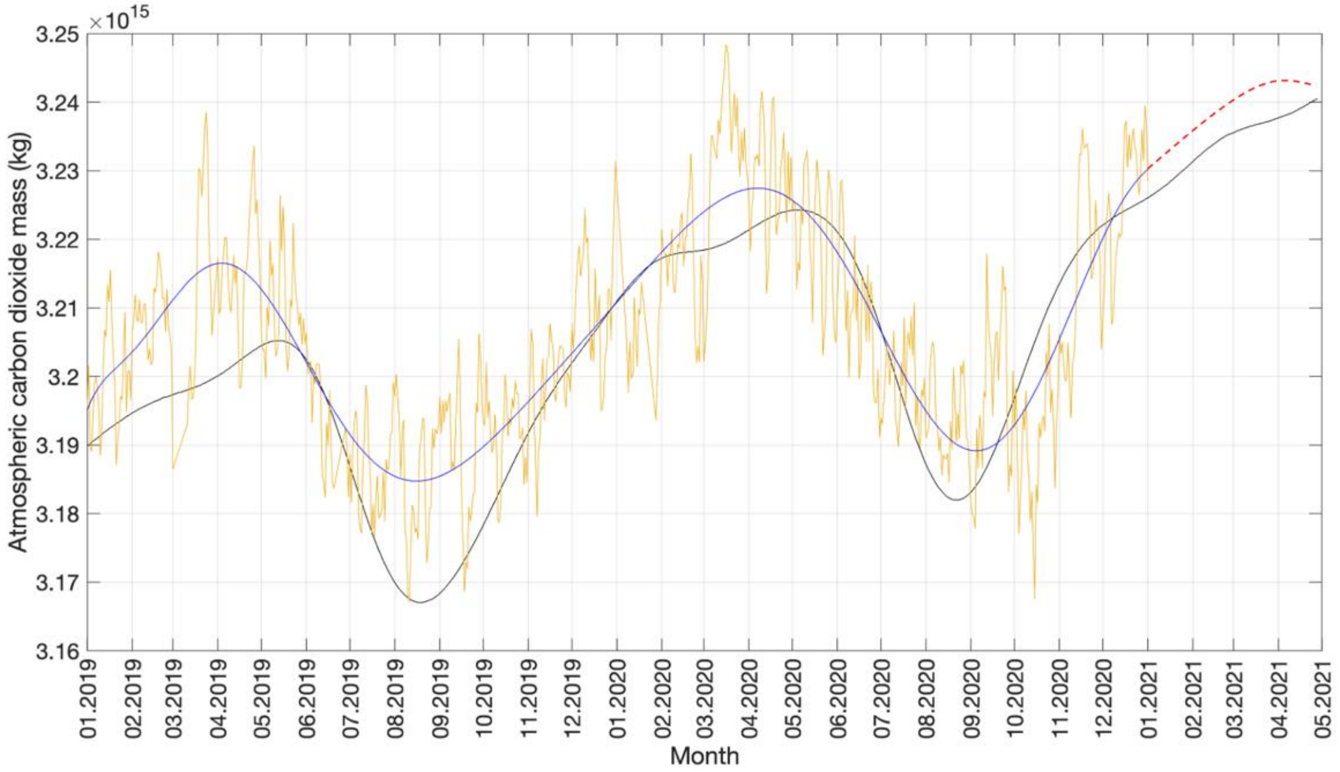

Figure 1. 3 OCO2 global 4-day carbon dioxide mass estimation in the period 2019–2021. The orange is 4-day global atmospheric carbon dioxide mass estimation, the black curve is related to NOAA data, and the blue is the fitting curve. The red dashed line is the prediction of global carbon dioxide mass since the data was not available for OCO2.

Carbon dioxide mass reaches its peak around March and May, while the minimum value occurs in the period between August and November. In general, an upward seasonal trend of global atmospheric carbon dioxide mass appears. The seasonal variations are probably because of various natural and anthropogenic parameters, which are different between the NH and SH. Global atmospheric carbon dioxide mass reaches its annual maximum value during spring and the beginning of summer in the NH. At the same time, the minimum occurs at the end of summer and during the NH's autumn.

Figure 1. 3 covers the 2019–2021 period; the same cyclic trend appears in the global mass calculation using Fraser's method and NOAA data. In this figure, a good agreement can be seen between the two methodologies. A slight difference can be seen between Fraser's methodology using the NOAA dataset and the proposed methodology. By comparing the fitting curve and black curve it is seen that May-July is the period with the best consistency of results and the whole results are almost the same except for extremums.

Table 1. 2 shows the summary of the differences between methods during the period 2019–2020. As shown, a slightly higher amount of carbon dioxide is calculated with the proposed methodology in this study. A maximum difference of 1.25% is calculated for August 2019, while the maximum

difference is around 0.3% for 2020. Finally, the average difference of 0.15% is calculated for the entire period. These differences could be the result of various factors such as the assumptions made in Fraser's method, a lower number of observations, and the amount of total water vapor column and surface pressure in each cell for the calculation of dry air moles in each cell instead of the whole Earth. It is not possible to strictly determine which method is more accurate. However, given the use of more observation and the process of considering parameters separately for each observation column in the methodology proposed in this study, it can be claimed that the proposed method of this study is more accurate.

Table 1. 2 Comparison of the global atmospheric carbon dioxide mass using NOAA data and OCO2 data, 2019–2020.

	NOAA CO_2 Mass Results	**OCO2 Data CO_2 Mass Results**
Average value (kg)	3.201×10^{15}	3.206×10^{15}
Maximum value (kg)	3.226×10^{15}	3.248×10^{15}
Minimum value (kg)	3.167×10^{15}	3.167×10^{15}
Maximum difference ((OCO2-–NOAA)/NOAA)	1.23%	
Average difference	0.15%	

Based on the abovementioned results, the validation of the methodology proposed in this study is assumed successful. One of the most attractive aspects of the proposed methodology in this study is its Spatio-temporal flexibility; which is possible to estimate the global atmospheric CO_2 mass with acceptable accuracy for specific dates; Furthermore, it is possible to define the CO_2 mass and its variation in desired locations because the amount of CO_2 mass is calculated for each cell. A similar approach for carbon dioxide column-averaged concentrations was investigated by Prasad et al. [84] to define the trend over the Indian region. For this purpose, data from SCHIAMACHY and GOSAT satellites were used. They defined the potential links between seasonal concentration trends and anthropogenic behaviour. Similarly, Rossi et al. [85] investigated the spatial distribution of the annual average atmospheric carbon dioxide for the state of Mato Grosso (Brazil) using data from the OCO2 lite version (V8r). Both studies do not estimate the CO_2 mass quantity in the atmosphere as done by the proposed model in this study. Thus, they cannot be used to determine the nominal capacity of the CO_2 carbon capture, storage, and utilization systems. Furthermore, the flexibility of the method proposed in this study can be used for anthropogenic activities control and monitoring the performance of the mitigation and adaptation strategies.

1.4 Conclusions

Carbon dioxide plays an important role in global warming and climate change because of its long-lasting presence in the atmosphere and negative impact on climate change. Carbon dioxide concentration can be used to define the capacity of carbon capturing systems for climate change mitigation, but to define the size of the plants it is required to know the quantity of carbon dioxide. In addition, in some cases, high concentration could be due to temporary local emission and decision making based on concentration could lead to waste of investment. Thus, the accurate estimation of the atmospheric CO_2 mass is essential to define mitigation measures and assess their impact. The method of carbon dioxide mass calculation has not changed since 1983, even though new measuring platforms such as satellites are available, and more data are accessible. Especially, satellite observation is more reliable for global scale estimation, due to its spatial and temporal resolution. The mean average of the comparison between satellites and TCCON is calculated as -0.08 ppm, and the pooled standard deviation is reported as ±1.66 ppm in this study. Among the satellites capable of CO_2 measurement, the most recently launched satellites, OCO2 and OCO3, were investigated to assess their applicability in the methodology proposed in this study. Due to a low fraction of acceptable data (after quality flag filtration and data cleaning), and the high number of missing days in the OCO3 observation, it was decided to use only data from the OCO2 satellite.

The proposed methodology in this chapter ensures high resolution to calculate the global atmospheric carbon dioxide through a wide range of observations from satellites and better results compared to the ones that can be obtained by Fraser’s methodology as currently applied. The maximum and the average difference between the proposed method and the results of Fraser’s method application on NOAA data were 1.23% and 0.15%, respectively.

It is possible to assess the local and global atmospheric carbon dioxide mass distribution by using the proposed method in this study because the Earth’s surface is divided into cells according to the satellite spatial resolution. The main issues in this study are related to the availability of data from satellites and passing the quality check, which might be solved by the combination of satellites or using proper algorithms to reproduce missed data. The result of this study could be useful in decision-making for the installation of systems for carbon capture. In addition, the result can be used to find the most critical locations in the world to make a proper plan for climate change mitigation and adaptation.

1.5 Appendix 1.A

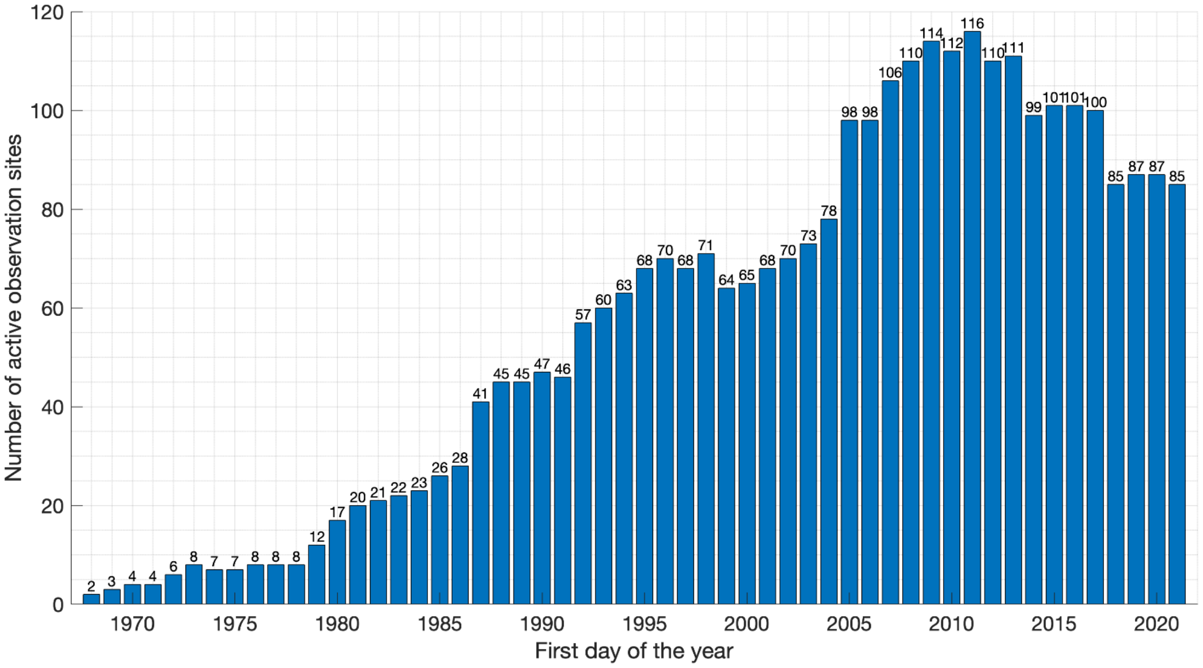

Figure 1.A. 1 The number of active observation sites at the beginning of each year. Data elaborated from the information reported in Table 1.A. 3 in the Appendix.

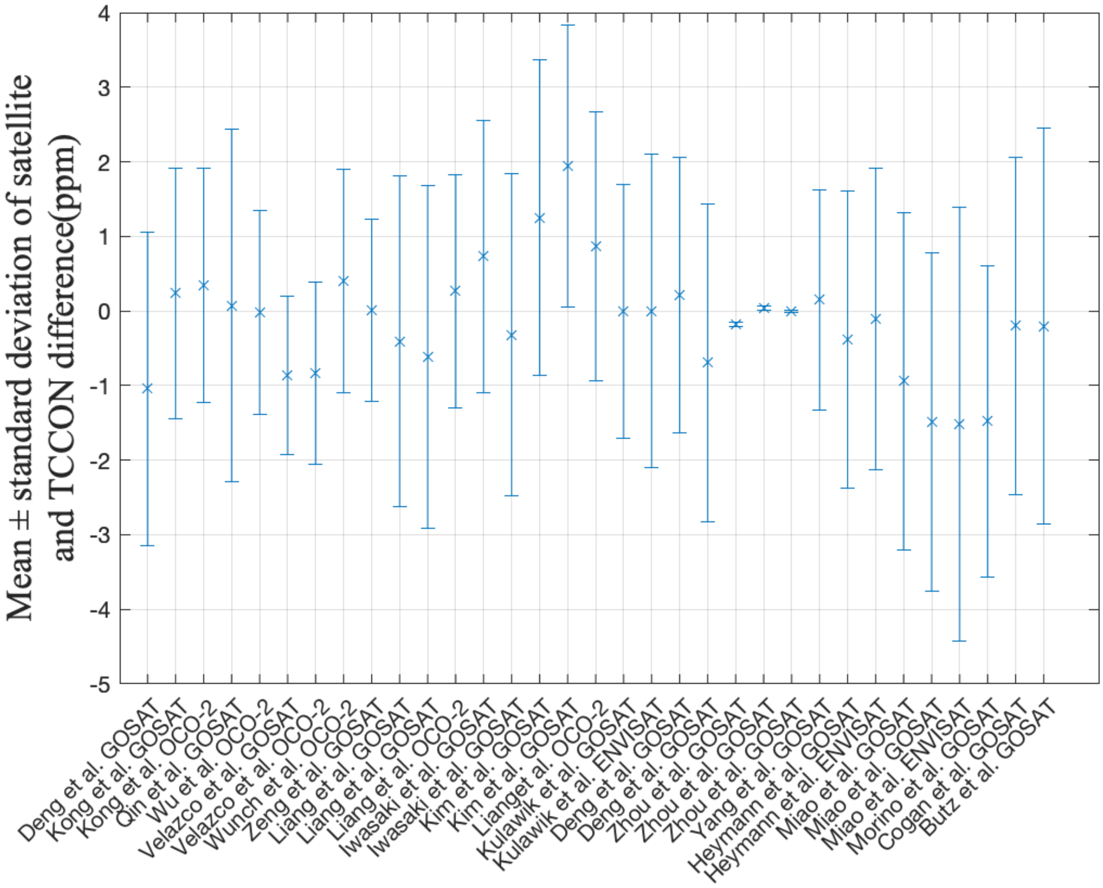

Figure 1.A. 2 Comparison of satellite observations and TCCON stations (References detail are provided in the Table 1.A. 4 in the Appendix.). The different studies are labelled based on references.

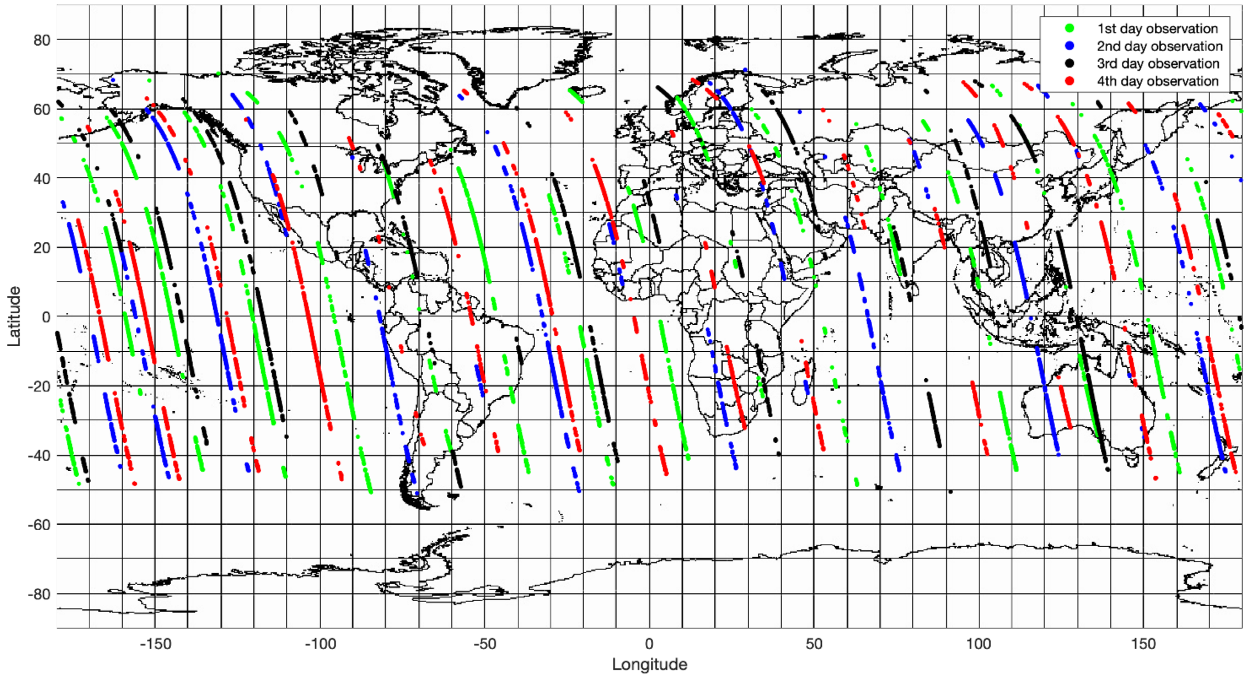

Figure 1.A. 3 OCO2 4-day observation, 22.04.2019–25.04.2019.

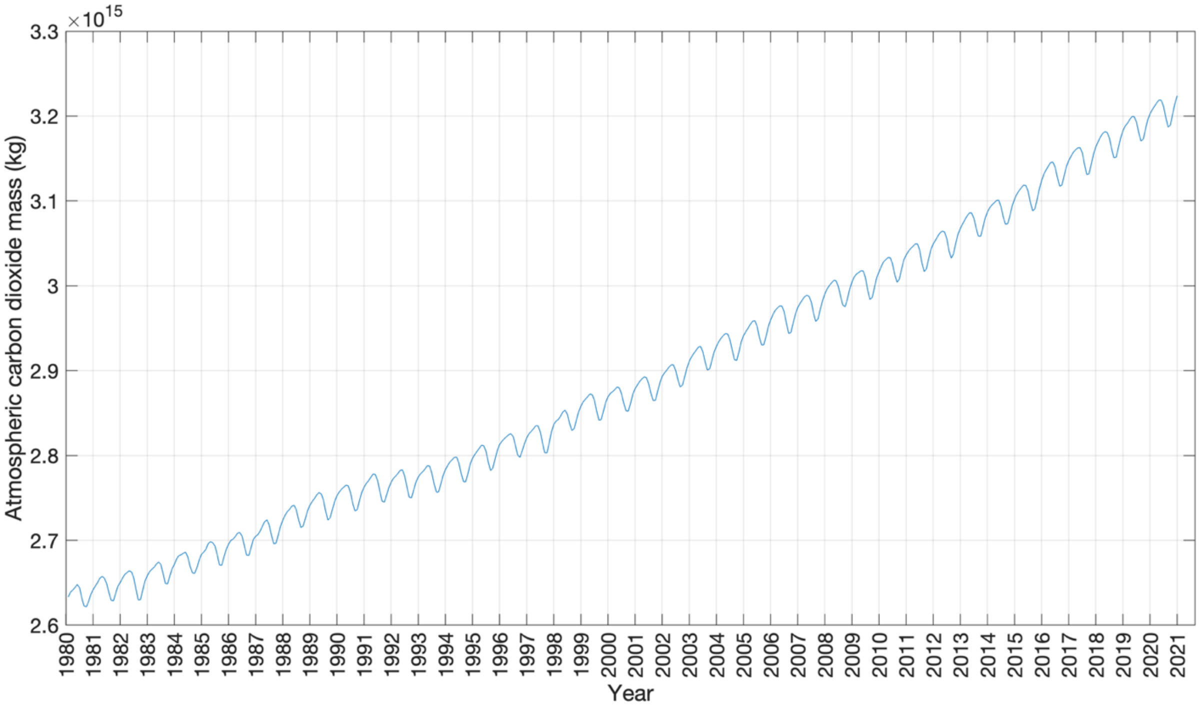

Figure 1.A. 4 Global atmospheric carbon dioxide mass 1980–2021.

Table 1.A. 1 Stations data adapted with permission from Fraser et al. *[8]* for 1980. Copyright 1983 by the American Geophysical Union.flask is sampling and in-situ is the measurement performed in the site.

No.	**Name**	**Symbol**	**Latitude**	**Longitude**	**Flask (F) or In Situ (I)**	**Concentration [a], [ppmv]**
1	Bass Strait	BAS	−40°	150°	F	336.7
2	Cape Grim	CGO	−41°	145°	F I	335.5 336.5
3	Macquarie Island	MAQ	−54°	159°	F	336.9
4	Mawson	MAW	−68°	61°	F	335.5
5	Amsterdam Island	AMS	−38°	78°	F	337.4
6	Ascension Island	ASC	−8°	−14°	F	338.5
7	Azores	AZO	38°	−27°	F	340.2
8	Barrow	BRW	71°	−157°	F I	340.7 339.7
9	Cape Kumukahi	KUM	20°	−145°	F	340
10	Cold Bay	CBA	55°	−163°	F	340.2

11	Guam	GUA	13°	145°	F	340.9
12	Key Biscayne	KEY	26°	−80°	F	340.7
13	Mauna Loa	MLO	20°	−156°	F	341.2
					I	338.1
14	Mould Bay	MOB	76°	−119°	F	340.5
15	Niwot Ridge	NWR	40°	−105°	F	340.4
16	Point Six Mount	PSM	47°	−114°	F	341
17	Samoa	SMO	−14°	−170°	F	337.9
					I	337.9
18	Seychelles	SEY	−5°	55°	F	338.6
19	South Pole	SPO	−90°	0	F	336.1
					I	335.9
					F	337

20	St. Croix	AVI	18°	−65°	F	339.9
21	Fanning Island	FAN	4°	−159°	F	339.1

Note: (a) the concentration was referred to 1980.

Table 1.A. 2 Effective parameters on carbon dioxide concentration.

No.	Author	year of publishment	CO_2 Sources[1]	Meteorological parameters[2]	Atmospheric boundary layer height cycle[3]	Vegetation and climate	Population, GDP and employment	Surface complexity and albedo	Soil respiration and terrestrial ecosystem	Sampling time[4]	Observation characteristics and height	Wildfire	phytoplankton and Ocean	Aerosols, clouds and fog
1	M. N. Patil et al. [86]	2020												✓
2	Yanfen Li et al. [87]	2019												✓
3	Zhaleh Siabi et al. [88]	2019		✓		✓								
4	Ivakhov V. et al. [89]	2019										✓		
5	Swma Jamalalden Al-jaf, Osama Tareq Al-Taai [90]	2019				✓								
6	Irène Xueref-Remy et al. [91]	2018	✓	✓	✓									
7	Mahesh Patakothi et al. [92]	2018		✓										
8	Shuai Yin et al. [93]	2018		✓		✓							✓	
9	Michael Buchwitz et al. [63]	2018		✓										
10	Nian Bie et al. [94]	2018						✓						✓
11	Ge Han et al. [95]	2018									✓			
12	Xun Jiang et al. [96]	2017		✓										
13	Seyed Mohsen Mousavi et al. [97]	2017				✓								
14	Samereh Falahatkar et al. [98]	2017		✓		✓								
15	LEI Li Ping et al. [99]	2017	✓											
16	Debra Wunch et al. [37]	2017						✓						✓

17	Jacob K. Hedelius et al. [100]	2017	✓	✓	✓					
18	Koorosh Esteki et al. [101]	2017	✓	✓						
19	Chen Pan et al. [102]	2016	✓			✓				
20	Thomas E. Taylor et al. [103]	2016								✓
21	Yeonjin Jung et al. [104]	2016								✓
22	Hernández-Paniagua et al. [105]	2015		✓						
23	Min Liu et al. [106]	2015	✓							
24	LIU Xiao-Man et al. [107]	2015	✓			✓				
25	H. Ohyama et al. [48]	2015								✓
26	Loretta Gratani and Laura Varone [108]	2014	✓			✓				
27	Moon-Soo Park et al. [109]	2014		✓	✓		✓			
28	S. X. Fang et al. [110]	2014		✓						
29	Qin XC et al. [111]	2014							✓	
30	Yanli Li et al. [112]	2014	✓	✓				✓		
31	M. Górka and D. Lewicka-Szczebak [113]	2013	✓					✓		
32	Li Yan-li et al. [114]	2013		✓						
33	Christian Büns and Wilhelm Kuttler [115]	2012	✓	✓						
34	Jiabing Wu et al. [116]	2012		✓		✓				
35	Ma Ángeles García et al. [117]	2012		✓						
36	Yanfang H. [118]	2012	✓			✓		✓		

37	Andrew Rice and Gregory Bostrom [119]	2011	✓		✓	✓								
38	Ramamurthy P. and Pardyjak ER. [120]	2011				✓								
39	Irène Xueref-Remy et al. [121]	2011				✓								
40	Ke Wang et al. [122]	2011	✓	✓					✓					
41	Nawo Eguchi et al. [47]	2011	✓			✓							✓	✓
42	Y. Yoshida et al. [123]	2011						✓			✓			✓
43	C. Sirignano et al. [124]	2010								✓				
44	Ch. Gurk et al. [125]	2008				✓								
45	George L. H. Ziska et al. [126]	2007	✓				✓							
46	I. Aben et al. [127]	2007												✓
47	Yang Y. et al. [128]	2006		✓										✓
48	Loretta Gratani and Laura Varone [129]	2005	✓	✓										
49	Hassan A. Nasrallah et al. [130]	2003	✓	✓		✓								
50	P. Chamard et al. [131]	2003		✓										
51	Yuesi et al. [132]	2002								✓				
52	Elizabeth A. Wentz et al. [133]	2002	✓				✓							
53	Richard J. Engelen et al. [134]	2001												✓
54	T. J. Conway et al. [135]	1988			✓									

1.anthropogenic sources such as urban sources (heating, and traffic), industry
2.wind speed and direction, precipitation, humidity, temperature, pressure, solar radiation and drought, La Niña and El Niño events
3. depends on the elevation of the location
4. in the afternoon for well mixing of the air

Table 1.A. 3 Sites that are currently included in the global gas reference network [136].

Site	Name	Location	First Carbon Dioxide Dataset	Status Carbon Dioxide Dataset	Air Sample Collection Method
1	Airborne Aerosol Observatory	Bondville (USA)	07.06.2006	Terminated 18.09.2009	Airborne Flasks *
2	Arembepe, Bahia	Brazil	27.10.2006	Terminated 13.01.2010	Surface Flasks *
3	Alaska Coast Guard	United States	30.04.2009	Terminated 21.10.2017	Airborne Flasks *
4	Alert, Nunavut	Canada	10.06.1985	ongoing	Surface Flasks
5	Amsterdam Island	France	05.01.1979	Terminated 07.12.1990	Surface Flasks *
6	Argyle, Maine	United States	18.09.2003 22.11.2008	Terminated 29.12.2008 ongoing	In Situ Tall Tower Surface Flasks
7	Anmyeon-do	Republic of Korea	03.12.2013	ongoing	Surface Flasks
8	Ascension Island	United Kingdom	27.08.1979	ongoing	Surface Flasks

9	Assekrem	Algeria	12.09.1995	ongoing	Surface Flasks
10	St. Croix, Virgin Islands	United States	16.02.1979	Terminated 29.08.1990	Surface Flasks *
11	Terceira Island, Azores	Portugal	26.12.1979	ongoing	Surface Flasks
12	Baltic Sea	Poland	31.08.1992	Terminate 22.06.2011	Surface Flasks *
13	Boulder Atmospheric Observatory, Colorado	United States	16.08.2007	Terminated 06.07.2016	In Situ Tall Tower * Airborne Flasks * Surface Flasks *
14	Bradgate, Iowa	United States	13.09.2004	Terminated 18.11.2005	Airborne Flasks *
15	Baring Head Station	New Zealand	14.10.1999	ongoing	Surface Flasks
16	Bukit Kototabang	Indonesia	08.01.2004	ongoing	Surface Flasks
17	St. Davids Head, Bermuda	United Kingdom	13.02.1989	Terminated 25.01.2010	Surface Flasks *
18	Tudor Hill, Bermuda	United Kingdom	11.05.1989	ongoing	Surface Flasks
19	Beaver Crossing, Nebraska	United States	15.09.2004	Terminated 11.05.2011	Airborne Flasks *

20	Barrow Atmospheric Baseline Observatory	United States	25.04.1971	ongoing	In Situ Observatory Surface Flasks
21	Black Sea, Constanta	Romania	11.10.1994	Terminated 26.12.2011	Surface Flasks *
22	Brentwood, Maryland	United States	25.09.2018	ongoing	Surface Flasks
23	Briggsdale, Colorado	United States	09.11.1992	ongoing	Airborne Flasks
24	Cold Bay, Alaska	United States	21.08.1978	ongoing	Surface Flasks
25	Cape Grim, Tasmania	Australia	19.04.1984	ongoing	Surface Flasks
26	Christmas Island	Republic of Kiribati	08.03.1984	ongoing	Surface Flasks
27	Cherskii	Russia	Not for CO_2	Not for CO_2	Surface In Situ *
28	Centro de Investigacion de la Baja Atmosfera (CIBA)	Spain	05.05.2009	ongoing	Surface Flasks
29	Offshore Cape May, New Jersey	United States	17.08.2005	ongoing	Airborne Flasks
30	Cape Meares, Oregon	United States	10.03.1982	Terminate 18.03.1998	Surface Flasks *
31	Cosmos	Peru	23.06.1979	Terminate 28.05.1985	Surface Flasks *

32	Cape Point	South Africa	11.02.2010	ongoing	Surface Flasks
33	Carbon in Arctic Reservoirs Vulnerability Experiment (CARVE)	United States	29.06.2012	ongoing	In Situ Tall Tower Airborn Flasks * Surface Flasks
34	Crozet Island	France	03.03.1991	ongoing	Surface Flasks
35	Dahlen, North Dakota	United States	21.09.2004	Terminated 15.11.2016	Airborne Flasks
36	Drake Passage	N/A	07.04.2003	ongoing	Surface Flasks
37	Dongsha Island	Taiwan	05.03.2010	ongoing	Surface Flasks
38	Easter Island	Chile	04.01.1994	ongoing	Surface Flasks
39	Estevan Point, British Columbia	Canada	22.11.2002	ongoing	Airborne Flasks
40	East Trout Lake, Saskatchewan	Canada	15.10.2005	Terminated 22.03.2020	Airborne Flasks *
41	Falkland Islands	United Kingdom	31.10.1980	Terminated 04.02.1982	Surface Flasks *
42	Fortaleza	Brazil	09.12.2000	Terminated 25.03.2003	Airborne Flasks *

43	Fairchild, Wisconsin	United States	20.09.2004	Terminated 18.11.2005	Airborne Flasks *
44	Mariana Islands	Guam	24.09.1978	ongoing	Surface Flasks
45	Dwejra Point, Gozo	Malta	11.10.1993	Terminated 12.02.1999	Surface Flasks *
46	Molokai Island, Hawaii	United States	31.05.1999	Terminated 22.04.2008	Airborne Flasks *
47	Halley Station, Antarctica	United Kingdom	17.01.1983	ongoing	Surface Flasks
48	Harvard Forest, Massachusetts	United States	02.03.2016	ongoing	Airborne Flasks * Surface Flasks
49	Homer, Illinois	United States	16.09.2004	ongoing	Airborne Flasks
50	Hohenpeissenberg	Germany	06.04.2006	ongoing	Surface Flasks
51	Humboldt State University	United States	17.05.2008	Terminated 31.05.2017	Surface Flasks *
52	Hegyhatsal	Hungary	02.03.1993	ongoing	Surface Flasks
53	Storhofdi, Vestmannaeyjar	Iceland	02.10.1992	ongoing	Surface Flasks
54	INFLUX (Indianapolis Flux Experiment)	United States	09.10.2010	ongoing	Airborne Flasks *

					Surface Flasks
55	Grifton, North Carolina	United States	30.07.1992	Terminated 09.06.1999	In Situ Tall Tower * Surface Flasks *
56	Izana, Tenerife, Canary Islands	Spain	16.11.1991	ongoing	Surface Flasks
57	Kaashidhoo	Republic of Maldives	02.03.1998	Terminated 15.07.1999	Surface Flasks *
58	Key Biscayne, Florida	United States	13.12.1972	ongoing	Surface Flasks
59	Kitt Peak, Arizona	United States	20.12.1982	Terminated 31.10.1989	Surface Flasks *
60	Cape Kumukahi, Hawaii	United States	12.01.1971	ongoing	Surface Flasks
61	Sary Taukum	Kazakhstan	12.10.1997	Terminated 15.08.2009	Surface Flasks *
62	Plateau Assy	Kazakhstan	15.10.1997	Terminated 05.08.2009	Surface Flasks *
63	LA Megacities	United States	05.11.2014	Terminated 08.10.2017	Surface Flasks *
64	Park Falls, Wisconsin	United States	29.11.1994 05.10.2006	ongoing ongoing	In Situ Tall Tower Airborne Flasks

					Surface Flasks
65	Lewisburg, Pennsylvania	United States	28.02.2013	ongoing	Surface Flasks
66	Lac La Biche, Alberta	Canada	30.01.2008	Terminated 26.02.2013	Surface Flasks *
67	Lulin	Taiwan	01.08.2006	ongoing	Surface Flasks
68	Lampedusa	Italy	12.10.2006	ongoing	Surface Flasks
69	Mould Bay, Northwest Territories	Canada	13.04.1980	Terminated 26.05.1997	Surface Flasks *
70	Mt. Bachelor Observatory	United States	14.10.2011	ongoing	Surface Flasks
			03.05.2012	ongoing	Surface in situ
71	McMurdo Station, Antarctica	United States	04.12.1985	Terminated 28.10.1987	Surface Flasks *
72	High Altitude Global Climate Observation Center	Mexico	09.01.2009	ongoing	Surface Flasks
73	Mace Head, County Galway	Ireland	03.06.1991	ongoing	Surface Flasks
74	Sand Island, Midway	United States	03.05.1985	ongoing	Surface Flasks

75	Mt. Kenya	Kenya	23.12.2003	Terminated 21.06.2011	Surface Flasks *
76	Mauna Kea, Hawaii	United States	N/A	N/A	Surface Flasks *
77	Mauna Loa, Hawaii	United States	N/A	N/A	Surface Flasks *
78	Mauna Loa, Hawaii	United States	20.08.1969	ongoing	In Situ Observatory Surface Flasks
79	Marcellus Pennsylvania	United States	03.08.2015	ongoing	Airborne Flasks * Surface Flasks
80	Mashpee, Massachusetts	United States	11.05.2016	ongoing	Surface Flasks
81	Marthas Vineyard, Massachusetts	United States	27.04.2007	Terminated 04.03.2011	Surface Flasks *
82	Mt. Wilson Observatory	United States	30.04.2010	ongoing	Surface Flasks
83	Farol De Mae Luiza Lighthouse	Brazil	12.09.2010	Terminated 11.03.2020	Surface Flasks *
84	NE Baltimore, Maryland	United States	04.04.2018	ongoing	Surface Flasks

85	Offshore Portsmouth, New Hampshire (Isles of Shoals)	United States	12.09.2003	ongoing	Airborne Flasks
86	Gobabeb	Namibia	13.01.1997	ongoing	Surface Flasks
87	NW Baltimore	United States	17.04.2018	ongoing	Surface Flasks
88	Niwot Ridge Forest, Colorado	United States	20.01.2006	Terminated 08.11.2009	Surface Flasks *
89	Niwot Ridge, Colorado	United States	18.05.1967	ongoing	Airborne Flasks *
			16.09.2005	ongoing	Surface Flasks
90	Kaitorete Spit	New Zealand	26.10.1982	Terminated 09.04.1985	Surface Flasks *
91	Oglesby, Illinois	United States	16.09.2004	Terminated 19.11.2005	Airborne Flasks *
92	Olympic Peninsula, Washington	United States	06.01.1984	Terminated 30.05.1990	Surface Flasks *
93	Ochsenkopf	Germany	13.03.2003	Terminated 04.06.2019	Surface Flasks *
94	Pallas-Sammaltunturi, GAW Station	Finland	21.12.2001	ongoing	Surface Flasks
95	Pico, Azores	Portugal	02.08.2010	Terminated 18.07.2011	Surface Flasks *

96	Poker Flat, Alaska	United States	27.06.1999	ongoing	Airborne Flasks
97	Pacific Ocean (0 N)	N/A	20.12.1986	Terminated 10.07.2017	Surface Flasks *
98	Pacific Ocean (5 N)	N/A	19.12.1986	Terminated 11.07.2011	Surface Flasks *
99	Pacific Ocean (10 N)	N/A	14.01.1987	Terminated 12.07.2017	Surface Flasks *
100	Pacific Ocean (15 N)	N/A	17.12.1986	Terminated 13.07.2017	Surface Flasks *
101	Pacific Ocean (20 N)	N/A	16.12.1986	Terminated 14.07.2017	Surface Flasks *
102	Pacific Ocean (25 N)	N/A	15.12.1986	Terminated 15.07.2017	Surface Flasks *
103	Pacific Ocean (30 N)	N/A	14.12.1986	Terminated 16.07.2017	Surface Flasks *
104	Pacific Ocean (35 N)	N/A	21.01.1987	Terminated 18.06.2007	Surface Flasks *
105	Pacific Ocean (40 N)	N/A	04.06.1987	Terminated 14.08.1996	Surface Flasks *
106	Pacific Ocean (45 N)	N/A	05.06.1987	Terminated 15.08.1996	Surface Flasks *
107	Pacific Ocean (5 S)	N/A	21.12.1986	Terminated 09.07.2017	Surface Flasks *
108	Pacific Ocean (10 S)	N/A	22.12.1986	Terminated 08.07.2017	Surface Flasks *

109	Pacific Ocean (15 S)	N/A	25.12.1986	Terminated 07.07.2017	Surface Flasks *
110	Pacific Ocean (20 S)	N/A	28.12.1986	Terminated 05.07.2017	Surface Flasks *
111	Pacific Ocean (25 S)	N/A	29.12.1986	Terminated 04.07.2017	Surface Flasks *
112	Pacific Ocean (30 S)	N/A	29.12.1986	Terminated 03.07.2017	Surface Flasks *
113	Pacific Ocean (35 S)	N/A	30.12.1986	Terminated 03.01.2012	Surface Flasks *
114	Palmer Station, Antarctica	United States	27.01.1978	ongoing	Surface Flasks
115	Point Six Mountain, Montana	United States	28.04.1978	Terminated 24.12.1982	Surface Flasks *
116	Point Arena, California	United States	05.01.1999	Terminated 25.05.2011	Surface Flasks *
117	Ragged Point	Barbados	14.11.1987	ongoing	Surface Flasks
118	Rarotonga	Cook Islands	16.04.2000	ongoing	Airborne Flasks
119	Santarem	Brazil	07.12.2000	Terminated 20.08.2003	Airborne Flasks *
120	Offshore Charleston, South Carolina	United States	22.08.2003	ongoing	Airborne Flasks
121	South China Sea (3 N)	N/A	05.07.1991	Terminated 07.10.1998	Surface Flasks *

122	South China Sea (6 N)	N/A	05.07.1991	Terminated 09.10.1998	Surface Flasks *
123	South China Sea (9 N)	N/A	06.07.1991	Terminated 10.10.1998	Surface Flasks *
124	South China Sea (12 N)	N/A	06.07.1991	Terminated 10.10.1998	Surface Flasks *
125	South China Sea (15 N)	N/A	07.07.1991	Terminate 15.10.1998	Surface Flasks *
126	South China Sea (18 N)	N/A	08.07.1991	Terminated 14.10.1998	Surface Flasks *
127	South China Sea (21 N)	N/A	08.07.1991	Terminated 14.10.1998	Surface Flasks *
128	Beech Island, South Carolina	United States	14.08.2008	ongoing	in Situ Observatory Surface Flasks
129	Shangdianzi	China	03.09.2009	Terminated 02.09.2015	Surface Flasks *
130	Mahe Island	Seychelles	15.01.1980	ongoing	Surface Flasks
131	Bird Island, South Georgia	United Kingdom	02.02.1989	Terminated 13.08.1992	Surface Flasks *
132	Southern Great Plains, Oklahoma	United States	02.04.2002	ongoing	Airborne Flasks
			29.10.2010	ongoing	Surface Flasks

133	Shemya Island, Alaska	United States	04.09.1985	ongoing	Surface Flasks
134	La Jolla, California	United States	01.01.1968	Terminated 25.09.1986	Surface Flasks *
135	Tutuila	American Samoa	15.01.1972	ongoing	in Situ Observatory Surface Flasks
136	Shenandoah National Park	United States	26.08.2008	ongoing	Surface in Situ
137	South Pole, Antarctica	United States	21.01.1975	ongoing	in Situ Observatory Surface Flasks
138	Ocean Station Charlie	United States	21.11.1968	Terminated 12.05.1973	Surface Flasks *
139	Ocean Station M	Norway	08.03.1981	Terminated 27.11.2009	Surface Flasks *
140	Sutro Tower, San Francisco, California	United States	02.10.2007	ongoing	Surface Flasks
141	Summit	Greenland	23.06.1997	ongoing	Surface Flasks
142	Syowa Station, Antarctica	Japan	25.01.1986	ongoing	Surface Flasks
143	Tacolneston	United Kingdom	06.06.2014	Terminated 04.01.2016	Surface Flasks *

144	Tae-ahn Peninsula	Republic of Korea	24.11.1990	ongoing	Surface Flasks
145	Tambopata	Peru	N/A	N/A	Surface in Situ
146	Offshore Corpus Christi, Texas	United States	09.09.2003	ongoing	Airborne Flasks
147	Trinidad Head, California	United States	19.04.2002	Terminated 01.06.2017	Airborne Flasks Surface Flasks *
148	Hydrometeorological Observatory of Tiksi	Russia	15.08.2011	Terminated 03.09.2018	Surface Flasks *
149	Thurmont, Maryland	United States	01.08.2017	ongoing	Surface Flasks
150	Taiping Island	Taiwan	28.05.2019	ongoing	Surface Flasks
151	Ulaanbaatar	Mongolia	25.03.2004	Terminated 05.03.2009	Airborne Flasks *
152	Ushuaia	Argentina	14.09.1994	ongoing	Surface Flasks
153	Wendover, Utah	United States	06.05.1993	ongoing	Surface Flasks
154	Ulaan Uul	Mongolia	01.01.1992	ongoing	Surface Flasks
155	West Branch, Iowa	United States	28.06.2007	ongoing	In Situ Tall Tower

					Airborn Flasks Surface Flasks
156	Walnut Grove, California	United States	20.09.2007	ongoing	In Situ Tall Tower Airborne Flasks * Surface Flasks
157	Weizmann Institute of Science at the Arava Institute, Ketura	Israel	27.11.1995	ongoing	Surface Flasks
158	Moody, Texas	United States	11.02.2001 07.07.2006	Terminated 01.10.2010 ongoing	In Situ Tall Tower Surface Flasks
159	Mt. Waliguan	Peoples Republic of China	05.08.1990	ongoing	Surface Flasks
160	Western Pacific Cruise (0 N)	N/A	10.05.2004	Terminated 27.05.2013	Surface Flasks *
161	Western Pacific Cruise (5 N)	N/A	11.05.2004	Terminated 29.05.2013	Surface Flasks *
162	Western Pacific Cruise (10 N)	N/A	11.05.2004	Terminated 29.05.2013	Surface Flasks *
163	Western Pacific Cruise (15 N)	N/A	12.05.2004	Terminated 30.05.2013	Surface Flasks *

164	Western Pacific Cruise (20 N)	N/A	12.05.2004	Terminated 31.05.2013	Surface Flasks *
165	Western Pacific Cruise (25 N)	N/A	13.05.2003	Terminated 01.06.2013	Surface Flasks *
166	Western Pacific Cruise (30 N)	N/A	14.05.2004	Terminated 01.06.2013	Surface Flasks *
167	Western Pacific Cruise (5 S)	N/A	09.05.2004	Terminated 27.05.2013	Surface Flasks *
168	Western Pacific Cruise (10 S)	N/A	08.05.2004	Terminated 26.05.2013	Surface Flasks *
169	Western Pacific Cruise (15 S)	N/A	08.05.2004	Terminated 25.05.2013	Surface Flasks *
170	Western Pacific Cruise (20 S)	N/A	07.05.2004	Terminated 25.05.2013	Surface Flasks *
171	Western Pacific Cruise (25 S)	N/A	06.05.2004	Terminated 24.05.2013	Surface Flasks *
172	Western Pacific Cruise (30 S)	N/A	05.05.2004	Terminated 23.05.2013	Surface Flasks *
173	Ny-Alesund, Svalbard	Norway and Sweden	11.02.1994	ongoing	Surface Flasks

*–Indicates discontinued site or project.

Table 1.A. 4 Comparison of satellite data and TCCON stations.

No.	location	coordination	period	Satellite name	Satellite difference with ground station	number of observations	note		reference
1	China	NH	2010 to 2016	GOSAT	-1.04±2.10 ppm	chinese text	correlation coefficient of 0.90		Deng A. et al. 2020 [137]
2	27 TCCON stations		July 2009-May 2016	GOSAT	0.24 ± 1.68 ppm	1913 NH 575 SH	0.349±1.699 ppm NH -0.128±1.561 ppm SH	2488 matched observations	Yawen Kong et al. 2019 [138]
			Sep 2014-July 2017	OCO-2	0.34 ± 1.57 ppm	779 NH 294 SH	0.283±1.584 ppm NH 0.494±1.127 ppm SH	1073 matched observations	
3	Tsukuba	36.05°N, 140.12°E	Sep 2014 – August2016	GOSAT	0.07± 2.36ppm	N/A			Qin et al. 2019 [44]
4	Various TCCON stations	Both Hemisphere	Sep 2014 and July 2016	OCO-2	-0.02 ± 1.36ppm	34560	RemoTeC algorithm version 7 data		Lianghai Wu et al. 2018 [139]
5	Burgos, Ilocos Norte, Philippines	18.52°N, 120.65°E	2017	GOSAT	-0.86 ± 1.06 ppm	N/A			Voltaire A. Velazco et al. 2017 [140]
				OCO-2	-0.83 ± 1.22ppm	164			
6	Various TCCON stations			OCO-2	0.4± 1.50ppm	2790			Wunch et al. 2017 [37]
7	global TCCON stations			GOSAT	0.01 ± 1.22 ppm				Zhao-Cheng Zeng et al. 2017 [52]

8	Various TCCON stations	Both Hemisphere	2009-2016	GOSAT	-0.4107±2.216 ppm	1813 NH 596 SH	-0.214±2.009 ppm NH -1.016±1.956 ppm SH		Ailin Liang et al. 2017 [141]
			2014-2016	GOSAT	-0.62±2.3 ppm	563 NH 151 SH	-0.312±2.006 ppm NH -1.778±2.096 ppm SH		
			September 2014 to December 2016	OCO-2	0.2671±1.56 ppm	730 NH 321 SH	0.175±1.402 ppm NH 0.476±1.065 ppm SH		
9	11 TCCON stations	Both Hemisphere	2009-2014	GOSAT	0.73±1.83 ppm	1484 NH 634 SH	0.959±1.724 ppm NH 0.209±1.706 ppm SH	Photon path length Probability Density Function-Simultaneous (PPDF-S) retrieval method	Chisa Iwasaki et al. 2017 [142]
				GOSAT	-0.32±2.16 ppm	1484 NH 634 SH	-0.299±1.860 ppm NH -0.384±2.104 ppm SH	standard products for General Users (GU) of XCO2	
10	Tsukuba and Saga	NH		GOSAT	1.25 ± 2.12 ppm	207	NIES algorithm		Woogyung Kim et al. 2016 [65]
				GOSAT	1.94 ± 1.89 ppm	205	ACOS algorithm		
11	Various TCCON stations		Sep 2014-Nov 2015	OCO-2	0.87 ± 1.8 ppm	not provided in the paper			Liang A. et al. 2016 [143]

12	11 TCCON stations	45°S–80°N	Jun 2009–Apr 2014	GOSAT	±1.7 ppm	not provided in the paper	ACOS b3.5		Susan Kulawik et al. 2016 [144]
		45°S–80°N	Jan 2003–Apr 2012	ENVISAT (SCIAMACHY)	±2.1ppm	not provided in the paper	Bremen Optimal Estimation DOAS, BESD v2.00.08		
13	12 TCCON stations		2010 to 2012	GOSAT	0.21 ± 1.85 ppm	2409 NH 915 SH	0.062±1.815 ppm NH 0.597±1.684 ppm SH	ACOS data	Anjian Deng et al. 2016 [145]
			2010 to 2012	GOSAT	-0.69 ± 2.13 ppm	407 NH 191 SH	-0.679±2.103 ppm NH -0.720±1.401 ppm SH	NIES data (National Institute for Environmental Studies of Japan)	
14	Izaña Ascension Island Darwin Reunion Island Wollongong	28.3°N, 16.5°W 7.9°S, 14.3°W 12.4°S, 130.9°E 20.9°S, 55.5°E 34.4°S, 150.8°E	Apr 2009–May 2014	GOSAT	-0.184 ± 0.028 ppm	1137 NH 5877 SH	-0.064±0.032 ppm NH -0.207±0.027 ppm SH	NIES version 02.21	Minqiang Zhou et al. 2016 [146]
			Apr 2009–Dec 2013	GOSAT	0.038 ± 0.032 ppm	726 NH 6532 SH	0.057±0.056 ppm NH 0.035±0.028 ppm SH	SRON/KIT algorithm, SRFP v2.3.5	
			Apr 2009–Jun 2014	GOSAT	-0.006 ± 0.019 ppm	1519 NH 8960 SH	-0.001±0.026 ppm NH -0.007±0.018 ppm SH	ACOS version 3.5	

15	TCCON stations			GOSAT	0.15±1.48 ppm	not provided in the paper	modification of the algorithm from Institute of Atmospheric Physics, Chinese Academy of Sciences		Dongxu Yang et al. 2015 [66]
16	Various TCCON stations		2004-2013	GOSAT	-0.38 ± 1.992 ppm	5522 NH 1530 SH	-0.364±2.078 ppm NH -0.439±1.640 ppm SH	Bremen Optimal Estimation DOAS (BESD) algorithm	J. Heymann et al. 2015 [147]
				ENVISAT (SCIAMACHY)	-0.105 ± 2.017 ppm	32619 NH 15336 SH	-0.071±2.097 ppm NH -0.179±1.836 ppm SH		
17	Eureka, Park Falls, Lamont, Sodankyla, Bialystok, Orleans and Garmisch	NH	April 2010 to March 2012	GOSAT	-0.94 ± 2.26 ppm	659	ACOS		ZHANG Miao et al. 2014 [148]
				GOSAT	-1.49 ± 2.27 ppm	755	NIES		
				ENVISAT	-1.52 ± 2.91 ppm	378	SCIAMACHY		
18	Various TCCON stations			GOSAT	-8.85 ± 4.75 ppm	62	SWIR L2 product version 01.xx	The old version with low accuracy and precision (neglected in calculations and figure)	I. Morino et al. 2011 [149] Y. Yoshida et al. 2013 [150]
			April 2009 to May 2011	GOSAT	-1.48 ± 2.09 ppm	567 NH 152 SH	-1.485±1.734 ppm NH -1.447±2.276 ppm SH	SWIR L2 product version 02.xx 719 observations	

19	Bialystok, Bremen, Orleans, Park falls, Lamont, Darwin, Wollongong	2009-2011	GOSAT	-0.20 ± 2.26 ppm	467 NH 110 SH	0.214±2.197 ppm NH -0.035±2.391 ppm SH	577 observations	A. J. Cogan et al. 2012 [151]
20	Bialystok, Orleans, Park Falls, Lamont, Darwin, Wollongong	April 2009 and July 2010	GOSAT	-0.05 ± 0.37 % -0.203 ± 2.654 ppm	759 NH 128 SH	-0.528±2.586 ppm NH 1.721±3.029 ppm SH	TANSO-FTS 887 observation	A. Butz et al. 2011 [152]

NH = Northern Hemisphere, SH = Sothern Hemisphere.

Table 1.A. 5 worldwide ground-based station.

No.	location	coordination	elevation *a.s.l: above sea level	period	instrument	note	reference
1	Bharati, the Indian Antarctic research station	69.24° S, 76.11° E	35m a.s.l*	austral summer (January–February) of 2016	Li-Cor CO2/H2O analyzer (model Li-840A)		Mahesh Patakothi et al. 2018 [92]
2	Bahir Dar and Hawassa	11°36′N, 37°23′E 07°15′N, 38°45′E	1786-1886m 1708 m a.s.l		Aeroqual Series 500 portable gas monitor and YuanTe SKY 2000-M4 handheld multi-gas detector	correlation coefficient between instrument was 0.986	Oluwasinaayomi Faith Kasim et al. 2018 [153]
3	Peterhof station (St. Petersburg, Russia)	59.88° N, 29.82° E		2009-2017	Fourier transform IR spectrometry (FTIR) using a Bruker 125HR	total error of 4.18 ± 0.02%, with 0.36 ± 0.06% and 4.16 ± 0.02% for random and systematic errors respectively	Virolainen Ya. A. 2018 [154]
4	Hefei, China	31°54′ N, 117°10′ E	29m a.s.l	July 2014-April 2016	Bruker IFS 125HR spectrometer and solar tracker InGaAs detector from July 2015	similar variation phase and seasonal amplitude with Tsukuba TCCON station	Wei Wang et al. 2017 [155]
5	Ny-Ålesund	78.92° N, 11.92° E		2005-2015	Bruker IFS 120HR FTIR spectrometer	lower sensitivity in the troposphere in comparison to TCCON (by a factor of 2)	Matthias Buschmann et al. 2016 [156]
6	Karlsruhe	49.094° N, 8.4336° E	133m a.s.l	3 February 2012-22 June 2012	EM27 spectrometer	commercial low-resolution (0.5 cm^{-1}) (FTS) agreement with Karlsruhe TCCON station, (0.12 ± 0.08) %	Gisi M. et al. 2012 [157]

7	China: Lin’an, Longfengshan, Shangdianzi, and Waliguan			January 2009 to December 2011	cavity ring-down spectroscopy systems (G1301, Picarro Inc.)	according to Chen et al., 2010; Crosson, 2008, this type of instrument is suitable for making precise measurement	S. X. Fang et al. 2014 [110]
8	Kitt Peak, Arizona	31.9° N, 111.6° W	2070 m a.s.l	1977-1995	Fourier transform spectrometer on the McMath telescope.	precisions better than 0.5% similar behavior to the Mauna Loa	Zhonghua Yang et al. 2002 [158]
9	Tsukuba, Meteorological Research Institute	36°04’ N, 140°07’ E	25m a.s.l	1986-1996	NDIR analyzer (Beckman model 864) from 1986-1992 NDIR analyzer (Beckman model 880) from 1992-1994		Hisayuki Yoshikawa Inoue and Hidekadzu Matsueda 1996 [159]
10	Mt. Cimone Station, Italy	44°11’ N, 10°42’ E	2165 m a.s.l	1979-1992	URAS-2T NDIR analyzer, from 1979 ULTRAMAT- 5E NDIR from 1988 URAS-3G NDIR (to control)	URAS-2T NDIR precision is ±0.3p.p.m.v. ULTRAMAT- 5E NDIR precision is ±0.1p.p.m.v.	V.Cundari et al. 1995 [160]
11	Izaña, Tenerife, Canary Islands	28°18’ N, 16°29’ W	2367 m a.s.l	1984-1988	Siemens Ultramat -3 NADIR	the samples were representative of free troposphere in the southern part of the North Atlantic because of the high altitude of the location	Beatriz Navascués et al. 1991 [161]
12	Amsterdam island	37°47’ S, 77°31’ E		1980-1989	non-dispersive infrared analyzer URAS 2T		A. Gaudry et al. 1991 [162]
13	La Jolla, California Mauna Loa, Hawaii Cape Kumukahi, Hawaii Fanning island and South pole	32.9° N, 117.3° W 19.5° N, 155.6° W 19.5° N, 154.8° W 3.9° N, 159.3° W 90°S, 59°E		March 1977-February 1982	non-dispersive infrared gas analyzer		Illem g. Mook and Marjan Koopmans 1983 [163]

14	Shetland Isles, Scotland	60.2°N, 1.2°W		1992–1996	Carle Series 400 gas chromatograph Finnigan MAT 252 mass spectrometer with MT Box-C gas preparationsystem	a part of CSIRO network	R.J. Francey et al. 1998 [164]
15	Schauinsland station, southwest Germany	47°55' N, 7°55' E	1205 m a.s.l	1972-2002	nondispersive infrared analysis (NDIR) Until August 1980,URAS-2 (Hartmann & Braun), from September 1980 until the end of 1993,Ultramat-3 (Siemens) and from 1994 onward with URAS-3 (Hartmann & Braun)	The accuracy of the data was estimated: better than ±1 ppm for the period 1972–1991 and better than ±0.5 ppm later on.	M. Schmidt et al. 2003 [165]
16	Kasprowy Wierch Kraków in southern Poland	49°14’N, 19°59’E 50°04’N, 19°55’E	1989m a.s.l 220 m a.s.l	1996-2006	Automated gas chromatographs (Hewlett Packard, Series 5890, with FID detector and Ni catalyst for conversion of CO2 to CH4 and Porapak Q column)		L. Chmura et al. 2008 [166]
17	Moscow to Khabarovsk			1997–2004	LI6262 gas analyzer (LICOR, United States)	mobile measurement at surface layer with the error of ±1 ppm at a CO2 concentration of 350 ppm. The intrinsic noise was 0.2 ppm	I. B. Belikov et al. 2006 [167]
18	ZOTTO international observatory, Krasnoyarsk krai, Russia	60° N, 90° E	114 m a.s.l	January 2006-December 2013	NDIR CO2 Analyzer (Siemens AG, Ultramat 6F) up to April 2007 EnviroSense 3000i gas-analyzing system (Picarro Inc., USA) from May 2009	using the tall tower (302 m) measurement error does not exeed 0.1 ppm	A. V. Timokhina et al. 2015 [168] E. A. Kozlova and A. C. Manning 2009 [169]
19	Cabauw	51.971° N, 4.927° E	-0.7m a.s.l	1992-2010	Siemens Ultramat NDIR 1992-2004 NDIR (LICOR 7000) after 2004	sampling in tall tower Siemens Ultramat NDIR resolution in the range of 0-500 ppm was 0.5 ppm	A. T. Vermeulen et al. 2011 [170]

20	Barrow (Alaska)	71.32° N, 156.61°W	11.00 m a.s.l	stablished in 1973	non-dispersive infrared analyzer		https://www.esrl.noaa.gov/gmd/obop/brw/
21	American Samoa	14.24°S, 170.56°W	42.00 m a.s.l	stablished in 1974	non-dispersive infrared analyzer		https://www.esrl.noaa.gov/gmd/obop/smo/ https://cdiac.ess-dive.lbl.gov/trends/co2/sio-sam.html
22	South Pole	90°S, 59°E	2,837 m a.s.l	stablished in 1957	non-dispersive infrared gas analyzer		https://www.esrl.noaa.gov/gmd/obop/spo/ Illem g. Mook and Marjan Koopmans 1983 [163]
23	Ascension Island (SH)	7.92°S, 14.33°W	10 m a.s.l	Available data from 22.05.2012-31.10.2018		TCCON station	https://tccondata.org/ https://tccon-wiki.caltech.edu/Main/TCCONSites
24	Anmeyondo (KR)	36.54°N, 126.33°E	30 m a.s.l	Available data from 02.02.2015-18.04.2018		TCCON station	https://tccondata.org/ https://tccon-wiki.caltech.edu/Main/TCCONSites
25	Bialystok (PL)	53.23°N, 23.025°E	180 m a.s.l	Available data from 01.03.2009-01.10.2018		TCCON station	https://tccondata.org/ https://tccon-wiki.caltech.edu/Main/TCCONSites

26	Bremen (DE)	53.10°N, 8.85°E	27 m a.s.l	Available data from 22.01.2010-23.08.2019	TCCON station	https://tccondata.org/ https://tccon-wiki.caltech.edu/Main/TCCONSites
27	Burgos	18.533°N, 120.650°E	35 m a.s.l	Available data from 03.03.2017-31.01.2020	TCCON station	https://tccondata.org/ https://tccon-wiki.caltech.edu/Main/TCCONSites
28	Caltech (US)	34.136°N, 118.127°W	230 m a.s.l	Available data from 20.09.2012-03.10.2020	TCCON station	https://tccondata.org/ https://tccon-wiki.caltech.edu/Main/TCCONSites
29	Darwin (AU)	12.42°S, 130.89°E 12.46°S, 130.93°E	30 m a.s.l 37 m a.s.l	Available data from 28.08.2005-31.01.2020	TCCON station	https://tccondata.org/ https://tccon-wiki.caltech.edu/Main/TCCONSites
30	Edwards (US)			Available data from 20.07.2013-03.10.2020	TCCON station	https://tccondata.org/ https://tccon-wiki.caltech.edu/Main/TCCONSites
31	East Trout Lake	54.35 °N, 104.99 °W	501.8 m a.s.l	Available data from 07.10.2016-06.09.2020	TCCON station	https://tccondata.org/ https://tccon-wiki.caltech.edu/Main/TCCONSites

32	Eureka (CA)	80.05°N, 86.42°W	610 m a.s.l	Available data from 24.07.2010-06.07.2020		TCCON station	https://tccondata.org/ https://tccon-wiki.caltech.edu/Main/TCCONSites
33	Four Corners (US)	36.80°N, 108.48°W	1643 m a.s.l	Available data from 16.03.2013-04.10.2013		TCCON station	https://tccondata.org/ https://tccon-wiki.caltech.edu/Main/TCCONSites
34	Garmisch (DE)	47.476°N, 11.063°E	740 m a.s.l	Available data from 16.07.2007-18.10.2019		TCCON station	https://tccondata.org/ https://tccon-wiki.caltech.edu/Main/TCCONSites
35	Hefei (PRC)	31.90°N, 118.67°E	29 m a.s.l	Available data from 18.09.2015-31.12.2016		TCCON station	https://tccondata.org/ https://tccon-wiki.caltech.edu/Main/TCCONSites
36	Indianapolis (US)	39.86°N, 86.00°W	270 m a.s.l	Available data from 23.08.2012-01.12.2012		TCCON station	https://tccondata.org/ https://tccon-wiki.caltech.edu/Main/TCCONSites
37	Izana (ES)	28.3°N, 16.5°W	2370 m a.s.l	Available data from 18.05.2007-02.11.2020		TCCON station	https://tccondata.org/ https://tccon-wiki.caltech.edu/Main/TCCONSites

38	Jet Propulsion Laboratory (US)	34.20°N, 118.175°W	390 m a.s.l	Available data from 31.07.2007-22.06.2008	TCCON station	https://tccondata.org/ https://tccon-wiki.caltech.edu/Main/TCCONSites
39	Jet Propulsion Laboratory (US)	34.20°N, 118.175°W	390 m a.s.l	Available data from 19.05.2011-14.05.2018	TCCON station	https://tccondata.org/ https://tccon-wiki.caltech.edu/Main/TCCONSites
40	Saga (JP)	33.24°N, 130.29°E	7 m a.s.l	Available data from 28.07.2011-04.08.2020	TCCON station	https://tccondata.org/ https://tccon-wiki.caltech.edu/Main/TCCONSites
41	Karlsruhe (DE)	49.10°N, 8.44°E	116 m a.s.l	Available data from 19.04.2010-31.10.2020	TCCON station	https://tccondata.org/ https://tccon-wiki.caltech.edu/Main/TCCONSites
42	Lauder (NZ)	45.04°S, 169.68°E	370 m a.s.l	Available data from 29.06.2004-09.12.2010	TCCON station	https://tccondata.org/ https://tccon-wiki.caltech.edu/Main/TCCONSites
43	Lauder (NZ)	45.04°S, 169.68°E	370 m a.s.l	Available data from 02.02.2010-31.10.2018	TCCON station	https://tccondata.org/ https://tccon-wiki.caltech.edu/Main/TCCONSites
44	Lauder (NZ)	45.04°S, 169.68°E	370 m a.s.l	Available data from 03.10.2018-31.07.2020	TCCON station	https://tccondata.org/ https://tccon-wiki.caltech.edu/Main/TCCONSites

45	Manaus (BR)	3.21°S, 60.59°W	50 m a.s.l	Available data from 01.10.2014-24.06.2015	TCCON station	https://tccondata.org/ https://tccon-wiki.caltech.edu/Main/TCCONSites
46	Nicosia	35.14°N, 33.38°E	185 m a.s.l	Available data from 31.08.2019-31.01.2020	TCCON station	https://tccondata.org/ https://tccon-wiki.caltech.edu/Main/TCCONSites
47	Lamont (US)	36.60°N, 97.48°W	320 m a.s.l	Available data from 06.07.2008-03.10.2020	TCCON station	https://tccondata.org/ https://tccon-wiki.caltech.edu/Main/TCCONSites
48	Orléans (FR)	47.97°N, 2.11°E	130 m a.s.l	Available data from 29.08.2009-18.09.2019	TCCON station	https://tccondata.org/ https://tccon-wiki.caltech.edu/Main/TCCONSites
49	Park Falls (US)	45.94°N, 90.27°W	440 m a.s.l	Available data from 02.06.2004-03.10.2020	TCCON station	https://tccondata.org/ https://tccon-wiki.caltech.edu/Main/TCCONSites
50	Paris (FR)	48.84°N, 2.35°E	60 m a.s.l	Available data from 23.09.2014-24.01.2020	TCCON station	https://tccondata.org/ https://tccon-wiki.caltech.edu/Main/TCCONSites

51	Réunion Island (RE)	20.90°S, 55.48°E	87 m a.s.l	Available data from 16.09.2011-18.07.2020	TCCON station	https://tccondata.org/ https://tccon-wiki.caltech.edu/Main/TCCONSites
52	Rikubetsu (JP)	43.45 °N, 143.77 °E	380 m a.s.l	Available data from 16.11.2013-30.09.2019	TCCON station	https://tccondata.org/ https://tccon-wiki.caltech.edu/Main/TCCONSites
53	Sodankylä (FI)	67.37°N, 26.63°E	188 m a.s.l	Available data from 16.05.2009-30.09.2020	TCCON station	https://tccondata.org/ https://tccon-wiki.caltech.edu/Main/TCCONSites
54	Ny Ålesund	78.9°N, 11.9°E	20 m a.s.l	Available data from 06.04.2014-15.09.2019	TCCON station	https://tccondata.org/ https://tccon-wiki.caltech.edu/Main/TCCONSites
55	Tsukuba (JP)	36.05°N, 140.12°E	30 m a.s.l	Available data from 04.08.2011-30.09.2019	TCCON station	https://tccondata.org/ https://tccon-wiki.caltech.edu/Main/TCCONSites
56	Wollongong (AU)	34.41°S, 150.88°E	30 m a.s.l	Available data from 26.06.2008-31.01.2020	TCCON station	https://tccondata.org/ https://tccon-wiki.caltech.edu/Main/TCCONSites
57	Zugspitze (DE)	47.42°N, 10.98°E	2960 m a.s.l	Available data from 24.04.2015-17.10.2019	TCCON station	https://tccondata.org/ https://tccon-wiki.caltech.edu/Main/TCCONSites

Table 1.A. 6 Tall towers in the NOAA Earth System Research Laboratory's Global Greenhouse Gas Reference Network [171].

No.	**Name**	**Location**	**Coordination**	**Surface Elevation**	**Intake Height**	**Carbon Dioxide Measurement Period**	**Note**
1	Argyle, Maine Tower (AMT)	Argyle, Maine	45.03° N, 68.68° W	50 m a.s.l.	12, 30, 107 m above ground	2003-ongoinssg	
2	Boulder Atmospheric Observatory (BAO)	Erie, Colorado	40.05° N, 105.01° W	1584 m a.s.l.	22, 100, 300 m above ground	2007–2016	Discontinued
3	Barrow Observatory (BRW)	Barrow, Alaska	71.323° N, 156.6114° W	11 m a.s.l.	16.46 m above ground	1971-ongoing	
4	WITN Tower (ITN)	Grifton, North Carolina	5.53° N, 77.38° W	9 m a.s.l.	51, 123, 496 m above ground	1992–1999	Discontinued
5	WLEF Tower (LEF)	Park Falls, Wisconsin	45.9451° N, 90.2732° W	472 m a.s.l.	1, 30, 76, 122, 244, 396 m above ground	2003-ongoing	
6	Mount Bachelor Observatory (MBO)	Mount Bachelor, Oregon	43.9775° N, 121.6861° W	2731 m a.s.l.	11 m above ground	2011-ongoing 2012-ongoing	
7	Mauna Loa Observatory (MLO)	Mauna Loa, Hawaii	19.5362° N, 155.5763° W	3397 m a.s.l.	40 m above ground	1969-ongoing	

8	South Carolina Tower (SCT)	Beech Island, South Carolina	33.406° N, 81.833° W	115 m a.s.l.	30, 61, 305 m above ground	2008-ongoing
9	American Samoa Observatory (SMO)	Tutuila Island, American Samoa	14.2474° S, 170.5644° W	42 m a.s.l.	18 m above ground	1972-ongoing
10	Shenandoah National Park (SNP)	Shenandoah National Park, Virginia	38.617° N, 78.35° W	1008 m a.s.l.	5, 10, 17 m above ground	2008-ongoing
11	South Pole Observatory (SPO)	South Pole, Antarctica	89.98° S, 24.8° W	2810 m a.s.l.	11 m above ground	1975-ongoing
12	West Branch, Iowa (WBI)	West Branch, Iowa	41.725° N, 91.353° W	242 m a.s.l.	31, 99, 379 m above ground	2007-ongoing
13	Walnut Grove, California (WGC)	Walnut Grove, California	38.265° N, 121.4911° W	0 m a.s.l.	30, 91, 483 m above ground	2007-ongoing
14	WKT Tower (WKT)	Moody, Texas	31.32° N, 97.33° W	251 m a.s.l.	30, 122, 457 m above ground	2003-ongoing

1.6 References

[1] V. Brovkin, S. Lorenz, T. Raddatz, T. Ilyina and I. Stemmler, “What was the source of the atmospheric CO2 increase during the Holocene?,” *Biogeosciences,* vol. 16, pp. 2543-2555, 2019.

[2] G. I. Pearman, D. Etheridge, F. d. Silva and P. J. Fraser, “Evidence of changing concentrations of atmospheric CO2, N2O and CH4 from air bubbles in Antarctic ice,” *Nature,* no. 320, pp. 248-250, 1986.

[3] Y. TianXiang, Z. LiLi, Z. M. Wei, W. YiFu and J. WILSON, “Space-and ground-based CO2 measurements: A review,” *Science China Earth Science,* vol. 59, no. 11, pp. 2089-2097, 2016.

[4] E. D. a. P. Tans, “Global Monitoring Laboratory,” NOAA/GML, 5 February 2022. [Online]. Available: www.esrl.noaa.gov/gmd/ccgg/trends/. [Accessed 09 January 2023].

[5] J. McElwain, I. Montañez, J. White, J. Wilson and C. Yiotis, “Was atmospheric CO2 capped at 1000 ppm over the past 300 million years?,” *Palaeogeography, Palaeoclimatology, Palaeoecology,* vol. 441, pp. 653-658, 2016.

[6] F. Goldberg, “Rate of Increasing Concentrations of Atmospheric Carbon Dioxide Controlled by Natural Temperature Variations,” *Energy and Environment,* vol. 19, no. 7, pp. 995-1011, 2008.

[7] M. S. a. V. Vajda, “Early Jurassic (late Pliensbachian) CO2 concentrations based on stomatal analysis of fossil conifer leaves from eastern Australia,” *Gondwana Research,* vol. 27, pp. 932-939, 2015.

[8] P. J. FRASER, G. I. PEARMAN and P. HYSON, “The Global Distribution of Atmospheric Carbon Dioxide 2. A Review of Provisional Background Observations, 1978-1980,” *Journal of Geophysical Research,* vol. 88, no. C6, pp. 3591-3598, 1983.

[9] e. Pierre Friedlingstein, “Global Carbon Budget 2019,” *Earth System Science Data,* vol. 11, pp. 1783-1838, 2019.

[10] X. J. a. Y. L. Yung, “Global Patterns of Carbon Dioxide Variability from Satellite Observations,” *Annual Review of Earth and Planetary Sciences,* vol. 47, pp. 225-245, 2019.

[11] “Carbon Cycle Greenhouse Gases,” NOAA, [Online]. Available: https://www.esrl.noaa.gov/gmd/ccgg/. [Accessed 02 2021].

[12] “TCCON,” [Online]. Available: https://tccondata.org/. [Accessed 22 05 2020].

[13] “CONTRAIL,” [Online]. Available: https://www.cger.nies.go.jp/contrail/index.html. [Accessed 02 2021].

[14] H. B. Singh, D. Jacob, L. Pfister and R. S. Hipskind, “INTEX-NA: Intercontinental Chemical Transport Experiment - North America,” 2002.

[15] “HIAPER Pole-to-Pole Observation,” NCAR Earth Observing Laboratory, [Online]. Available: https://www.eol.ucar.edu/field_projects/hippo-1. [Accessed 02 2021].

[16] “In-service Aircraft for a Global Observing System,” LAGOS, [Online]. Available: https://www.iagos.org/. [Accessed 02 2021].

[17] “Carbon in Arctic Reservoirs Vulnerability Experiment (CARVE),” NASA, [Online]. Available: https://carve.ornl.gov/. [Accessed 02 2021].

[18] “Ships Of Opportunity Program (SOOP) Data,” NCEI (NOAA National Centers for Environmental Information, 06 08 2020. [Online]. Available: https://www.ncei.noaa.gov/access/ocean-carbon-data-system/oceans/VOS_Program/. [Accessed 17 02 2021].

[19] T. Takahashi, S. C. Sutherland and A. Kozyr, “Global Surface pCO2 (LDEO) Database V2019,” NCEI (NOAA National Centers for Environmental Information), 2020. [Online]. Available:

https://www.ncei.noaa.gov/access/ocean-carbon-data-system/oceans/LDEO_Underway_Database/. [Accessed 17 02 2021].

[20] A. Sutton, C. Sabine, J. Mathis and A. Kozyr, “A high-frequency atmospheric and seawater pCO2 data set from 14 open ocean sites using a moored autonomous system,” Carbon Dioxide Information Analysis Center, Oak Ridge National Laboratory, US Department of Energy, Oak Ridge, Tennessee., 2014. [Online]. Available: https://www.ncei.noaa.gov/access/ocean-carbon-data-system/oceans/Moorings/ndp092.html. [Accessed 02 2021].

[21] G. Pan, Y. Xu and a. J. Ma, “The potential of CO2 satellite monitoring for climate governance: A review.,” *Journal of Environmental Management,* vol. 277, p. 111423, 2021.

[22] “Orbiting Carbon Observatory-3,” NASA, [Online]. Available: https://ocov3.jpl.nasa.gov/. [Accessed 02 2021].

[23] “Orbiting Carbon Observatory-2,” NASA, [Online]. Available: https://ocov2.jpl.nasa.gov/. [Accessed 02 2021].

[24] “GOSAT,” European Space Agency, [Online]. Available: https://earth.esa.int/eogateway/missions/gosat. [Accessed 02 2021].

[25] “TES Get Data,” NASA, [Online]. Available: https://tes.jpl.nasa.gov/data/. [Accessed 02 2021].

[26] “AIRS Atmospheric Infrared Sounder,” NASA, [Online]. Available: https://airs.jpl.nasa.gov/data/get-data/standard-data/. [Accessed 02 2021].

[27] “NOAA comprehensive large array-data stewardship system(class),” NOAA, [Online]. Available: https://www.avl.class.noaa.gov/saa/products/search?datatype_family=IASI. [Accessed 02 2021].

[28] “SciSat-1/ACE (Science Satellite/Atmospheric Chemistry Experiment),” eoPortal Directory, [Online]. Available: https://directory.eoportal.org/web/eoportal/satellite-missions/s/scisat-1. [Accessed 02 2021].

[29] “SCHIAMACHY,” [Online]. Available: https://www.sciamachy.org/. [Accessed 02 2021].

[30] W. D, T. GC, B. JF, W. RA and N. J, “The total carbon column observing network.,” *Philos Trans A Math Phys Eng Sci.,* vol. 369, pp. 2087-2112, 2011.

[31] P. S. Bakwin, P. P. Tans, C. Zhao, W. Ussler and E. Quesnell, “Measurements of carbon dioxide on a very tall tower,” *Tellus,* vol. 47B, pp. 535-549, 1995.

[32] P. S. BAKWIN, P. P. TANS, D. F. HURST and C. ZHAO, “Measurements of carbon dioxide on very tall towers: Results of the NOAA/CMDL program,” *Tellus B,* vol. 50, no. 5, pp. 401-415, 1998.

[33] “Measuring & Analyzing Greenhouse Gases: Behind the Scenes,” NOAA, [Online]. Available: https://www.esrl.noaa.gov/gmd/ccgg/behind_the_scenes/towers.html. [Accessed February 2021].

[34] W. Bischof, “Carbon Dioxide Measurements from Aircraft,” *Tellus,* vol. 22, no. 5, pp. 545-549, 1970.

[35] Y. Hou, S. Wang, Y. Zhou, F. Yan and J. Zhu, “Analysis of the carbon dioxide concentration in the lowest atmospheric layers and the factors affecting China based on satellite observations,” *International Journal of Remote Sensing,* vol. 34, no. 6, pp. 1981-1994, 2012.

[36] Y. O. a. R. IMASU, “CO2 Retrieval Using Thermal Infrared Radiation Observation by Interferometric Monitor for Greenhouse Gases (IMG) Onboard Advanced Earth Observing Satellite (ADEOS),” *Journal of the Meteorological Society of Japan,* vol. 94, no. 6, 2016.

[37] D. Wunch, P. O. Wennberg, G. Osterman, B. Fisher and B. Naylor, “Comparisons of the Orbiting Carbon Observatory-2 (OCO-2) XCO2 measurements with TCCON,” *Atmospheric Measurement Techniques,* vol. 10, p. 2209–2238, 2017.

[38] Y. BI, Q. WANG, Z. YANG, J. CHEN and W. BAI, “Validation of Column-Averaged Dry-Air Mole Fraction of CO2 Retrieved from OCO-2 Using Ground-Based FTS Measurements,” *Journal of Meteorological Research,* vol. 32, pp. 433-443, 2018.

[39] Y. M. Timofeyev, I. A. Berezin, Y. A. Virolainen, M. V. Makarova, A. V. Polyakov and A. V. Poberovsk, “Spatial–Temporal CO2 Variations near St. Petersburg Based on Satellite and Ground-Based Measurements,” *Atmospheric and Oceanic Physics,* vol. 55, no. 1, pp. 59-64, 2019.

[40] L. Wu, O. Hasekamp, H. Hu, J. a. d. Brugh, J. Landgraf, A. Butz and I. Aben, “Full-physics carbon dioxide retrievals from the Orbiting Carbon Observatory-2 (OCO-2) satellite by only using the 2.06 μm band,” *Atmospheric Measurement Techniques,* vol. 12, pp. 6049-6058, 2019.

[41] C. W. O'Dell, A. Eldering, P. O. Wennberg, D. Crisp and M. R. Gunson, “Improved retrievals of carbon dioxide from Orbiting Carbon Observatory-2 with the version 8 ACOS algorithm,” *Atmospheric Measurement Techniques,* vol. 11, pp. 6539-6576, 2018.

[42] L. Ailin, H. Ge, G. Wei, Y. Jie and X. Chengzhi, “Comparison of Global XCO2 Concentrations From OCO-2 With TCCON Data in Terms of Latitude Zones,” *IEEE Journal of Selected Topics in Applied Earth Observations and Remote Sensing,* vol. 10, no. 6, pp. 2491-2498, 2017.

[43] L. A., H. G., X. H., G. W. and Z. T., “Evaluation of XCO2 from OCO-2 Lite File Product compared with TCCON data,” *International Geoscience and Remote Sensing Symposium (IGARSS),* vol. 8127389, pp. 2070-2073, 2017.

[44] X.-. X.-C. Qin, T. Nakayama, Y. Matsumi, M. Kawasaki, R. Imasu, I. Morino and Y. Tanaka, “Observation of column-averaged molar mixing ratios of carbon dioxide in Tokyo,” *Atmospheric Environment: X,* vol. 2, p. 100022, 2019.

[45] L. Dan-dan, H. Yin-bo, C. Zhen-song, L. Xing-ji and S. Yu-song, “Analysis of Total Columns of Greenhouse Gas Based on Direct Observation and Comparison with Satellite Data in Hefei,” *Acta Photonica Sinica,* vol. 49, no. 3, 2020.

[46] V. A. Velazco, N. M. Deutscher, I. Morino, O. Uchino and B. Bukosa, “Satellite and ground-based measurements of XCO2 in a remote semiarid region of Australia,” *Earth System Science Data,* vol. 11, pp. 935-946, 2019.

[47] N. Eguchi, Y. Yoshida, I. Morino, N. Kikuchi and T. Saeki, “SEASONAL VARIATIONS OF GREENHOUSE GAS COLUMN-AVERAGED DRY AIR MOLE FRACTIONS RETRIEVED FROM SWIR SPECTRA OF GOSAT TANSO-FTS,” *IGRASS,* no. 10.1109/IGARSS.2011.6049986., pp. 3542-3545, 2011.

[48] H. Ohyama, S. Kawakami, T. Tanaka, I. Morino and O. Uchino, “Observations of XCO2 and XCH4 with ground-based high-resolution FTS at Saga, Japan, and comparisons with GOSAT products,” *Atmospheric Measurement Techniques,* vol. 8, pp. 5263-5276, 2015.

[49] N. V. Rokotyan, R. Imasu, V. I. Zakharov, K. G. Gribanov and M. Y. Khamatnurova, “The Amplitude of the CO2 Seasonal Cycle in the Atmosphere of the Ural Region Retrieved from Ground□Based and Satellite Near□IR Measurements,” *Atmospheric and Oceanic Optics,* vol. 28, no. 1, pp. 49-55, 2015.

[50] E. L. Yates, K. Schiro, M. Lowenstein, E. J. Sheffner and L. T. Iraci, “Carbon Dioxide and Methane at a Desert Site—A Case Study at Railroad Valley Playa, Nevada, USA,” *Atmosphere,* vol. 2, pp. 702-714, 2011.

[51] Y. Qu, C. Zhang, D. Wang, P. Tian, W. Bai and X. Zhang, “Comparison of atmospheric CO2 observed by GOSAT and two ground stations in China,” *International journal of remote sensing,* vol. 34, no. 11, pp. 3938-3946, 2014.

[52] Z.-C. Zeng, L. Lei, K. Strong, D. B. A. Jones and L. Guo, “Global land mapping of satellite-observed CO2 total columns using spatio-temporal geostatistics,” *International Journal of Digital Earth,* vol. 10, no. 4, pp. 426-456, 2017.

[53] D. Wunch, P. O. Wennberg, G. C. Toon, B. J. Connor, B. Fisher, G. B. Osterman and C. Frankenberg, “A Method for Evaluating Bias in Global Measurements of CO2 Total Columns from Space.,” *Atmospheric Chemistry and Physics,* vol. 23, pp. 12317-12337, 2011.

[54] Y. Yuan, R. Sussmann, M. Rettinger, L. Ries, H. Petermeier and A. Menzel, “Comparison of Continuous In-Situ CO2 Measurements with Co-Located Column-Averaged XCO2 TCCON/Satellite Observations and CarbonTracker Model Over the Zugspitze Region,” *Remote sensing,* vol. 11, p. 2981, 2019.

[55] M. Buchwitz, M. Reuter, O. Schneising, W. Hewson and R. Detmers, “Global satellite observations of column-averaged carbon dioxide and methane: The GHG-CCI XCO2 and XCH4 CRDP3 data set,” *Remote Sensing of Environment,* vol. 203, pp. 276-295, 2017.

[56] M. Buchwitz, M. Reuter, O. Schneising, H.Boesch and S. Guerlet, “The Greenhouse Gas Climate Change Initiative (GHG-CCI): Comparison and quality assessment of near-surface-sensitive satellite-derived CO2 and CH4 global data sets,” *Remote Sensing of Environment,* vol. 162, pp. 344-362, 2015.

[57] R. Miao, N. Lu, L. Yao, Y. Zhu, J. Wang and J. Sun, “Multi-Year Comparison of Carbon Dioxide from Satellite Data with Ground-Based FTS Measurements (2003–2011),” *Remote Sens.,* vol. 5, no. 7, pp. 3431-3456, 2013.

[58] Y. M. A. a. F. A. Jr, “The characteristics of tropospheric CO2 retrieved by AIRS, GOSAT and IASI in East Asia,” *Disaster Advances,* vol. 8, no. 9, pp. 1-13, 2015.

[59] L. Zhang, X. Zhang and H. Jiang, “Accuracy comparisons of AIRS, SCIAMACHY and GOSAT with ground-based data based on global CO2 concentration,” *21st International Conference on Geoinformatics, Kaifeng,* pp. 1-5, 2013.

[60] Linjing Zhang, H. Jiang and X. Zhang, “Comparison analysis of the global carbon dioxide concentration column derived from SCIAMACHY, AIRS, and GOSAT with surface station measurements,” *International Journal of Remote Sensing,* vol. 36, no. 5, pp. 1406-1423, 2015.

[61] X. Jiang, D. Crisp, E. T. Olsen, S. S. Kulawik and C. E. Miller, “CO2 annual and semiannual cycles from multiple satellite retrievals and models,” *Earth and Space Science,* vol. 3, no. 2, pp. 78-87, 2016.

[62] R. M., B. M., S. O., N. S. and B. H., “Ensemble-based satellite-derived carbon dioxide and methane column-averaged dry-air mole fraction data sets (2003-2018) for carbon and climate applications,” *Atmospheric Measurement Techniques,* vol. 13, no. 2, pp. 789-819, 2020.

[63] M. Buchwitz, M. Reuter, O. Schneising, S. Noël and B. Gier, “Computation and analysis of atmospheric carbon dioxide annual mean growth rates from satellite observations during 2003–2016,” *Atmospheric Chemistry and Physics,* vol. 18, pp. 17355-17370, 2018.

[64] B. Dils, B. M., R. M., S. O. and B. H., “The Greenhouse Gas Climate Change Initiative (GHG-CCI): comparative validation of GHG-CCI SCIAMACHY/ENVISAT and TANSO-FTS/GOSAT CO2 and CH4 retrieval algorithm products with measurements from the TCCON,” *Atmospheric Measurement Techniques,* vol. 7, pp. 1723-1744, 2014.

[65] W. Kim, J. Kim, Y. Jung, H. Boesch and H. Lee, “Retrieving XCO2 from GOSAT FTS over East Asia Using Simultaneous Aerosol Information from CAI,” *remote sensing,* vol. 8, no. 994, 2016.

[66] D. Yang, Y. Liu, Z. Cai, J. Deng, J. Wang and X. Chen, “An advanced carbon dioxide retrieval algorithm for satellite measurements and its application to GOSAT observations,” *Science Bulletin,* vol. 60, no. 23, pp. 2063-2066, 2015.

[67] L. H., O. C. W., B. S., B. H. and C. F., “Does GOSAT capture the true seasonal cycle of carbon dioxide?,” *Atmospheric Chemistry and Physics,* vol. 15, pp. 13023-13040, 2015.

[68] Y. YI, Y. LIU, Z. CAI, S. FANG, D. YANG, Y. WANG, M. LIANG, B. YAO, Q. MA and M. WANG, “Measuring and comparing in-situ CO2 and CO profiles with satellite observations and model data,” *Atmospheric and Oceanic Science Letters,* vol. 12, no. 6, pp. 444-450, 2019.

[69] J. M. Tadić and a. A. M. Michalak, “On the effect of spatial variability and support on validation of remote sensing observations of CO2,” *Atmospheric Environment,* vol. 132, pp. 309-316, 2016.

[70] E. S. Maddy, C. D. Barnet, M. Goldberg, C. Sweeney and X. Liu, “CO2 retrievals from the Atmospheric Infrared Sounder: Methodology and validation,” *Journal of Geophysical Research, Atmospheres,* vol. 113, no. D11301, 2008.

[71] C. M., C. Barnet, E. T. Olsen, L. Chen and E. Maddy, “On the determination of atmospheric minor gases by the method of vanishing partial derivatives with application to CO2.,” *Geophysical Research Letters,* vol. 322, no. 22, 2005.

[72] A. B. Uspensky, A. V. Kukharsky, S. V. Romanov and a. A. N. Rublev, “Monitoring the Carbon Dioxide Mixing Ratio in the Troposphere and the Methane Total Column over Siberia According to the Data of the AIRS and IASI IR Sounders,” *Atmospheric and Oceanic Physics,* vol. 47, no. 9, pp. 1097-1103, 2011.

[73] A. V. K. a. A. B. Uspenskii, “Determination of Tropospheric Mean Carbon Dioxide Concentration from Satellite High Spectral Resolution IR-Sounder Data,” *Russian Meteorology and Hydrology,* vol. 34, no. 4, pp. 292-211, 2009.

[74] F. Christian, K. S. S., W. S. C., C. Frédéric and D. Bruce, “Using airborne HIAPER Pole-to-Pole Observations (HIPPO) to evaluate model and remote sensing estimates of atmospheric carbon dioxide,” *Atmospheric Chemistry and Physics,* vol. 16, pp. 7867-7878, 2016.

[75] S. Glen., “StatisticsHowTo.com,” [Online]. Available: https://www.statisticshowto.com/pooled-standard-deviation/.

[76] NASA, “GES DISK,” NASA, [Online]. Available: https://disc.gsfc.nasa.gov/datasets/OCO2_L2_Lite_FP_9r/summary. [Accessed 2019-2021].

[77] “User's guide,” NASA, [Online]. Available: https://docserver.gesdisc.eosdis.nasa.gov/public/project/OCO/OCO2_DUG.V9.pdf. [Accessed 12 November 2021].

[78] NASA, [Online]. Available: https://ocov2.jpl.nasa.gov/observatory/instrument/. [Accessed 11 November 2021].

[79] “GES DISK documentation,” NASA, [Online]. Available: https://docserver.gesdisc.eosdis.nasa.gov/public/project/OCO/OCO2_OCO3_B10_DUG.pdf.

[80] G. I. Pearman, P. Hyson and P. J. Fraser, “The global distribution of atmospheric carbon dioxide: 1. Aspects of observations and modeling,” *Journal of Geophysical Research,* vol. 88, no. C6, pp. 3581-3590, 1983.

[81] K. T. a. C. Guillemot, “The total mass of the atmosphere,” *Journal of Geophysical Research,* 1994.

[82] K. E. T. A. L. SMITH, “The Mass of the Atmosphere: A Constraint on Global Analyses,” *JOURNAL OF CLIMATE,* vol. 18, pp. 864-875, 2005.

[83] A. Müller, H. Tanimoto, T. Sugita, T. Machida and S.-i. Nakaoka, “New approach to evaluate satellite derived XCO2 over oceans by integrating ship and aircraft observations,” *Atmospheric Chemistry and Physics,* vol. 21, p. 8255–8271, May 2021.

[84] P. Prasad, S. Rastogi and a. R. P. Singh, “Study of satellite retrieved CO2 and CH4 concentration over India.,” *Advances in Space Research,* vol. 54, no. 9, pp. 1933-1940, 2014.

[85] F. S. Rossi, G. A. d. A. Santos, L. d. S. Maria, T. Lourençoni, P. T. Deoti, J. L. Della-Silva and J. W. O. J. e. al., “Carbon dioxide spatial variability and dynamics for contrasting land uses in central

Brazil agricultural frontier from remote sensing data.," *Journal of South American Earth Sciences,* vol. 116, p. 103809, 2022.

[86] M. N. Patil, T. Dharmaraj, R. T. Waghmare, S. Singh, P. Pithani, R. Kulkarni, N. Dhangar, D. Siingh, G. R. Chinthalu, R. Singh and S. Ghude, "Observations of carbon dioxide and turbulent fluxes during fog conditions in north India," *Journal of Earth System Science,* vol. 129, no. 51, 2020.

[87] Y. Li, C. Zhang and F. Li, "Influence of thin cirrus clouds on the short-wave infrared satellite observation of atmospheric CO2," *Optik - International Journal for Light and Electron Optics,* vol. https://doi.org/10.1016/j.ijleo.2019.164140, 2019.

[88] Z. Siabi, S. Falahatkar and S. J. Alavi, "Spatial distribution of XCO2 using OCO-2 data in growing seasons," *Journal of Environmental Management,* vol. 224, pp. 110-118, 2019.

[89] I. V., P. Nina, P. V., Z. Alexander and L. M., "Atmospheric Concentration of Carbon Dioxide at Tiksi and Cape Baranov Stations in 2010-2017," *Russian Meteorology and Hydrology,* vol. 44, no. 4, pp. 291-299, 2019.

[90] S. J. A.-j. a. O. T. Al-Taai, "IMPACT OF CARBON DIOXIDE CONCENTRATIONS ON ATMOSPHERIC TEMPERATURE CHANGES OVER IRAQ AND SOME NEIGHBORING COUNTRIES," *Plant Archives,* vol. 19, pp. 1450-1456, 2019.

[91] I. Xueref-Remy, E. Dieudonné, C. Vuillemin, M. Lopez and C. Lac, "Diurnal, synoptic and seasonal variability of atmospheric CO2 in the Paris megacity area," *Atmospheric Chemistry and Physics,* vol. 18, pp. 3335-3362, 2018.

[92] M. Pathakoti, S. Gaddamidi, B. Gharai, P. S. Syamala and P. V. N. Rao, "Influence of meteorological parameters on atmospheric CO2 at Bharati, the Indian Antarctic research station," *Polar Research,* vol. 37, p. 1442072, 2018.

[93] S. Yin, X. Wang, H. Tani, X. Zhang and G. Zhong, "Analyzing temporo-spatial changes and the distribution of the CO2 T concentration in Australia from 2009 to 2016 by greenhouse gas monitoring satellites," *Atmospheric Environment,* vol. 192, pp. 1-12, 2018.

[94] N. Bie, L. Lei, Z. Zeng, B. Cai and S. Yang, "Regional uncertainty of GOSAT XCO2 retrievals in China: quantification and attribution," *Atmospheric Measurement Techniques,* vol. 11, pp. 1251-1272, 2018.

[95] H. Ge, X. Hao, G. Wei, L. Jiqiao and D. Juan, "Feasibility Study on Measuring Atmospheric CO2 in Urban Areas Using Spaceborne CO2-IPDA LIDAR," *Remote Sensig,* vol. 10, p. 985, 2018.

[96] X. Jiang, A. Kao, A. Corbett, E. Olsen and T. Pagano, "Influence of Droughts on Mid-Tropospheric CO2," *remote sensing,* vol. 9, no. 852, 2017.

[97] S. M. Mousavi, S. Falahatkar and M. Farajzadeh, "Assessment of seasonal variations of carbon dioxide concentration in Iran using GOSAT data," *Natural Resources Forum,* vol. 41, pp. 83-91, 2017.

[98] S. Falahatkar, S. M. Mousavi and M. Farajzadeh, "Spatial and temporal distribution of carbon dioxide gas using GOSAT data over IRAN," *Environmental Monitoring and Assessment,* vol. 189, no. 627, 2017.

[99] L. L. Ping, Z. Hui, H. ZhongHua, C. BoFeng and Y. ShaoYuan, "Assessment of atmospheric CO2 concentration enhancement from anthropogenic emissions based on satellite observations," *Chinese Journal,* vol. 62, no. 25, pp. 2941-2950, 2017.

[100] J. K. Hedelius, S. Feng, C. M. Roehl, D. Wunch and P. W. Hillyard, "Emissions and topographic effects on column CO2 (X CO2) variations, with a focus on the Southern California Megacity," *Journal of Geophysical Research: Atmospheres,* vol. 122, pp. 7200-7215, 2017.

[101] K. Esteki, N. Prakash, Y. Li, C. Mu and K. Du, "Seasonal Variation of CO2 Vertical Distribution in the Atmospheric Boundary Layer and Impact of Meteorological Parameters.," *International Journal of Environmental Research,* vol. 11, no. 19, 2017.

[102] C. Pan, X. Zhu, N. Wei, X. Zhu and Q. She, "Spatial variability of daytime CO2 concentration with landscape structure across urbanization gradients, Shanghai, China," *Climate Research,* vol. 69, pp. 107-116, 2016.

[103] T. E. Taylor, C. W. O'Dell, C. Frankenberg, P. T. Partain and H. Q. Cronk, "Orbiting Carbon Observatory-2 (OCO-2) cloud screening algorithms: validation against collocated MODIS and CALIOP data," *Atmospheric Measurement Techniques,* vol. 9, pp. 973-989, 2016.

[104] Y. Jung, J. Kim, W. Kim and H. B. H. Lee, "Impact of Aerosol Property on the Accuracy of a CO2 Retrieval Algorithm from Satellite Remote Sensing," *remote sensing,* vol. 8, no. 322, 2016.

[105] Hernández-Paniagua, L. I.Y., C. D., F. K.C. and F. R.E., "Diurnal, seasonal, and annual trends in atmospheric CO2 at southwest London during 2000–2012: Wind sector analysis and comparison with Mace Head, Ireland," *Atmospheric Environment,* vol. 105, pp. 138-147, 2015.

[106] M. Liu, J. Wu, X. Zhu, H. He, W. Jia and W. Xiang, "Evolution and variation of atmospheric carbon dioxide concentration over terrestrial ecosystems as derived from eddy covariance measurements," *Atmospheric Environment,* vol. 114, pp. 75-82, 2015.

[107] L. Xiao-Man, C. Xue-Ling and H. Fei, "Gradient characteristics of CO2 concentration and flux in Beijing urban area part I: Concentration and virtual temperature," *Chinese Journal of Geophysics-Chinese Edition,* vol. 58, no. 5, pp. 1502-1512, 2015.

[108] L. G. a. L. Varone, "Atmospheric carbon dioxide concentration variations in Rome: relationship with traffic level and urban park size," *Urban Ecosyst,* vol. 17, pp. 501-511, 2014.

[109] M.-S. PARK, S. J. JOO and S.-U. PARK, "Carbon Dioxide Concentration and Flux in an Urban Residential Area in Seoul, Korea," *ADVANCES IN ATMOSPHERIC SCIENCES,* vol. 31, pp. 1101-1112, 2014.

[110] S. X. Fang, L. X. Zhou, P. P. Tans, P. Ciais and M. Steinbacher, "In situ measurement of atmospheric CO2 at the four WMO/GAW stations in China," *Atmospheric Chemistry and Physics,* vol. 14, pp. 2541-2554, 2014.

[111] Q. XC, L. LP, K. M, M. O, T. K, Z. ZC and Z. B., "Retrieval and analysis of atmospheric XCO2 using ground-based spectral observation.," *Guang Pu Xue Yu Guang Pu Fen Xi/Spectroscopy and Spectral Analysis,* vol. 34, no. 7, pp. 1729-1735, 2014.

[112] Y. Li, J. Deng, C. Mu, Z. Xing and K. Du, "Vertical distribution of CO2 in the atmospheric boundary layer: Characteristics and impact of meteorological variables," *Atmospheric Environment,* vol. 91, pp. 110-117, 2014.

[113] M. G. a. D. Lewicka-Szczebak, "One-year spatial and temporal monitoring of concentration and carbon isotopic composition of atmospheric CO2 in a Wrocław (SW Poland) city area," *Applied Geochemistry,* vol. 35, pp. 7-13, 2013.

[114] L. Yan-li, M. Chao, D. Junjun, Z. Shuhui and D. Ke, "Near surface atmospheric CO2 variations in autumn at suburban Xiamen, China," *Huanjing Kexue/Environmental Science,* vol. 34, pp. 2018-2024, 2013.

[115] B. C. a. W. Kuttler, "Path-integrated measurements of carbon dioxide in the urban canopy layer," *Atmospheric Environment,* vol. 46, 2012.

[116] J. Wu, D. Guan, F. Yuan, H. Yang, A. Wang and C. Jin, "Evolution of atmospheric carbon dioxide concentration at different temporal scales recorded in a tall forest," *Atmospheric Environment,* vol. 61, pp. 9-14, 2012.

[117] M. A. García, M. L. Sánchez and I. A. Pérez, “Differences between carbon dioxide levels over suburban and rural sites in Northern Spain,” *Environmental Science and Pollution Research,* vol. 19, pp. 432-439, 2012.

[118] Y. H., S. W., Y. Z., F. W., W. L. and Y. H., “Variations of Greenhouse Gas carbon dioxide concentration over the Chinese mainland based on Satellite and Background Measurements.,” *Disaster Advances,* vol. 5, pp. 871-876, 2012.

[119] A. R. a. G. Bostrom, “Measurements of carbon dioxide in an Oregon metropolitan region,” *Atmospheric Environment,* vol. 45, no. 5, pp. 1138-1144, 2011.

[120] R. P. a. P. ER, “Toward understanding the behaviour of carbon dioxide and surface energy fluxes in the urbanized semi-arid Salt Lake Valley, Utah, USA,” *Atmos Environ,* vol. 45, pp. 73-84, 2011.

[121] I. Xueref-Remy, C. Messager, D. Filippi, M. Pastel and P. Nedelec, “Variability and budget of CO2 in Europe: analysis of the CAATER airborne campaigns – Part 1: Observed variability,” *Atmospheric Chemistry and Physics,* vol. 11, pp. 5655-5672, 2011.

[122] K. Wang, H. Jiang, X. Zhang and G. Zhou, “Analysis of spatial and temporal variations of carbon dioxide over China using SCIAMACHY satellite observations during 2003–2005,” *International Journal of Remote Sensing,* vol. 32, no. 3, pp. 815-832, 2011.

[123] Y. Yoshida, Y. Ota, N. Eguchi, N. Kikuchi and K. Nobuta, “Retrieval algorithm for CO2 and CH4 column abundances from short-wavelength infrared spectral observations by the Greenhouse gases observing satellite,” *Atmospheric Measurement Techniques,* vol. 4, pp. 717-734, 2011.

[124] C. Sirignano, R. E. M. Neubert, C. Rödenbeck and H. A. J. Meijer, “Atmospheric oxygen and carbon dioxide observations from two European coastal stations 2000–2005: continental influence, trend changes and APO climatology,” *Atmospheric Chemistry and Physics,* vol. 10, pp. 1599-1615, 2010.

[125] G. Ch., F. H., H. P., L. M. G., L. J. and W. H., “Airborne in-situ measurements of vertical, seasonal and latitudinal distributions of carbon dioxide over Europe,” *Atmospheric Chemistry and Physics,* vol. 8, pp. 6395-6403, 2008.

[126] K. George, L. H. Ziska, J. A. Bunce and B. Quebedeauxb, “Elevated atmospheric CO2 concentration and temperature across an urban–rural transect,” *Atmospheric Environment,* vol. 41, no. 35, pp. 7654-7665, 2007.

[127] I. Aben, O. Hasekamp and W. Hartmann, “Uncertainties in the space-based measurements of CO2 columns due to scattering in the Earth's atmosphere,” *Journal of Quantitative Spectroscopy and Radiative Transfer,* vol. 104, no. 3, pp. 450-459, 2007.

[128] Y. Y., T. J., Z. Y. and C. S., “Study on the atmospheric stabilities and the thickness of atmospheric mixed layer during recent 15 years in Shanghai.,” *Sci Meteorol Sin,* vol. 26, pp. 536-541, 2006.

[129] L. G. a. L. Varone, “Daily and seasonal variation of CO2 in the city of Rome in relationship with the traffic volume,” *Atmospheric Environment,* vol. 39, pp. 2619-2624, 2005.

[130] H. A. Nasrallah, R. C. B. Jr., S. M. Madic and L. Al-Ansari, “Temporal variations in atmospheric CO2 concentrations in Kuwait City, Kuwait with comparisons to Phoenix, Arizona, USA,” *Environmental Pollution,* vol. 121, pp. 301-305, 2003.

[131] P. CHAMARD, F. THIERY, A. D. SARRA, L. CIATTAGLIA and L. D. SILVESTRI, “Interannual variability of atmospheric CO2 in the Mediterranean: measurements at the island of Lampedusa,” *Tellus,* vol. 55B, pp. 83-93, 2003.

[132] W. Yuesi, W. Changke, G. Xueqing, L. Guangren and H. Yao, “Trend, seasonal and diurnal variations of atmospheric CO2 in Beijing,” *Chinese Science Bulletin,* vol. 47, no. 24, pp. 2050-2055, 2002.

[133] E. A. Wentz, P. Gober, R. C. B. Jr. and T. A. Day, "Spatial Patterns and Determinants of Winter Atmospheric Carbon Dioxide Concentrations in an Urban Environment," *Annals of the Association of American Geographers,* vol. 92, no. 1, pp. 15-28, 2002.

[134] R. J. Engelen, A. S. Denning, K. R. Gurney and G. L. Stephen, "Global observations of the carbon budget 1. Expected satellite capabilities for emission spectroscopy in the EOS and NPOESS eras," *JOURNAL OF GEOPHYSICAL RESEARCH,* vol. 106, no. D17, pp. 20055-20068, 2001.

[135] T. J. Conway, P. Tans, L. S. Waterman, K. W. Thoning, K. A. Masarie and R. H. Gammon, "Atmospheric carbon dioxide measurements in the remote global troposphere, 1981-1984," *Tellus B: Chemical and Physical Meteorology,* vol. 40, no. 2, pp. 81-115, 1988.

[136] "Global Monitoring Laboratory," NOAA, [Online]. Available: https://www.esrl.noaa.gov/gmd/dv/site/index.php?program=ccgg. [Accessed 10 February 2021].

[137] D. A., G. H., H. J., J. C., L. P. and J. H., "Temporal and distribution characteristic of CO2 concentration over China based on GOSAT satellite data," *Yaogan Xuebao/Journal of Remote Sensing,* vol. 24, no. 3, pp. 319-325, 2020.

[138] Y. Kong, B. Chen and S. Measho, "Spatio-Temporal Consistency Evaluation of XCO2 Retrievals from GOSAT and OCO-2 Based on TCCON and Model Data for Joint Utilization in Carbon Cycle Research," *Atmosphere,* vol. 10, p. 354, 2019.

[139] L. Wu, O. Hasekamp, H. Hu, J. Landgraf and A. Butz, "Carbon dioxide retrieval from OCO-2 satellite observations using the RemoTeC algorithm and validation with TCCON measurements," *Atmospheric Measurement Techniques,* vol. 11, pp. 3111-3130, 2018.

[140] V. A. Velazco, I. Morino, O. Uchino, A. Hori and M. Kie, "TCCON Philippines: First Measurement Results, Satellite Data and Model Comparisons in Southeast Asia," *Remote Sensing,* vol. 9, no. 1228, 2017.

[141] L. Ailin, G. Wei, H. Ge and X. Chengzhi, "Comparison of Satellite-Observed XCO2 from GOSAT, OCO-2, and Ground-Based TCCON," *Remote Sensing,* vol. 9, p. 1033, 2017.

[142] I. Chisa, I. Ryoichi, B. Andrey, Y. Tatsuya and Y. Yukio, "Validation of GOSAT SWIR XCO2 and XCH4 Retrieved by PPDF-S Method and Comparison with Full Physics Method," *Scientific online letters on the atmosphere: SOLA,* vol. 13, pp. 168-173, 2017.

[143] L. A., G. W. and H. G., "OCO-2 XCO2 validation using TCCON data," *International Geoscience and Remote Sensing Symposium (IGARSS),* vol. 7729210, pp. 830-833, 2016.

[144] S. Kulawik, D. Wunch, C. O'Dell, C. Frankenberg and M. Reuter, "Consistent evaluation of ACOS-GOSAT, BESD-SCIAMACHY, CarbonTracker, and MACC through comparisons to TCCON," *Atmospheric Measurement Techniques,* vol. 9, pp. 683-709, 2016.

[145] D. Anjian, Y. Tao, C. Tianhai, G. Xingfa, Z. Fengjie and G. Hong, "Intercomparison of Carbon Dioxide Products Retrieved from GOSAT Short-Wavelength Infrared Spectra for Three Years (2010–2012)," *Atmosphere,* vol. 7, no. 109, 2016.

[146] M. Zhou, B. Dils, P. Wang, R. Detmers and Y. Yoshida, "Validation of TANSO-FTS/GOSAT XCO2 and XCH4 glint mode retrievals using TCCON data from near-ocean sites," *Atmospheric Measurement Techniques,* vol. 9, pp. 1415-1430, 2016.

[147] J. Heymann, M. Reuter, M. Hilker, M. Buchwitz and O. Schneising, "Consistent satellite XCO2 retrievals from SCIAMACHY and GOSAT using the BESD algorithm," *Atmospheric Measurement Techniques,* vol. 8, pp. 2961-2980, 2015.

[148] Z. Miao, Z. Xing-Ying, L. Rui-Xia and H. Lie-Qun, "A study of the validation of atmospheric CO2 from satellite hyper spectral remote sensing," *Advances in Climate Change Research,* vol. 5, pp. 131-135, 2014.

[149] I. Morino, O. Uchino, M. Inoue, Y. Yoshida and T. Yokota, “Preliminary validation of column-averaged volume mixing ratios of carbon dioxide and methane retrieved from GOSAT short-wavelength infrared spectra,” *Atmospheric Measurement Techniques,* vol. 4, pp. 1061-1076, 2011.

[150] Y. Yoshida, N. Kikuchi, I. Morino, O. Uchino and S. Oshchepkov, “Improvement of the retrieval algorithm for GOSAT SWIR XCO2 and XCH4 and their validation using TCCON data,” *Atmospheric Measurement Techniques,* vol. 6, pp. 1533-1547, 2013.

[151] J. C. A., H. Boesch, J. P. R., L. Feng and I. P. P., “Atmospheric carbon dioxide retrieved from the Greenhouse gases Observing SATellite (GOSAT): Comparison with ground-based TCCON observations and GEOS-Chem model calculations,” *Journal of Geophysical Research, Atmospheres,* vol. 117, no. D21, 2012.

[152] B. A., G. S., H. O., S. D. and G. A., “Toward accurate CO2 and CH4 observations from GOSAT,” *GEOPHYSICAL RESEARCH LETTERS,* vol. 38, no. L14812, 2011.

[153] O. F. Kasim, M. W. Abshare, T. E. Mukuna and B. Wahab, “Land Use and Ambient Air Quality in Bahir Dar and Hawassa, Ethiopia,” *Air, Soil and Water Research,* vol. 11, pp. 1-10, 2018.

[154] Y. A. Virolainen, “METHODICAL ASPECTS OF THE DETERMINATION OF CARBON DIOXIDE IN ATMOSPHERE USING FTIR SPECTROSCOPY,” *Journal of Applied Spectroscopy,* vol. 85, no. 3, 2018.

[155] W. Wang, Y. Tian, C. Liu, Y. Sun and W. Liu, “Investigating the performance of a greenhouse gas observatory in Hefei, China,” *Atmospheric Measurement Techniques,* vol. 10, pp. 2627-2643, 2017.

[156] M. Buschmann, N. M. Deutscher, V. Sherlock, M. Palm, T. Warneke and J. Notholt, “Retrieval of xCO2 from ground-based mid-infrared (NDACC) solar absorption spectra and comparison to TCCON,” *Atmospheric Measurement Techniques,* vol. 9, pp. 577-585, 2016.

[157] G. M., H. F., D. S., B. T., S. A. and K. A., “XCO2-measurements with a tabletop FTS using solar absorption spectroscopy,” *Atmospheric Measurement Techniques,* vol. 5, no. 11, pp. 2969-2980, 2012.

[158] Z. Yang, G. C. Toon, J. S. Margolis and P. O. Wennberg, “Atmospheric CO2 retrieved from ground-based near IR solar spectra,” *GEOPHYSICAL RESEARCH LETTERS,* vol. 29, no. 9, 2002.

[159] I. H. Y. a. H. Matsueda, “Variations in Atmospheric CO2 at the Meteorological Research Institute, Tsukuba, Japan,” *Journal Of Atmospheric Chemistry,* vol. 23, pp. 137-161, 1996.

[160] V. CUNDARI, T. COLOMBO and L. CIATTAGLI, “Thirteen Years of Atmospheric Carbon Dioxide Measurements at Mt. Cimone Station, Italy.,” *Il Nuovo Cimento,* vol. 18C, no. 1, pp. 33-47, 1995.

[161] B. NAVASCUES, C. Jardin and C. RUS, “Carbon dioxide observations at Izaña baseline station, Tenerife (Canary Islands): 1984-1988,” *Tellus,* vol. 43B, pp. 118-125, 1991.

[162] G. A., M. P., P. G., B. G., A. B., A. Jegou and L. G., “Non-seasonal variations of atmospheric CO2 concentrations at Amsterdam Island,” *Tellus B: Chemical and Physical Meteorology,* vol. 43B, pp. 136-143, 1991.

[163] M. W. G., M. Koopmans, A. F. Carter and C. D. Keeling, “Seasonal, Latitudinal, and Secular Variations in the Abundance and Isotopic Ratios of AtmosphericCarbon Dioxide 1. Results From Land Stations,” *Journal of Geophysical Research,* vol. 88, no. C15, pp. 10915-10933, 1983.

[164] R. J. Francey, L. P. Steele, R. L. Langenfelds, C. E. Allison and L. N. Cooper, “Atmospheric carbon dioxide and its stable isotope ratios, methane, carbon monoxide, nitrous oxide and hydrogen from Shetland Isles,” *Atmospheric Environment,* vol. 32, no. 19, pp. 3331-3338, 1998.

[165] S. M., G. R., S. H. and L. I., “The Schauinsland CO2 record: 30 years of continental observations and their implications for the variability of the European CO2 budget,” *Journal of Geophysical Research Atmospheres,* vol. 108, no. 19, 2003.

[166] L. Chmura, K. Rozanski, J. M. Necki, M. Zimnoch, A. Korus and M. Pycia, “Atmospheric Concentrations of Carbon Dioxide in Southern Poland: Comparison of Mountain and Urban Environments,” *Polish J. of Environ. Stud.,* vol. 6, pp. 859-867, 2008.

[167] I. B. Belikov, C. A. M. Brenninkmeijer, N. F. Elansky and A. A. Ral’ko, “Methane, Carbon Monoxide, and Carbon Dioxide Concentrations Measured in the Atmospheric Surface Layer over Continental Russia in the TROICA Experiments,” *Atmospheric and Oceanic Physics,* vol. 42, no. 1, pp. 46-59, 2006.

[168] A. V. Timokhina, A. S. Prokushkin, A. A. Onuchin, A. V. Panov and G. B. Kofman, “Long-term Trend in CO2 Concentration in the Surface Atmosphere over Central Siberia,” *Russian Meteorology and Hydrology,* vol. 40, no. 3, pp. 186-190, 2015.

[169] E. A. a. A. C. M. Kozlova, “Methodology and calibration for continuous measurements of biogeochemical trace gas and O2 concentrations from a 300-m tall tower in central Siberia.,” *Atmospheric Measurement Techniques,* vol. 2, no. 1, pp. 205-220, 2009.

[170] A. T. Vermeulen, A. Hensen, M. E. Popa, W. C. M. v. d. Bulk and a. P. A. C. Jongejan, “Greenhouse gas observations from Cabauw Tall Tower (1992–2010),” *Atmospheric Measurement Techniques,* vol. 4, pp. 617-644, 2011.

[171] “In-Situ Measurement Program,” NOAA, [Online]. Available: https://gml.noaa.gov/ccgg/insitu/. [Accessed 02 2021].

2 CHAPTER 2: Assessment of an Innovative Ejector Plant for Port Sediment Management

ABSTRACT

The necessity of removing deposited materials from the seabed is common and has been done since the earliest settlements along coasts and rivers. The most widely used method of sediment deposit removal is dredging, which is a reliable and widespread technology. Although dredging restores the desired water depth, it does not have any impact on the reasons for sedimentation, therefore it cannot guarantee navigability over time. In addition, dredging operation has a huge environmental impact and it is relatively expensive. Therefore, market demand for alternative sustainable sediment removal technology is growing. In this chapter, an innovative technology which is called the ejector plant is investigated to assess the effectiveness of guaranteeing a minimum water depth over time at the port entrance at Marina of Cervia (Italy). This demo plant is the first industrial-scale ejector demo plant that has been installed and operated since June 2019. This system is designed to remove continuously the sediments which are naturally settling in a certain area and cause navigability problems. The focus of this study is on a three-year analysis of bathymetries from 2017 to 2020 at the port inlet before and after the ejector demo plant installation. In addition, metocean data are considered to define the possible net impact of the ejector plant. The assessment of effectiveness is carried out based on the variation in the water depth which is calculated based on the bathymetry data and using QGIS. It is found that in the period from January to April 2020, the water depth in the area of influence of the ejectors increased by 0.72 mm/day, while in the whole port inlet area a decrease of 0.95 mm/day was calculated. The estimated variation of volume in this period ranges from 245 to 750 m^3.

Keywords:

ejectors; sediment transport rate; port sediment management; effectiveness assessment

2.1 Introduction

Anthropogenic activities in the coastal area affect significantly waves, currents, and sediment transport pattern. Especially, extreme wave-induced currents and sediment transport paces can be seen near ports and influence recreational and commercial activities. The accumulated sediments lead to navigation problems inside the channel on the one hand and cause erosional effects on the leeside coasts on the other. Thus, harbours need frequent maintenance dredging to remove the accumulated sediments [1]. Dredging is a consolidated and mature technology but has considerable weaknesses [2, 3, 4, 5]. Dredging impacts the marine environment, as a result, contributes to the mobility and diffusion of pollutants present in the accumulated sediments. Furthermore, it becomes an obstacle for navigation during its operational phases. For the determination of the timing and number of maintenance dredging, periodic hydrographic surveys of the harbour area are required. Since maintenance dredging is usually executed on an as-needed basis, periodic surveys become a necessary tool to properly schedule the work [6]. Moreover, for the estimation of the removed sediment volume bathymetries are surveyed before and after dredging. In other words, dredging assists the measurement of the dredged material, which is usually defined by a contract.

Considering the high carbon dioxide emission of dredging the research questions are:
-Is there any reliable technology as an alternative to dredging?
-How the alternative technology performance can be approved?
-Do the natural phenomena affect the result?
-Is the proposed technology sustainable?

Various technologies have been developed over the past years as alternative methods of dredging. Bianchini et al. [7] He classifies alternative solutions of dredging into three categories: (i) anti-sedimentation structures, (ii) remobilizing sediment systems, and (iii) sand by-passing plants. Anti-sedimentation structures reduce significantly the volume of sediment which should be removed from harbour inlets, though present environmental troubles and still sediment removal is necessary [8]. Remobilizing sediment systems lift and separate the grains from the seabed by means of the injection of water or the movement of mechanical devices such as dredger propellers. An important advantage of water injection dredging is its low cost and less environmental impact compared with traditional dredging, which leads to wide application of this technology [9]. However, environmental problems due to the lack of resuspended sediment control require further investigation [10, 11], Sand by-passing plants have limited environmental impacts, but the problem is its high installation costs and often uncertain operational costs.

An innovative sand by-passing technology tested in the framework of the LIFE MARINAPLAN PLUS and STIMARE projects [12, 13, 14], which is based on ejector technology. Ejector technology provides the opportunity to keep the designed draft of the entrance channel over time through the continuous removal of settling sediments. By proper sediment management, it is possible to eventually produce benefits by counteracting neighbouring erosion processes. The ejector which is shown in Figure 2. 1 is an open jet pump (which does not have a closed suction chamber and mixing throat) with a converging section instead of a diffuser and a series of nozzles positioned circularly around the ejector. The diameter and whole length of ejector are around 250 mm, and 400 mm, respectively. Each ejector is located on the seabed and transfer sediments by transferring momentum from a high-speed primary water jet flow to a secondary flow which is a mixture of sediment and. The water-sediment mixture is conveyed via a pipeline and discharged to an area far from the port inlet, where it is not an obstacle for navigation. Both water inlet and outlet pipelines are DN80 spiral tubes (external diameter of around 90 mm). according to the preliminary test performed in 2017 [14], it is known that with a primary water input flowrate of approximately 27 m^3/h, a working pressure of 2.4 bar, and a 60-meter discharge pipeline, it is possible to transfer of about 2 m^3/h sediment at the discharge pipeline while using a water pump with the power consumption of about 3.5 kW. At this condition, the whole discharge flowrate of one ejector is about 34 m^3/h of water–sediment mixture, or approximately peak sediment concentration of about 6% (volume). Each ejector has specific influence radius and can work on a limited circular area which is created by the pressurized water outgoing from the central and circular nozzles. It is possible to manage the seabed level and maintain the path suitable for navigation by integration of ejectors in series and parallel.

This technology is reliable because it is based on the jet pumps which have been applied since the 1970s for coastal applications. The ejector technology has been invented and tested in 2001 at the University of Bologna. The first experimental plant was installed and tested in 2005 at the port of Riccione (Italy). The second experimental plant was installed in 2012 [15, 16] in Portoverde Marina (Italy). Both installations have been installed at port inlet and were designated to manage sand. The third experimental plant was in 2018 in Cattolica (Italy), which was the first time that the ejectors were applied for the silt and clay sediments management and installed in a river channel [17].

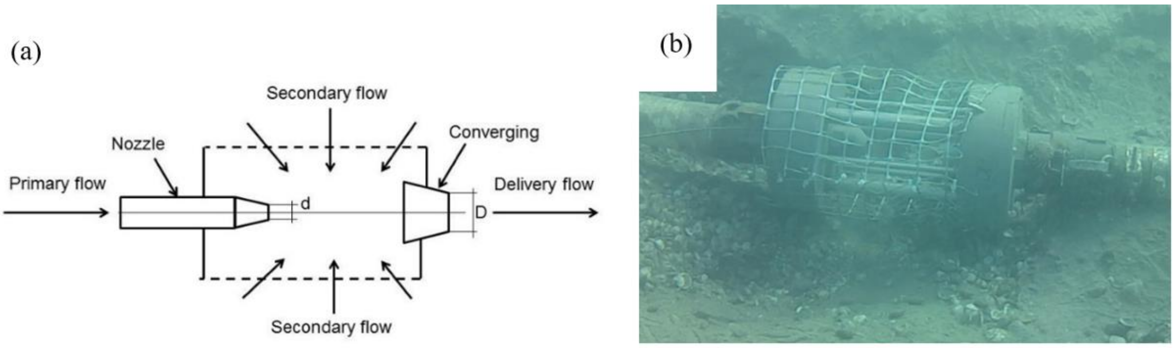

Figure 2. 1 (**a**) Sketch of the ejector *[14]* and (**b**) underwater picture of the ejector in operation.

An ejector demo plant has been installed at the port inlet of the Marina of Cervia (Italy) and operated from June 2019 to September 2020.

The aim of this chapter is to assess the ejector demo plant effectiveness, in other words, to define the ability of successful maintaining of the navigability at the port entrance over time. The novelty of the approach which is used in this study is related to the methodology applied to evaluate the impact of the ejector demo plant on both water-depth and sediment volume changes at the harbour entrance. The benefit of ejector system in comparison to dredging is the possibility of continuous monitoring the effect over a long period while for dredging it is necessary to compare bathymetries of the interested area before and after sediment removal to determine the impacts. Thus, natural sediment transport should be considered in the effectiveness assessment. Sediment transport prediction is very complex, and accurate phase of calibration and validation based on measurements is required, in addition, a suitable sediment transport model driven by reliable input data of waves and currents, initial bathymetry, sediment characteristics, etc. is needed. Several pieces of literature are available which provide useful examples [18, 19, 20, 21, 22]. However, the analysis of effectiveness of a continuous working sand by-passing system has never been investigated, and in previous studies the by-passed amount of sediment has been always evaluated starting from dredging needs [23]. In this study comparison of water-depth and sediment volume changes over time is performed, during the periods before and after ejector demo plant installation, through the analysis of bathymetries and metocean data. For this purpose, the sediment transport pace in the area of Cervia port inlet was assessed by using the bathymetries analysis in the last 3 years. In addition, the assessment of 3-year metocean climate on the Cervia site was used and discussed together with the bathymetric information. Furthermore, the operational period of the ejector demo plant is compared with the two previous years, from June 2017 to June 2019. The effectiveness of the demo plant is evaluated based on the different operation and control strategies.

2.2 Description of the Ejector Demo Plant

2.2.1 Description of the Study Site: Cervia, North Italy

Cervia harbour is located in the coast of Emilia-Romagna region, Italy (Figure 2. 2). It was designed along an artificial canal to convey the salt produced in the near salt flats. Thus, the harbour played a very important role in the past by interconnecting the land and the maritime markets. Maintenance dredging have been used since the first half of nineteenth century. In 1970s local municipality decided to modernize the existing infrastructure and redesigned the harbour.

The area of Marina of Cervia currently is approximately 43,000 m^2 with a capacity of around 300 berths. A further lengthening of the docks (20 m for the southern dock and 40 m for the northern dock) was planned and constructed in 2009 by the municipality to prevent coast advancement and port inlet sedimentation.

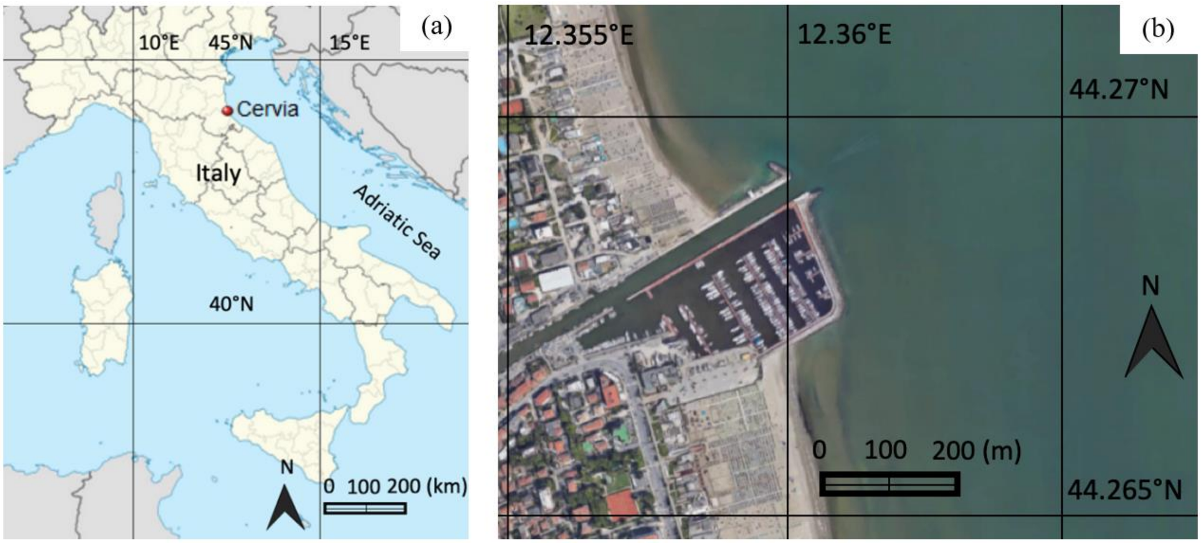

Figure 2. 2 Cervia position (**a**) and harbour aerial picture of the study area (**b**).

Sediment handling through dredger propellers, that is the remobilizing sediment technique in which dredger propellers are used to remobilize the sediment, and Traditional dredging have been still planned and periodically operated at the port inlet [14]. In the period 2009–2015, the removed sediment was approximately more than 17,000 m^3 per year. The cost of dredging was EUR 1 million, i.e., a weighted average cost of EUR 8.31 per dredged cubic meter of sediment. In addition, the cost of propeller operation was around EUR 350,000, almost once a year. The physical-chemical characterization of the sediment indicates that, at the port inlet, the sediment is mainly sand (97%), and the specific weight is 1.9 g/mL.

The total annual longshore sediment transport in the area offshore Cervia port is estimated to be equal to zero [24]. Which means that the Cervia port area can be considered as a convergence point for the annual longshore sediment transport, with the convergence point position being affected by annual wave climate. As in all the Northern Adriatic Sea, the wave climate is characterized by severe storms mainly generated by north-easterly winds, called Bora, even if Sirocco, south-easterly winds, might have relevant seasonal impacts [25, 26], the latter generally causes the highest surge levels [27]. Details on the wave buoy can be found at [28]. Figure 2. 3 shows the wave roses of the annual distribution of the significant wave height (a) and the peak period (b) versus the mean wave directions at the buoy. It shows: (i) the most energetic waves, up to 4.0 m in height, propagating from the sector 50–60° N; (ii) the most frequent conditions, with wave heights up to 1.0 m, coming from 90° N; (iii) the high-wave periods with values ranging from 9 to 11 s, coming from 90° N; (iv) the most frequent values range from 5 to 7 s.

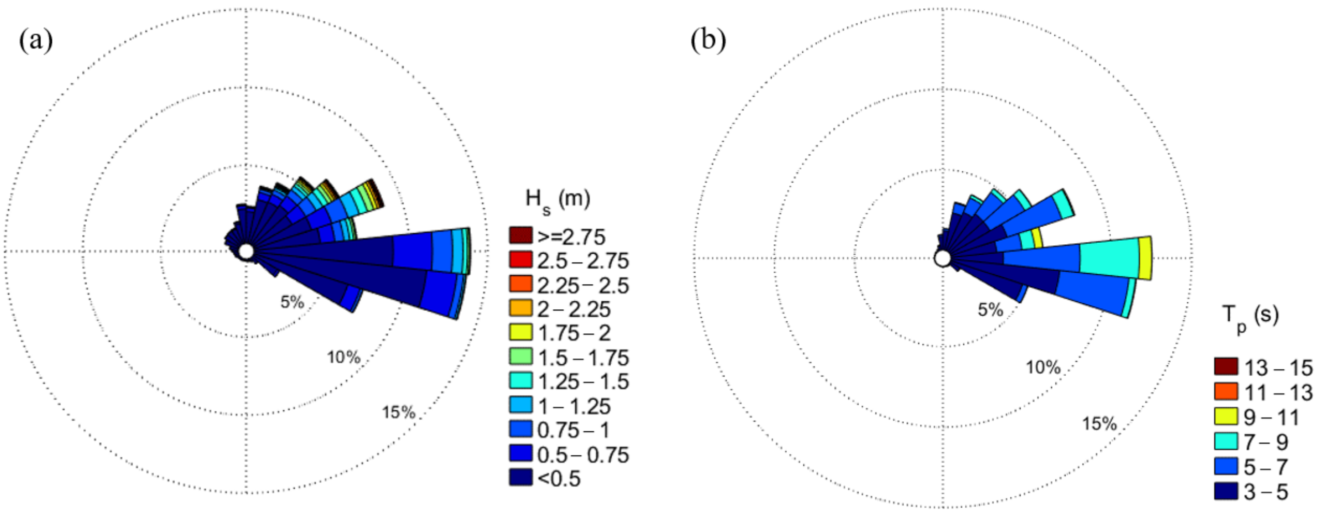

Figure 2. 3 Wave rose from the Nausicaa buoy in the period 2010–2020: polar distribution of the significant wave height (**a**) and peak period (**b**) [29]..

2.2.2 The Ejector Demo Plant of Cervia

The ejector demo plant in Cervia was tested from 13 June of 2019 as a possible alternative solution of the port sedimentation problem. The main objective of this demo plant was guaranteeing navigability at the port entrance while operating. This plant includes 10 ejectors located at the port entrance, as shown in Figure 2. 4 in green boundary. In- and out-flow pipelines laying on the seabed, which deliver the water and water-sediment mixture, respectively. Discharge pipelines convey sediments and water to a location at the south of the port entrance channel.

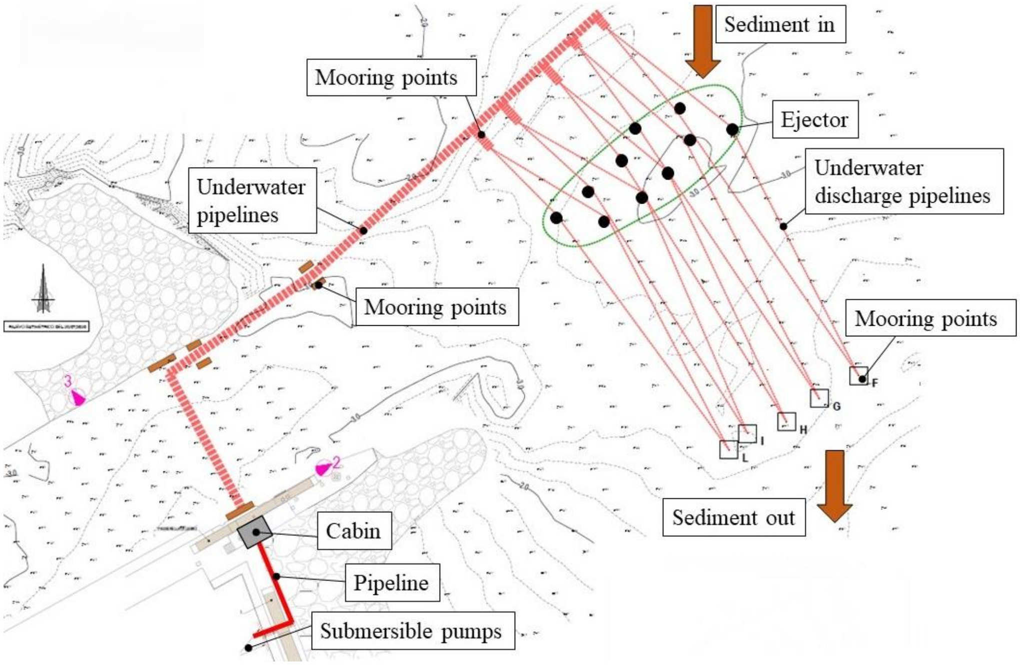

Figure 2. 4 Location of ejectors in the demo plant of Cervia.

The Cervia plant includes a fully automated and remotely accessible pumping station. There are two submersible pumps, each one is allocated to five ejectors. The pumped water flowrate is controlled by an inverter, while electrovalves are used to control the flowrate of each ejector. It is possible to use an air compressor to inject compressed air in the line to identify the positions of the ejectors on the seabed. The total installed power is around 80 kW. To relate plant operation with sea weather conditions a meteorological station installed which measure wind speed and direction. When wind speed becomes higher than the the predefined threshold, the water flowrate feeding the ejectors is set at the maximum value (approximately 30 m^3/h per ejector) to guarantee a sufficient sediment suction and transfer capacity.

2.3 Materials and Methods

2.3.1 Ejector Demo Plant Operation and Monitoring

Cervia's ejector demo plant was operated continuously in the period between June 2019 to September 2020, according to the objective of the LIFE MARINAPLAN PLUS project, the monitoring of performance and impacts produced [14] for a minimum 15-month operation. Ejector demo plant operation was divided to five phases which is shown in Figure 2. 5. At the first and second phases, the ejector demo plant was operated with a lower load, 25% and 50%, respectively, and manual control; these strategies were considered to limit pressure and power consumption, since some demo plant devices showed lower performances than the declaration of the suppliers. At the third and fourth phases, demo plant operated at the full load. However, at these two phases there was a growing problem related to mussels (Mytilus galloprovincialis) fouling in the pipes and filters. The performance of the demo plant was significantly affected by fouling, since a reduced water flowrate was pumped for the ejectors, and a higher pressure was needed. As a result, dramatically higher power was required. This is the reason that only 2 ejectors were in operation in the fifth phase. Therefore, only the bathymetric survey related to the period from June 2019 (before ejector demo plant operation) to April 2020 have been considered and analysed to investigate the effectiveness of the ejector demo plant. The bathymetries after May 2020 refer to the demo plant in operation with only two ejectors and are not comparable with the others.

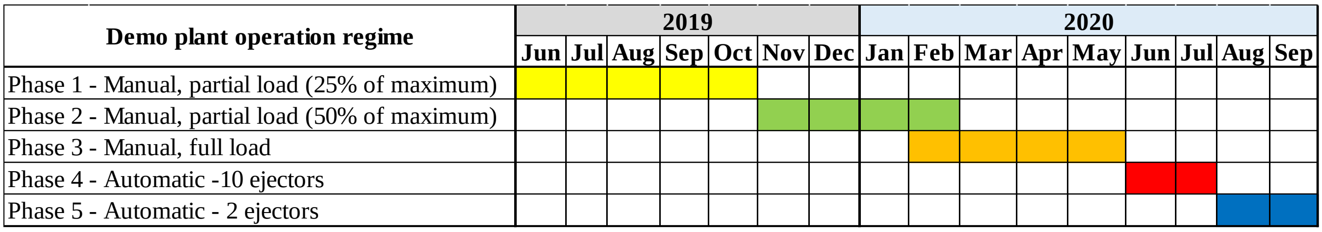

Demo plant operation regime	**2019**							**2020**								
	Jun	**Jul**	**Aug**	**Sep**	**Oct**	**Nov**	**Dec**	**Jan**	**Feb**	**Mar**	**Apr**	**May**	**Jun**	**Jul**	**Aug**	**Sep**
Phase 1 - Manual, partial load (25% of maximum)	🟨	🟨	🟨	🟨	🟨											
Phase 2 - Manual, partial load (50% of maximum)						🟩	🟩	🟩	🟩							
Phase 3 - Manual, full load									🟧	🟧	🟧	🟧				
Phase 4 - Automatic -10 ejectors													🟥	🟥		
Phase 5 - Automatic - 2 ejectors															🟦	🟦

Figure 2. 5 Classification by phases of the ejector demo plant operation in Cervia.

2.3.2 Analysis of Bathymetries: Water Depth and Sediment Volume Variation over Time

The analysis of the sediment transport at the port entrance was carried out over 3 years, from June 2017 to June 2020 for two periods: (i) with propeller operation and dredging (2017–2019) and (ii) during the operation of ejectors (2019–2020). The chosen periods are characterized by similar wave climates as shown in the frequency tables in Appendix 2.A. All the bathymetries collected was provided by the Municipality of Cervia and carried out through a digital hydrographic ultrasound system (Hydrotrac model, manufactured by Odom Hydrographic Systems, Baton Rouge, Louisiana, U.S.) with narrow emission cone, with the resulting error estimated as not more than 3 cm. The mean water level is the water depths reference.

Table 2. 1 provides information about 10 bathymetries (see Appendix 2.B) considered for the aim of the study, including timeframe and the relationship with sediment movement method, i.e., dredging, propellers, and ejector demo plant operations.

The provided bathymetries by the Municipality of Cervia include information about the water depth and the corresponding coordination in AutoCAD files format. QGIS 3.14 built-in Python is used to generate a model. TIN interpolation is used since it is more useful for elevation. To have more accurate result the area is divided to the cells with 5 m dimensions. The X and Y coordinate numbers are in the Project Coordinate Reference System (CRS) of WGS 84 (EPSG:4326) and the chosen unit is meters. In all the bathymetries, a common area can be identified (Figure 2. 6). This common area is defined by comparing all available bathymetries.

Table 2. 1 Bathymetries considered in the analysis for the period June 2017–April 2020.

Bathymetry ID	Date	Note
01	13 June 2017	Realized after dredging (2200 m^3 of removed sediments) and 5 days of propellers operation completed in April–June 2017
02	28 December 2017	
03	7 April 2018	
04	11 May 2018	Realized after 5 days of propeller operation, completed in April 2018
05	10 October 2018	
06	10 April 2019	Realized after 2.5 days of propeller operation and dredging (20,000 m^3 of removed sediments), completed in January–April 2019
07	12 June 2019	Realized one day before the ejector demo plant was put into in operation
08	6 September 2019	Ejector demo plant in operation (phase 1, see Figure 2. 5)
09	9 January 2020	Ejector demo plant in operation (phase 2, see Figure 2. 5)
10	30 April 2020	Ejector demo plant in operation (phase 3, see Figure 2. 5)

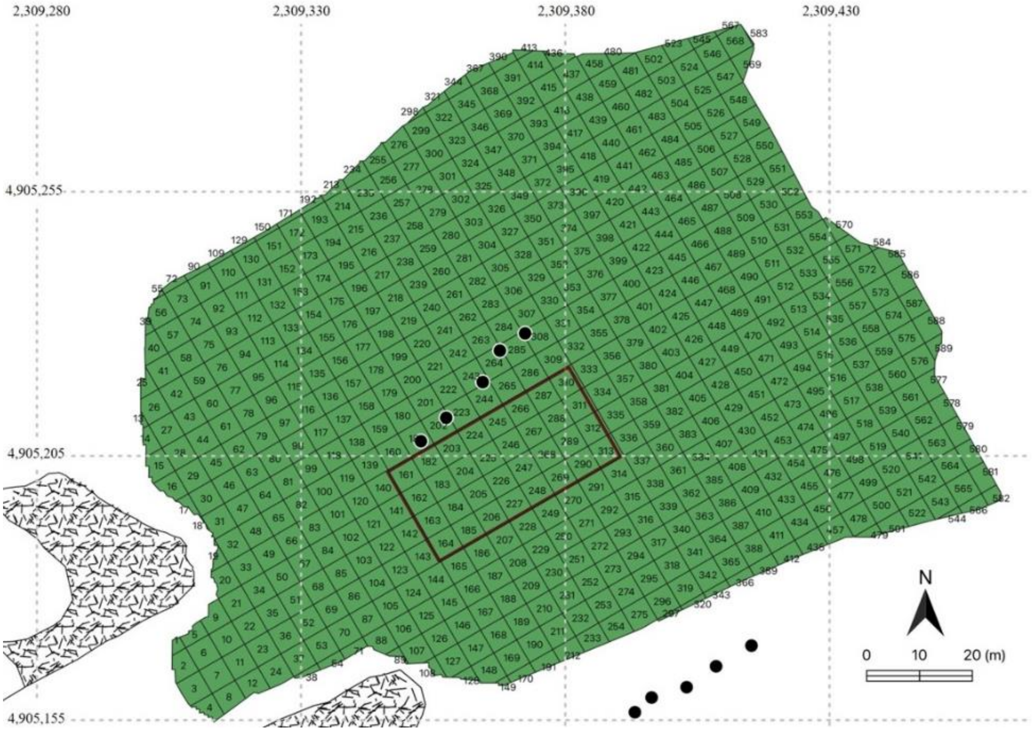

Figure 2. 6 Grids in the common area of the analysed bathymetries. The box identifies the area primarily impacted by ejector operation. The black dots represent the mooring points of inlet (north) and outlet (south) ejectors' pipes.

The point water depth measurements in the common area are present in all analysed bathymetry. Cells determination and interpolation was necessary, because comparing water depth variation at each measured point of the available bathymetries is rather impossible due to the relatively low accuracy in measured point. The whole area of common region is approximately 12,150 m^2. The size of the cell (5 × 5 m) is compatible with the area of the influence of one ejector. There is a red in Figure 2. 6

which shows the area directly impacted by ejector demo plant operation, which is composed of 32 cells and the area is 800 m^2. The black dots represent the mooring points of the inlet (north) and outlet (south, outside the surveyed area) ejectors' pipes (see also Figure 2. 4).

QGIS built-in Python is used to calculate the average water depth and volume for each cell at each bathymetry. The base level was assumed to be −7 m which is only for computing purposes. After calculation, it is possible to compare water depth and volume change over time by considering subsequent bathymetries. In case of the period related to dredging and/or propeller operation, after each operation the relative bathymetry was considered as the baseline for the following ones.

2.3.3 Analysis of 3-Year Metocean Climate on the Cervia Site

According to Aguzzi et al. [24] the annual net longshore sediment transport in the area offshore of the port of Cervia is estimated to be zero, in addition, sea storms are the most contributor to driving forces leading to sediment transport and coastal changes; Thus, it is important to identify each single sea storm to be able to define the impact of ejectors on the port sediment management in Cervia. According to the studies including the information about the sea storm in the port Cervia [30, 31, 29] a sea storm is defined for the storm which the wave height is higher than 1.5 m (the chosen threshold value) and remaining for at least 6 h over this height. Two storms are considered as separate if the wave height decays below the threshold for 3 or more consecutive hours.

According to Pellegrini et al. [29] the total energy E of each storm can be calculated using Eq.2. 1, which means through the integration of the significant height of the wave H_s for the duration of the storm (dur):

$$E = \int_{dur} H_s^2 dt \qquad \text{Eq.2. 1}$$

The sea storm is classified based on Dolan et al. study [32], which is shown in Table 2. 2, it includes the energy classification scale. This classification is done only to provide the opportunity of comparison of the periods in which the sea storm characterization is similar. For this purpose, some assumptions are made: (i) the longshore sediment transport can be considered constant in the area and (ii) the higher the storm energy registered in a certain period, the lower the contribution to sedimentation or erosion of longshore sediment transport. These assumptions are made based on Pellegrini et al. [29] study.

Table 2. 2 Energy-based classification of the sea storm.

Class	Storm Energy (m^2 h)
I—weak	$E \leq 58.4$
II—moderate	$58.4 < E \leq 127.9$
III—significant	$127.9 < E \leq 389.7$
IV—severe	$389.7 < E \leq 706.9$
V—extreme	$E > 706.9$

Table 2. 3 which is extracted from Pellegrini et al. [29] study includes a list and characteristics of the identified sea storms occurring in the period 2017–2020, which is under investigation in this study, together with the contemporary sea level and the maximum sea level during storm measured at a close tidal station, and with the bathymetry surveys and sediment movimentation actions at the port entrance.

Table 2. 3 Sea storm events in the period 2017–2020, together with the list of bathymetry surveys and sediment movimentation at the port entrance: peak wave significant height (H_s), mean (T_m), and peak (T_p) wave period, mean wave direction (MWD), compass sector, storm duration (dur), storm energy (E), energetic class, sea level at the H_s instant, and maximum sea level during storm. [a] Sea level data not available; [b] Nausicaa data not available. [29]

Date	H_s (m)	T_m (s)	T_p (s)	MWD (° N)	Compass Sector	dur (h)	E (m^2 h)	Class	Level (m)	Level Max (m)
April–June 2017	Propeller movimentation									
13 June 2017	Bathymetry 01									
6 November 2017	2.79	5.6	8.3	61	I	19.5	89.68	II—moderate	0.53	0.83
13 November 2017	3.68	6.7	9.1	59	I	50.5	302.96	III—significant	0.44	0.93
26 November 2017	3.07	5.0	7.7	46	I	11	50.77	I—weak	0.13	0.36
2 December 2017	2.39	5.3	7.7	58	I	22	86.48	II—moderate	0.27	0.69
28 December 2017	Bathymetry 02									
3 February 2018	2.51	5.3	8.3	55	I	9.5	36.15	I—weak	0.29	0.70
13 February 2018	1.78	4.4	6.2	24	I	7	20.33	I—weak	0.40	0.52
18 February 2018	2.70	5.6	8.3	59	I	15	70.10	II—moderate	0.10	0.45
24 February 2018	3.00	6.0	8.3	75	I	67.5	331.37	III—significant	0.36	0.70
26 February 2018	2.49	5.5	7.1	48	I	59	248.20	III—significant	0.28	0.61
21 March 2018	3.10	6.0	9.1	65	I	37	182.44	III—significant	0.43	0.83
23 March 2018	2.13	5.1	7.1	42	I	12.5	42.66	I—weak	0.38	0.72
7 April 2018	Bathymetry 03									
April 2018	Propeller movimentation									
11 May 2018	Bathymetry 04									
26 August 2018	2.00	5.1	7.7	37	I	9	28.14	I—weak	0.27	0.53
24 September 2018	2.75	5.8	8.3	316	IV	47	188.87	III—significant	0.14	0.59
2 October 2018	2.36	5.3	7.7	23	I	11.5	49.20	I—weak	0.32	0.40
10 October 2018	Bathymetry 05									
21 October 2018	2.76	5.6	7.1	340	IV	20	73.58	II—moderate	0.26	0.57
29 October 2018	2.63	6.2	9.1	46	I	16.5	75.98	II—moderate	0.79	1.06
17 November 2018	2.33	5.5	7.7	44	I	34.5	121.52	II—moderate	[a]	[a]
20 November 2018	2.66	5.4	7.7	42	I	11.5	55.93	I—weak	[a]	[a]
27 November 2018	2.30	5.1	6.2	66	I	16.5	53.12	I—weak	[a]	[a]
January 2019	Propeller movimentation									
23 February 2019	2.84	6.1	9.1	66	I	32	145.29	III—significant	−0.39	0.04
20 March 2019	1.89	4.8	7.1	63	I	6.5	20.10	I—weak	−0.07	0.15
26 March 2019	3.60	6.3	8.3	38	I	7.5	67.50	II—moderate	0.56	0.83
4 April 2019	1.94	6.2	9.1	82	I	8	22.13	I—weak	0.34	0.57
March–April 2019	Dredging sand volume of 20,000 m^3									
10 April 2019	Bathymetry 06									
5 May 2019	2.77	5.6	7.1	52	I	19.5	80.04	II—moderate	0.42	0.48
12 May 2019	2.75	5.3	7.1	32	I	31	143.70	III—significant	0.30	0.46
14 May 2019	2.02	4.9	6.7	38	I	23.5	28.65	I—weak	0.07	0.14
12 January 2019	Bathymetry 07									

18 January 2019	Ejectors on									
3 September 2019	1.85	4.8	6.7	55	I	6.5	18.8	I—weak	0.22	0.33
6 September 2019	Bathymetry 08									
3 October 2019	2.5	5.4	7.7	28	I	9	38.4	I—weak	0.56	0.56
17 November 2019	1.87	6.5	9.1	83	I	7.5	22.8	I—weak	0.76	0.90
24 November 2019	1.77	5.5	8.3	82	I	13.5	34.8	I—weak	0.55	0.68
10 December 2019	1.75	5.1	6.7	66	I	11	30.9	I—weak	0.20	0.20
23 December 2019	[b]	[b]	[b]	[b]	[b]	[b]	[b]	[b]	[b]	1.0
9 January 2020	Bathymetry 09									
20 January 2020	1.73	4.7	5.9	61	I	21	55.1	I—weak	0.12	0.13
6 February 2020	2.54	5.3	7.1	44	I	18.5	84.1	II—moderate	−0.05	0.19
25 March 2020	4.05	7.8	25	58	I	76.5	369.6	III—significant	−0.13	0.25
31 March 2020	2.24	5.2	7.1	48	I	17	56.0	I—weak	0.16	0.18
1 April 2020	1.88	4.7	6.2	61	I	10.5	29.9	I—weak	0.05	0.07
14 April 2020	2.58	5.5	7.7	59	I	16	58.5	I—weak	−0.04	0.0
30 April 2020	Bathymetry 10									

The yearly analyses of the sea storm event which is shown in Figure 2. 7 indicates the similarity among the considered years, with an average 13 sea storm events per year. However, the temporal distribution during each year is different, Figure 2. 8. It can be seen that:

- the most energetic year ($E > 1400$ m^2 h) was 2017–2018, with the higher amount of storm energy in winter and autumn, 700 m^2 h and 520 m^2 h, respectively.
- 2018–2019 shows the most energetic sea in autumn, more than 600 m^2 h;
- 2019–2020 shows the lowest energy approximately 800 m^2 h, the highest amount is seen in spring, 500 m^2 h;
- In all years, the low level of energy values was observed in summer, as expected.

To evaluate the net impact of ejectors plant it is necessary to find periods which the sea storm energy is the same. According to Table 2. 4 the first (13 June 2017–28 December 2017) and last (9 January 2020–30 April 2020) periods have almost similar released energy, 530 and 650 m^2 h, respectively. In addition, the number of sea storms are close, four and six, respectively. Therefore, these two periods could be useful for the assessment of ejector demo plant performance.

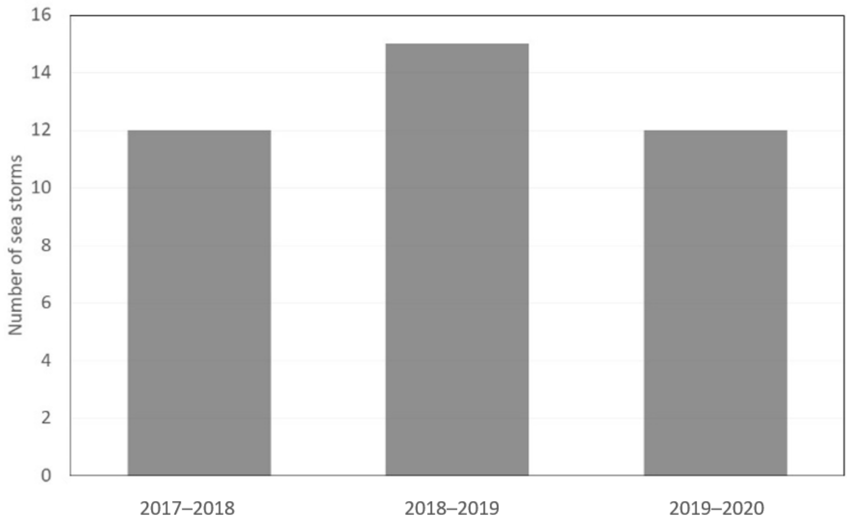

Figure 2. 7 Annual number of sea storm events in the period 2017–2020. [29]

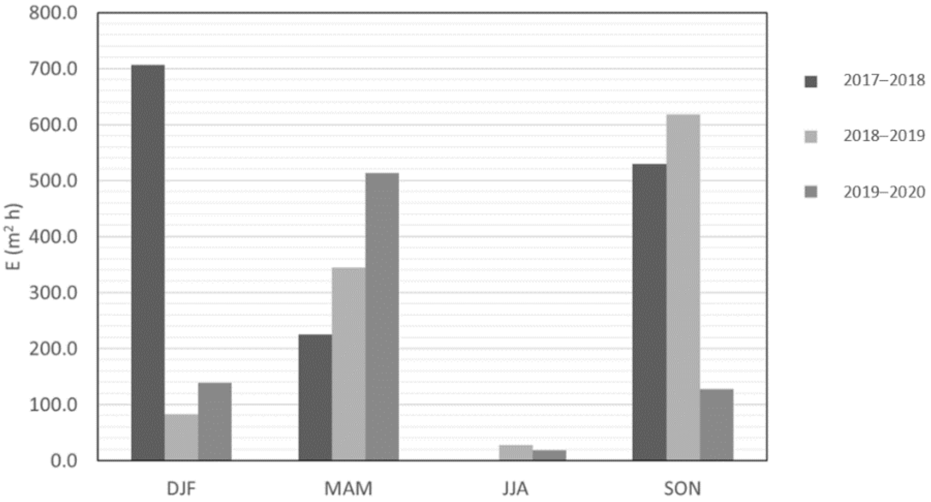

Figure 2. 8 Seasonal distribution of the sea storm energy in the period 2017–2020: winter (DJF), spring (MAM), summer (JJA), and autumn (SON). [29]

Table 2. 4 Summary of number of storms, related energy in periods under analysis, and the mean energy per day. [29]

Period	**N° of Storms**	**Energy Released in the Period (m^2 h)**	**Mean Energy Per Day (m^2 h/day)**
13 June 2017–28 December 2017	4	530	2.68
28 December 2017–7 April 2018	7	930	9.30
11 May 2018–10 October 2018	3	266	1.75
10 April 2019–12 June 2019	4	275	4.37
12 June 2019–6 September 2019	1	19	0.22
6 September 2019–9 January 2020	4	127	1.02
9 January 2020–30 April 2020	6	653	5.83

2.4 Results

2.4.1 Analysis of Water Depth Variation before and after Ejector Demo Plant Operation

The water depth at the port entrance after operation of propellers began in June 2017is shown in Figure 2. 9, where the navigation channel presented a draft around −4 m, with 100 m width and 200 m length, while the northern area had a water depth less than 2 m. The black dots indicate the positions of the mooring points of the ejectors' inlet and outlet pipelines in Figure 2. 9.

Figure 2. 10 shows the maps of water depth changes between two consecutive surveys from June 2017 to April 2018, where a hot–cold colour scale is representative of accumulated or eroded sediment volumes, as it is seen in the legend. In Figure 2. 10 a, seabed modification after summer and autumn seasons was observed, shows that the navigation channel is impacted, while in the second figure, the water depth variation was focused very close to the port docks with higher sedimentation.

In May 2018, propeller operation was required due to substantially closure of the port entrance i.e., water depth under 2 m at the port inlet. Figure 2. 11 depicts the bathymetry after propeller operation, which is similar to the one obtained in Figure 2. 9. The water depth changes measured in the following bathymetry are shown in Figure 2. 12 and reveal the same behaviour as observed in Figure 2. 11; the sedimentation is higher in the central navigation channel, while sediment moved from the surrounding areas.

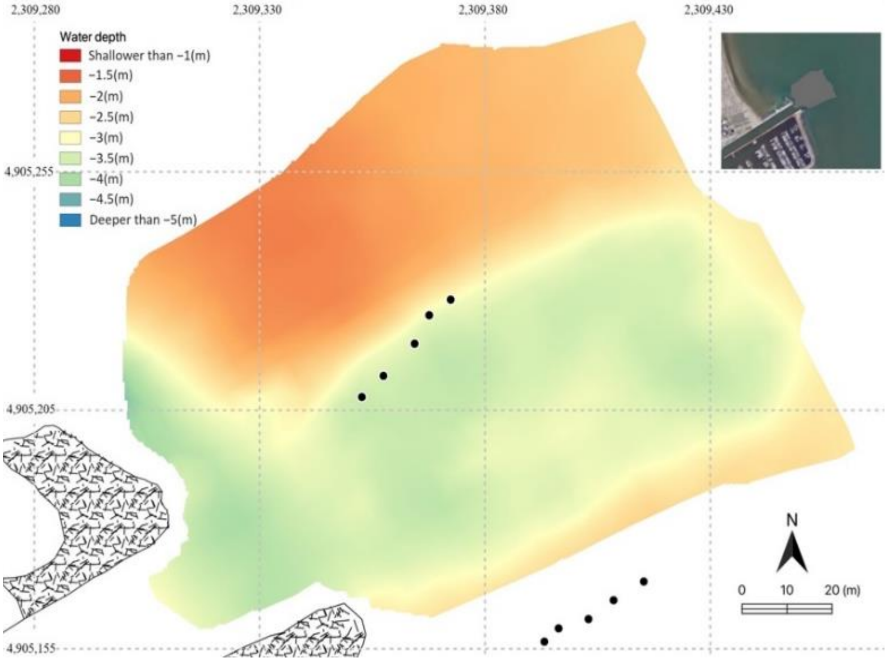

Figure 2. 9 Maps of water depth at the port entrance after dredging and propeller operation on 13 June 2017. The positions of the mooring points of the ejectors' inlet and outlet pipelines are also reported as black dots.

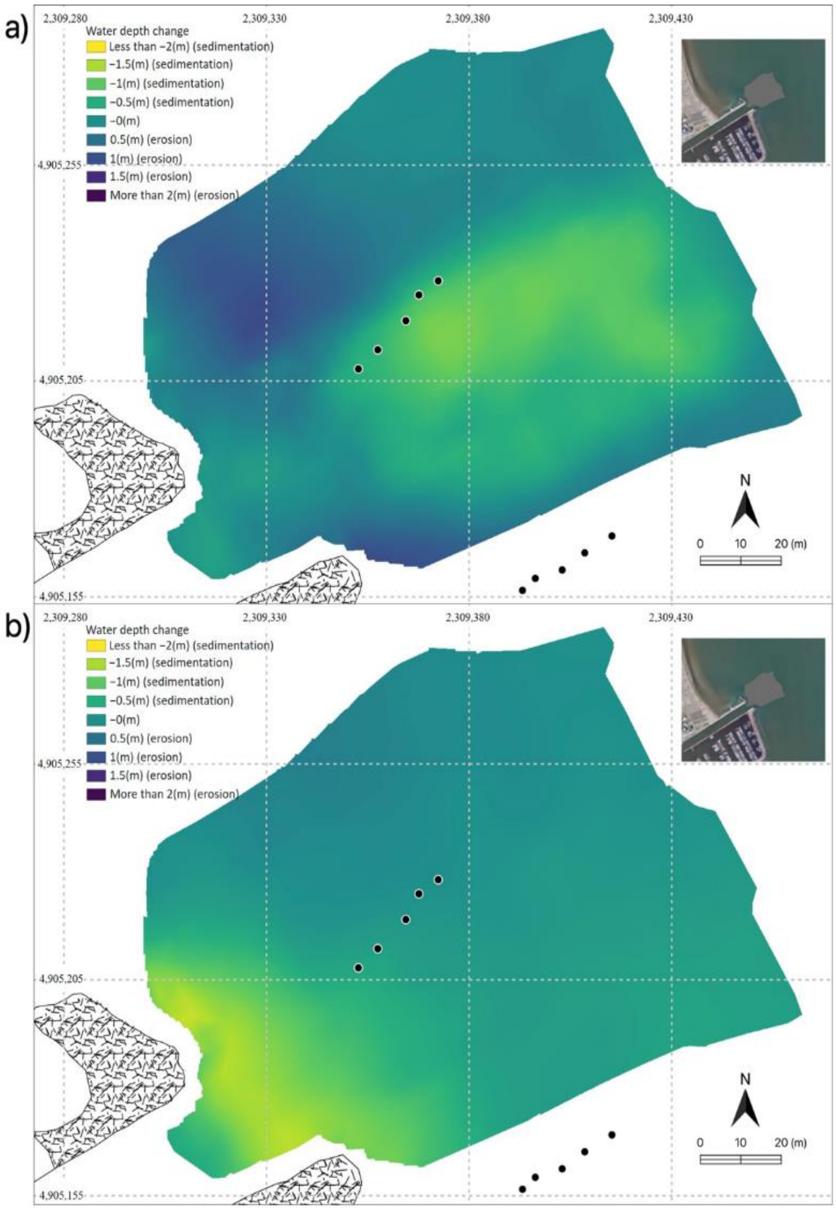

Figure 2. 10 Water depth changes in the period: (**a**) 13 June 2017–28 December 2017 and (**b**) 28 December 2017–7 April 2018. The positions of the mooring points of the ejectors’ inlet and outlet pipelines are also reported as black dots for reference purposes.

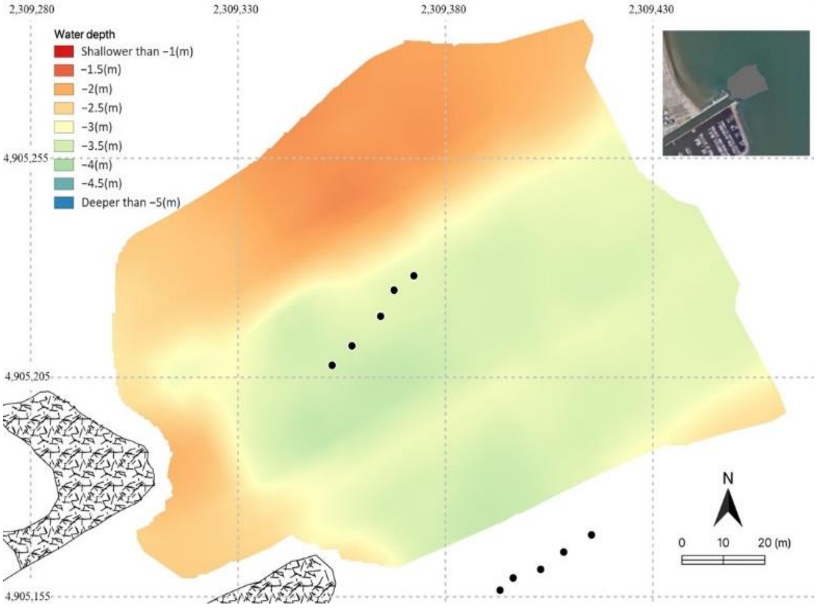

Figure 2. 11 Maps of water depth at the port entrance after propeller operation on 11 May 2018. The positions of the mooring points of the ejectors’ inlet and outlet pipelines are also reported as black dots.

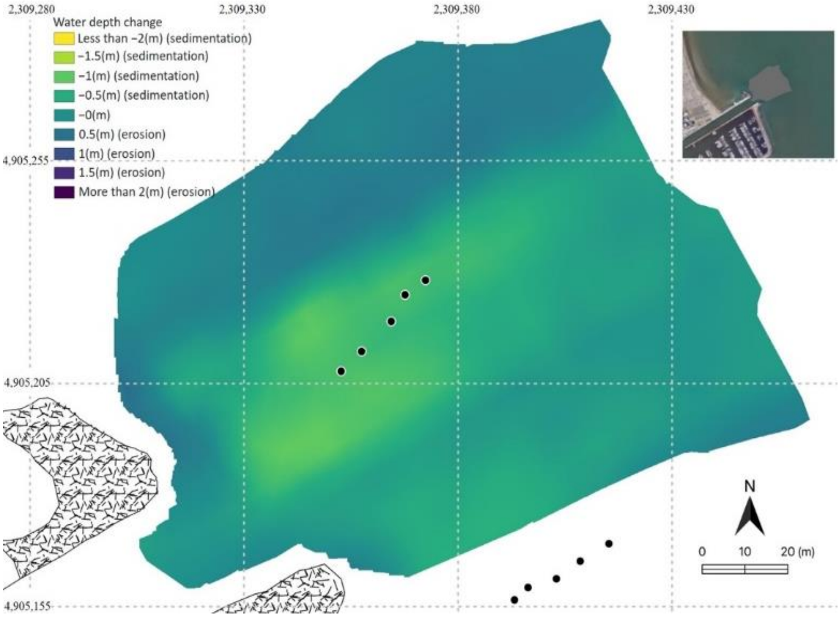

Figure 2. 12 Water depth change in the period 11 May 2018–10 October 2018. The positions of the mooring points of the ejectors’ inlet and outlet pipelines are also reported in black dots.

The last dredging and propeller operation before ejector demo plant installation was from January to April 2019. Figure 2. 13 shows the bathymetry of 10 April of 2019. During this period, the sediment management activities affected a wider area, including the entrance to the docks and the inner channel. However, after 2 months, sedimentation occurred in the area in front of the port entrance (see Figure 2. 14a).

On 13 June 2019, the ejector demo plant was activated. The reference bathymetry which is used to assess the performance of the plant is related to 12 June 2019 (Figure 2. 14b). The minimum water depth at the port entrance to guarantee navigability was 2.5 m because below this level there could be navigability issue for fisherman and leisure boats that use the Marina of Cervia. Figure 2. 15 is provided based on the bathymetries from June 2019 to April 2020 (included in Appendix 2.B), it provides information about the occurrence of the minimum water-depth and its location in the common area at the port inlet.

It is seen that at the end of the monitoring period (end of April 2020) there is still a navigable channel (i.e., water depth over 2.5 m) to enter the port of Cervia. It should be noted that in January 2020 the situation appeared critical in the area of influence of the ejectors. However, it should be considered that until February 2020, the ejector demo plant was not operating at full load, while starting from February 2020, the technical issues that limited the operation of the demo plant were solved.

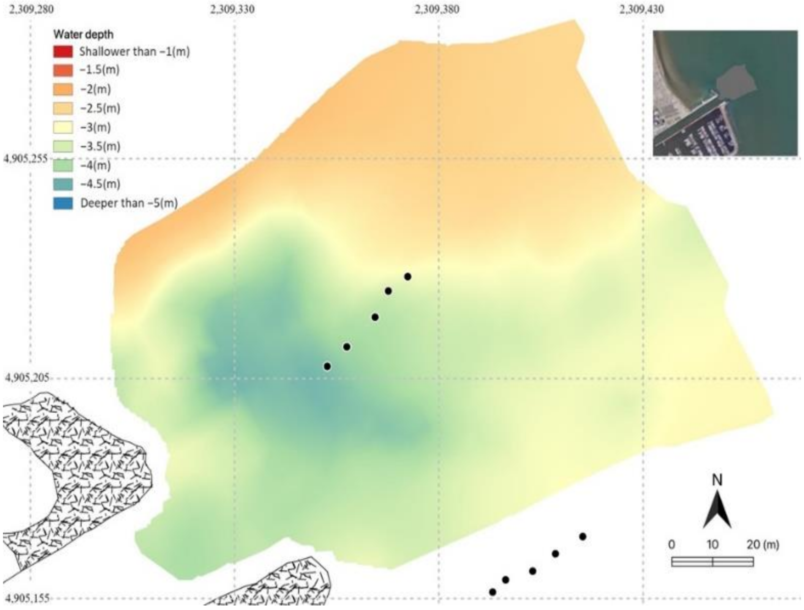

Figure 2. 13 Maps of water depth at the port entrance after dredging and propeller operation on 10 April 2019. The positions of the mooring points of the ejectors' inlet and outlet pipelines are also reported as black dots.

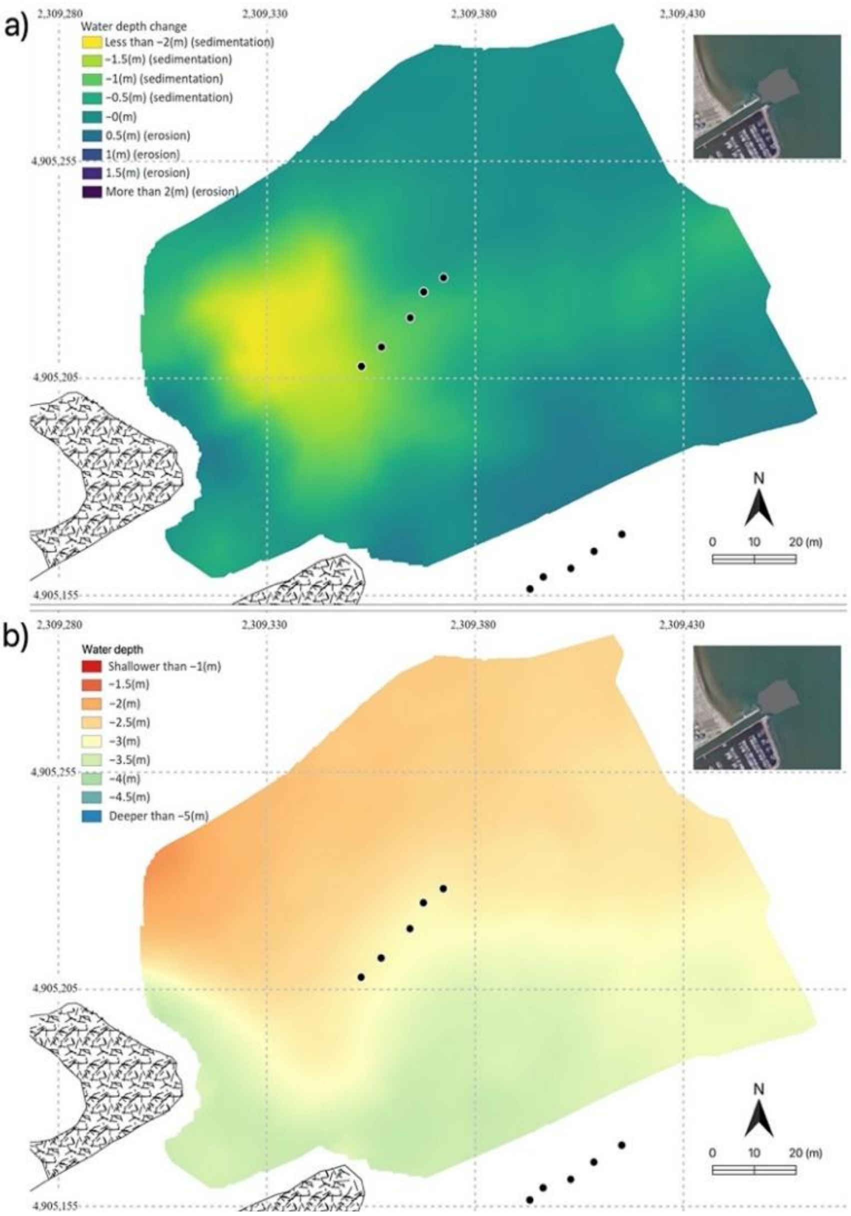

Figure 2. 14 (**a**) Water depth change in the period 10 April 2019–12 June 2019, and (**b**) water depth measured on 12 June 2019. The positions of the mooring points of the ejectors' inlet and outlet pipelines are also reported as black dots.

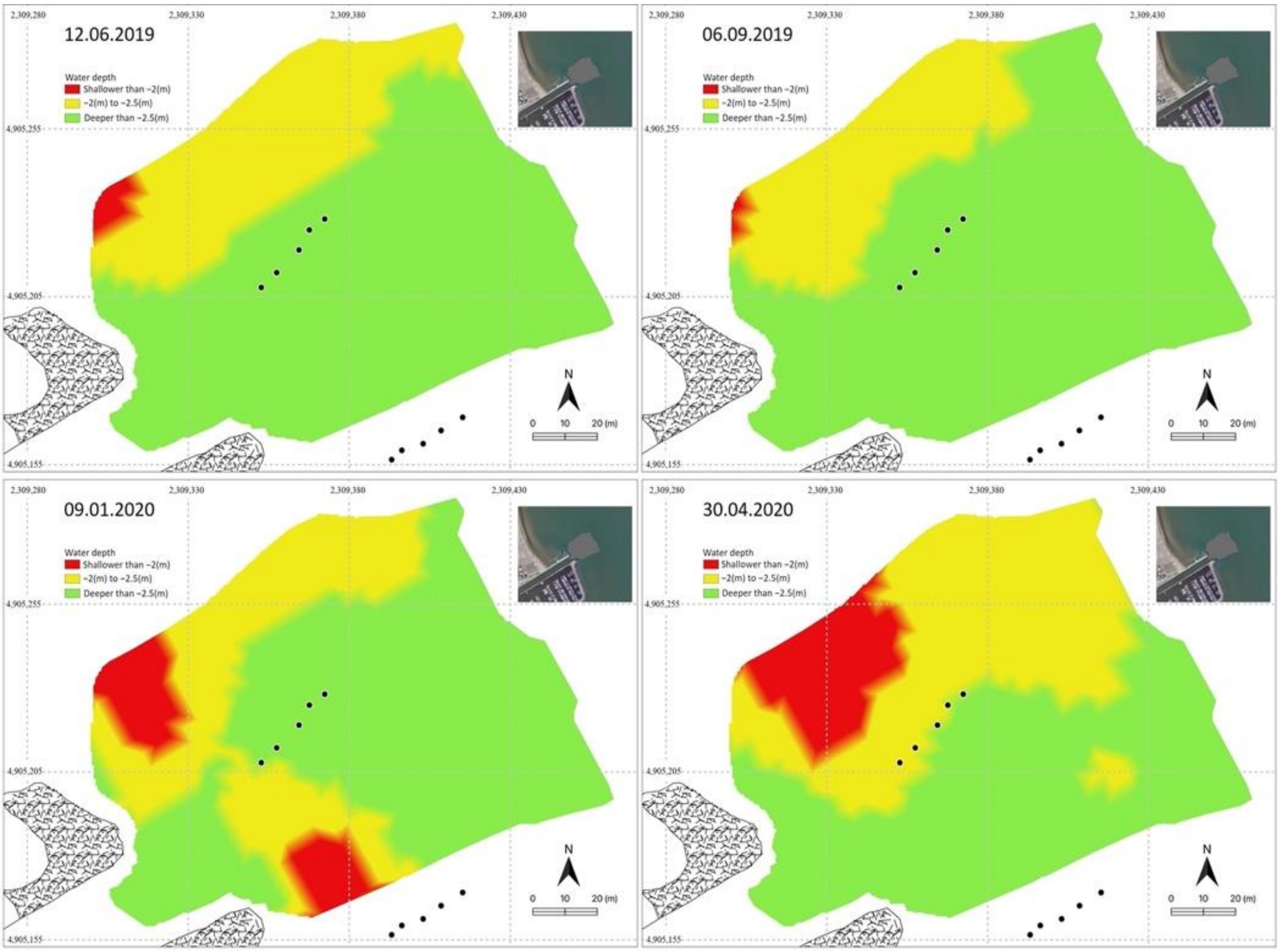

Figure 2. 15 Critical areas (i.e., water depth < 2.5 m) during the ejector operation (12 June 2019–30 April 2020). The positions of the mooring points of the ejectors' inlet and outlet pipelines are also reported as black dots.

2.4.2 Analysis of Volume Variation before and after Ejector Demo Plant Operation

Volume variation over time is shown in common area and ejector area in Figure 2. 6. The mean water depth variation is considered as the parameter for comparison, expressed in mm per day, which is calculated by dividing the volume change between two consecutive bathymetries by the area under consideration (i.e., common area or ejector area) and by the number of days between two consecutive bathymetries. The results are shown in Figure 2. 16.

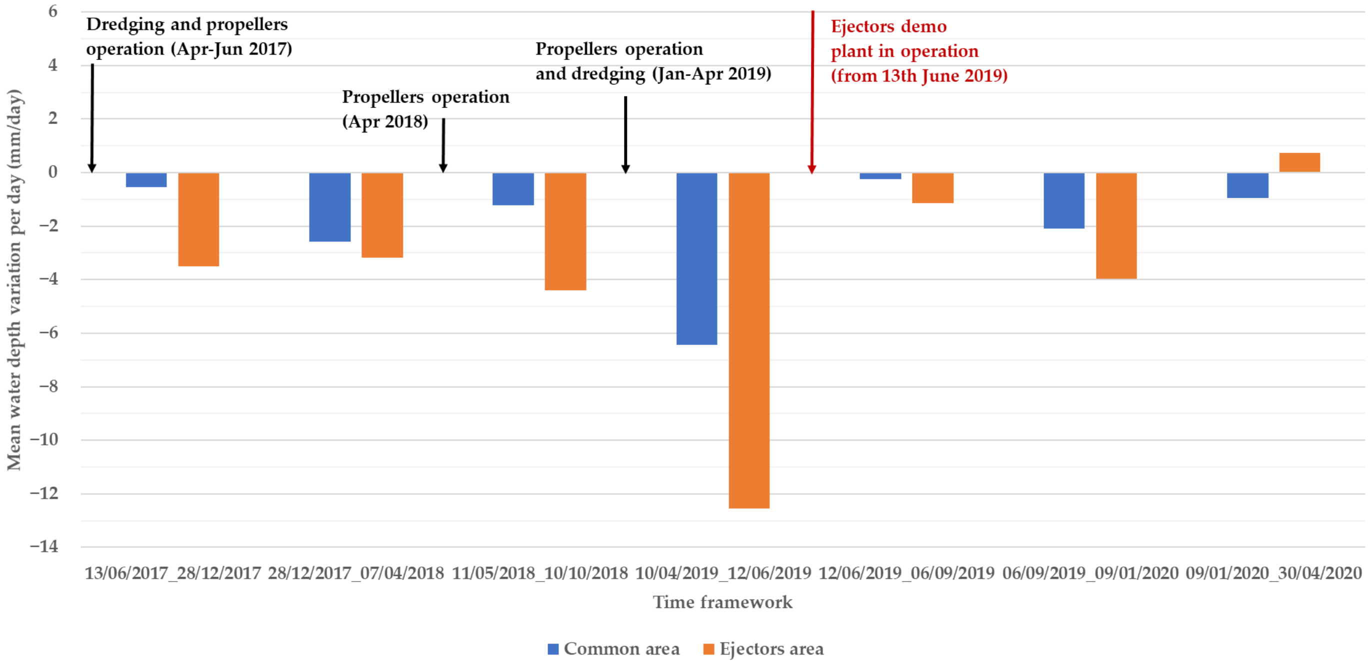

Figure 2. 16 Mean water depth variation per day (in mm/day) between two consecutive bathymetries in the common area and in the ejector area before and after ejector demo plant operation.

To check if the positive water depth variation observed in Figure 2. 16 might somehow be influenced by the natural sediment transport dynamic the volume variation has been related to the metocean data. For this purpose, the parameter computed for the comparison is the water depth variation per storm energy unit, expressed in mm per m^2 h, which is calculated by dividing the volume variation between two consecutive bathymetries by the area under consideration and by the cumulated energy produced by the storms registered between two consecutive bathymetries (see Table 2. 3 for metocean data). The results are shown in Figure 2. 17.

It is seen in Figure 2. 17 that implicitly storm is the main reason for sediment transport in both areas under investigation. Thus, different periods considered in the analysis can be compared only if similar storm conditions occur.

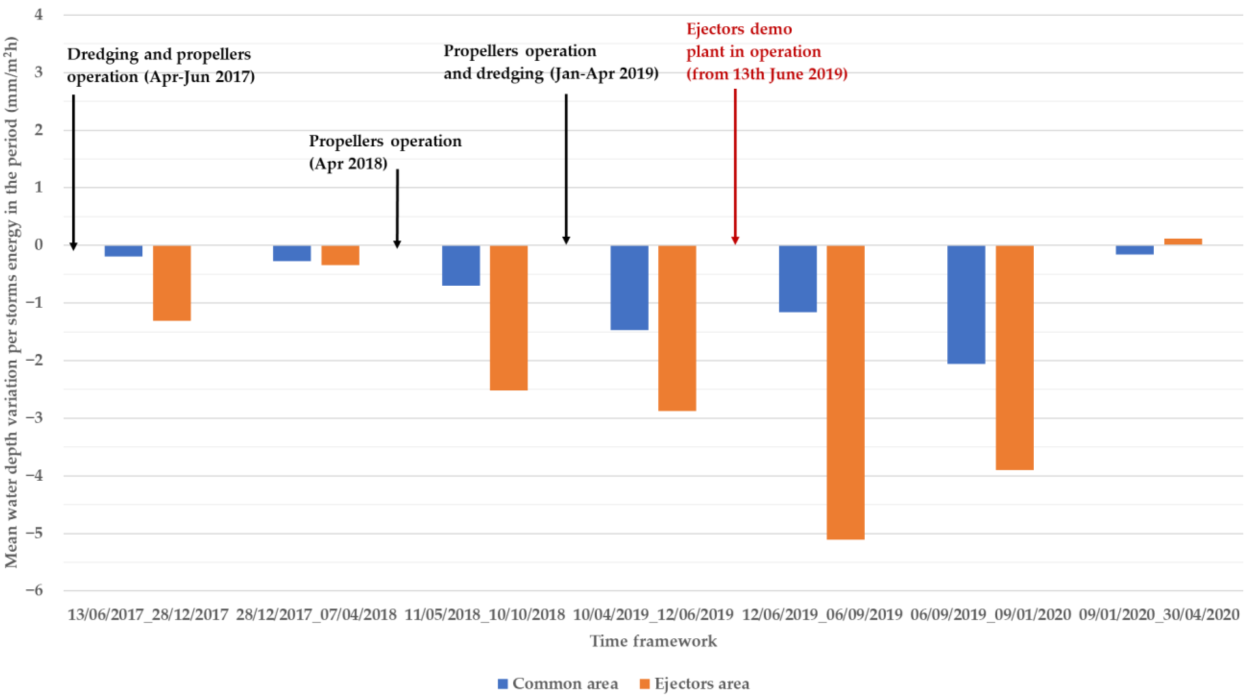

Figure 2. 17 Mean water depth variation per energy of storms in the period (in mm/m^2 h) between two consecutive bathymetries in the common area and in the ejector area before and after ejector demo plant operation.

2.5 Discussion

By the analysis of Figures 9–14, it is realized that dredging and propeller operation in the centre of the navigation channel partially solve the problem of navigability of the port inlet. In a few months the hole at the centre of the channel was covered by sediment. Part of the sediment came from the surrounding area, as it is expected that the natural sediment transport in the area produced by storm and longshore transport also contributes. The effect of dredging and propeller operation on the water depth change pace is confirmed by the analysis of Figure 2. 16 and Figure 2. 17. These two figures indicate sediment dynamics that seem to affect more the area of ejectors rather than the whole common area. The ejector area is directly influenced by dredging and propeller operation, which means that after artificial deepening of the seabed the ejector area is characterized by a water depth that is higher than the mean value of the common area. It is realized that the ejector area works as a sediment trap after dredging or propeller operation. In addition, in the ejector area, in the first period after dredging or propeller operation (13 June 2017–28 December 2017, 11 May 2018–10 October 2018, 10 April 2019–12 June 2019 periods), a higher water depth variation is observed than in the common area, while during the period 28 December 2017–7 April 2018, which is characterized by the highest number of storms, related energy in the period as well as energy per day, the water depth changes in both areas are comparable. It is seen in Figure 2. 17 that there is a relevant decreasing water depth change rate per storm energy unit in the two consecutive periods from June to December

2017 and from December 2017 to April 2018. The rate is −1.31 mm/m^2 h and−0.34 mm/m^2 h in the first and second period, respectively. It is concluded that after a faster water depth variation in the ejector area, mainly affected by dredging and propeller operation, the water depth changes tend to homogenize in the common area. Therefore, the increase in water depth which is provided artificially modifies the natural sediment transport by collecting the sediment from nearby which is naturally transported to the area. Thus, it is better to work on the sediment in southern or northern areas instead of dredge or move the sediment via propeller operation along the navigable channel.

Figure 2. 16 shows that there is not a constant relationship between the water depth change in the ejector area and the common areas. This figure indicates that water depth variation in the common area, before and after ejector demo plant operation has a considerable intensity, −0.5 ÷ 2.5 mm/day of mean variation, with the exception of the period 10 April 2019–12 June 2019, in which the water depth variation in the common area reaches −6.5 mm/day. This huge water depth variation rate is related to combination of the effects of (i) dredging and propeller operation realized on a wide area at the port entrance (Figure 2. 13) and (ii) high storm energy measured in the period. In the 12 June 2019–6 September 2019 period the storm energy is almost zero and has the highest value in Figure 2. 17. In this case, probably it is related to natural longshore sediment transport.

By a detailed look at Figure 2. 16 and Figure 2. 17 it can be recognized that in the last period of ejector demo plant operation, which overlaps with phase 3 of operation, a positive water depth variation in the area of the ejectors can be observed, while in the common area, a negative water depth change was observed at the same period. This period can be compared to the first period 13 June 2017–28 December 2017 since the two periods show similar energetic forcing from sea and similar metocean characteristics (see Table 2. 3 and Table 2. 4). It is worth mentioning that, in the comparing period, there is a relevant negative water depth change, especially in the common area. It shows the impact of ejector demo plant operation which helps to keep the water depth almost constant in the ejector area.

If the same mean rate of water depth variation for the period 13 June 2017–28 December 2017 is assumed, −1.31 mm/m^2 h, it can be estimated that, without the ejector demo plant the water depth would vary by about −0.855 m in the ejector area in the period 9 January 2020–30 April 2020, while a mean water depth variation of about 0.081 m has been calculated. Thus, the contribution of the ejector demo plant could be calculated with a maximum water depth variation of 0.936 m (0.081+0.855), which is equivalent to a maximum volume of sediment by-passed of about 750 m^3. However, the water depth change rate in the period of 13 June 2017 to 28 December 2017 might be affected by the previous dredging operation, the potential impact of the ejectors has been calculated by assuming the same mean rate of water depth variation of 28 December 2017–7 April 2018, i.e., −0.34 mm/m^2 h. By application of this water depth variation rate, it can be estimated that without the ejector demo plant in operation in the similar period, 9 January 2020–30 April 2020, the water depth would vary by about −0.223 m in the ejector area. Therefore, the net contribution of the ejector demo plant can be calculated in a maximum water depth variation of 0.304 m, which the maximum volume of sediment would be around 245 m^3.

2.6 Conclusions

An innovative sediment management technology, as an alternative to dredging systems, has been installed in the first industrial sized demo plant at the port entrance of the Marina of Cervia (Italy) and the performance assessment is performed in this chapter. This study evaluates the effectiveness achieved and it is found that the ejector demo plant was able to guarantee navigability at the port entrance after almost one year of operation (June 2019–April 2020). Especially, in the period between January and April 2020 the maximum impact of the ejector demo plant by keeping the water depth at the desired level (i.e., over the minimum threshold of 2.5 m) was observed. In this period the ejector demo plant was operated at the design water flowrates and the total by-passed sediment volume is estimated between 245 and 750 m^3. This estimation is based on the consideration of the storm energy and its probable sediment movement at the same period. Since the proposed technology has very low electricity consumption, carbon dioxide emission is very low. Furthermore, electricity source can be renewable energies, which could lead to a zero emission sediment removal. Therefore, the proposed technology is a sustainable alternative to dredging technology.

Considering the acceptable performance of the ejector demo plant in the last period of operation (January–April 2020), ejectors arrangement modification could be evaluated to optimize demo plant operation. It can be done by spacing out the ejectors and, at the same time, move them closer to the port entrance. In addition, number of ejectors installed can be reduced to reduce whole power consumption, however, it needs deep investigation.

2.7 Appendix 2.A Frequency Tables of the Sea Climate

Table 2.A. 1 Frequency table of significant wave heights H_s and mean direction MWD for the year 2017–2018 *[29]*.

MWD [°N]	**Hs [m]**												
	<0.50	**0.50–0.75**	**0.75–1.00**	**1.00–1.25**	**1.25–1.5**	**1.5–1.75**	**1.75–2.00**	**2.00–2.25**	**2.25–2.5**	**2.5–2.75**	**2.75–3**	**>3.00**	**Total**
0–15	2.43	0.36	0.10	0.03	0.01	0.00	0.01	0.00	0.00	0.00	0.00	0.00	2.94
15–30	3.27	0.78	0.26	0.24	0.04	0.09	0.06	0.00	0.03	0.00	0.00	0.00	4.78
30–45	4.36	1.28	0.54	0.53	0.34	0.22	0.27	0.10	0.03	0.02	0.01	0.01	7.71
45–60	3.79	1.32	1.05	0.79	0.63	0.40	0.49	0.58	0.48	0.15	0.02	0.01	9.70
60–75	4.61	1.33	0.81	0.52	0.39	0.29	0.43	0.63	0.25	0.21	0.21	0.02	9.70
75–90	9.64	2.44	1.36	1.25	0.87	0.16	0.01	0.01	0.00	0.00	0.00	0.01	15.74
90–105	16.46	3.73	1.37	0.46	0.18	0.07	0.00	0.00	0.00	0.00	0.00	0.00	22.26
105–120	10.53	1.42	0.26	0.11	0.00	0.00	0.00	0.00	0.00	0.00	0.00	0.00	12.32
120–135	2.23	0.16	0.06	0.00	0.00	0.00	0.00	0.00	0.00	0.00	0.00	0.00	2.45
135–150	0.54	0.03	0.00	0.00	0.00	0.00	0.00	0.00	0.00	0.00	0.00	0.00	0.58
150–165	0.20	0.00	0.00	0.00	0.00	0.00	0.00	0.00	0.00	0.00	0.00	0.00	0.20
165–180	0.07	0.01	0.00	0.00	0.00	0.00	0.00	0.00	0.00	0.00	0.00	0.00	0.08
180–195	0.15	0.01	0.00	0.00	0.00	0.00	0.00	0.00	0.00	0.00	0.00	0.00	0.16
195–210	0.17	0.00	0.00	0.00	0.00	0.00	0.00	0.00	0.00	0.00	0.00	0.00	0.17
210–225	0.11	0.00	0.00	0.00	0.00	0.00	0.00	0.00	0.00	0.00	0.00	0.00	0.11
225–240	0.10	0.00	0.00	0.00	0.00	0.00	0.00	0.00	0.00	0.00	0.00	0.00	0.10
240–255	0.27	0.08	0.00	0.00	0.00	0.00	0.00	0.00	0.00	0.00	0.00	0.00	0.35
255–270	0.32	0.00	0.00	0.00	0.01	0.00	0.00	0.00	0.00	0.00	0.00	0.00	0.33
270–285	0.68	0.00	0.00	0.00	0.00	0.00	0.00	0.00	0.00	0.00	0.00	0.00	0.68
285–300	0.98	0.04	0.03	0.00	0.00	0.00	0.00	0.00	0.00	0.00	0.00	0.00	1.05
300–315	1.71	0.05	0.00	0.02	0.00	0.00	0.00	0.00	0.00	0.00	0.00	0.00	1.78
315–330	1.69	0.03	0.06	0.01	0.00	0.00	0.00	0.00	0.00	0.00	0.00	0.00	1.79
330–345	1.63	0.13	0.07	0.02	0.00	0.00	0.00	0.00	0.00	0.00	0.00	0.00	1.84
345–360	2.68	0.33	0.09	0.07	0.01	0.00	0.00	0.00	0.00	0.00	0.00	0.00	3.18
Total	68.62	13.53	6.06	4.05	2.48	1.23	1.26	1.32	0.79	0.37	0.24	0.05	100

Table 2.A. 2 Frequency table of significant wave height H_s and mean direction MWD for the year 2018–2019 [29].

MWD [°N]	Hs [m]												
	<0.50	**0.50–0.75**	**0.75–1.00**	**1.00–1.25**	**1.25–1.5**	**1.5–1.75**	**1.75–2.00**	**2.00–2.25**	**2.25–2.5**	**2.5–2.75**	**2.75–3**	**>3.00**	**Total**
0–15	3.16	0.53	0.16	0.06	0.03	0.02	0.01	0.05	0.03	0.01	0.01	0.00	4.06
15–30	4.78	1.13	0.55	0.20	0.12	0.02	0.02	0.03	0.05	0.02	0.01	0.00	6.92
30–45	4.86	1.38	0.99	0.57	0.37	0.26	0.21	0.19	0.06	0.04	0.01	0.00	8.94
45–60	5.34	1.49	1.39	0.92	0.79	0.39	0.32	0.15	0.07	0.04	0.01	0.00	10.92
60–75	5.42	1.34	1.35	1.08	0.95	0.50	0.23	0.11	0.08	0.09	0.02	0.00	11.16
75–90	6.02	1.31	0.89	0.86	0.43	0.22	0.03	0.02	0.00	0.00	0.00	0.00	9.80
90–105	9.81	2.56	1.01	0.49	0.24	0.05	0.01	0.00	0.00	0.00	0.00	0.00	14.19
105–120	5.89	0.86	0.31	0.04	0.01	0.06	0.03	0.00	0.00	0.00	0.00	0.00	7.21
120–135	3.07	0.25	0.05	0.00	0.01	0.01	0.02	0.00	0.00	0.00	0.00	0.00	3.40
135–150	2.21	0.10	0.02	0.00	0.01	0.00	0.00	0.00	0.00	0.00	0.00	0.00	2.33
150–165	1.54	0.06	0.01	0.00	0.01	0.01	0.01	0.01	0.00	0.00	0.00	0.00	1.65
165–180	1.41	0.02	0.01	0.00	0.01	0.01	0.01	0.00	0.00	0.00	0.00	0.00	1.46
180–195	1.09	0.03	0.00	0.00	0.00	0.00	0.01	0.00	0.00	0.00	0.00	0.00	1.13
195–210	0.73	0.01	0.01	0.00	0.00	0.00	0.01	0.00	0.00	0.00	0.00	0.00	0.75
210–225	0.95	0.01	0.01	0.00	0.00	0.00	0.00	0.00	0.00	0.00	0.00	0.00	0.96
225–240	0.84	0.00	0.01	0.00	0.01	0.00	0.00	0.01	0.00	0.00	0.00	0.00	0.86
240–255	0.70	0.01	0.00	0.00	0.00	0.00	0.00	0.00	0.00	0.00	0.00	0.00	0.71
255–270	0.95	0.00	0.01	0.00	0.00	0.00	0.00	0.00	0.00	0.01	0.00	0.00	0.96
270–285	1.13	0.01	0.00	0.00	0.00	0.00	0.01	0.00	0.00	0.00	0.00	0.00	1.14
285–300	1.64	0.02	0.01	0.00	0.00	0.01	0.00	0.00	0.00	0.01	0.01	0.00	1.69
300–315	1.93	0.06	0.00	0.00	0.01	0.02	0.01	0.02	0.01	0.01	0.00	0.00	2.06
315–330	1.81	0.08	0.02	0.00	0.01	0.02	0.03	0.05	0.01	0.00	0.01	0.00	2.03
330–345	2.00	0.08	0.01	0.00	0.03	0.01	0.04	0.03	0.01	0.00	0.01	0.00	2.21
345–360	2.95	0.16	0.10	0.05	0.03	0.05	0.05	0.05	0.02	0.01	0.00	0.00	3.47
Total	70.22	11.49	6.90	4.28	3.06	1.64	1.06	0.72	0.34	0.22	0.08	0.00	100

Table 2.A. 3 Frequency table of significant wave height H_s and mean direction MWD for the year 2019–2020 [29].

MWD [°N]	**Hs [m]**												
	<0.50	**0.50–0.75**	**0.75–1.00**	**1.00–1.25**	**1.25–1.5**	**1.5–1.75**	**1.75–2.00**	**2.00–2.25**	**2.25–2.5**	**2.5–2.75**	**2.75–3**	**>3.00**	**Total**
0–15	3.27	0.41	0.09	0.03	0.03	0.01	0.01	0.01	0.01	0.00	0.00	0.00	3.86
15–30	4.40	0.55	0.17	0.10	0.02	0.02	0.02	0.02	0.02	0.01	0.00	0.00	5.32
30–45	4.38	0.78	0.56	0.24	0.10	0.08	0.08	0.10	0.05	0.02	0.02	0.00	6.42
45–60	3.90	1.39	1.42	0.97	0.52	0.49	0.25	0.20	0.14	0.17	0.01	0.00	9.46
60–75	4.91	1.49	2.00	0.86	0.50	0.66	0.18	0.10	0.08	0.04	0.00	0.00	10.84
75–90	7.48	2.11	1.33	0.93	0.63	0.24	0.05	0.00	0.01	0.00	0.00	0.00	12.77
90–105	17.20	4.54	1.32	0.42	0.04	0.02	0.01	0.00	0.00	0.00	0.00	0.00	23.55
105–120	10.82	1.07	0.25	0.04	0.01	0.00	0.00	0.00	0.00	0.00	0.00	0.00	12.19
120–135	2.79	0.35	0.07	0.02	0.00	0.00	0.00	0.00	0.00	0.00	0.00	0.00	3.23
135–150	0.33	0.02	0.02	0.00	0.00	0.00	0.00	0.00	0.00	0.00	0.00	0.00	0.37
150–165	0.09	0.00	0.00	0.00	0.00	0.00	0.00	0.00	0.00	0.00	0.00	0.00	0.09
165–180	0.09	0.00	0.00	0.00	0.00	0.00	0.00	0.00	0.00	0.00	0.00	0.00	0.09
180–195	0.08	0.01	0.00	0.00	0.00	0.00	0.00	0.00	0.00	0.00	0.00	0.00	0.09
195–210	0.09	0.00	0.00	0.00	0.00	0.00	0.00	0.00	0.00	0.00	0.00	0.00	0.09
210–225	0.05	0.01	0.00	0.00	0.00	0.00	0.00	0.00	0.00	0.00	0.00	0.00	0.06
225–240	0.14	0.04	0.00	0.00	0.00	0.00	0.00	0.00	0.00	0.00	0.00	0.00	0.18
240–255	0.28	0.06	0.00	0.00	0.00	0.00	0.00	0.00	0.00	0.00	0.00	0.00	0.34
255–270	0.38	0.03	0.01	0.00	0.00	0.00	0.00	0.00	0.00	0.00	0.00	0.00	0.42
270–285	0.46	0.04	0.00	0.00	0.00	0.00	0.00	0.00	0.00	0.00	0.00	0.00	0.50
285–300	0.91	0.01	0.00	0.00	0.00	0.00	0.00	0.00	0.00	0.00	0.00	0.00	0.91
300–315	1.52	0.02	0.00	0.00	0.01	0.00	0.00	0.00	0.00	0.00	0.00	0.00	1.55
315–330	1.78	0.03	0.02	0.01	0.01	0.00	0.00	0.00	0.00	0.00	0.00	0.00	1.84
330–345	1.77	0.08	0.03	0.04	0.00	0.00	0.00	0.00	0.00	0.00	0.00	0.00	1.91
345–360	3.43	0.29	0.17	0.02	0.01	0.00	0.00	0.00	0.00	0.00	0.00	0.00	3.92
Total	70.57	13.31	7.47	3.67	1.88	1.50	0.60	0.43	0.31	0.23	0.03	0.00	100

2.8 Appendix 2.B. Bathymetric Maps of the Study Area

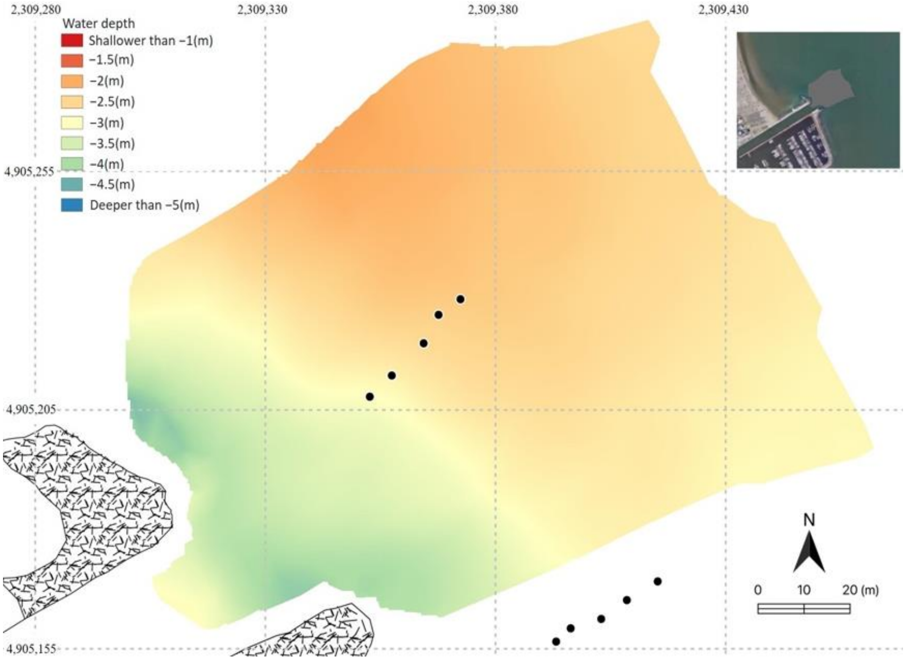

Figure 2.B. 1 Bathymetry of 28 December 2017.

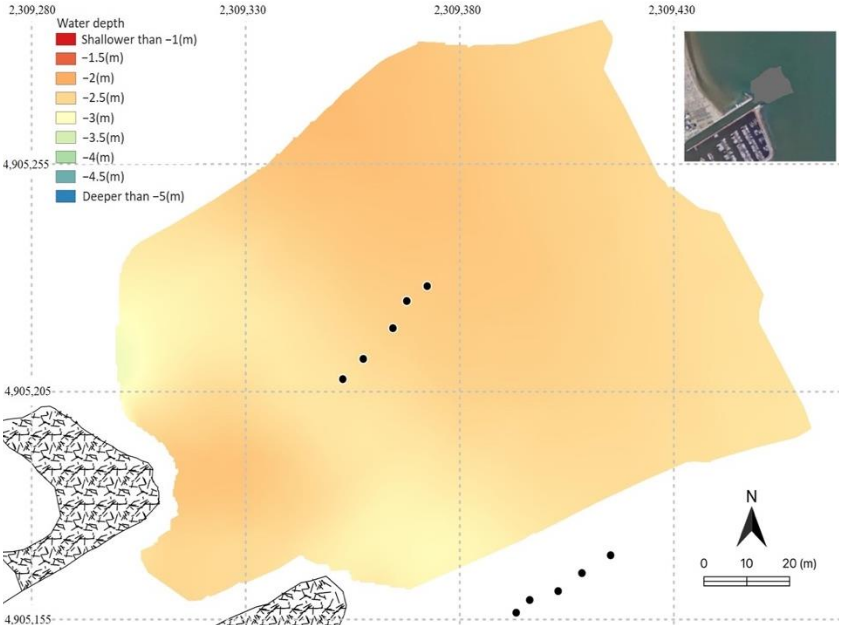

Figure 2.B. 2 Bathymetry of 7 April 2018.

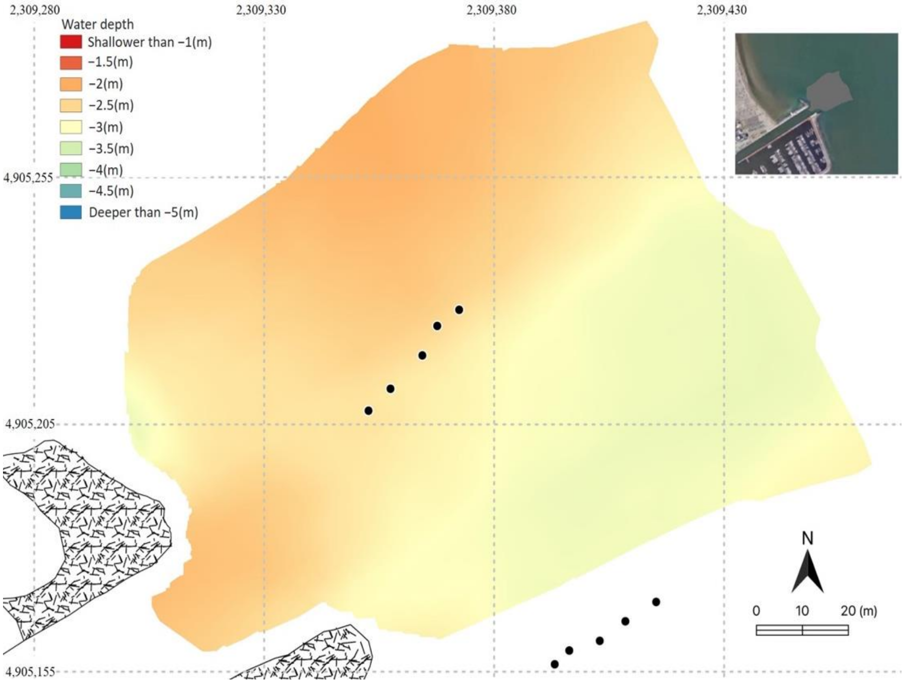

Figure 2.B. 3 Bathymetry of 10 October 2018.

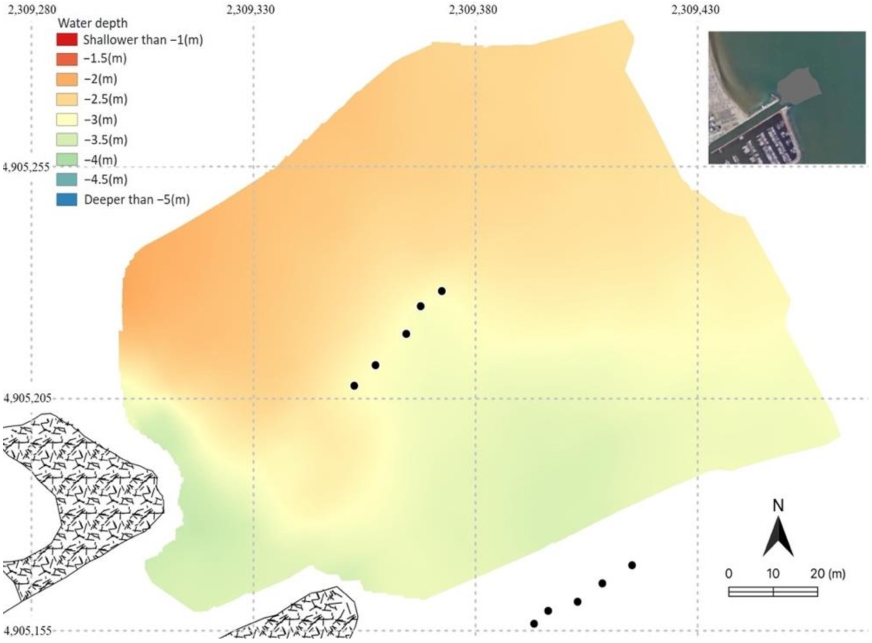

Figure 2.B. 4 Bathymetry of 6 September 2019.

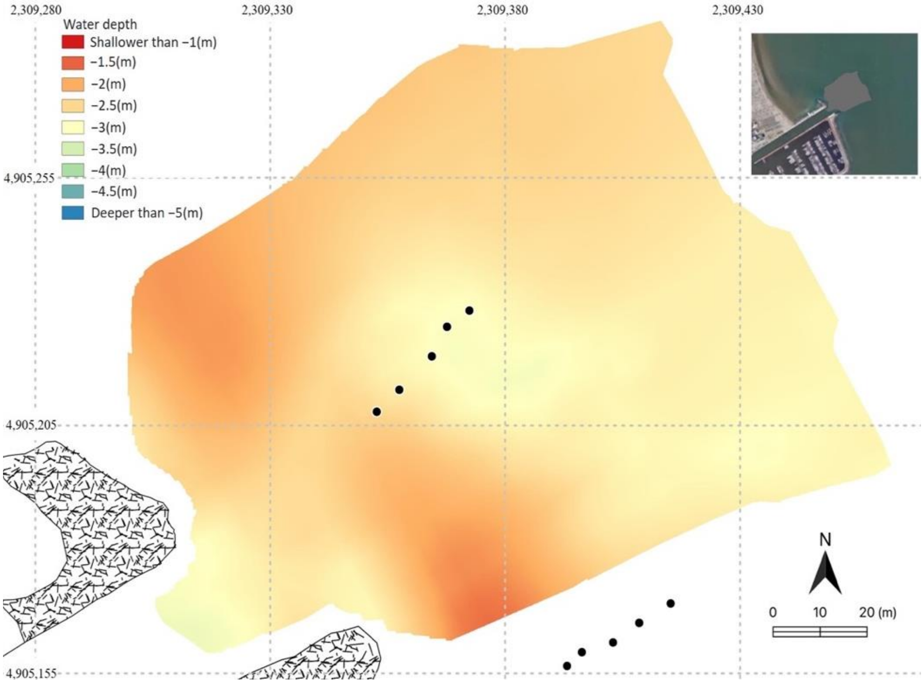

Figure 2.B. 5 Bathymetry of 9 January 2020.

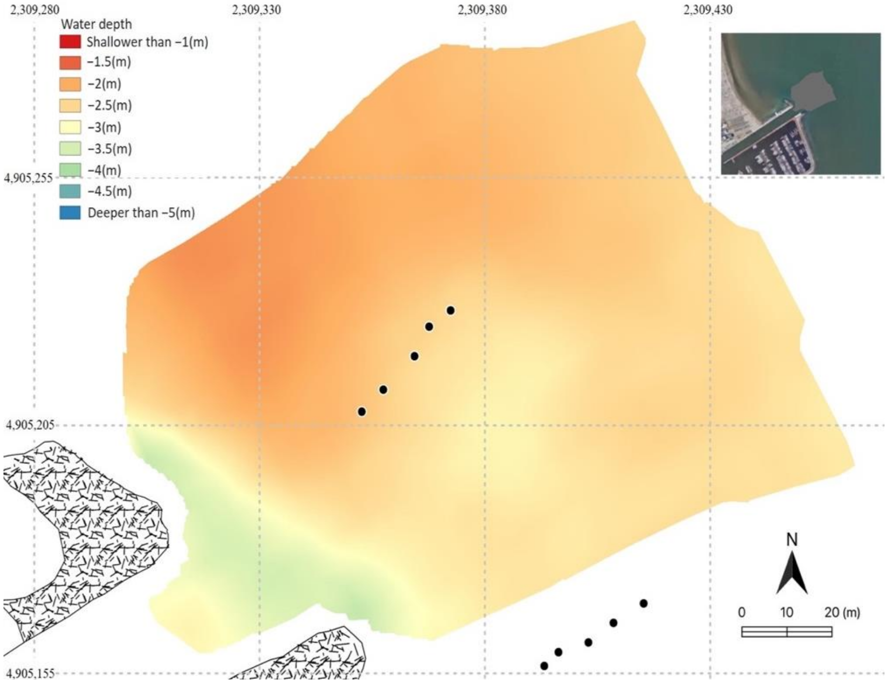

Figure 2.B. 6 Bathymetry of 30 April 2020.

2.9 References

[1] L. Palumbo, “Sediment management of nations in Europe.,” *In Sustainable management of sediment resources,* vol. 2, pp. 11-58, 2007.

[2] P. Magaña, M. Á. Reyes-Merlo, Á. Tintoré, C. Zarzuelo and a. M. Ortega-Sánchez., “An Integrated GIS Methodology to Assess the Impact of Engineering Maintenance Activities: A Case Study of Dredging Projects.,” *Journal of Marine Science and Engineering,* vol. 8, no. 3, p. 186, 2020.

[3] R. Guerra, A. Pasteris and a. M. Ponti., “Impacts of maintenance channel dredging in a northern Adriatic coastal lagoon. I: Effects on sediment properties, contamination and toxicity.,” *Estuarine, Coastal and Shelf Science,* vol. 85, no. 1, pp. 134-142, 2009.

[4] M. Ponti, A. Pasteris, R. Guerra and a. M. Abbiati., “Impacts of maintenance channel dredging in a northern Adriatic coastal lagoon. II: Effects on macrobenthic assemblages in channels and ponds.,” *Estuarine, Coastal and Shelf Science,* vol. 85, no. 1, pp. 143-150, 2009.

[5] A. D. McQueen, B. C. Suedel, C. d. Jong and a. F. Thomsen, “Ecological risk assessment of underwater sounds from dredging operations,” *Integrated Environmental Assessment and Management,* vol. 16, no. 4, pp. 481-493, 2020.

[6] C. Memos, P. Chiavaccini, R. Dornhelm, R. Hoekstra, P. Inglis, S. Sannasiraj, O. Stoschek, A. Willemsen, E. Mink and V. Sundar, “Anti-Sedimentation Systems for Marinas and Yacht Harbours,” PIANC report 130, Brussel, Belgium, 2015.

[7] A. Bianchini, F. Cento, A. Guzzini, M. Pellegrini and a. C. Saccani, “Sediment management in coastal infrastructures: Techno-economic and environmental impact assessment of alternative technologies to dredging.,” *Journal of environmental management,* vol. 248, p. 109332, 2019.

[8] M. Sane, H. Yamagishi, M. Tateishi and a. T. Yamagishi, “Environmental impacts of shore-parallel breakwaters along Nagahama and Ohgata, District of Joetsu, Japan.,” *Journal of environmental management,* vol. 82, no. 4, pp. 399-409, 2007.

[9] “Water Injection Dredging, Facts about–An Information Update from the IADC; International Association of Dredging Companies,” International Association of Dredging Companies (IADC). , Voorburg, South Holland,, 2013.

[10] K. L. Spencer, R. E. Dewhurst and a. P. Penna, “Potential impacts of water injection dredging on water quality and ecotoxicity in Limehouse Basin, River Thames, SE England, UK,” *Chemosphere,* vol. 63, no. 3, pp. 509-521, 2006.

[11] A. G. Pledger, P. Brewin, K. L. Mathers, J. Phillips, P. J. Wood and a. D. Yu, “The effects of water injection dredging on low-salinity estuarine ecosystems: Implications for fish and macroinvertebrate communities,” *Ecological Indicators,* vol. 122, p. 107244, 2021.

[12] R. Archetti, L. Damiani, A. Bianchini, C. Romagnoli, M. Abbiati, F. Addona, L. Airoldi and e. al., “Innovative strategies, monitoring and analysis of the coastal erosion risk: The STIMARE project,” in *In The 29th International Ocean and Polar Engineering Conference,* OnePetro, 2019.

[13] A. Bianchini, A. Guzzini, M. Pellegrini, C. Saccani, M. G. Gaeta and a. R. Archetti., “Coastal erosion mitigation through ejector devices application,” *Italian journal of engineering geology and environment,* pp. 13-22, 2020.

[14] M. Pellegrini, M. Abbiati, A. Bianchini, M. A. Colangelo, A. Guzzini, B. Mikac, M. Ponti, G. Preda, C. Saccani and a. A. Willemsen, “Sustainable sediment management in coastal infrastructures through an innovative technology: preliminary results of the MARINAPLAN PLUS LIFE project,” *Journal of Soils and Sediments,* vol. 20, no. 6, pp. 2685-2696, 2020.

[15] A. Bianchini, M. Pellegrini and a. C. Saccani, “Zero environmental impact plant for seabed maintenance,” in *In Proceedings of the International Symposium on Sediment Management I2SM,* Ferrara, Italy, 2014.

[16] M. Pellegrini and a. C. Saccani, “Laboratory and field tests on photo-electric probes and ultrasonic Doppler flow switch for remote control of turbidity and flowrate of a water-sand mixture flow.,” *In Journal of Physics: Conference Series,* vol. 882, no. 1, p. 012008, 2017.

[17] M. Pellegrini, G. Preda and a. C. Saccani, “Application of an innovative jet pump system for the sediment management in a port channel: Techno-economic assessment based on experimental measurements,” *Journal of Marine Science and Engineering,* vol. 8, no. 9, p. 686, 2020.

[18] D. Bonaldo, F. Antonioli, R. Archetti, A. Bezzi, A. Correggiari, S. Davolio, G. D. Falco and e. al., “Integrating multidisciplinary instruments for assessing coastal vulnerability to erosion and sea level rise: Lessons and challenges from the Adriatic Sea, Italy,” *Journal of coastal conservation,* vol. 23, no. 1, pp. 19-37, 2019.

[19] R. Archetti, A. Paci, S. Carniel and a. D. Bonaldo, “Optimal index related to the shoreline dynamics during a storm: the case of Jesolo beach.,” *Natural hazards and earth system sciences,* vol. 16, no. 5, pp. 1107-1122, 2016.

[20] M. G. Gaeta, D. Bonaldo, A. G. Samaras, S. Carniel and a. R. Archetti, “Coupled wave-2D hydrodynamics modeling at the Reno river mouth (Italy) under climate change scenarios.,” *Water,* vol. 10, no. 10, p. 1380, 2018.

[21] M. G. Gaeta, A. G. Samaras, I. Federico, R. Archetti, F. Maicu and a. G. Lorenzetti, “A coupled wave–3-D hydrodynamics model of the Taranto Sea (Italy): a multiple-nesting approach,” *Natural hazards and earth system sciences,* vol. 16, no. 9, pp. 2071-2083, 2016.

[22] A. G. Samaras, M. G. Gaeta, A. M. Miquel and a. R. Archetti, “High-resolution wave and hydrodynamics modelling in coastal areas: operational applications for coastal planning, decision support and assessment.,” *Natural hazards and earth system sciences,* vol. 16, no. 6, pp. 1499-1518, 2016.

[23] P. Loza, “Sand Bypassing Systems. Master Thesis in Environmental Engineering, Master′s Thesis,” University of Porto, Porto, Portugal, 2008.

[24] M. Aguzzi, F. Bonsignore, N. D. Nigris, M. Morelli, T. Paccagnella, C. Romagnoli and S. Unguendoli, “Stato del Litorale Emi-liano-Romagnolo al 2012,” in *Erosione e Interventi di difesa; Arpae Emilia-Romagna,* Bologna, Italy, 2016.

[25] B. Cushman-Roisin, M. Gacic, P.-M. Poulain and a. A. Artegiani, “Physical oceanography of the Adriatic Sea: past, present and future,” Springer Science & Business Media, 2013.

[26] P. Lionello, L. Cavaleri, K. M. Nissen, C. Pino, F. Raicich and a. U. Ulbrich, “Severe marine storms in the Northern Adriatic: Characteristics and trends.,” *Physics and Chemistry of the Earth, Parts A/B/C,* vol. 40, pp. 93-105, 2012.

[27] L. Perini, L. Calabrese, P. Luciani, M. Olivieri, G. Galassi and a. G. Spada., “Sea-level rise along the Emilia-Romagna coast (Northern Italy) in 2100: scenarios and impacts.,” *Natural Hazards and Earth System Sciences,* vol. 17, no. 12, pp. 2271-2287, 2017.

[28] ARPAE, ARPAE, [Online]. Available: (https://www.arpae.it/sim/?mare/boa. [Accessed 27 Dec 2020].

[29] M. Pellegrini, A. Aghakhani, M. G. Gaeta, R. Archetti, A. Guzzini and a. C. Saccani, “Effectiveness Assessment of an Innovative Ejector Plant for Port Sediment Management.,” *Journal of Marine Science and Engineering,* vol. 9, no. 2, p. 197, 2021.

[30] L. Perini, L. Calabrese, M. Deserti, A. Valentini, P. Ciavola and a. C. Armaroli, “Le mareggiate e gli impatti sulla costa in Emilia-Romagna 1946–2010.,” *C 15* , 2011.

[31] C. Armaroli, P. Ciavola, L. Perini, L. Calabrese, S. Lorito, A. Valentini and a. M. Masina, “Critical storm thresholds for significant morphological changes and damage along the Emilia-Romagna coastline, Italy,” *Geomorphology,* vol. 143, pp. 34-51, 2012.

[32] R. Dolan and a. R. E. Davis, “An intensity scale for Atlantic coast northeast storms,” *Journal of coastal research,* pp. 840-853, 1992.

[33] E. T. Mendoza and a. J. A. Jiménez, “Storm-induced beach erosion potential on the Catalonian coast,” *Journal of Coastal Research,* pp. 81-88, 2006.

3 CHAPTER 3: CO_2 emission of hydrogen generation via PEM and Alkaline electrolysers, and sensitivity analysis regarding cell characteristics and energy source

ABSTRACT

The major hydrogen business worldwide is related to industrial consumers. Currently, hydrogen is almost entirely generated from fossil fuel energy sources. In the last few years, interest in hydrogen has grown for the decarbonization of multiple sectors, such as industry, transport, and buildings. However, the mix of various technologies and energy sources applied for hydrogen production affects the substitution of natural gas and other fossil fuels with hydrogen.

This chapter's objective is the investigation of current carbon dioxide emissions related to hydrogen production in Australia and Italy through PEM and alkaline electrolysers, and to assess the potential impact regarding cell characteristics variation and three energy scenarios. A sensitivity analysis is performed to determine the critical parameters. Based on experimental data extracted from the literature and the equation obtained for sensitivity analysis it is found that the energy consumption for hydrogen production using PEM technology is more sensitive to cell voltage compared to current density. This result indicates the importance of cell manufacturing and electrolyte resistance. Furthermore, by performing sensitivity analysis regarding energy sources scenarios it is found that carbon dioxide emission in Australia has higher sensitivity to renewable energy sources rather than in Italy.

Keywords:

Hydrogen, CO_2, Electrolysis, Australia, Italy, Renewable energy sources (RES)

3.1 Introduction

The growth of human population and increase in anthropogenic activities have significantly impacted the total world energy consumption, which is mostly based on fossil fuel sources. The result of more fossil fuel consumption is more Greenhouse gas (GHG) emissions which cause climate change and global warming. To reach the Paris agreement objective, which is limiting the global mean temperature increase to 2°C it is estimated that approximately 80% of GHG emissions should be reduced by 2050, compared to 1990 [1]. In 2021, the global carbon dioxide emissions from energy generation are estimated around 33885 million tonnes of carbon dioxide [2]. Due to the increase in global energy demand, the potential diminishing of fossil fuels, and huge environmental impact of fossil fuels, researchers and industries have focused on the transition from fossil fuel sources to low carbon systems and sources of energy, especially renewable energy sources (RES). In recent decades, renewable energies such as wind, solar, and hydropower have significant contributions to world energy production. Figure 3. 1 presents the electricity generation via various sources in the period between 1985 and 2020. The data are extracted from the BP Statistical Review of World Energy [2]. It is seen that a bit lower than 60% of the world's electricity in 2020 was generated by fossil fuels, and the fluctuation of contribution ranges between 60 to 70 during the mentioned period. However, RES contribution to the total energy production of Australia in 2020, according to the Department of Industry, Science, Energy, and Resources, was around 24% [3]. While the percentage of RES contribution in Italy in 2019 was 18% [4].

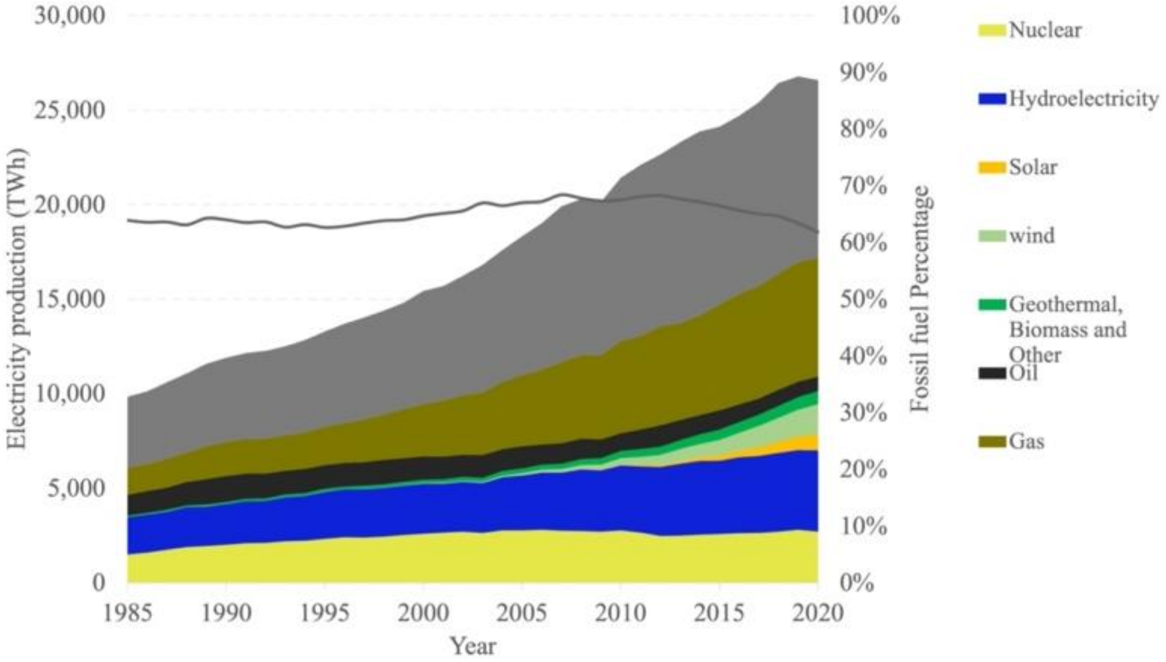

Figure 3. 1 Electricity production by source, World (data from *[2]*).

The contribution of different energy sources arises several research questions as follow:

-How to increase the contribution of RES for climate change mitigation?

-Which technology can be the possible solution for low contribution of RES?

-What are the effective parameters on the performance of the proposed technology?

-Is the proposed technology sustainable?

The issue associated with RES is its intermittency and unpredictability, which results in contribution restriction in the supply chain. To raise the contribution and increase the ability of RES to supply energy demand it is required to use energy storage systems. There are several challenges for storage systems to be able to supply immediately when it is required [5]. Hydrogen technology could be considered as a solution to store energy generated from RES. However, it is required to prove hydrogen technology as a solution for reaching net zero emission and an alternative to fossil fuels. For this purpose, various aspects should be assessed, such as hydrogen applications, production, and environmental impact, which are discussed in this chapter. This first section of the chapter includes hydrogen applications, production, literature review of proton exchange membrane (PEM) and alkaline electrolysers, energy consumption, and manufacturers to find out the reason of this study regarding the lag of previous studies, which are explained in the scope section. The main scope of this study is the carbon dioxide footprint of hydrogen generation using PEM and alkaline electrolyser at operational lever and sensitivity analysis regarding cell characteristics and source of energy which are discussed in section 3.23.3.

3.1.1 literature review

3.1.1.1 Hydrogen application

Application of hydrogen could be in internal combustion engines as fuel in transport, such as hydrogen-fuelled buses, or in fuel cells. It can be used for industrial consumption, such as production of ammonia, methanol, pharmaceutical [6], petroleum refining, metal treating [5], and the food and beverages sector. In the near future it is predicted that hydrogen can be utilized in power generation, transport sector, and heating in residential, although even if many technical and regulatory gaps are still unsolved [5]. In addition, hydrogen can be considered as solution for the integration of gas and electricity sectors. This integration can be achieved by injecting hydrogen into the natural gas network. However, specific values of hydrogen concentration are provided in legislation documents of different countries. The application of hydrogen integration to the natural gas network in real networks is hindered due to several challenges such as gas leakages check, material degradation, safety, quality management, and appliance proper and safe performance [7].

Hydrogen combustion products is large amount of water and energy. In addition, hydrogen combustion does not release GHG. Another benefit of the hydrogen industry is related to social impact by creating employment [6].In comparison to other hydrocarbons it has high combustion temperatures which leads to the need of special material or combustion control to avoid material degradation.

3.1.1.2 Hydrogen production

Although hydrogen is not a primary energy source [8] it can be considered a source of energy that is capable of producing direct energy that facilitates energy production [6]. Hydrogen can be considered a suitable net zero-emission alternative to fossil fuels since it is the only carbon-free with the highest energy content per kg in comparison to any known fuel [5].

3.1.1.2.1 Production methods

If the input source is considered for the classification of hydrogen generation, there are two main categories of hydrogen production: conventional and renewable technologies. The conventional class contains the consumption of fossil fuels and methods of hydrocarbon reforming and pyrolysis. The process could be steam reforming, dry reforming, cracking natural gas, coal gasification, and partial oxidation which are highly energy-consuming processes [5, 6]. The second type includes hydrogen generation using water or biomass. Water can be split by various methods such as electrolysis, thermolysis, and photo-electrolysis [5]. There are several electrolysis technologies: Alkaline, PEM, solid oxide electrolysis cells (SOEC), and Anion exchange membrane (AEM). Alkaline and PEM technologies are the most widespread. Currently, 96% of the hydrogen generation in the world is based on conventional class and the most commonly used hydrogen generation technology is the steam methane reforming (SMR) method. The cheapest technology is SMR and around half of the world’s hydrogen is produced by this method [9, 10]. However, Hurtubia et al. [11] stated that the contribution of fossil fuels is 98% in 70 Mt of annual hydrogen production, including 75% natural gas and 23% coal, and only 2% is produced by electrolysis. Hydrogen produced through SMR is called grey hydrogen. If the emitted carbon dioxide in SMR process is captured by carbon capture and storage technologies, it results in blue hydrogen. If RES is used as the electricity source for hydrogen production, this hydrogen is called green hydrogen. Green hydrogen is known as the cleanest energy carrier [5].

To reduce the carbon dioxide emission of hydrogen generation it is recommended to use RES as an energy source [12], however, there are other methods without GHG emission, such as microalgae, which are under the early stage of investigation [11].

3.1.1.2.2 Hydrogen production challenges

One of the main challenges in hydrogen generation is its unavailability in nature in pure form. Hydrogen can be found only in compound form. However, very low concentrations of hydrogen molecule can be found in the atmosphere in gaseous form which is not affordable to be captured. Another important challenge which has played an essential role over the past two decades is policies in investment, market development, and renewable energy-related industries development [9]. Cost of hydrogen production is another challenge which should be taken into account to reach a sustainable technology. Hydrogen generation cost is reported differently in various studies. Kopteva et.al [13] reported that the cost of hydrogen production ranges approximately from 2 to 5 US dollars per kg. While, in another study, [5, 14], the range of hydrogen generation cost from solar thermal, solar PV, nuclear, and wind, in 2010, for electrolysis was reported 4.15 to 23.27 dollars per kilogram of hydrogen. One kg hydrogen contains 33.33 kWh primary energy, therefore, the energy will be 0.06 to 0.7 US dollars per kWh which is higher than the price of fossil fuel. Australia objective is reaching under $2 per kilogram of hydrogen production which can be competitive with conventional fuels, however, there would be other expenses such as compressing, storing, and transportation of hydrogen which could cost up to $2 per kilogram of hydrogen [15]. The projection of the Australian government for 2030 is 2 to 4 A$ per kilogram of clean hydrogen [16]. Janssen et. al [17] predicted that the cost of hydrogen generation by means of RES can be less than 2 €/kg until 2050 in several countries in Europe. This wide range of hydrogen generation costs through electrolysis indicates that the production considerably depends on RES availability and its cost.

Hydrogen blending with natural gas is another issue with hydrogen technology. It is impossible to blend considerably high quantities of pure hydrogen into the natural gas network. Only a few countries allow direct injection into the infrastructure under determined circumstances and below the defined threshold. Thus, separate distribution infrastructures or suitable hydrogen carriers are needed which could be another challenging issue [7].

Therefore, applicable, and sustainable methods and efficient distribution network are needed to produce and deliver affordable clean hydrogen. This chapter focuses on hydrogen production via electrolysis and the impact assessment of using RES as energy source. Market-ready technologies, i.e., PEM and alkaline electrolysers, and their operational environmental and GHG impact are assessed in this study.

3.1.1.2.3 PEM electrolysis

The core of a PEM electrolyser cell is membrane, which is usually sulfonated tetrafluoroethylene is located at the centre of each cell. The anode and cathode layers are located on two sides of the membrane. The most common materials of anode and cathode are Iridium and platinum, respectively, which are used as noble metal catalysts. The next layer right after anode and cathode layers is porous transport layer (sometimes called the gas diffusion layer, or current collectors), which titanium is mostly used on the anode side and carbon paper is used on the cathode side. The last layer of each cell is the bipolar plate, which is attached on both sides, titanium is mostly used as a bipolar plate. It is possible to connect several single cells in series to reach the desired capacity of the system, which provide the PEM stack. To fix the cells in a stack end plates, bolts, nuts, and sealings are used [18]. In this study, hydrogen generation at the stack level is investigated.

The water electrolysis overall reaction is as in Eq.3. 1, which is an endothermic reaction:

$$\mathrm{H_2O} \rightarrow {}^{1}/_{2}\,\mathrm{O_2} + \mathrm{H_2} \qquad \text{Eq.3. 1}$$

In PEM technology water is oxidized on the anode side which oxygen is produced while the reduction reaction occurs on the cathode side to generate hydrogen, as it is seen in Eq.3. 2 and Eq.3. 3.

$$\mathrm{H_2O} \rightarrow {}^{1}/_{2}\,\mathrm{O_2} + 2\mathrm{H^+} + 2\mathrm{e^-} \qquad \text{Eq.3. 2}$$

$$2\mathrm{H^+} + 2\mathrm{e^-} \rightarrow \mathrm{H_2} \qquad \text{Eq.3. 3}$$

PEM technology can produce dry hydrogen with a purity of 99.99% [19] at a pressure of less than 30 bar and a temperature of 323–353 K [20]. The efficiency of the PEM system can be around 70 % and the stack energy consumption could be 4.2-5.6 kWh/m^3 [20]. Based on Zhao et al. [21] study, considering the electricity production from a 3 MW wind plant in Denmark and using the ecoinvent database for the emissions factors, electricity consumption contribution to the global warming potential (GWP) index of hydrogen generation through the PEM technology is around 90%, which indicates the importance of stack operational level assessment.

To produce pure hydrogen other units are required in the PEM electrolysis plant, such as water pump, water purification, heat exchanger, ion exchanger, circulation pump, gas/water separator, demister, and deoxidizer which are not in the scope of this study and are discussed in chapter 4.

The solid polymer electrolyte which is used in the PEM system eliminates the necessity of circulating aqueous electrolyte and resists against gas bubbles [21]. The thickness of a PEM cell with can be around 20–300μm, which is capable of operating at high pressures, more than 30 bar. Furthermore, since PEM system can operate with high energy density, the gases have high purity, and this technology is effective at high voltages the operational cost of PEM is lower in comparison to other electrolysis [6]. In comparison to alkaline technology, PEM system can operate more flexible regarding load range, which makes this technology more reliable for RES electricity production, in addition, PEM technology has higher cell efficiency [11]. Moreover, PEM electrolyser can operate with higher current density [21]. SOEC technology operates at significantly greater temperature in comparison to PEM technology. Furthermore, SOEC has some issues in terms of degradation and stability which should be solved before commercialization for large-scale industrial projects [22].

Despite the advantages of the PEM electrolyser compared with other electrolysis technologies, it has several drawbacks. PEM system components, such as catalyst materials, are relatively expensive. In addition, PEM system is complex due to high-pressure operation. The other issues are high water purity, low durability, and significant corrosion in systems with high capacity which require profound study in future research to find solutions [6, 11].

3.1.1.2.4 Alkaline electrolyser

The most mature and oldest water electrolysis method is alkaline technology [23]. The overall reaction of electrolysis in an alkaline electrolyser is the same as PEM electrolyser while the reactions in the cathode and anode are different as in Eq.3. 4 and Eq.3. 5, respectively [24]:

$$2H_2O + 2e^- \rightarrow H_2 + 2OH^- \qquad \text{Eq.3. 4}$$

$$2OH^- \rightarrow {}^1\!/_2\, O_2 + H_2O + 2e^- \qquad \text{Eq.3. 5}$$

Two configurations of the alkaline cell are available, conventional and zero-gap. In conventional configuration, there is a specific distance between electrodes, while in zero-gap, electrodes are directly pressed to the separator to minimize ohmic losses in the electrolyte. Various parameters influence the ohmic resistance of the cell such as the electronic conductivity of the electrode material , the ionic conductivity of the separator membrane, the specific conductivity of the electrolyte, and gas bubble effects. The separator could be a ZIRFON product (Agfa) or dense anion exchange membrane. The widely used type of electrodes are made of nickel. Nickel causes overvoltage for reactions which could be reduced by adding catalysts such as iron and molybdenum to anode and cathode reactions, respectively. KOH (Potassium hydroxide, 20-30% at 50-80°C) is mostly used as an electrolyte which is an aqueous solution. Cheaper choice is diluted sodium hydroxide for the electrolyte, but it has lower conductivity. The hydrogen gas products purity without any additional purification is higher than 99.9 vol.% through alkaline electrolyser and it is between 99.0 to 99.5 vol.% for oxygen gas. Alkaline system operates under 1 to 20 bar pressure and the current density of 0.05 to 0.7 $A.cm^{-2}$ [24]. The operating temperature ranges between 20-100 °C [25]. This range can be up to 150 °C which could be proper for large-scale hydrogen production [26]. Alkaline system efficiency could be 65-75 % and the stack energy consumption can be 4.2-5.9 kWh/m^3 [20]. According to Zhao et al. [21] study, considering the electricity production from a 3 MW wind plant in Denmark and using the ecoinvent database for the emissions, the contribution of electricity consumption to the GWP index of hydrogen generation through alkaline technology is more than 95%.

Relatively low cost (electrodes can be made of inexpensive and abundant materials), long-term service life, limited water purification requirements, simple design, and high reliability in operation are some of alkaline electrolyser advantages. Despite the advantages it has an important issue which is related to its high energy consumption which needs improvement [27].

3.1.1.2.5 Cell characteristics and hydrogen yield

3.1.1.2.5.1 PEM electrolyser

Table 3.A. 1 and Table 3.A. 2 in the appendix includes studies about PEM technology which provided direct or indirect information about cell voltage, current density, and hydrogen yield. In this chapter, “Case” term refers to various experimental test conditions in each study.

The range of cell voltage and current density in studies provided in the Table 3.A. 1 is, 1.63-2.46 V and 0.5-3 A/cm^2, respectively. The minimum current density was used in Kumar et al. [28], and Millet et al. [29] studies, and the maximum one was used by Bareiß et al. [30], Rakousky et al. [31], and Bernt and Gasteiger [32]. The maximum and minimum cell voltage were studied by Di Blasi et al. [33] and Kumar et al. [28], respectively.

Power density is calculated by the product of cell voltage level and current density. Cell efficiency range according to the studies provided in Table 3.A. 1 is 0.85-6.3. To provide a comparison between studies it is assumed that the experimental units are modular, and it is possible to add them together to reach 1 MW capacity without any impact on performance. The active area for 1 MW in each study is calculated as in Eq.3. 6:

$$A_A(m^2) = Capacity(10^6 W)/(power\ density\left(\frac{W}{m^2}\right)) \qquad \text{Eq.3. 6}$$

Where A_A is the active area (m^2)

Cell efficiency regarding lower heating value, $\boldsymbol{\eta}$cell (LHV), is calculated as follow [30]:

$$\eta_{cell,LHV} = 1.23V/E_{cell} \qquad \text{Eq.3. 7}$$

Where E_{cell} is cell voltage (V).

The range of cell efficiency based on the studies provided in Table 3.A. 1 is 0.5-0.75. The cell voltage under typical operating conditions is reported between 1.5 to 2V by Buttler and Spliethoff [34], which lead to 62% to 82% based on LHV.

Theoretical and experimental energy consumptions for hydrogen generation are provided in Table 3.A. 1 and Table 3.A. 2 in the appendix.

The theoretical hydrogen yield of the cell (l/h) is calculated by modification of the equation in Atlam and Kolhe *[35]* study after unit conversion as follow:

$$v_H = v_M\left(\frac{3600s}{1h}\right)(\frac{I}{2F}) \qquad \text{Eq.3. 8}$$

Where:

v_H = Theoretical hydrogen yield of cell [l/h];

v_M = one molar volume which can be calculated by ideal gas expression $v_M = \frac{R(T)}{P}$;

R = ideal gas constant 0.08206 [$\frac{l.atm}{mol.K}$];

T = temperature [K];

P = pressure [atm];

I = current [A] or [C/s], calculated by the product of single cell area and current density;

F = Faraday constant [C/mol], 96,485.332;

Theoretical total hydrogen yield (m^3/h) is calculated as follow:

$$v_{T,theoretical} = A_{1MW} \times \frac{v_H}{cell\ area(m^2)} \times 10^{-3} \qquad \text{Eq.3. 9}$$

Where:

A_{1MW} = active area for 1MW (m^2)

$v_{T,theoretical}$ = Theoretical total hydrogen yield [m^3/h];

Theoretical specific energy consumption (kWh/kg) to produce 1 kg hydrogen can be calculated by the following equation, considering that each kg of hydrogen is equal to 11.1 Nm^3:

$$E_{c,theoretical} = (1000\ kW/\ v_{T,theoretical}) \times 11.1\ (\frac{m^3}{kg}) \qquad \text{Eq.3. 10}$$

The information about the experimental hydrogen yield of the cell is extracted directly from literature or calculated by means of the faradaic efficiency and theoretical yield. Experimental total hydrogen yield and experimental specific energy consumption are calculated with the same method as the theoretical one, it should be noted that the experimental hydrogen yield of cell is used instead of the theoretical one. The ratio between the experimental hydrogen yield and the theoretical one is called faradaic efficiency. Faradaic efficiency range according to the studies provided in Table 3.A. 2 is 83.39-93.81 %. The average experimental and theoretical hydrogen yields in the studies in the Table 3.A. 2 are approximately 250 and 285 m^3/h, respectively. The maximum theoretical hydrogen yield is estimated for Millet et al. [29] study, 323 m^3/h, and the maximum experimental was obtained by Di Blasi et al. [33], 306 m^3/h.

3.1.1.2.5.2 Alkaline electrolyser

Table 3.A. 3 provides information of studies about alkaline electrolysis which include information about electricity consumption for 1 kg hydrogen production and cell efficiency and hydrogen yield are represented. Cell voltage and current density information in these studies is not enough to be shown in the table. The cell efficiency range, referred to LHV, in these studies is 0.5-0.78. The average experimental hydrogen yield is 25 m^3/h. It is not possible to use Eq.3. 8 to calculate the theoretical hydrogen yield since the information on current density is not completely provided in these studies.

Energy consumption and the source of energy for electricity generation are the most important concerns regarding hydrogen production. “Theoretical specific energy consumption kWh/kg” and “experimental specific energy consumption kWh/kg (using Faradaic efficiency or data in articles)” columns from Table 3.A. 2 are used to produce Figure 3. 2, which can be used to visually compare the reviewed literature in terms of energy consumption. Change in Gibbs free energy can be calculated as the following equation [36]. Change in Gibbs free energy is considered 237.22 kJ/mol as in Kumar and Himabindu study [22]. This value is also considered by Millet et al. [37] and Selamet et al. [38]:

$$\Delta G = \Delta H - T\Delta S \qquad \text{Eq.3. 11}$$

Where:

ΔG = change in Gibbs free energy, kJ/mol

ΔH = change in enthalpy, 285.83 kJ/mol [36]

T = temperature in Kelvin

ΔS = change in entropy kJ/mol.K

The minimum required energy to produce 1 kilogram of hydrogen is calculated 32.95 kWh/kg, which is calculated considering that the Gibbs free energy in the hydrogen production reaction, 237.22 kJ, is used to produce 2 grams of hydrogen. It is shown as the theoretical minimum required energy based on Gibbs free energy in Figure 3. 2 and Figure 3. 3.

It is possible to use the change of enthalpy instead of Gibbs free energy in hydrogen production reaction to define the theoretical minimum required energy based on enthalpy. The amount of change of enthalpy in this reaction is 285.83 kJ, which is used to produce 2 grams of hydrogen. Therefore, the energy required to produce 1 kilogram of hydrogen is 39.70 kWh/kg, which is shown as the theoretical minimum required energy based on enthalpy in Figure 3. 2 and Figure 3. 3.

By applying cell voltage greater than 1.23 V the required Gibbs free energy is supplied and the thermal energy from the environment helps the water split. A minimum voltage of 1.48 V is required to supply the whole reaction enthalpy [30], which is compatible with the voltages shown in Table 3.A. 1.

It is seen in Figure 3. 2 and Figure 3. 3 that all results of collected literature are in the mentioned range or above it. By comparing these figures, it can be recognized that, generally, PEM electrolysers uses less energy than alkaline electrolysers to generate 1 kg hydrogen.

3.1.2 Manufacturers

Several manufacturers all around the world produce PEM and alkaline electrolysis systems. Information about power consumption for hydrogen generation is available in their public datasheet. However, it should be noted that several additional units are installed to ensure proper operations of the electrolysers like, for example, but not limited to water pumps, cooling fans, and control system components that increases the total electricity consumption. Table 3.B. 1 is provided as the best knowledge of the author and the availability of data. The energy consumption ranges from 42.2 to 65.6 kWh/kg of hydrogen which is generally higher than the experimental values shown in Figure 3. 2 and Figure 3. 3. This difference could be due to various reasons such as difference in stack characteristics, scaling and balance of plant, and the system efficiency. The average energy consumption for alkaline and PEM technology technologies is 54.7 and 53 kWh/kg, respectively.

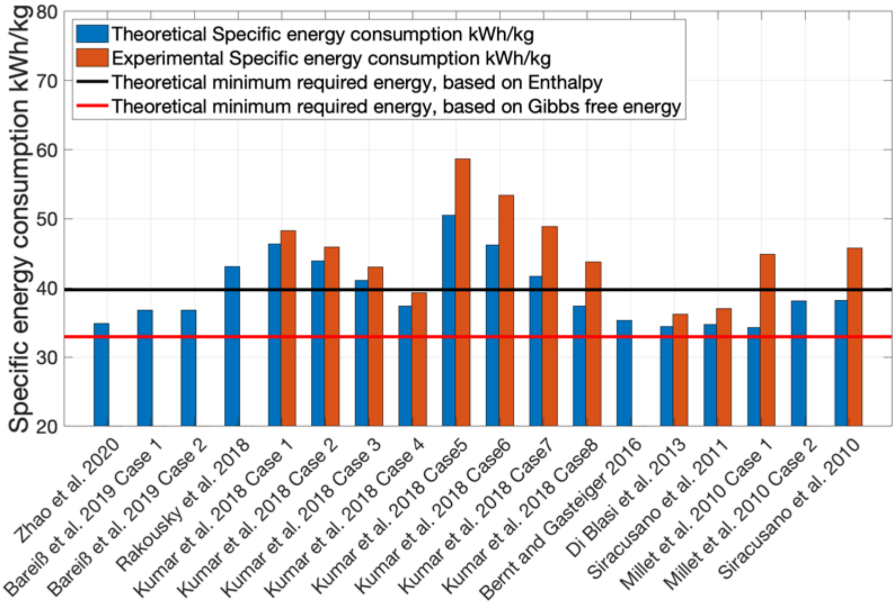

Figure 3. 2 Specific energy consumption kWh per kilogram of hydrogen production using PEM electrolyser

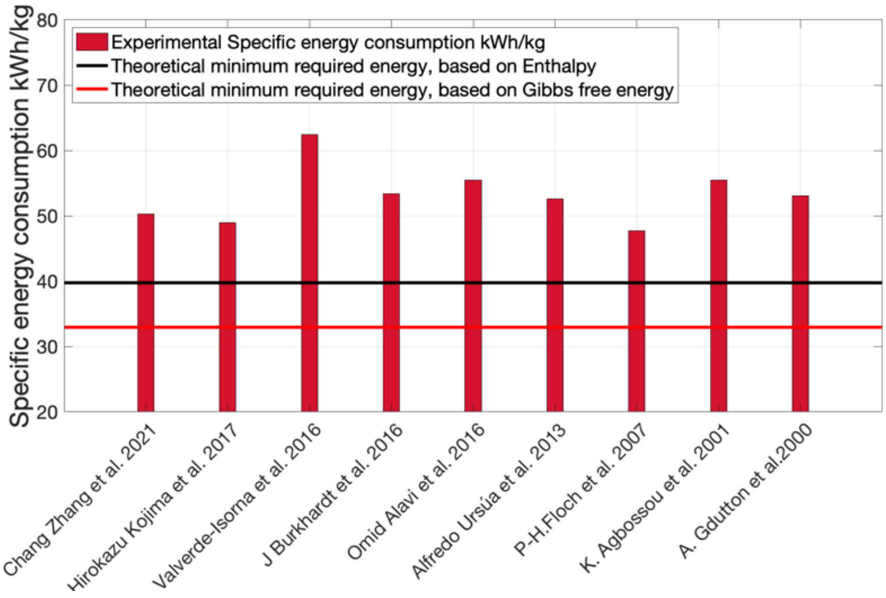

Figure 3. 3 Specific energy consumption kWh per kilogram of hydrogen production using Alkaline electrolyser

3.1.3 Scope of the chapter

Previous studies focused mainly on the techno-economic analysis [22], [39], [40], [41], life cycle assessment of hydrogen production, and defining the most important contributor to carbon dioxide emission among the components and procedures of hydrogen generation. Furthermore, the main comparison review has been related to the materials, methods, and components in publications [42]. Considering the difference in electrolysers characteristics and the variety of input energy sources in different countries, lack of comprehensive comparative assessment of environmental impact and sensitivity analysis of cell characteristics and energy sources is obvious and is discussed in this chapter.

The aims of this study are 1) the assessment of the minimum amount of various fuel types for hydrogen generation via PEM and alkaline technologies and their CO_2 emission, 2) the estimation of the CO_2emission to produce 1 kg hydrogen through PEM and alkaline technologies in Europe and Australia by means of the current electricity generation condition, 3) projection of the carbon dioxide emission to produce 1 kg hydrogen using PEM and alkaline systems in Europe and Australia in 2030, 4) sensitivity analysis of energy consumption for hydrogen production via PEM and alkaline regarding cell characteristics, and 5) sensitivity analysis of energy consumption for hydrogen generation via PEM and alkaline regarding energy scenarios.

In this chapter, carbon dioxide emissions regarding the fuel type and the location of energy production for the current grid condition and prediction for 2030 are assessed. In addition, empirical equations to define the most effective cell characteristics and the impact of the transition from fossil fuels to RES in hydrogen generation through PEM and alkaline electrolysis are provided as a result of sensitivity analysis regarding cell characteristics and energy sources.

3.2 Methodology

3.2.1 Environmental impact

In this Chapter carbon dioxide footprint of hydrogen generation at the stack operational level through PEM and alkaline electrolysers is investigated. Emission factors vary regarding energy sources and the location of energy generation.

3.2.1.1 Energy sources

The electrical energy input to generate hydrogen can be provided by means of different fuel types and RES. The Australian government, Department of Industry, Science, Energy, and Resources [43] provides the energy content of various fuels which is listed in Table 3.C. 1 in the appendix.

By using "experimental required energy" reported in Table 3.A. 2 and Table 3.A. 3 and the energy contents in Table 3.C. 1, the minimum required amount of each fuel to generate 1 kg hydrogen can be calculated as in Eq.3. 12:

$$F_m = \frac{E_{esc} \times (0.0036\ (GJ)/1\ kWh)}{E_c} \times \frac{1000\ (kg)}{1\ (t)} / \eta_f \qquad \text{Eq.3. 12}$$

F_m = Minimum required fuel (kg)

E_{esc} = Experimental specific energy consumption (kWh)

E_c = Energy content (GJ/t)

η_f = Thermal to power energy conversion efficiency of fuel kind

Thermal to power energy conversion efficiency of fuel kind varies regarding the fuel type, generator type, and process of electricity generation. In this study, for simplification, a combined gas/steam turbine with an average efficiency of thermal to mechanical energy of 50% [44] is assumed for any fuel type, and mechanical to electrical conversion efficiency of 98% is considered. Thus, thermal to power energy conversion, which is the product of thermal to mechanical energy efficiency and mechanical to electrical conversion efficiency, is considered 49% for the calculations (590%×98%=49%).

It is assumed that 100% of energy from fuel combustion is used to generate hydrogen, energy consumption in other units of the plant is not considered in this study.

3.2.1.2 Carbon dioxide emission based on fuel type

The Australian government, Department of Industry, Science, Energy, and Resources [43] provides also the emission factor of various fuels which is listed in Table 3.C. 1 in the appendix. By using the emission factor and the experimental required energy represented in Table 3.A. 2 and Table 3.A. 3, CO_2 emission amount of 1 kg of hydrogen generation using various fuel sources can be calculated as follow:

$$E_{fuel} = F_m(kg) \times \frac{1\ (t)}{1000\ (kg)} \times E_c \times E_f \qquad \text{Eq.3. 13}$$

Where:

E_{fuel} = Carbon dioxide emission regarding fuel type (kg CO_2)

E_f = Emission factor (kg CO_2/GJ)

3.2.1.3 CO2 emission of electricity generation for hydrogen production, Australia states, current situation

Australia has a high potential for hydrogen generation via RES. In addition, its geographical location provides the opportunity to supply the hydrogen demand of Asian countries. Thus, a part of this study is allocated to carbon dioxide emission from electricity production to produce hydrogen in this country. The “current situation” term in this study refers to the current condition of electricity generation which is transferred via electricity grid. Scope 2 and Scope 3 Electricity emission factors are provided by the Australian government, Department of Industry, Science, Energy, and Resources [43] since 1989 for Australia and its states. The last estimate of the combination of carbon dioxide emission for Scope 2 and Scope 3 in Australia is used at the same time with the required energy for electrolysis represented in Table 3.A. 2 and Table 3.A. 3 to estimate the carbon dioxide emission.

3.2.1.4 CO_2 emission of electricity generation for hydrogen production, Europe, current situation

Europe region, like Australia, is one of the most important regions in terms of hydrogen generation using RES to reach net zero emission. The same method, as for the Australian states, is applied to European countries. Similarly, electricity generation CO_2 emission factor and studies in Table 3.A. 2 and Table 3.A. 3 are used for the estimation of carbon dioxide emission of 1 kg hydrogen generation in Europe. The carbon dioxide emission estimation is performed on EU28 countries. Furthermore, carbon dioxide emission of 1 kg hydrogen generation in seven European countries is assessed to provide the possible range of emission.

3.2.1.5 CO_2 *emission of electricity generation for hydrogen production, Australia, 2030 Prediction*

Governments have struggled to reduce CO_2 emissions regarding the Paris agreement goals. According to the Australian government, Department of Industry, Science, Energy, and Resources *[45]*, the emission reduction aims in Australia up to 2030 is 26%-28% lower than 2005 levels. It is possible to define the CO_2 emission trend of hydrogen generation over the years by using electricity emission factors since 1989, which is provided by the Australian government, Department of Industry, Science, Energy, and Resources *[43]*. This information could be used to predict carbon dioxide emissions in the future.

Electricity generation carbon dioxide emission prediction for 2030 by using a linear trend is provided in Table 3. 1. The highest reduction trend is predicted for South Australia. Tasmania is predicted to have negative values, which means that the emission is projected to increase. It means that the linear trend for this state is inappropriate for prediction. In addition, Victoria has supplied a part of Tasmania's electricity in previous years which could be the reason for the inappropriately chosen trend as this supply was not constant. The prediction for Australia is 18% reduction in carbon dioxide emissions in 2030 compared to 2019. It is achievable by proper management regarding the source of electricity production and using more efficient and sustainable technologies.

State	Scope 2 and 3 predictions for 2030 kg CO_2 e/kWh	reduction respect to 2019
New South Wales and Australian capital territory	0.777	9%
Victoria	0.847	15.3%
Queensland	0.804	12.6%
South Australia	0.003	99.0%
Western Australia-south west	0.447	35.2%

interconnected system (SWIS)		
Tasmania	0.218	-36.3%
Northern territory	0.490	15.6%
Australia	0.664	18.0%

Table 3. 1 Prediction of CO_2 emission for electricity generation in 2030

3.2.1.6 CO2 emission of electricity generation for hydrogen production, Europe, 2030 Prediction

The same procedure as for Australia is applied to the European countries for the prediction of the emission factor in 2030. To predict the CO_2 emission for hydrogen generation through PEM and alkaline electrolysers in 2030 the predicted emission factors and required energy for electrolysis provided in Table 3.A. 2 and Table 3.A. 3 are used in this study.

3.2.2 Sensitivity analysis

Cell characteristics and energy sources are investigated as the parameters for sensitivity analysis of electricity consumption and carbon dioxide emission in this study. Italy and Australia have a high potential for green hydrogen generation, furthermore, their strategic geographical position allows supplying hydrogen to numerous countries. Therefore, in this study, for the energy sources sensitivity analysis, energy sources in Australia and Italy are considered.

3.2.2.1 Sensitivity analysis- Cell characteristics

3.2.2.1.1 PEM electrolyser

To perform sensitivity analysis, in this section, the first step is to define the parameters in Table 3.A. 1 which have a logical relationship with experimental energy consumption. These parameters are used to define the general equation which can be used for sensitivity analysis.

Figure 3. 4 and Figure 3. 5 represent experimental energy consumption to produce 1 kg hydrogen through a PEM electrolyser versus “cell voltage, cell efficiency, and current density” and “cell faradaic efficiency”, respectively. The linear trendline is shown in Figure 3. 4 for each parameter. It is seen that cell voltage and current density have almost linear relationships with experimental energy consumption, the coefficient of determination is 0.77 and 0.57, respectively. The maximum residual (difference between actual value and trendline) occurs around 45 kWh/kg energy consumption for all 3 parameters. According to Eq.3. 7, the cell voltage is the denominator of the cell efficiency equation, therefore, it is logical when cell voltage has a linear relationship with experimental energy

consumption there could not be a linear relation between cell efficiency and experimental energy consumption. According to the Figure 3. 5, specific relationship between experimental energy consumption and cell faradaic efficiency is not recognized. Thus, cell voltage, and current density are considered the parameters to find the general equation for the sensitivity analysis. Figure 3. 5 shows a sudden drop in the faradaic efficiency at approximately 45-50 kWh/kg that can be used as a criterion to have two clusters to formulate the estimated experimental specific energy including faradaic efficiency. It requires more investigation and is not considered in this study.

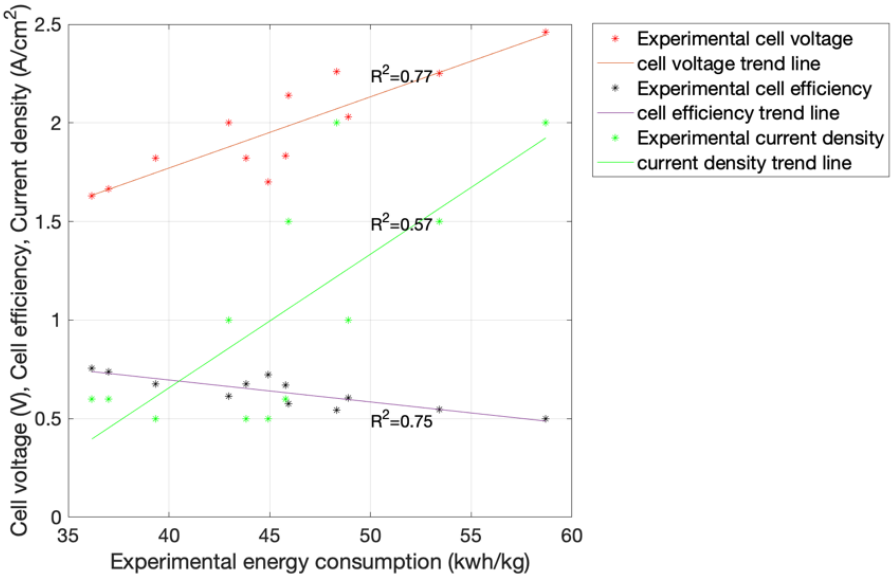

Figure 3. 4 Experimental energy consumption for 1 kg hydrogen production by means of PEM electrolyser versus cell voltage, cell efficiency and current density

Eq.3. 14 is provided based on the information provided in Table 3.A. 1 and Table 3.A. 2, the relation between current density, cell voltage, and experimental specific energy consumption for 1 kg hydrogen generation through the PEM electrolyser (R^2=0.82). This equation is created by the application of multiple regression in python, using pandas and sklearn libraries. The correlation coefficient is 0.91, which is shown in Figure 3. 6. This figure represents the relation between the experimental and estimated energy consumption. The black line is the linear trendline, and the maximum residual occurs almost around experimental energy consumption equal to 45 kWh/kg.

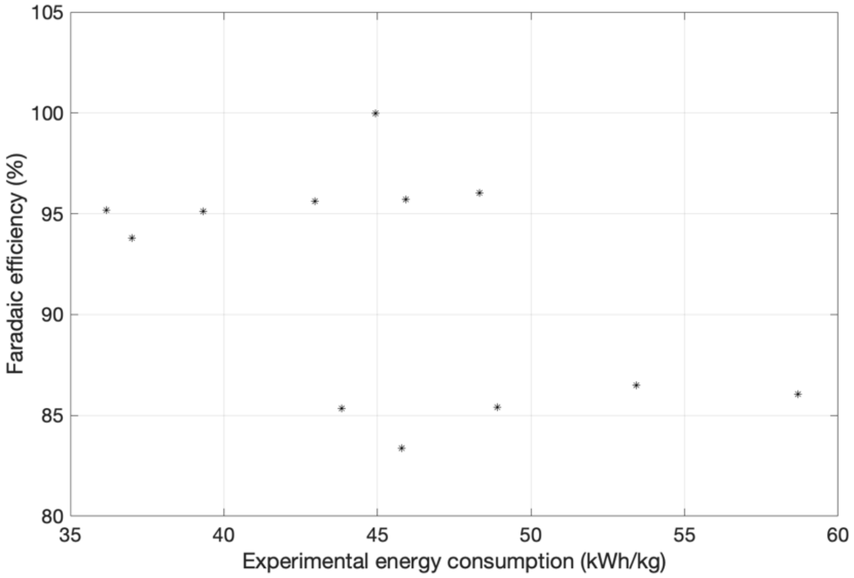

Figure 3. 5 Experimental energy consumption for 1 kg hydrogen production by means of PEM electrolyser versus cell faradaic efficiency

$$E_{e,experimental,PEM} = -6.90 \times I_{density} + 35.63 \times E_{cell} - 17.59 \qquad \text{Eq.3. 14}$$

where:

$E_{e,experimental,PEM}$ = Estimated experimental specific energy consumption for 1 kg hydrogen generation (kWh) by means of PEM electrolyser

E_{cell} = cell voltage (V)

$I_{density}$ = current density (A/cm^2)

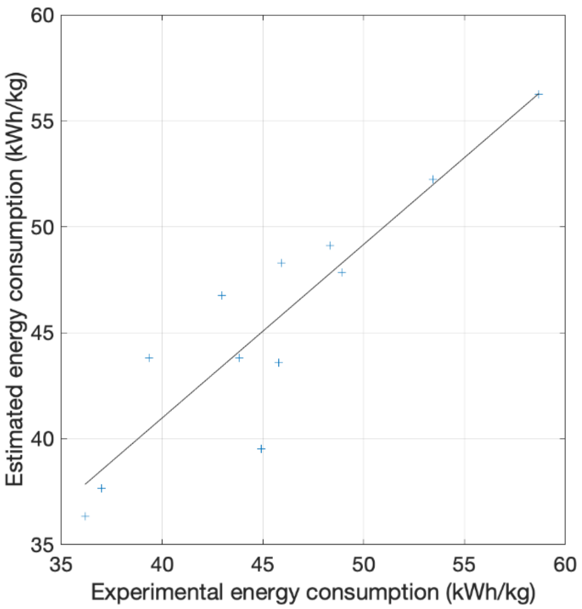

Figure 3. 6 correlation between experimental and estimated energy consumption for 1 kg hydrogen production by means of PEM electrolyser

Eq.3. 14 can be modified by combination with Eq.3. 7 as follow:

$$E_{e,experimental,PEM} = \frac{44.07}{\eta_{cell,LHV}} - 6.90 \times I_{density} - 17.59 \qquad \text{Eq.3. 15}$$

The average current density and cell voltage are considered 1.025 (A/cm^2) and 1.967 (V) respectively (average of 12 cases with information about experimental energy consumption, current density, and cell voltage) as initial values to perform the sensitivity analysis of energy consumption. The corresponding Cell efficiency of the cell voltage equal to 1.967V is %62.5. For each sensitivity analysis regarding the desired parameter, the other parameter in Eq.3. 14 and Eq.3. 15 is considered as the fixed one. In the last step, -30% to 30% tolerance is applied to the variable parameter for the sensitivity analysis.

3.2.2.1.2 Alkaline electrolyser

For the alkaline electrolyser the same procedure, as in PEM sensitivity analysis, is used. The only available information for the alkaline system, according to the literature review, is cell efficiency and experimental energy consumption. The obtained equation between estimated experimental energy consumption and cell efficiency is shown in Eq.3. 16 (R^2=0.64)

$$E_{e,experimental,alkaline} = -53.16 \times \eta_{cell,LHV} + 88.33 \quad \text{Eq.3. 16}$$

where:

$E_{e,experimental,alkaline}$ = Estimated experimental specific energy consumption for 1 kg hydrogen production (kWh) by means of alkaline electrolyser

This equation has only one variable, moreover, the coefficient of determination is low; Thus, it is not reliable to investigate the sensitivity analysis by this equation. It requires in-depth research that could be covered in future studies.

3.2.2.2 Sensitivity analysis- Energy source

The method of sensitivity analysis of CO_2 emission regarding renewable energy sources, including solar, wind, and hydro energies in Australia and Italy, is provided in this section. The median values of carbon dioxide emission for hydrogen generation through PEM and alkaline technologies in Australia and Italy are extracted from Figure 3. 13 and Figure 3. 14. The median emissions for PEM technology in Australia and Italy are 38.1 and 13.15 kg CO_2/kg hydrogen, respectively. And the median emissions for alkaline technology in Australia and Italy are 43.01 and 15.4 kg CO_2/kg hydrogen, respectively.

Three energy scenarios are considered as follow:

1) Constant share of wind and hydro, and replacement of the other sources with solar

2) Constant share of solar and hydro, and replacement of the other sources with wind

3) Constant share of solar and wind, and replacement of the other sources with hydro

According to the IPCC report, 2018, Annex III, table AIII.2, CO_2 emissions for 1MWh electricity generation by solar (utility), wind (onshore), and hydropower are 48, 11, and 24 kg, respectively [46]. According to the Department of Industry, Science, Energy, and Resources, RES contribution to total energy production in Australia in 2020, was 24% (Solar 9%, wind 9%, hydro 6%) [3]; While RES contribution in Italy in 2019 was 18 % (Solar 1.7%, wind 1.4%, hydro 3.4%, other renewable sources 11.5%) [4].

To estimate the average emission of the other sources of CO_2 emission, the following equation is used:

$$E_T = E_{consumption} \times (C_s \times E_s + C_w \times E_w + C_h \times E_h + C_o \times E_o) \quad \text{Eq.3. 17}$$

Where:

E_T = Total carbon dioxide emission, (kg CO_2)

$E_{consumption}$ = Average electricity consumption for 1 kg hydrogen generation, (kg CO_2/MWh)

C_s = solar contribution, (percentage of the total, in MWh)

E_s = electricity production carbon dioxide emission by means of solar energy, (kg CO_2/MWh)

C_w = wind contribution, (percentage of the total, in MWh)

E_w = electricity production carbon dioxide emission by means of wind energy, (kg CO_2/MWh)

C_h = hydro contribution, (percentage of the total, in MWh)

E_h = electricity production carbon dioxide emission by means of hydro energy, (kg CO_2/MWh)

C_o = other energies contribution, (percentage of the total, in MWh)

E_o = electricity production carbon dioxide emission by means of other sources of energy, (kg CO_2/MWh)

According to the studies provided in Table 3.A. 2 and Table 3.A. 3, the average electricity consumption is 45.44 and 53.29 kWh/kg hydrogen in PEM and alkaline technology, respectively. Table 3. 2 shows the contribution of other sources and their average CO_2 emission using Eq.3. 17 and average electricity consumption. C_o is calculated by subtracting solar, wind, and hydro contribution from 100%. The only unknown parameter is E_o, which is calculated by using Eq.3. 17

To perform the sensitivity analysis, considering the defined scenarios, contribution variations is applied to each energy source (reduction of C_o at the same time), and the CO_2 emission is calculated using Eq.3. 17.

	Italy (PEM)	Australia (PEM)	Italy (alkaline)	Australia (alkaline)
E_T (kg CO_2/kg Hydrogen)	13.15	38.1	15.4	43.01
C_s	1.70%	9.00%	1.70%	9.00%
E_s (kg CO_2/MWh)	48	48	48	48
C_w	1.40%	9.00%	1.40%	9.00%
E_w (kg CO_2/MWh)	11	11	11	11
C_h	3.40%	6.00%	3.40%	6.00%
E_h (kg CO_2/MWh)	24	24	24	24
C_o	93.50%	76.00%	93.50%	76.00%
E_o (kg CO_2/MWh)	307.6	1094.37	307.16	1053.08

Table 3. 2 Contribution of energy sources and average emission of sources

3.3 Result and discussion

3.3.1 Environmental impact

3.3.1.1 Energy sources

The minimum amount of required fuel to generate 1 kg of hydrogen using PEM and alkaline electrolysers at stack level is calculated according to Eq.3. 12 and shown in Figure 3. 7 and Figure 3. 8. The real required amount of fuel, in reality, is more than the reported quantities in Figure 3. 7 and Figure 3. 8. By comparing Figure 3. 7 and Figure 3. 8 it is realized that the minimum required fuel amount in Alkaline technology is greater than in PEM.

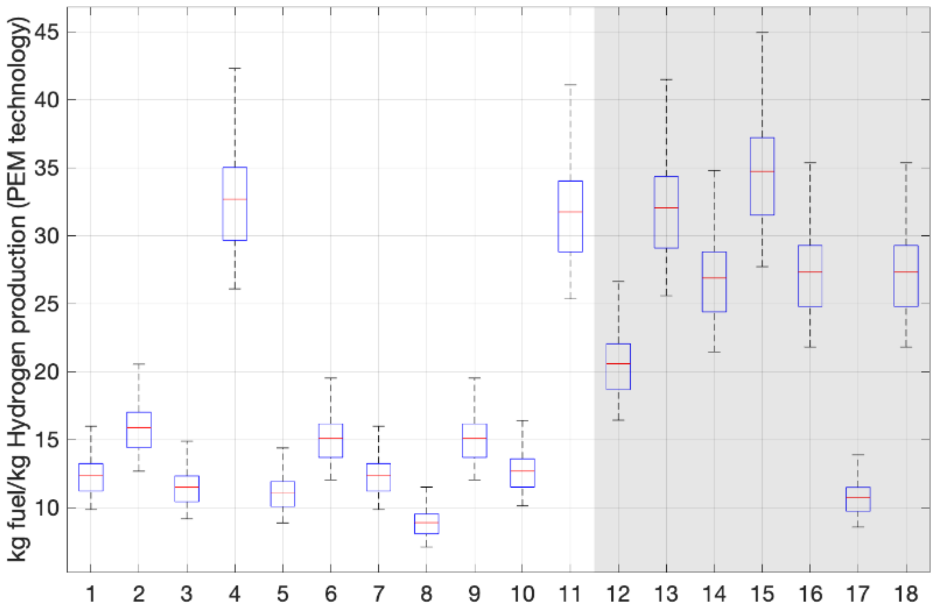

Figure 3. 7 Minimum required fuel to generate 1 kg hydrogen (based on experimental energy values) by means of PEM technology, numbers in the x axis is the fuel row number in Table 3.A. 1. Highlighted part is related to zero emission fuels.

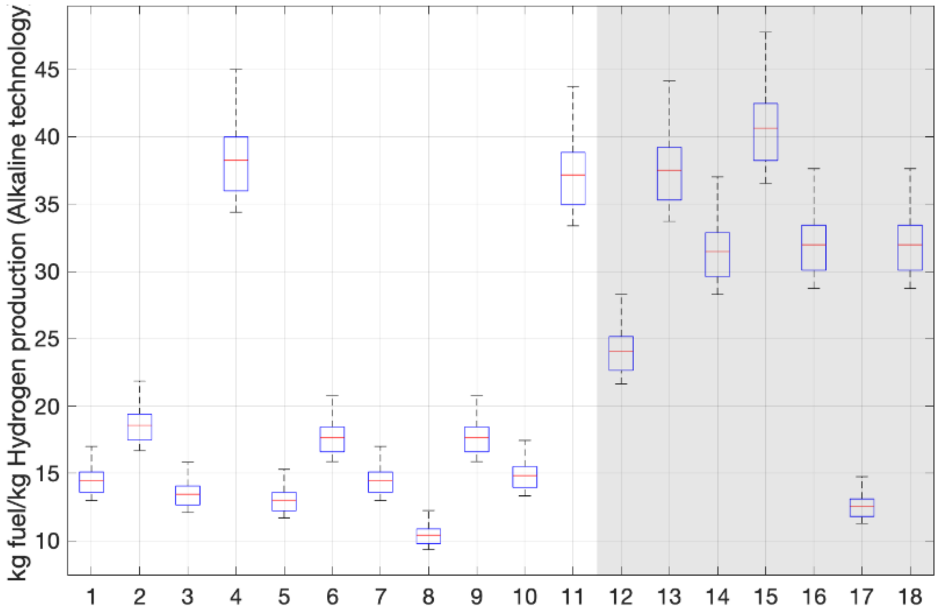

Figure 3. 8 Minimum required fuel to produce 1 kg hydrogen (based on experimental energy values) by means of Alkaline technology, numbers in the x axis is the fuel row number in Table 3.A. 1. Highlighted part is related to zero emission fuels.

The boxplot of each number in x axis represents the results based on studies provided in Table 3.A. 2, and Table 3.A. 3, and using the relevant fuel type in Table 3.A. 1. Figure 3. 7 and Figure 3. 8 show that, in general, the required mass of fuels with zero emission factor is considerably higher than fuels with non-zero emissions, except some fuels, such as brown coal, “non-biomass municipal materials, if combusted to produce heat or electricity”, and charcoal. The minimum required fuel is related to coal tar; however, its emission is dramatically high. Among the zero emission fuels, charcoal is the fuel with the minimum weight required to generate 1 kg of hydrogen because of its high energy content. It should be noted that fuel type and its energy content are not the only parameters to determine the amount of fuel consumption; the other parameters, such as technology type plays an important role in the determination of fuel consumption. As an example (see Figure 3. 7), the minimum fuel amount of dry wood which is zero emission fuel is around 15 kg fuel/kg hydrogen which is almost equal to or less than the maximum values of bituminous coal, sub-bituminous coal, coal briquettes, coal coke, “Solid fossil fuels other than those mentioned in the items above”, and “industrial materials and tyres that are derived from fossil fuels, if recycled and combusted to produce heat or electricity”. Thus, charcoal is not the only fuel with zero emission factor with a low amount of fuel consumption if charcoal is sourced from sustainably managed biomass.

3.3.1.2 Carbon dioxide emission based on fuel type

CO_2 emission corresponding to fuel type to generate 1 kg hydrogen via PEM and alkaline electrolysers at stack level is provided in Figure 3. 9 and Figure 3. 10. CO_2 emission at stack level, if non-zero emission fuels are used in hydrogen generation, assuming 100% efficiency of burning fuels, could be approximately 25-40 kg for 1 kg of hydrogen generation through PEM technology and around 30-40 kg for alkaline, except coal coke which is a bit greater. Coal coke has the greatest carbon dioxide emission, while coal tar and “industrial materials and tyres” have the lowest values among the non-zero fuels. The abovementioned ranges are related only to fuel burning, without consideration of other emissions such as extraction and transportation. It is seen that the CO_2 emission associated with alkaline technology is around 5 kg higher than PEM.

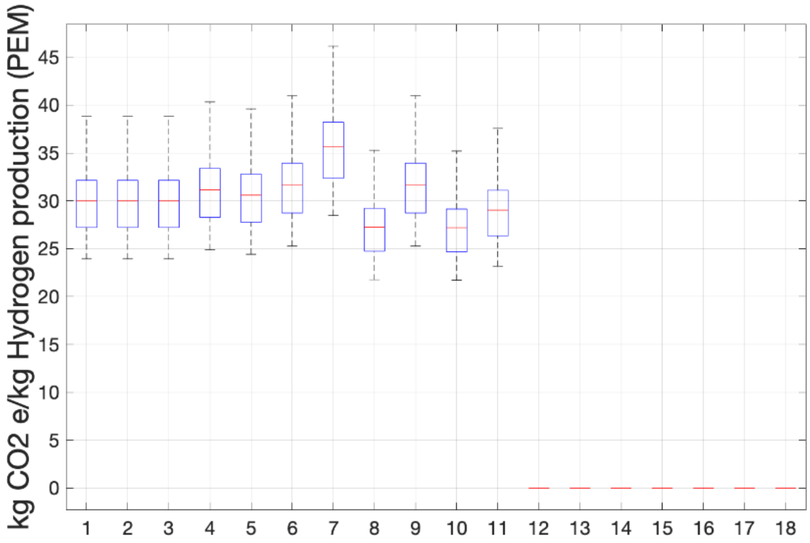

Figure 3. 9 CO_2 emission of 1 kg hydrogen generation only from fuel burning (based on experimental energy values) by means of PEM technology, numbers in the x axis is the fuel row number in Table 3.A. 1.

3.3.1.3 Australia states, current situation

The last estimate of the combination of carbon dioxide emission for Scope 2 and Scope 3 in Australia and its states to produce 1 kg hydrogen, based on studies provided in Table 3.A. 2 and Table 3.A. 3 are shown in Figure 3. 11 and Figure 3. 12. These figures can be used to define the range of carbon dioxide emission in Australia and its state to generate 1 kg of hydrogen via PEM and alkaline electrolyser at the stack operational level.

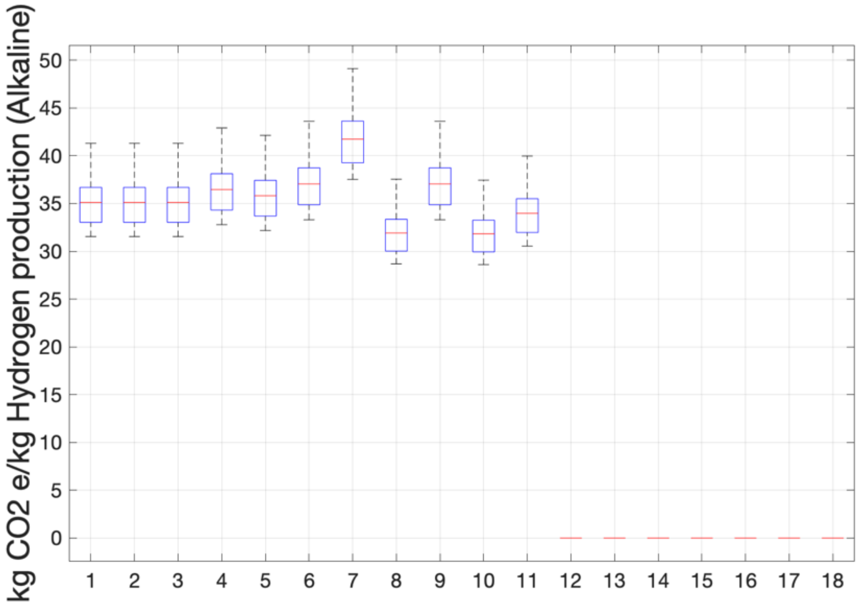

Figure 3. 10 CO_2 emission of 1 kg hydrogen generation only from fuel burning (based on experimental energy values) by means of Alkaline technology, numbers in the x axis is the fuel row number in Table 3.A. 1.

The emission quantities of the alkaline technology are higher than PEM. The overall range of CO_2 emission to generate 1 kg hydrogen, using electricity from the grid, in the current condition, is around 30-45 and 38-50 kg CO_2 via PEM and alkaline systems, respectively., Tasmania has the lowest emission intensity among the Australian states and Victoria has the greatest one.

There is a significant difference between the range in “Figure 3. 9 and Figure 3. 10 “, and “Figure 3. 11 and Figure 3. 12” which can be due to the consumption of other fuel types and the powerplants efficiency. Moreover, Figure 3. 9 and Figure 3. 10 are based only on the emission related to fuel combustion, not other emissions such as transportation and extraction. Therefore, if the technologies represented in Table 3.A. 2 and Table 3.A. 3 are used, the carbon dioxide emission to produce 1 kg of hydrogen in Australia could be approximately 30 to 40 kg and 40-50 kg, at stack level, via PEM and alkaline technologies, respectively.

Annually approximately 350 kt of hydrogen is generated in Australia, including export to other countries such as Japan and Korea (according to the council of Australian government (COAG) energy council report) [47]. Only 55 t of generated hydrogen in Australia is clean hydrogen [16]. If fuels with zero-emission and RES are not completely used as energy sources, the results would be 10.5 to 14 and 14 to 17.5 Mt of carbon dioxide emission for PEM and alkaline technologies, respectively. If the required energy represented in the manufacturer list in Table 3.C. 1 is considered instead of the experimental required energy, carbon dioxide emission can be closer to the upper boundary of this range; because the required energy in the manufacturer list is closer to the maximum quantities in experimental tests. Thus, it is expected to have annually 17.5 Mt of CO_2 emission due to hydrogen generation using PEM and alkaline technology in Australia.

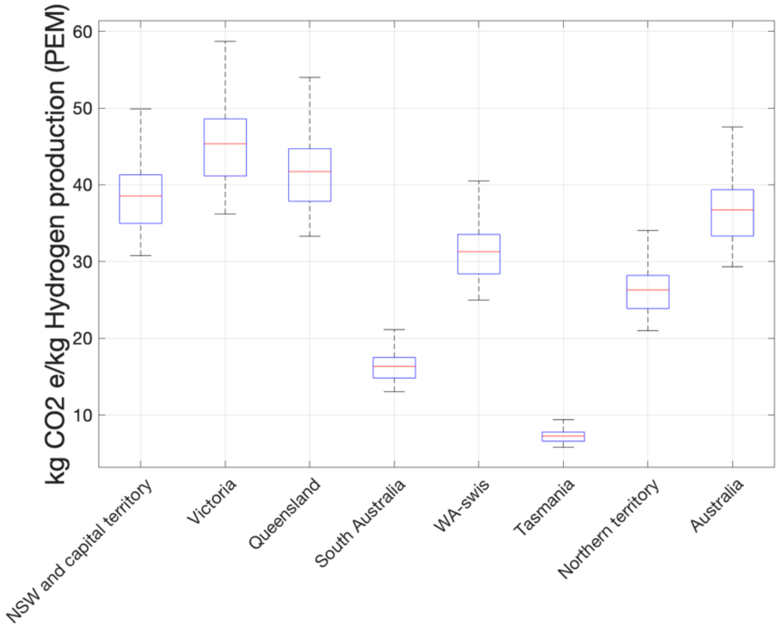

Figure 3. 11 Scope 2 and Scope 3 combination CO2 emission of 1 kg hydrogen generation in Australia and its states based on studies provided in Table 3.A. 2 (last estimate after 2019), PEM technology

3.3.1.4 Europe, current situation

Based on the information provided in Table 3.A. 2 and Table 3.A. 3 and the GHG emission factor of the electricity sector for the electricity generation, extracted from the ISPRA report [48], the carbon dioxide emission, at the current situation, to produce 1 kg hydrogen through PEM and Alkaline in Europe and main countries is calculated. The results are shown in Figure 3. 13 and Figure 3. 14. For the sake of comparison, Australia is included in these figures.

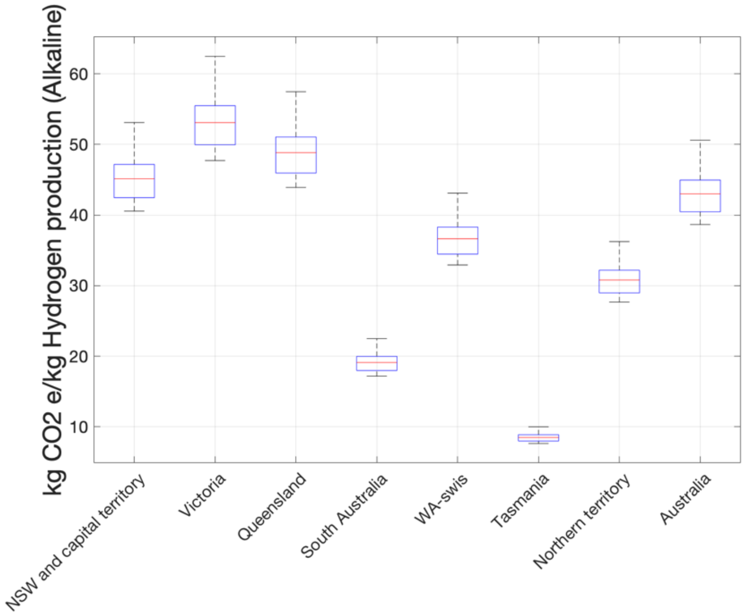

Figure 3. 12 Scope 2 and Scope 3 combination CO2 emission of 1 kg hydrogen generation in Australia and its states based on studies provided in Table 3.A. 3 (last estimate after 2019), Alkaline technology

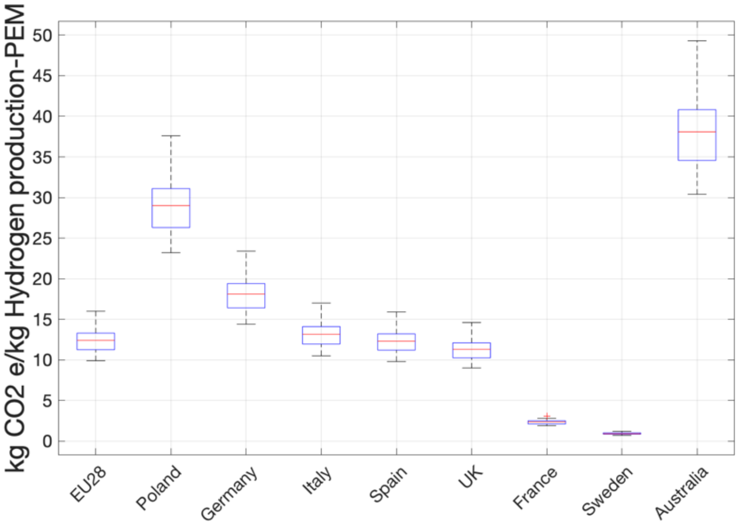

Figure 3. 13 CO_2 emission of the generation of 1 kg hydrogen in Europe and Australia based on studies provided in Table 3.A. 2, PEM technology.

Australia has dramatically higher carbon dioxide emissions for hydrogen production in comparison to European countries on average; the difference is around 25 and 30 kg of carbon dioxide emission via PEM and alkaline, respectively. Despite the significant difference between Eu28 and Australia, some countries like Poland could have high emissions close to Australia's emissions. However, countries like Sweden and France show significantly lower carbon dioxide emissions to produce hydrogen by PEM and Alkaline.

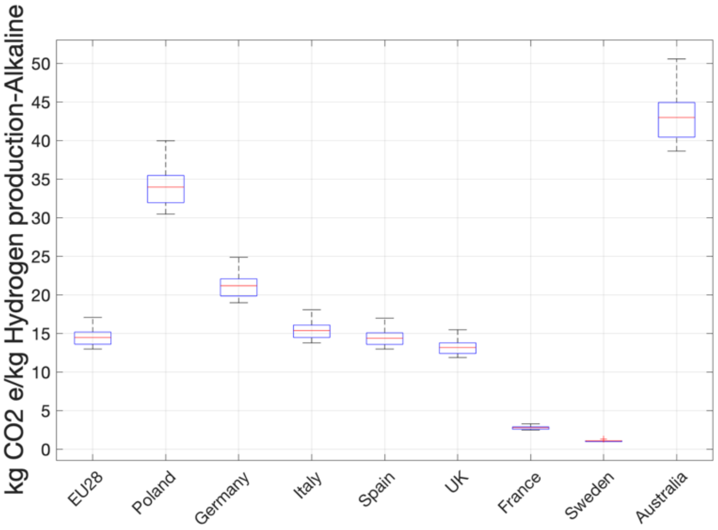

Figure 3. 14 CO_2 emission of the production of 1 kg hydrogen in Europe and Australia based on studies represented in Table 3.A. 3, Alkaline technology

3.3.1.5 Australia, 2030 prediction

According to the information provided in Table 3.A. 2 and Table 3.A. 3, carbon dioxide emission for 1 kg hydrogen generation using PEM and alkaline technology in Australia, if electricity is drawn from the national and State grids, in 2030, is predicted and provided in Figure 3. 15 and Figure 3. 16.

It is seen that carbon dioxide emission to produce 1 kg of hydrogen in Australia via PEM electrolyser at stack operational level is projected to be approximately 25-35 kg in 2030 and 30-40 kg for Alkaline technology. Hydrogen generation in Australia in 2030 is predicted to be approximately 1 Mt per year (according to COAG energy council report) [47]. It results in 25 to 35 and 30 to 40 Mt of carbon dioxide emission via PEM and Alkaline technologies, respectively, if the trend is the same as predicted values. According to Figure 3. 15 and Figure 3. 16, it is anticipated that, in 2030, South Australia would almost reach zero-emission hydrogen production while Victoria might have the highest CO_2 emission for hydrogen production. Thus, energy production patterns and management in South Australia could be applied as a guide in other states for the overall carbon dioxide emission reduction in Australia.

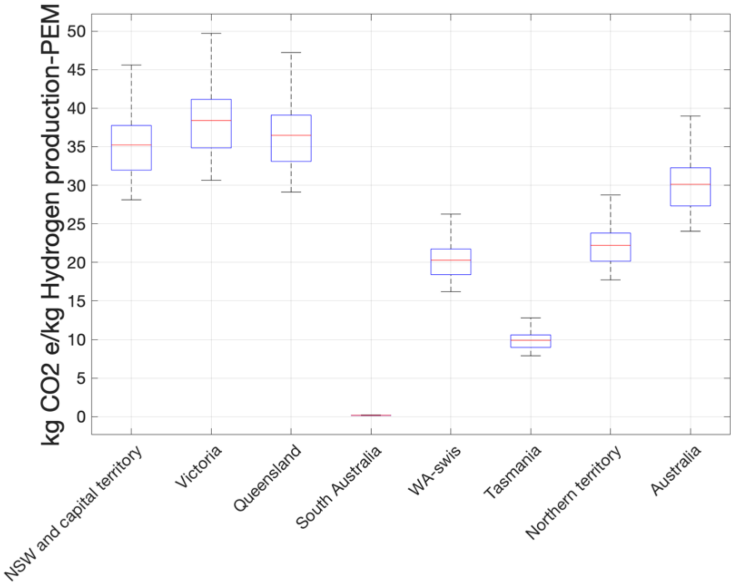

Figure 3. 15 Emission for 1 kg hydrogen generation using PEM technology (based on experimental energy values)-2030 prediction, Australia states

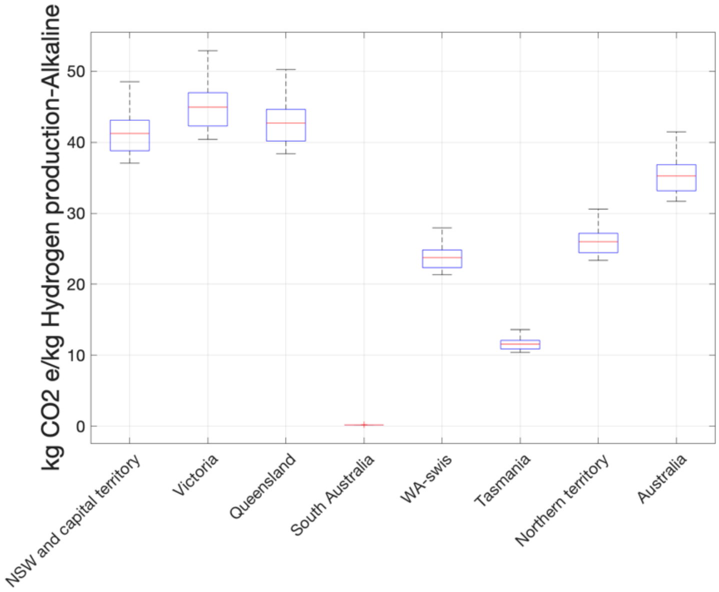

Figure 3. 16 Emission for 1 kg hydrogen generation using alkaline technology (based on experimental energy values)-2030 prediction, Australia states

3.3.1.6 Europe, 2030 prediction

The carbon dioxide emission prediction in 2030 for European countries is shown in Figure 3. 17 and Figure 3. 18. For the sake of comparison, these figures contain predicted emissions related to Australia.

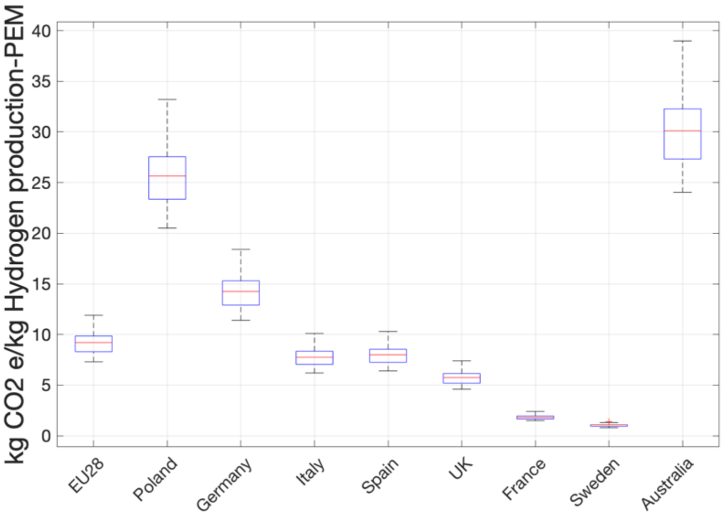

Figure 3. 17 Emission for 1 kg hydrogen generation using PEM technology (based on experimental energy values)-2030 prediction, European countries and Australia

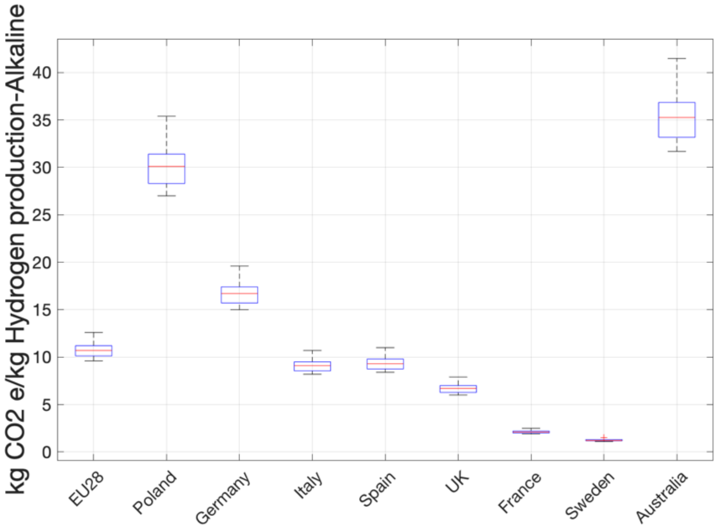

Figure 3. 18 Emission for 1 kg hydrogen generation using PEM technology (based on experimental energy values)-2030 prediction, European countries and Australia

It is recognized that Australia could have dramatically higher emissions for hydrogen generation using PEM and alkaline electrolysers in comparison to European countries. Poland might have the highest emission among European countries, with values close to Australia's emission. Therefore, it is required to make proper decisions in countries like Australia and Poland to reach the Paris agreement objectives. The emission difference between Australia and EU28 in 2030, could be around 20 and 25 kg of carbon dioxide via PEM and alkaline, respectively. This difference is almost 5 kg lower than the current situation.

3.3.2 Sensitivity analysis

3.3.2.1 Sensitivity analysis- Cell characteristics-PEM technology

The result of the sensitivity analysis of estimated energy consumption to produce 1 kg hydrogen via PEM electrolyser is shown in Figure 3. 19. It is seen that energy consumption for hydrogen generation is more sensitive to the cell voltage and cell efficiency, which are related concepts according to Eq.3. 7. Sensitivity of estimated energy consumption to current density is very low. The variation of estimated energy consumption is around -46 to 46%, 65 to -35%, and 4.6 to -4.6% for cell voltage, cell efficiency, and current density variation, respectively. It is realized that the impact of cell voltage could be almost 10 times greater than the current density effect with an inverse direction.

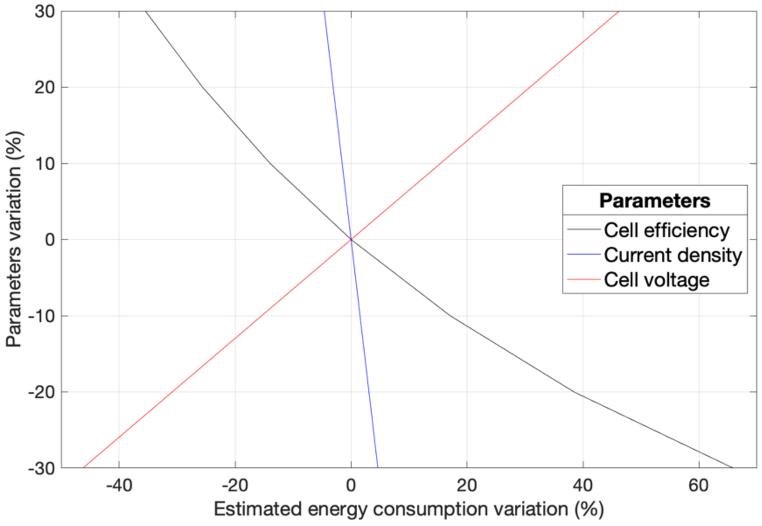

Figure 3. 19 variation of parameters (-30 to 30%) and variation of estimated energy consumption for 1 kg hydrogen generation through PEM electrolyser

According to Faraday's 1st law, the amount of generated hydrogen is proportional to the current density, not the cell voltage. The result of sensitivity analysis, based on experimental test results in the literature, shows more sensitivity of energy consumption to cell voltage compared to current density. It indicates the importance of cell manufacturing and electrolyte resistance that could lead to lower faradaic efficiency due to undesirable reactions or electrolyte impurities.

3.3.2.2 Sensitivity analysis- Energy source

The result of sensitivity analysis based on energy source is shown in Figure 3. 20 and Figure 3. 21 for Italy and Australia, respectively. The maximum amount of contribution increment is determined based on the C_o values.

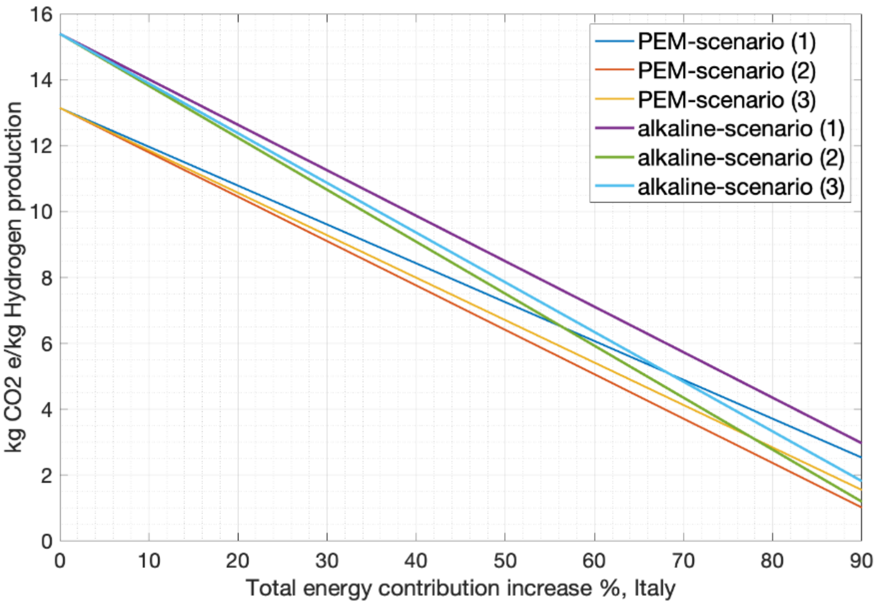

Figure 3. 20 variation of energy source contribution and impact on CO_2 emission for 1 kg hydrogen production by means of PEM and alkaline electrolyser in Italy.

It is seen in Figure 3. 20 that the result of a 90 % increment of renewable sources can be in the range of 1-3 kg CO_2/kg hydrogen production and the minimum CO_2 emission can be reached by scenario 2 via PEM technology. However, the most considerable change is related to scenario 2 with alkaline technology (according to the lines' slope). Furthermore, by comparing the line slopes, it is recognized that scenario 1 via PEM technology has the lowest sensitivity. The result of 70% increment of RES in Australia could be 3.5-5.5 kg CO_2/kg hydrogen production and the minimum emission and most considerable change are like Italy. By comparing the lines' slope, it can be recognized that carbon dioxide emission in Australia is more sensitive to RES rather than in Italy. By comparing the CO_2 emission, considering the maximum contribution percentage in Australia, 70 %, it is realized that the emission range for both countries would be 3.5-6 kg CO_2, at this percentage. It is worth mentioning that Australia can reach this condition with an initial amount of around 40 kg CO_2 emission, while Italy's initial emission value is around 14 kg CO_2 emission.

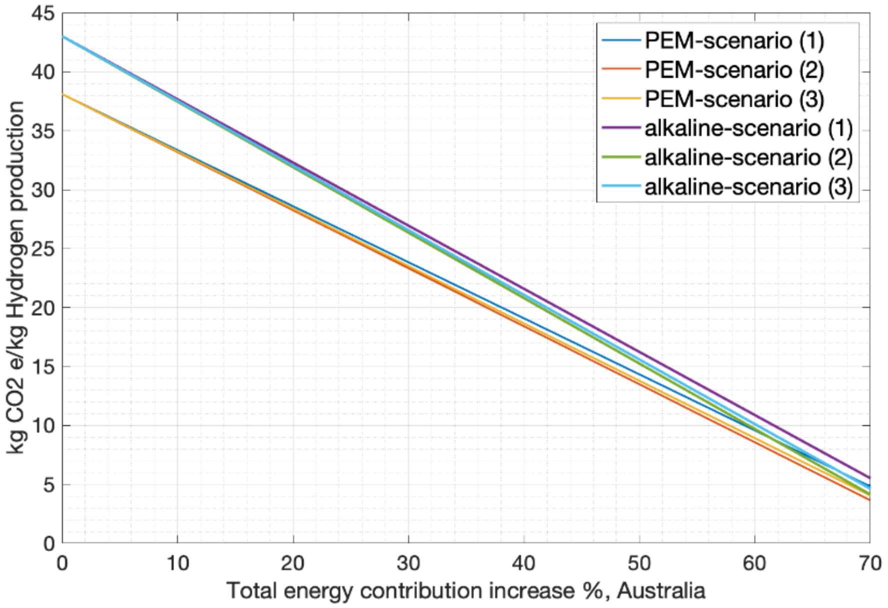

Figure 3. 21 variation of energy source contribution and impact on CO_2 emission for 1 kg hydrogen generation by means of PEM and alkaline electrolyser in Australia.

Considering the net zero emission goal of Australia by 2050, a complete transition from fossil fuels to RES in hydrogen generation will be required. This transition is achievable, considering 262,000 square kilometers of land suitable for hydrogen generation using renewable electricity. This area is about 3% of Australia's total land area [15].

3.4 Conclusion

RES has low contribution to global electricity generation which roots from the storage problem. Hydrogen technology can be a solution to solve electricity storage problem and increase the RES contribution to global electricity contribution. Hydrogen generation using PEM and alkaline electrolysers and their potential CO_2 emission are investigated in this chapter. The minimum energy required to generate 1 kilogram of hydrogen based on the Gibbs free energy and enthalpy is 32.95 kWh/kg and 39.70 kWh/kg, respectively. However, the experimental quantities and the ones provided by manufacturers are greater due to variations in stack configuration and system efficiency. The energy consumption range reported by manufacturers is 42.2 to 65.6 kWh/kg of hydrogen. Various fuel sources with different carbon dioxide emissions could be consumed to provide electricity for water electrolysis. Considering the current consumption of various fuel types in Australia, with different contributions, if PEM and alkaline technologies represented in Table 3.A. 2, and Table 3.A. 3 are used, the carbon dioxide emission to generate 1 kg of hydrogen in Australia could be approximately 30 to 40 kg and 40 to 50 kg, at stack operational level, through PEM and alkaline technologies, respectively. Considering the current amount of hydrogen generation in Australia, if it is produced by the PEM electrolyser the emission equivalent is 10.5 to 14 Mt of CO_2 and the emission for alkaline technology could be 14 to 17.5 Mt of CO_2. It is anticipated that in 2030, compared to 2019, there would around 18% reduction in carbon dioxide emissions of the national electricity grid in Australia. It could result in around 25 to 35 kg of CO_2 emission for 1 kg of hydrogen generation by PEM technology and 30-40 kg for Alkaline technology. The current carbon dioxide emission for 1 kg of hydrogen generation in Italy is around 12 to 15 kg CO_2 and the projected emission in 2030 is 5 -10 kg CO_2 using PEM or alkaline technologies. To overcome the CO_2 emissions problem, the transition from fossil fuels to RES is necessary, which can be achieved by the hydrogen technology. A sensitivity analysis is performed for the identification of the critical parameters regarding energy consumption and carbon dioxide emission. The results of sensitivity analysis, regarding cell characteristics, show more sensitivity of PEM energy consumption to cell voltage in comparison to current density. It might be due to undesirable reactions or electrolyte impurities that amplify the importance of cell manufacturing and electrolyte resistance. Furthermore, by performing sensitivity analysis regarding energy sources scenarios it is concluded that CO_2 emission in Australia is more sensitive to RES in comparison to Italy.

3.5 Appendix 3.A

Table 3.A. 1 PEM electrolyser characteristics in literature

Row	Name in diagrams	Year of estimation	Active area for 1MW (m^2)	Cell area (single cell format) (cm^2)	Cell voltage level (V)	Current density (A/cm^2)	Power density (W/cm^2)	ηcell (LHV)	Reference
1	Zhao et al. 2020	2020	39	800	1.7	1.5	2.6	0.72	[21]
2	Bareiß et al. 2019 Case 1	2017	37	500	1.79	1.5	2.7	0.69	[30]
3	Bareiß et al. 2019 Case 2	Near future	18.5	1000	1.79	3	5.4	0.69	[30]
4	Rakousky et al. 2018	2018	16	17.64	2.1	3	6.3	0.59	[31]
5	Kumar et al. 2018 Case 1	2018	22	25	2.26	2	4.52	0.54	[49]
6	Kumar et al. 2018 Case 2	2018	31	25	2.14	1.5	3.21	0.57	[49]
7	Kumar et al. 2018 Case 3	2018	50	25	2	1	2	0.62	[49]
8	Kumar et al. 2018 Case 4	2018	110	25	1.82	0.5	0.91	0.68	[49]
9	Kumar et al. 2018 Case5	2018	20.5	25	2.46	2	4.92	0.5	[28]
10	Kumar et al. 2018 Case6	2018	29.5	25	2.25	1.5	3.375	0.55	[28]
11	Kumar et al. 2018 Case7	2018	49.5	25	2.03	1	2.03	0.61	[28]

12	Kumar et al. 2018 Case8	2018	110	25	1.82	0.5	0.91	0.68	[28]
13	Bernt and Gasteiger 2016	2016	19.5	5	1.72	3	5.16	0.72	[32]
14	Di Blasi et al. 2013	2013	102	100	1.63	0.6	0.98	0.75	[33]
15	Siracusano et al. 2011	2011	100	100	1.67	0.6	1	0.74	[50]
16	Millet et al. 2010 Case 1	2010	117.5	250	1.7	0.5	0.85	0.72	[29]
17	Millet et al. 2010 Case 2	2010	53	250	1.88	1	1.88	0.65	[29]
18	Siracusano et al. 2010	2010	91	100	1.83	0.6	1.1	0.67	[51]

Table 3.A. 2 PEM electrolyser theoretical and experimental energy consumption for hydrogen production in literature

Row	Name in diagrams	Theoretical			Experimental			Faradaic efficiency %	Reference
		hydrogen yield of cell (l/h)	Total hydrogen yield (m3/h)	Specific energy consumption kWh/kg	hydrogen yield of cell (l/h)	total hydrogen yield (m3/h)	specific energy consumption kWh/kg		
1	Zhao et al. 2020	648.76	316.3	34.9	-	-	-	-	[21]
2	Bareiß et al. 2019 Case 1	405.47	300.1	36.8	-	-	-	-	[30]
3	Bareiß et al. 2019 Case 2	1621.9	300.1	36.8	-	-	-	-	[30]
4	Rakousky et al. 2018	28.61	259.5	43.1	-	-	-	-	[31]
5	Kumar et al. 2018 Case 1	27.03	237.9	46.4	25.96	228.4	48.3	96.04	[49]
6	Kumar et al. 2018 Case 2	20.27	251.3	43.9	19.4	240.6	45.9	95.7	[49]
7	Kumar et al. 2018 Case 3	13.52	270.4	41.1	12.92	258.4	43	95.63	[49]
8	Kumar et al. 2018 Case 4	6.76	297.4	37.4	6.42	282.5	39.3	95.11	[49]
9	Kumar et al. 2018 Case5	27.03	221.6	50.5	23.26	190.7	58.7	86.05	[28]

10	Kumar et al. 2018 Case6	20.27	239.2	46.2	17.53	206.9	53.4	86.48	[28]
11	Kumar et al. 2018 Case7	13.52	267.7	41.7	11.52	228.1	48.9	85.39	[28]
12	Kumar et al. 2018 Case8	6.76	297.4	37.4	5.76	253.4	43.8	85.33	[28]
13	Bernt and Gasteiger 2016	8.11	316.3	35.3	-	-	-	-	[32]
14	Di Blasi et al. 2013	31.52	321.5	34.4	30	306	36.2	95.18	[33]
15	Siracusano et al. 2011	31.98	319.8	34.7	30	300	37	93.81	[50]
16	Millet et al. 2010 Case 1	68.73	323	34.3	52.5	246.8	44.9	99.98	[29]
17	Millet et al. 2010 Case 2	137.07	290.6	38.1	-	-	-	-	[29]
18	Siracusano et al. 2010	31.98	291	38.2	26.67	242.7	45.8	83.39	[51]

Table 3.A. 3 Alkaline electrolyser energy consumption in literature

Row	Name in diagrams	Year of estimation	Cell efficiency (referred to LHV)	Experimental total hydrogen yield (m^3/h)	Faradaic efficiency	Electricity consumption (kWh) for 1 kg hydrogen production	Ref.
1	Chang Zhang et al. 2021		0.65	50.0	0.7	50.28	[52]
2	Hirokazu Kojima et al. 2017	2017	0.63	34.00	0.77	48.97	[53]
3	L.Valverde-Isorna et al. 2016	2016	0.5	5.33	0.92	62.48	[54]
4	J Burkhardt et al. 2016	2016	0.61	60.00	-	53.40	[55]
5	Omid Alavi et al. 2016	2016	-	-	-	55.50	[56]
6	Alfredo Ursúa et al. 2013	2013	0.78	0.94	0.86	52.61	[57]
7	P-H.Floch et al. 2007	2007	-	-	-	47.73	[58]
8	K. Agbossou et al. 2001	2001	0.65	1.00	-	55.50	[59]
9	A.Gdutton et al.2000	2000	0.627	-	-	53.10	[60]

3.6 Appendix 3.B

Table 3.B. 1 PEM and alkaline manufacturers based on publicly available information, in case of several models from a company an example is represented, only some leading manufacturers are included

Manufacturer	**Electrolyser type**	**Model**	**Nominal hydrogen flow Nm^3/h**	**Nominal input power MW**	**power consumption kWh/Nm^3**	**power consumption kWh/kg**	**Country of origin**	
Hydrogenics	PEM	HyLYZER® -300-30	300	1.5	5.2	57.7	Canada	[
Nel	PEM	MC400	413	1.87	4.53	50.3	Norway	[
Cummins	PEM	HyLYZER® 200-30	200	1	4.95	55	USA	[
Erre2Gas	PEM	SIRIO 200	2	0.01	4.8	53.3	Italy	[
SinoHy Energy	PEM	HGPS-200	200	1	5	55.5	China	[
ITM power	PEM	2 GEP Skid	999	5	5.01	55.6	UK	[
Hefei Sinopower technologies	PEM	-	300	1.35	4.5	50.0	China	[
Toplink	PEM	Series M	300	1.50	5.00	55.5	China	[
IGAS	PEM	-	205	0.92	4.47	49.6	Germany	[
Plugpower	PEM	1MW GENFUEL ELECTROLYZER	200	1	4.50	49.9	USA	[
Elogen	PEM	Elyte 200	200	0.86	4.3	47.7	Germany	[
Green H2 systems	PEM		200	1.00	5	55.5	Germany	[
H-TEC SYSTEMS	PEM	ME450/1400	210	1.00	4.8	53.3	Germany	[

Siemens energy	PEM	-	180	NA	NA	NA	Germany	[
Cockerill Jingli Hydtogen	PEM	DQ80	80	NA	NA	NA	China	[
Suzhou green hydrogen energy	Alkaline	GHM-100	100	NA	4.4	48.8	China	[
HyGear	Alkaline	Hy.GEN-E 250	250	NA	5.2	57.7	Netherland	[
Nel	Alkaline	A series	150-3880	NA	3.8	42.2	Norway	[
Green hydrogen systems	Alkaline	Aseries	90	NA	4.3	48.2	Denmark	[
McPhy	Alkaline	McLyzer (800-30)	800	NA	4.5	49.9	France	[
H2Gen	Alkaline	Mercury advanced G64	42.6	NA	5.35	59.4	Australia	[
Cockerill Jingli Hydtogen	Alkaline	-	50	NA	4.7	52.2	China	[
Cummins	Alkaline	HySTAT® 100-10	100	0.5	4.95-5.40	55-60	USA	[
Sunfire	Alkaline	HYLINK	2230	10	4.7	52.2	Germany	[
Asahi Kasei	Alkaline	Aqualyzer	2000	10	NA	NA	Japan	[
Idroenergy	Alkaline	Mod.8.0	5.33	NA	5.6	62.5	Italy	[

Pure energy centre	Alkaline	4Nm^3	4	NA	5.6	62	UK	[
Sagim	Alkaline	M5000	5	NA	5.0	55.6	France	[
Teledyne Energy Systems	Alkaline	NH-450	450	NA	5.9	65.6	USA	[

3.7 Appendix 3.C

Table 3.C. 1 Fuel combustion emission factors *[43]*

#No.	Fuel combusted	Energy content factor	Emission factor kg CO_2-e/GJ
		GJ/t	CO_2
1	Bituminous coal	27	90
2	Sub-bituminous coal	21	90
3	Anthracite	29	90
4	Brown coal	10.2	93.5
5	Coking coal	30	91.8
6	Coal briquettes	22.1	95
7	Coal coke	27	107
8	Coal tar	37.5	81.8
9	Solid fossil fuels other than those mentioned in the items above	22.1	95
10	Industrial materials and tyres that are derived from fossil fuels, if recycled and combusted to produce heat or electricity	26.3	81.6
11	Non-biomass municipal materials, if combusted to produce heat or electricity	10.5	87.1
12	Dry wood	16.2	0
13	Green and air-dried wood	10.4	0
14	Sulphite lyes	12.4	0

15	Bagasse	9.6	0
16	Biomass, municipal and industrial materials, if combusted to produce heat or electricity	12.2	0
17	Charcoal	31.1	0
18	Primary solid biomass fuels other than those mentioned in the items above	12.2	0

3.8 References

[1] C. Wulf and M. Kaltschmitt, “Life cycle assessment of hydrogen supply chain with special attention on hydrogen refuelling stations,” *international journal of hydrogen energy,* vol. 37, pp. 16711-16721, 2012.

[2] BP, “Statistical Review of World Energy,” 2021. [Online]. Available: https://www.bp.com/en/global/corporate/energy-economics/statistical-review-of-world-energy.html. [Accessed January 2022].

[3] “Australian electricity generation - fuel mix,” Department of Industry, Science, Energy, and Resources, 2020. [Online]. Available: https://www.energy.gov.au/data/australian-electricity-generation-fuel-mix. [Accessed January 2022].

[4] L. Jensen, “Climate action in Italy Latest state of play,” 2021. [Online]. Available: https://www.europarl.europa.eu/RegData/etudes/BRIE/2021/690663/EPRS_BRI(2021)690663_EN.pdf. [Accessed 15 August 2022].

[5] A. P. Pavlos Nikolaidis, “A comparative overview of hydrogen production processes,” *Renewable and Sustainable Energy Reviews,* vol. 67, pp. 597-611, 2017.

[6] K. G. d. Santos, C. T. Eckerta, E. D. Rossi, R. A. Bariccatti, E. P. Frigo, C. A. Lindino and H. J. Alves, “Hydrogen production in the electrolysis of water in Brazil, a review,” *Renewable and Sustainable Energy Reviews,* vol. 68, pp. 563-571, 2017.

[7] L. M.Romeo, M. Cavana, M. Bailera, P. Leone, B. Peña and P. Lisbona, “Non-stoichiometric methanation as strategy to overcome the limitations of green hydrogen injection into the natural gas grid,” *Applied Energy,* vol. 309, p. 118462, 2022.

[8] J. Lu, A. Zahedi, C. Yang, M. Wang and B. Peng, “Building the hydrogen economy in China: Drivers, resources and technologies,” *Renewable and Sustainable Energy Reviews,* vol. 23, pp. 543-556 , 2013.

[9] S. M. Alirahmi, E. Assareh, N. N. Pourghassab, M. Delpisheh, L. Barelli and A. Baldinelli, “Green hydrogen & electricity production via geothermal-driven multi-generation system: Thermodynamic modeling and optimization,” *Fuel,* vol. 308, p. 122049, 2022.

[10] T. Longden, F. Beck, F. Jotzo, R. Andrews and M. Prasad, “Clean’ hydrogen? – Comparing the emissions and costs of fossil fuel versus renewable electricity based hydrogen,” *Applied Energy* , Vols. Volume 306, Part B, p. 118145 , 2022.

[11] B. Hurtubia and E. Sauma, “Economic and environmental analysis of hydrogen production when complementing renewable energy generation with grid electricity,” *Applied Energy,* vol. 304, p. 117739, 2021.

[12] M. Delpierre, J. Quist, J. Mertens, A. Prieur-Vernat and S. Cucurachi, “Assessing the environmental impacts of wind-based hydrogen production in the Netherlands using ex-ante LCA and scenarios analysis,” *Journal of Cleaner Production,* vol. 299, p. 126866, 2021.

[13] A. Kopteva, L. Kalimullin, P. Tcvetkov and A. Soares, “Prospects and Obstacles for Green Hydrogen Production in Russia,” *Energies,* vol. 14, no. 3, p. 718, 2021.

[14] J. R. Bartels, M. B. Pate and N. K. Olson, “An economic survey of hydrogen production from conventional and alternative energy sources.,” *International Journal of Hydrogen Energy* , vol. 35, no. 16, p. 8371–84, 2010.

[15] A. Government, “State of Hydrogen 2021, Australia’s pathway for a clean hydrogen future,” Australian Government, Department of Industry, Science, Energy and

Resources, 2021. [Online]. Available: https://www.industry.gov.au/data-and-publications/state-of-hydrogen-2021/australias-pathway-for-a-clean-hydrogen-future. [Accessed February 2022].

[16] A. Government, "State of Hydrogen 2021-Hydrogen industry development," Australian Government, Department of Industry, Science, Energy and Resources, 2021. [Online]. Available: https://www.industry.gov.au/data-and-publications/state-of-hydrogen-2021/hydrogen-industry-development. [Accessed 1 February 2022].

[17] J. Janssen, M. Weeda, R. Detz and B. v. d. Zwaan, "Country-specific cost projections for renewable hydrogen production through off-grid electricity systems," *Applied Energy,* vol. 309, p. 118398, 2022.

[18] E. Schropp, G. Naumann and a. M. Gaderer, "Life Cycle Assessment of a Polymer Electrolyte Membrane Water Electrolysis," in *In Progress in Life Cycle Assessment ,* Springer, Cham, 2019, pp. 53-66.

[19] O. Schmidt, A. Gambhir, I. Staffell, A. Hawkes, J. Nelson and S. Few, "Future cost and performance of water electrolysis: An expert elicitation study," *international journal of hydrogen energy,* vol. 42, pp. 30470-30492, 2017.

[20] B. Lee, H. Lee, J. Heo, C. Moon, S. Moon and H. Lim, "Stochastic techno-economic analysis of H2 production from power-to-gas using a high- pressure PEM water electrolyzer for a small-scale H2 fueling station," *Sustainable energy and fuels,* vol. 3, p. 2521, 2019.

[21] G. Zhao, M. R. Kraglund, H. L. Frandsen, A. C. Wulff, S. H. Jensen, M. Chen and C. R. Graves, "Life cycle assessment of H2O electrolysis technologies," *international journal of hydrogen energy,* vol. 45, pp. 23765-23781, 2020.

[22] S. Kumar and V.Himabindu, "Hydrogen production by PEM water electrolysis – A review," *Materials Science for Energy Technologies,* vol. 2, no. 3, pp. 442-454 , 2019.

[23] D. M. Santos, C. A. Sequeira and a. J. L. Figueiredo, "Hydrogen production by alkaline water electrolysis," *Química Nova,* vol. 36, pp. 1176-1193, 2013.

[24] J. B. a. T. Turek, " Alkaline Water Electrolysis Powered by Renewable Energy: A Review," *Processes,* vol. 8, no. 248, 2020.

[25] M. Rashid, M. A. Mesfer, H. Naseem and M. Danish, "Hydrogen production by water electrolysis: a review of alkaline water electrolysis, PEM water electrolysis and high temperature water electrolysis," *International Journal of Engineering and Advanced Technology,* 2015.

[26] R. Bhandari, C. Trudewind and P. Zapp, "Life cycle assessment of hydrogen production via electrolysis–a review," *Journal of cleaner production,* vol. 85, pp. 151-163, 2014.

[27] N. Kuleshov, V. Kuleshov, S. Dovbysh, S. Grigoriev, S. Kurochkin and P. Millet, "Development and performances of a 0.5 kW high- pressure alkaline water electrolyser," *International journal of hydrogen energy,* vol. 44, p. 29441e29449, 2019.

[28] S. S. Kumar, S. U. B. Ramakrishna and D. B. &. V. Himabindu, " Preparation of RuxPd1-xO2 electrocatalysts for the oxygen evolution reaction (OER) in PEM water electrolysis," *Ionics,* vol. 24, pp. 2411-2419, 2018.

[29] P. Millet, R. Ngameni, S. A. Grigoriev, N. Mbemba, F. Brisset, A. Ranjbari and C. Etiévant, "PEM water electrolyzers: From electrocatalysis to stack development," *International Journal of Hydrogen Energy,* vol. 35, no. 10, pp. 5043-5052, 2010.

[30] K. Bareiß, C. d. l. Rua, M. Möckl and T. Hamacher, “Life cycle assessment of hydrogen from proton exchange membrane water electrolysis in future energy systems,” *Applied Energy,* vol. 237, pp. 862-872, 2019.

[31] C. Rakousky, G. P. Keeley, K. Wippermann, M. Carmo and D. Stolten, “The stability challenge on the pathway to high-current-density polymer electrolyte membrane water electrolyzers,” *Electrochimica Acta* , vol. 278, pp. 324-331, 2018.

[32] M. Bernt and H. Gasteiger, “Influence of Ionomer Content in IrO2/TiO2 Electrodes on PEM Water Electrolyzer Performance,” *Journal of The Electrochemical Society,* vol. 163, no. 11, p. F3179, 2016.

[33] A. D. Blasi, L. Andaloro, S. Siracusano, N. Briguglio, G. Brunaccini, A. Stassi, A. S. Aricò and V. Antonucci, “Evaluation of materials and components degradation of a PEM electrolyzer for marine applications,” *International Journal of Hydrogen Energy,* vol. 38, no. 18, pp. 7612-7615, 2013.

[34] A. Buttler and a. H. Spliethoff, “Current status of water electrolysis for energy storage, grid balancing and sector coupling via power-to-gas and power-to-liquids: A review,” *Renewable and Sustainable Energy Reviews,* vol. 82, pp. 2440-2454, 2018.

[35] O. Atlam and M. Kolhe, “Equivalent electrical model for a proton exchange membrane (PEM) electrolyser,” *Energy Conversion and Management,* vol. 52, pp. 2952-2957, 2011.

[36] C. Yilmaz and M. Kanoglu, “Thermodynamic evaluation of geothermal energy powered hydrogen production by PEM water electrolysis,” *Energy,* vol. 69, pp. 592-602, 2014.

[37] P. Millet, N. Mbemba, S. A. Grigoriev, V. N. Fateev, A. Aukauloo and a. C. Etiévant., “Electrochemical performances of PEM water electrolysis cells and perspectives,” *International Journal of Hydrogen Energy* , vol. 36, no. 6, pp. 4134-4142, 2011.

[38] Ö. F. Selamet, F. Becerikli, M. D. Mat and a. Y. Kaplan, “Development and testing of a highly efficient proton exchange membrane (PEM) electrolyzer stack.,” *International Journal of hydrogen energy,* vol. 36, no. 17, pp. 11480-11487, 2011.

[39] D. Jang, J. Kim, D. Kim, W.-B. Han and a. S. Kang., “Techno-economic analysis and Monte Carlo simulation of green hydrogen production technology through various water electrolysis technologies.,” *Energy Conversion and Management,* vol. 258, p. 115499, 2022.

[40] W. G. Colella, B. D. James, J. M. Moton, G. Saur and a. T. Ramsden, “Techno-economic analysis of PEM electrolysis for hydrogen production.,” *In Electrolytic Hydrogen Production Workshop. Golden, CO: NREL,* 2014.

[41] H. Nami, O. B. Rizvandi, C. Chatzichristodoulou, P. V. Hendriksen and a. H. L. Frandsen, “Techno-economic analysis of current and emerging electrolysis technologies for green hydrogen production,” *Energy Conversion and Management,* vol. 269, p. 116162, 2022.

[42] M. Carmo, D. L. Fritz, J. Mergel and D. Stolten, “A comprehensive review on PEM water electrolysis,” *international journal of hydrogen energy,* vol. 38, p. 4901e4934, 2013.

[43] d. o. I. S. E. a. R. Australian government, “NATIONAL GREENHOUSE ACCOUNTS FACTORS, Australian National Greenhouse Accounts,” 2021. [Online]. Available: https://www.industry.gov.au/sites/default/files/August%202021/document/national-greenhouse-accounts-factors-2021.pdf. [Accessed January 2022].

[44] M. M. Kostic, “Energy: Global and Historical Background,” in *Encyclopedia of Energy Engineering and Technology, Second Edition*, Taylor & Francis, 2007.

[45] A. Government, “Australia’s emissions projections 2021,” Australian Government, Department of Industry, Science, Energy and Resources, 6 October 2021. [Online]. Available: https://www.industry.gov.au/data-and-publications/australias-emissions-projections-2021. [Accessed 1 February 2022].

[46] T. B. (Germany), L. F. (USA), E. H. (Austria/Norway), A. M. (UK/Germany), D. P. (Argentina), J. R. (India), R. S. (Brazil), S. S. (Germany), R. S. (. Zealand) and P. S. (UK), “Technology-specific Cost and Performance Parameters,” IPCC, 2018. [Online]. Available: https://www.ipcc.ch/site/assets/uploads/2018/02/ipcc_wg3_ar5_annex-iii.pdf. [Accessed 10 August 2022].

[47] "Taskforce, COAG Energy Council" – "National Hydrogen Strategy", “Deloitte, Australian and Global Hydrogen Demand Growth Scenario Analysis,” COAG Energy Council, 2019.

[48] (ISPRA) and A. Caputo, “Fattori di emissione atmosferica di gas a effeto serra nel settore elettrico nazionale e nei principali Paesi Europei,” ISPRA, Rome, 2020.

[49] S. S. Kumar, S. U. B. Ramakrishna and B. R. D. &. V. Himabindu, “Phosphorus-doped carbon nanoparticles supported palladium electrocatalyst for the hydrogen evolution reaction (HER) in PEM water electrolysis,” *Ionics*, vol. 24, pp. 3113-3121, 2018.

[50] S. Siracusano, A. D. Blasi, V. Baglio, G. Brunaccini, N. Briguglio, A. Stassi, R. Ornelas, E. Trifoni, V. Antonucci and A. S. Aricò, “Optimization of components and assembling in a PEM electrolyzer stack,” *International Journal of Hydrogen Energy*, vol. 36, no. 5, pp. 3333-3339, 2011.

[51] S. Siracusano, V. Baglio, A. D. Blasi, N. Briguglio, A. Stassi, R. Ornelas, E. Trifoni, V. Antonucci and A. S. Aricò, “Electrochemical characterization of single cell and short stack PEM electrolyzers based on a nanosized IrO2 anode electrocatalyst,” *International Journal of Hydrogen Energy*, vol. 35, no. 11, pp. 5558-5568, 2010.

[52] C. Zhang, J. Wang, Z. Ren and Z. a. W. P. Yu, “Wind-powered 250 kW electrolyzer for dynamic hydrogen production: A pilot study.,” *International Journal of Hydrogen Energy*, vol. 46, no. 70, pp. 34550-34564, 2021.

[53] H. M. H. a. T. T. Kojima, “Development of large scale unified system for hydrogen energy carrier production and utilization: Experimental analysis and systems modeling.,” *International Journal of Hydrogen Energy*, vol. 42, no. 19, pp. 13444-13453, 2017.

[54] L. Valverde-Isorna, D. H. D. Ali and a. M. Abdel-Wahab, “Modelling the performance of wind–hydrogen energy systems: Case study the Hydrogen Office in Scotland/UK.,” *Renewable and Sustainable Energy Reviews*, vol. 53, pp. 1313-1332, 2016.

[55] J. Burkhardt, A. Patyk, P. Tanguy and C. and Retzke, “Hydrogen mobility from wind energy–A life cycle assessment focusing on the fuel supply,” *Applied energy*, vol. 181, pp. 54-64, 2016.

[56] O. Alavi, A. Mostafaeipour and M. and Qolipour, “Analysis of hydrogen production from wind energy in the southeast of Iran.,” *International Journal of Hydrogen Energy*, vol. 41, no. 34, pp. 15158-15171, 2016.

[57] A. Ursúa, I. San Martín, E. Barrios and P. and Sanchis, “Stand-alone operation of an alkaline water electrolyser fed by wind and photovoltaic systems,” *International Journal of Hydrogen Energy*, vol. 38, no. 35, pp. 14952-14967, 2013.

[58] P. Floch, S. Gabriel, C. Mansilla and F. and Werkoff, “On the production of hydrogen via alkaline electrolysis during off-peak periods.,” *International journal of hydrogen energy,* vol. 32, no. 18, pp. 4641-4647, 2007.

[59] K. Agbossou, R. Chahine, J. Hamelin, F. Laurencelle, A. Anouar, J. St-Arnaud and T. and Bose, “Renewable energy systems based on hydrogen for remote applications.,” *Journal of power sources,* vol. 96, no. 1, pp. 168-172, 2001.

[60] A. Dutton, J. Bleijs, H. Dienhart, M. Falchetta, W. Hug, D. Prischich and A. and Ruddell, “Experience in the design, sizing, economics, and implementation of autonomous wind-powered hydrogen production systems.,” *International Journal of Hydrogen Energy,* vol. 25, no. 8, pp. 705-722, 2000.

[61] D. THOMAS, “Hydrogenics shift power, energize your world,” Hydrogenics Europe N.V., 21 February 2019. [Online]. Available: https://etipwind.eu/wp-content/uploads/A2-Hydrogenics_v2.pdf. [Accessed December 2021].

[62] “Hydrogen generators,” Nel, [Online]. Available: https://nelhydrogen.com/wp-content/uploads/2020/03/High-Purity-Brochure-Rev-H-Single-Pages.pdf. [Accessed December 2021].

[63] Cummins, “Hydrogen: the next generation,” Cummins, [Online]. Available: https://www.cummins.com/sites/default/files/2021-08/cummins-hydrogen-generation-brochure-20210603.pdf. [Accessed December 2021].

[64] “Purity,” Amtronics, [Online]. Available: https://h2gen.com.au/wp-content/uploads/2020/11/Sirio-PEM-technical-datasheet.pdf. [Accessed December 2021].

[65] “PEM Electrolysis and Refueling Equipment,” SinoHy Energy, [Online]. Available: https://www.sinohyenergy.com/pem-electrolysis-and-refueling-equipment/. [Accessed December 2021].

[66] “2 GEP Skid,” ITM power, [Online]. Available: https://itm-power.com/products/2gep-skid. [Accessed December 2021].

[67] Hefei Sinopower technologies, [Online]. Available: https://sinopowerfc.en.alibaba.com/product/1600399351689-904325465/High_purity_H2_generator_water_electrolysis_1NM3_to_300NM3_Hour_pem_electrolyzer_electrolyzer_stack.html?spm=a2700.shop_index.104470.5.73997a7aIa4O3e. [Accessed December 2021].

[68] Toplink, [Online]. Available: https://toplinking.en.alibaba.com/product/62493439954-816861916/electrolyzed_water_machine_pem_hydrogen_generator_membrane_electrolyzer.html. [Accessed December 2021].

[69] “GREEN ELECTROLYZER Hydrogen from Renewable Energy,” IGAS, [Online]. Available: https://igas-energy.de/fileadmin/individual/igas-energy-de/editor/Broschueren/iGas_green_Elektrolyzer_E_170420.pdf . [Accessed December 2021].

[70] “ THE PLUG 1MW ELECTROLYZER,” Plug Power, [Online]. Available: https://www.plugpower.com/wp-content/uploads/2020/10/2021_1MWELXSpec_F101821.pdf. [Accessed December 2021].

[71] “Pem electrolysers,” Elogen, [Online]. Available: https://elogenh2.com/wp-content/uploads/2021/04/Elogen_Product_sheet-Elyte200.pdf . [Accessed December 2021].

[72] “PEM electrolyzers,” Green H2 systems, [Online]. Available: https://www.green-h2-systems.de/en/Technology.html. [Accessed December 2021].

[73] “H-TEC PEM Electrolyser ME450/1400,” H-Tec systems, [Online]. Available: https://www.h-tec.com/en/products/detail/h-tec-pem-electrolyser-me450-1400/me450-1400/. [Accessed December 2021].

[74] “Silyzer 300 The next paradigm of PEM electrolysis,” Siemens Energy, [Online]. Available: https://assets.siemens-energy.com/siemens/assets/api/uuid:a193b68f-7ab4-4536-abe2-c23e01d0b526/datasheet-silyzer300.pdf. [Accessed December 2021].

[75] “PEM water electrolysis,” Cocherill Jingli Hydrogen, [Online]. Available: https://www.jinglihydrogen.com/water-electrolyzer/pem-water-electrolysis.html. [Accessed 08 August 2022].

[76] “Hydrogen generator,” Suzhou green hydrogen energy, [Online]. Available: https://www.sghec.com/product/hydrogen-generator/. [Accessed 08 August 2022].

[77] “Hy.Gen-E on-site hydrogen generation system,” HyGear, [Online]. Available: https://hygear.com/wp-content/uploads/2021/06/HyGear_Hy.GEN-e_hydrogen-generation-system_electrolysis.pdf. [Accessed 08 August 2022].

[78] “Atmospheric Alkaline Electrolyser,” Nel, [Online]. Available: https://nelhydrogen.com/product/atmospheric-alkaline-electrolyser-a-series/?gclid=Cj0KCQjwxb2XBhDBARIsAOjDZ37QV2T59xJWKvDx-xqroMQCn81Ol7nf-A9M59CXnkOFNV47NA0OyXAaAlGREALw_wcB. [Accessed 08 August 2022].

[79] “Technical Specs A-series & X-series,” Green hydrogen systems, [Online]. Available: https://9441822.fs1.hubspotusercontent-na1.net/hubfs/9441822/Brochures/Technical%20specs.pdf. [Accessed 08 August 2022].

[80] “McLyzer range: 100 to 800 Nm3/h at 30 bar,” McPhy, [Online]. Available: https://mcphy.com/en/equipment-services/electrolyzers/large/. [Accessed 08 August 2022].

[81] “Hydrogen generators,” H2Gen, [Online]. Available: https://h2gen.com.au/wp-content/uploads/2020/05/Mercury-Hydrogen-Gen-brox-2019.pdf. [Accessed 08 August 2022].

[82] “Alkaline water electrolysis Machine,” Cockerill Jingli Hydrogen, [Online]. Available: https://www.jinglihydrogen.com/water-electrolyzer/water-electrolyzer-dq50.html. [Accessed 08 August 2022].

[83] “RENEWABLE HYDROGEN FOR ALL APPLICATIONS SUNFIRE-HYLINK ALKALINE,” Sunfire, [Online]. Available: https://www.sunfire.de/files/sunfire/images/content/Sunfire.de%20(neu)/Sunfire-Factsheet-HyLink-Alkaline_20220520.pdf. [Accessed 09 August 2022].

[84] “Aqualyzer,” Asahi Kasei, [Online]. Available: https://ak-green-solution.com/en/. [Accessed 09 August 2022].

[85] A. Pietra, M. Gianni, N. Zuliani, S. Malabotti and a. R. Taccani, “Experimental Characterization of an Alkaline Electrolyser and a Compression System for Hydrogen Production and Storage,” *energies,* vol. 14, no. 5347, 2021.

4 Chapter4: Life Cycle Assessment of hydrogen generation via PEM electrolyser regarding stack component weight and energy source variation

ABSTRACT

One of the most important aspects regarding the acceptance of hydrogen technology as an alternative to fossil fuels is its environmental impact. PEM and Alkaline technologies are the most commercialized water electrolysis systems. In addition, the electricity consumption of alkaline technology is higher than PEM technology to produce hydrogen. Therefore, in this study, the environmental impacts of hydrogen generation through PEM technology are investigated. For this purpose, nine energy and stack configuration scenarios in three regions, Australia, Italy, and the whole world, are considered. It is found that the biggest contributor to environmental impacts in hydrogen generation via the PEM system is electricity consumption. In addition, by a complete transition from fossil fuels to renewable energy sources, in general, for most indices stack materials become the main contributor. However, for some indices, such as global warming potential, electricity consumption is still the main contributor, with more than around 75% contribution. By comparing three regions at the current condition, which means the current electricity from the electricity grid, it is found that Australia and Italy have the highest and the lowest quantity of indices, respectively, with some exceptions. By a sensitivity analysis of environmental impact regarding the stack material variation it is realized that, at the current condition, the most effective elements on indices are iridium, platinum, and Nafion, and variation in other elements does not have a significant impact on the LCIA result. However, it is recognized that for the global warming index titanium, iridium, and platinum are the main contributors. In addition, it is found that by the transition from fossil fuels to RES, indices such as global warming show desirable results, carbon dioxide emission of 1 kg hydrogen production could reach the range of 1 to 2.3 kg from around 25 kg CO_2 emission. While, some indices, such as mineral resources scarcity do not show desirable results. Therefore, this transition could be a proper solution for global warming mitigation while the material intensity and cost become more important. Furthermore, it is recognized that the transition to wind energy sources should be investigated properly because of the undesirable result of several indices after the transition.

4.1 Introduction

The most famous renewable energy sources (RES) are solar energy, wind energy, hydro energy, geothermal energy, biomass energy, and tidal energy. Solar and wind energies are unpredictable and intermittent. Hydro and biomass energies are dependent upon water and land availability, while geothermal and tidal energies are limited to specific locations. These limitations lead to a low contribution to electricity generation. A solution to increase the RES contribution to the supply of energy is storage. Among others, hydrogen is an energy carrier that can be used to store energy from RES [1]. It arises several questions which should be addressed to prove the hydrogen technology:

-Which technology can be used to produce hydrogen?

-What is the environmental impact of proposed hydrogen generation technology for the whole generation procedure?

-Is the selected technology more sustainable in comparison to other widespread technologies for hydrogen generation?

Hydrogen is considered a suitable zero-emission alternative to fossil fuels since it has the potential of being carbon-free with the highest energy content per kg compared to any known fuel [2]. Hydrogen currently has applications in several industrial processes, such as petroleum refining, metal treating [2], production of ammonia, methanol, pharmaceutical [3], and the food and beverages sector for hydrogenation of amines and fatty acids [4]. In addition, it is expected that, in the near future, hydrogen generation will increase, and multiple options will be opened by decarbonization requirements, like being used for power generation, in the transport sector, and for space heating in residential buildings [2]. Hydrogen can be injected into the natural gas network up to specific values considering the legislations in different countries [5, 6, 7, 8]. Hydrogen blending provides the opportunity to further integrate hydrogen use in the natural gas and electricity sectors [9].

Currently, hydrogen is mostly produced by fossil fuel energy sources through processes characterized by high environmental impact [10], like steam methane reforming (SMR). Interest in water electrolysis systems using power from RES to produce hydrogen, or the so-called “green hydrogen”, is increasing because of its benefits related to CO_2 emission reduction and climate change mitigation [11]. Available water electrolysis technologies are alkaline, Proton Exchange membrane (PEM), solid oxide electrolysis cells (SOEC), and Anion exchange membrane (AEM). Among the electrolysis technologies, SOEC and AEM are the least evolved technologies [12], and further research is required to be commercially available. In addition, the conversion efficiency of alkaline is lower than PEM technology, which leads to higher energy consumption and environmental impact [13].

Life cycle assessment (LCA) is a standardized methodology to determine the environmental impact associated with the life cycle of products and services [14]. LCA includes four steps: (i) goal and scope definition, (ii) life cycle inventory, (iii) life cycle impact assessment (LCIA), and (iv) interpretation of results. Several researchers have focused on the LCA of hydrogen generation through PEM technology. Schropp et al. [15] investigated the LCA of hydrogen production in a 1.25 MW plant, in Germany, under 3 energy scenarios: current condition, the mixture of 70% wind and 30% solar energy, and 100% wind. They indicated that GWP100 of scenarios 1 to 3 would be 32.52, 2.02, and 0.93 kg CO_2-eq per kilogram hydrogen. The method of LCIA in their study was CML 2001. It should be noted that various methods provide different indices, however, some indices could be common among the methods, such as the global warming index. Zhao et al. [16] applied the LCIA method of ReCiPe 2016 (H) and estimated the LCA for the current condition with scenarios related to recycling, considering the average electricity mix in Denmark and using the Ecoinvent database. They estimated the GWP of around 72 kg CO_2-eq per kilogram hydrogen for the current condition. In addition, they stated that recycling can reduce GWP by around 30%. However, the contribution of BOP and stack materials should be checked to confirm if it is possible to reduce by 30 % or not. Zhang et al. [17] performed an LCA analysis of PEM technology in Switzerland, based on ILCD 2011 Midpoints method. They considered 3 scenarios of current grid condition, 100% wind, and 100% solar energy as the energy source. In addition, they compared the result with the current condition of the European grid. They estimated 10, 40, 60, and 247 g CO_2-eq per MJ of hydrogen, for wind, solar, current condition, and Europe scenarios, respectively. The conversion results in approximately, 1.2, 4.80, 7.20, and 29.64 kg CO_2-eq per kilogram hydrogen. Bareiß et al. [18] investigated the LCA of hydrogen generation through PEM technology in Germany at a 1 MW power plant based on 3 scenarios, the current condition in 2017, the prediction for 2050, and 65% wind-35% solar. The result was around 29, 11.5, and 3 kg CO_2-eq per kilogram hydrogen. The ReCiPe Midpoint method is used in Bareiß's study and only 7 indices among 16 indices of the ReCiPe method are analysed. Delpierre et al. [19] projected the environmental impact of PEM technology, using wind power in the Netherlands, considering 2 scenarios for the development of the technology in 2050, low development (100 MW plant) and high development (1 MW plant). They estimated that the carbon dioxide emission would be around 0.77 kg CO_2-eq per kilogram hydrogen.

It can be seen that previous studies have mostly focused on the LCA of hydrogen in one region or country [17], [18], [19], [20], [21] for small-scale experimental hydrogen production stacks or case studies of available hydrogen generation plants with a limited number of scenarios. Therefore, the comparison of various environmental indices among different regions is not covered properly in the literature. In addition, scenarios provided in the mentioned studies are mainly related to the complete transition from fossil fuels to solar and wind, while other RES are not considered. Furthermore, in the abovementioned studies, for future scenarios, the whole energy supply is considered to be replaced with RES, without the consideration of the current contribution of other RES, such as hydro, and nuclear energy. To the best knowledge of the authors, only in [16] the reduced material of the system is considered to estimate environmental impact which needs more investigation.

In this chapter, all stages of LCA are investigated to determine the environmental impact of hydrogen production through PEM electrolysis. In particular, the chapter provides a possible range for the environmental impact of 1 kg hydrogen production through a 1 MW PEM hydrogen generation plant. Various aspects are considered in this study to cover the lag of LCA studies in hydrogen generation through PEM technology. Instead of assessing only one region, three regions are considered, Australia, and Italy, as the countries with high potential for hydrogen production via RES and export to other countries, and the whole world for the sake of comparison. In addition, the comparison of 18 indices related to the ReCiPE LCIA method is provided in this study. Scenarios including the transition from fossil fuel to wind, solar, hydro, and their combination are provided to cover the lag of energy scenarios related to hydro energy. In the case of the energy scenarios investigated in this study, only the fossil fuel contribution is substituted by RES, which results in more reliable values compared to the 100% contribution of one type of RES. In addition, a sensitivity analysis is performed regarding the stack components' weight variation to assess the impact of material changes on environmental emissions for current and future scenarios of electricity sources. In the end, the comparison with the SMR method is provided for the clarification of scenarios' effects on environmental impact reduction. In addition, the contributions of materials and utilities in global warming potential are compared to define the most important part to be focused on by researchers.

This chapter is divided into two main sections, methodology and "results and discussion". The methodology includes goal and scope definition; life cycle inventory and scenarios are also explained in the methodology section. In the result and discussion section, LCIA and the interpretation of the results are provided.

4.2 Methodology

To determine the environmental impact of the PEM plant for hydrogen generation in this study, a life cycle assessment is performed on collected information from literature Table 4.A. 1. The LCA is performed based on the hydrogen generation LCA guidance developed by Lozanovski et al. [22] (this guidance is according to the ISO 14040 and 14044 standards.). LCA framework includes several phases such as goal and scope definition, life cycle inventory, life cycle impact assessment, and interpretation of the results which are discussed in this chapter.

4.2.1 Goal and scope definition

The main objective of this study is to quantify environmental impact indices of hydrogen production by PEM electrolyser under different energy and stack configuration scenarios. For this purpose, a PEM hydrogen generation plant including a stack (considering the variation of stack materials), Balance of plant (BOP) which the components are shown in the system boundary in Figure 4. 1, and energy consumption considering several scenarios in terms of energy source is considered. Various PEM plant details from the literature are collected in this study to provide an overview of the possible range of environmental impact indices of hydrogen production by PEM technology (Table 4.A. 1). Another goal of this study is the verification of the results stated by Bareiß et al. [18] and Wulf and Kaltschmitt [23], they revealed that the biggest contributor to environmental impact in hydrogen generation via PEM technology is electricity supply and the contribution of producing the hydrogen production plant is negligible.

The LCA, in this study, has been modelled as a cradle to gate system which is the life cycle assessment from raw material extraction to the product at the factory gate. The functional unit is defined as 1 kg of hydrogen produced in a 1 MW PEM electrolysis plant, with a standard quality of 5.0 and 30 bar pressure at 80°C operating temperature.

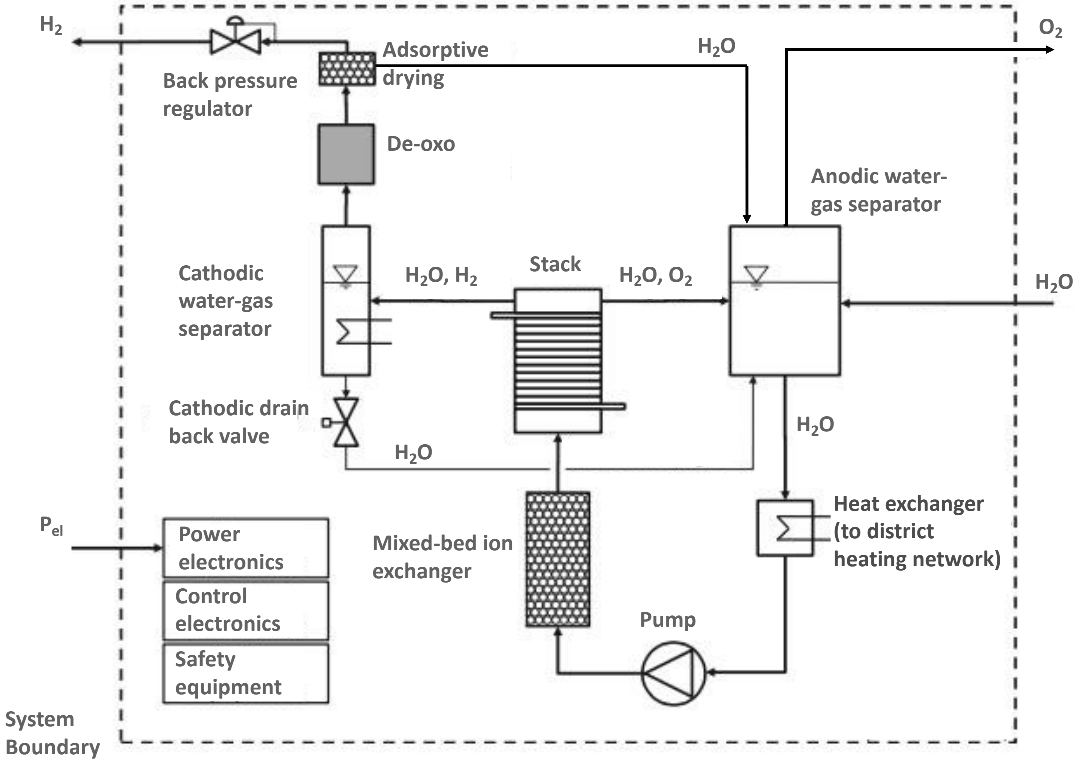

Figure 4. 1 Scheme of PEM system boundary, based on K. Bareiß et al. [18] with modification

Figure 4. 1 illustrates the components and hydrogen production stages included within the system boundaries. In the first stage, water is fed to the anode water-gas separator unit. Fed water to the system should have a conductivity of less than 0.1 µS/cm to prevent system degradation [18]. After the anode water-gas separator, there is a heat exchanger to control the temperature of water considering the difference between the required temperature of the stack and the temperature of water fed to the system or water in the cycle. In the next step, water is pumped to stack after passing through an ion exchange resin cartridge to maintain the conductivity of water. There are two outlets at the stack. One of them is to discharge water and oxygen which is connected to the anode water-gas separator to separate oxygen from water and use water again in the cycle. Procedures applied to oxygen after anode water-gas separator such as drying, and purification are assumed to be outside the system boundary of this study. Hydrogen and water leave the stack through the cathodic outlet. To separate hydrogen from water the mixture will be cooled down to ambient temperature in the cathodic water-gas separator, separated water is used again by connecting the cathodic water-gas separator to the anode water-gas separator. Hydrogen after the cathodic water-gas separator still has a small portion of oxygen and water content which should be reduced to less than 5ppm [18]. These reductions are carried out in de-oxo purification and adsorptive drying respectively for oxygen and water removal. For simplification, valves are neglected in this study. Other important system components are control systems, safety

equipment, and power electronics such as rectifiers, voltage transformers, and power inverters in case of using solar and wind energy.

Australia and Italy have high potential in hydrogen generation using RES, in addition, their strategic geographical position provides the opportunity to supply the hydrogen demand to numerous countries, therefore, a part of this study is allocated to the assessment of LCA in Australia and Italy and comparison of the result with the whole world result. SimaPro 9.4 is used for the estimation of environmental indices and data has been taken from the Ecoinvent v3 database. For the stack and BOP components, it is assumed that all components and activities in a global location can be used from the ecoinvent, and the transportation is negligible. However, in some cases, global information is not available and other locations such as Australia and Europe are used. For the electricity generation emission factors, ecoinvent v3 does not cover all desired sources of electricity in Italy, Australia, and the whole world. It is assumed that the emission factor of fuels has a negligible difference in different regions. Thus, for hard coal, oil, and nuclear energy, the Union for the Coordination of Transmission of Electricity (Europe) (UCTE) is used; for natural gas and solar energy, information in Italy and Australia is used, respectively; and for wind and hydro energy, Europe is considered. The method which is used for LCIA is Recipe 2016 Midpoint (H) which is related to 100 years' time horizon.

4.2.2 Life cycle inventory

Units and processes in the system boundary are depicted in Figure 4. 1 and the main assumptions are described in this section. It is assumed that clean water with conductivity less than 0.1 μS/cm is used, thus, the unit for water purification or water desalination is not included in the system boundary.

4.2.2.1 PEM stack

The main component of hydrogen production by PEM technology is the PEM stack, in which single cells are connected in series. Single cells inside the stack are separated by means of bipolar plates which are mostly titanium. Bipolar plates have a multifunctional character such as uniform distribution of gas and air, conduct electrical current from cell to cell, heat control, and gas leakage prevention. These characteristics are different in various types of bipolar plates which are mainly different in the flow field configuration. For electrical connection, there are two current collectors mostly made of aluminium and copper which are located at the top and bottom of the stack. To fix the structure of the stack and evenly compress individual cells together end plates, bolts, nuts, and flat springs are used. Commercial system stack lifetime is typically 40,000 to 60,000 [18] hours; in this study, the stack lifetime is assumed 7 years. Main materials and assumed masses of a 1 MW PEM plant stack are provided in Table 4. 1 and Table 4. 2 which are based on the literature review from studies provided in Table 4.A. 1 by scaling up to a 1 MW plant. For this purpose, the active area is calculated based on the power density and the materials' quantity is calculated according to the required active area.

4.2.2.2 Balance of plant

A rough estimation for the material of the BOP is provided based on the Bareiß et al. [18] study with modification. The system is assumed containerized in a standard 20 ft container that weighs approximately 3.9 t. The foundation is assumed 4 shallow single footings with 25 cm depth and an area of 2.25 m^2. Considering the concrete density of 2400 kg/m^3 the total weight of the concrete is 5.4 t. Assuming a mesh of rebar with a diameter of 12 at the top and bottom, with a spacing of 20 cm, the total weight of foundation reinforcement is approximately 0.2 t. A pump with a power of 10 kW is considered to provide sufficient water flow. The power electronics units including voltage adaption and rectifiers weigh 1 t and the control system is assumed to be 0.1 t. Considering the other components and processes such as piping and lubrication the weight of the main materials of the PEM BOP is provided in Table 4. 3 and Table 4. 4.

Material	Minimum mass (kg)	Maximum mass (kg)	Average mass (kg)
Titanium (Bipolar plate)	499.50	1,755.00	1,127.25
Gold coat (Bipolar plate)	0.11	0.11	0.11
Aluminum alloy (end plates)	27.00	27.00	27.00
Stainless steel (Bolt,nuts, and flat springs)	100.00	100.00	100.00
Copper (current collector)	4.50	4.50	4.50
Nafion	1.92	25.50	13.45
Activated carbon(Carbon paper (Cathode))	0.08	9.00	2.07
Iridium (Anode)	0.30	2.58	1.39
Titanium felt (Anode)	15.02	66.00	36.50

Material	Minimum mass (kg)	Maximum mass (kg)	Average mass (kg)
Platinum (Cathode)	0.04	0.60	0.18
gasket (synthetic rubber)	4.80	4.80	4.80
Total mass (kg)-stack	653.27	1,995.09	1,317.25
Total mass (t)-stack	0.65	2.00	1.32

Table 4. 1 Main materials and assumed masses of the PEM plant stack, divided by stack components and materials.

For water purification, a mixed-bed ion exchanger is considered which is used mostly where high water quality is needed. Mixed-bed ion exchanger has cation and anion resins (zeolites) that are mixed in a single vessel. Cations and anions dissolved in the water are exchanged for hydrogen ions and hydroxide ions, respectively. The depleted mixed-bed resins can be regenerated usually with hydrochloric acid (HCl) and sodium hydroxide (NaOH). This unit can be used as a last step for water purification after other demineralization steps (polishing mixed-bed) or as the main purifier (working mixed-bed) which in this study the latter is considered. The chemical consumption for resin regeneration of a working mixed-bed is approximately in the range of 10 to 100 g HCl and 25 to 250 g NaOH for each 1 m^3 polished water [24]. The assumed chemical consumption of mixed-bed ion exchanger in this study is 55 g HCl and 137.5 g NaOH for 1 m^3 purified water. Approximately 9 kg of water is needed to produce 1 kg hydrogen using a PEM electrolyser. Therefore, the quantity of HCl and NaOH are 0.495 and 1.2375 g/kg H_2.

Material	Minimum mass (kg)	Maximum mass (kg)	Average mass (kg)
Titanium	514.52	1,821.00	1,163.75
Stainless steel	100.00	100.00	100.00
Aluminum alloy	27.00	27.00	27.00
Nafion	1.92	25.50	13.45
synthetic rubber production	4.80	4.80	4.80

Material	Minimum mass (kg)	Maximum mass (kg)	Average mass (kg)
Copper	4.50	4.50	4.50
Activated carbon	0.08	9.00	2.07
Iridium	0.30	2.58	1.39
Platinum	0.04	0.60	0.18
Gold coat	0.11	0.11	0.11
Total mass (kg)-stack	653.27	1,995.09	1,317.25
Total mass (t)-stack	0.65	2.00	1.32

Table 4. 2 Main materials and assumed masses of the PEM plant stack, based on material separation.

During the hydrogen generation electrolysis process, heat is generated through the chemical reaction. A heat exchanger is needed to maintain the working temperature within 60 to 80 °C [18]. A suitable heat exchanger for PEM electrolysis could be stainless steel (alloy 316) plate heat exchanger to prevent hydrogen embrittlement of the materials. According to the "Experimental hydrogen yield for 1 MW (m^3/h)" column in Table 4.A. 1 in the appendix the average hydrogen yield is around 250 m^3/h (22.52 kg/h). The amount of water required for cooling is assumed 50 t/h according to SinoHy Energy [25]. A possible heat exchanger could be the LX-00 model from HISAKA WORKS, LTD. [26] which weighs around 0.21 t. The operating pressure could be higher than the capacity of the selected heat exchanger which could be reduced by using pressure-reducing valves. It is assumed that the water which is used in the heat exchanger is fed into a district heating network to use the waste heat of the reaction. Thus, the amount of water and the energy for pumping the water to the heat exchanger is not considered inside the system boundary.

The produced hydrogen after passing the cathodic water-gas separator is saturated with water vapor. The water vapor content at 30 bar pressure is approximately 7 g H_2O per kg of H_2. In addition, there is around 800 ppm oxygen impurity in the produced hydrogen which should be removed to have the desired hydrogen quality. De-oxo purification unit is used to remove the oxygen impurity. To remove 800 ppm, around 15 g water is produced per 1 kg of hydrogen [18]. The consumed hydrogen to remove oxygen at De-oxo is neglected. The total amount of 22 g water per kg of hydrogen should be removed in the adsorptive drying unit to have dry hydrogen. Silica gel is mostly used as an adsorbent which adsorbs water at its surface until saturated condition. The energy to evaporate 1 kg water from Silica is 7100-8400 kJ which results in 0.05 kWh per 1 kg dried hydrogen at 30 bar pressure [18].

According to Lehner et al. [27], most PEM systems operate at a pressure between 30 and 60 bar, without the installation of any additional compression unit, therefore, in this study, in which the aim is hydrogen at 30 bar, the compression unit is not required in the system boundary.

In addition to the abovementioned components some other construction and process materials such as piping (plastic and stainless steel), steel elements, and lubricants are considered in Table 4. 3 and Table 4. 4 based on Bareiß et al. [18] and Niklas Gerlof [28] studies with modification.

The lifetimes of the BOP components are assumed to be 20 years. For the energy scenarios related to intermittent renewable sources such as solar and wind, for simplification, it is assumed that the total equivalent time of operation is 20 years. It is assumed that 260 days of a year is working days and the rest is off day or allocated to maintenance. Therefore, the total hydrogen production in the lifetime of the system can be calculated as follow:

$$20 \times 260 \times 24 \times 22.52 = 2{,}810{,}496\ kg\ H_2$$

Unit	Materials	Mass (t)	Contribution to BOP weight
Water-gas separator	Copper	0.1	0.865%
Heat exchanger	High alloyed steel	0.21	1.816%
Tubing and pump	Low alloyed steel	0.9	7.784%
lubricant	grease	0.1	0.865%
piping	Plastic	0.3	2.595%
Ion exhanger	Zeolite (powder)	0.1	0.865%
	HCl	0.000495	0.004%
	NaOH	0.001238	0.011%

Unit	Materials	Mass (t)	Contribution to BOP weight
De-oxo and water treament	Aluminium	0.1	0.865%
container (20 ft standard)	Low alloyed steel	2.3	19.893%
Steel structure	chromium steel (high alloyed steel)	0.75	6.487%
Foundation	Concrete	5.4	46.706%
	Low alloyed steel (reinforcement)	0.2	1.730%
Power electronics (rectifier, voltage adaption)	Aluminium	0.1	0.865%
	Copper	0.2	1.730%
	Low alloyed steel	0.6	5.190%
	elastomere (tube insulation)	0.1	0.865%
control panel/electronics	electronics production	0.1	0.865%
Total mass of main materials of the PEM plant except stack (t)			11.56

Table 4. 3 Main materials and assumed masses of the PEM plant without stack, based on unit separation. Modification of the results from Bareiß et al. [18] and Niklas Gerlof [28].

Materials	Mass (t)	Contribution to BOP weight
Concrete	5.4	46.706%
Low alloyed steel	3.8	32.868%
High alloyed steel	0.96	8.304%
Copper	0.3	2.595%
Plastic	0.3	2.595%

Aluminium	0.2	1.730%
reinforcing steel	0.2	1.730%
grease	0.1	0.865%
Zeolite (powder)	0.1	0.865%
electronics production	0.1	0.865%
elastomere (tube insulation)	0.1	0.865%
NaOH	0.001238	0.011%
HCl	0.000495	0.004%
Total mass (t)	11.56	

Table 4. 4 Main materials and assumed masses of the PEM plant without stack, based on material separation.

4.2.2.3 Energy, water, and heat

Energy consumption for the assembly of the PEM stack and BOP in kWh of a 1MW system is extracted from Niklas Gerlof‘s *[28]* study. Considering 2,810,496 kg hydrogen generation during the lifetime of the plant, assembly energy per 1 kg hydrogen generation is calculated and shown in Table 4. 5. The Operational energy consumption and Water consumption to produce 1 kg hydrogen are provided in Table 4. 6.

Assembly energy in kWh of 1MW system	
PEM electrolysis Stack	311,672.3
PEM electrolysis BOP	50,000.0
Assembly energy kWh/kg H2	
PEM electrolysis Stack	0.110896
PEM electrolysis BOP	0.017790

Table 4. 5 Stack and BOP assembly energy

<table>
<tr><th>Water demand
H2 production (l)</th><th>Electricity demand
(kWh)-stack</th><th>Electricity demand
(kWh)-Pump^1</th><th>Heat ^{2}(kWh)</th></tr>
<tr><td>9</td><td>36.2-58.7</td><td>0.44</td><td>0.28</td></tr>
<tr><td colspan="4">1. 10 kW pump, 10 kWh to produce 22.52 kg hydrogen
2. extracted from Niklas Gerlof [28]</td></tr>
</table>

Table 4. 6 Operational energy consumption and Water consumption

The theoretically required water for 1 kg hydrogen production is 9 l. In this study it is considered that the water for other sections such as the cooling unit is recycled and reused in the process, thus, the amount of water for other sections is neglected.

4.2.3 Scenarios- stack materials and energy

To assess the LCIA of hydrogen generation through PEM technology several scenarios are considered in this study:

- Sc1: Minimum stack mass and minimum electricity for operation (at current electricity grid contributions condition which is called current condition or current situation hereafter in this study)
- Sc2: Average stack mass and average electricity for operation (current condition)
- Sc3: Maximum stack mass and maximum electricity for operation (current condition)
- Sc4: Minimum stack mass and average electricity for operation (current condition)
- Sc5: Maximum stack mass and average electricity for operation (current condition)
- Sc6: Average stack mass and average electricity for operation, the contribution of fossil fuels is allocated to solar for electricity generation
- Sc7: Average stack mass and average electricity for operation, the contribution of fossil fuels is allocated to wind for electricity generation
- Sc8: Average stack mass and average electricity for operation, the contribution of fossil fuels is allocated to hydro for electricity generation
- Sc9: Average stack mass and average electricity for operation, allocation of fossil fuels contributions to solar, hydro, and wind for electricity generation with the same weight.

Scenarios Sc1, Sc2, and Sc3 are compared to assess the current condition variation. It should be noted that the result of LCIA in scenario Sc1 is less than Sc2, and the Sc3 LCIA result is greater than Sc2. These scenarios are investigated to provide a possible range and the average value of the indices.

Scenarios Sc2, Sc4, and Sc5 are used to investigate the changes in indices by variation of the stack materials. For this purpose, the average electricity for operation is considered and the only variable is the stack component mass. Variation of the LCIA is calculated considering Sc2 as the base scenario.

Scenarios Sc2, Sc6, Sc7, Sc8, and Sc9 are used to assess the changes in indices by variation of the contribution of electricity generation via renewable energy sources. For this purpose, average stack mass is considered, and the only variable is the electricity source. Variation of the LCIA is calculated considering Sc2 as the base scenario.

4.3 Results and discussion

In this section, LCIA and the interpretation of the results are provided. The LCIA at the current grid situation, variation in stack materials, and variation in the source of electricity generation is investigated to numerically assess the variation of indices.

4.3.1 LCIA- Current situation- Australia, Global, Italy

Scaled relative LCIA is used in this section at the current situation. To calculate the values of scaled relative LCIA each index quantity is divided to the maximum value of the same index in all scenarios in all regions. Scaled relative LCIA is a comparative representation of the results. It provides the opportunity to simply find the scenarios with the highest values of desired indices, as it is shown in Figure 4. 2 and Figure 4. 3.

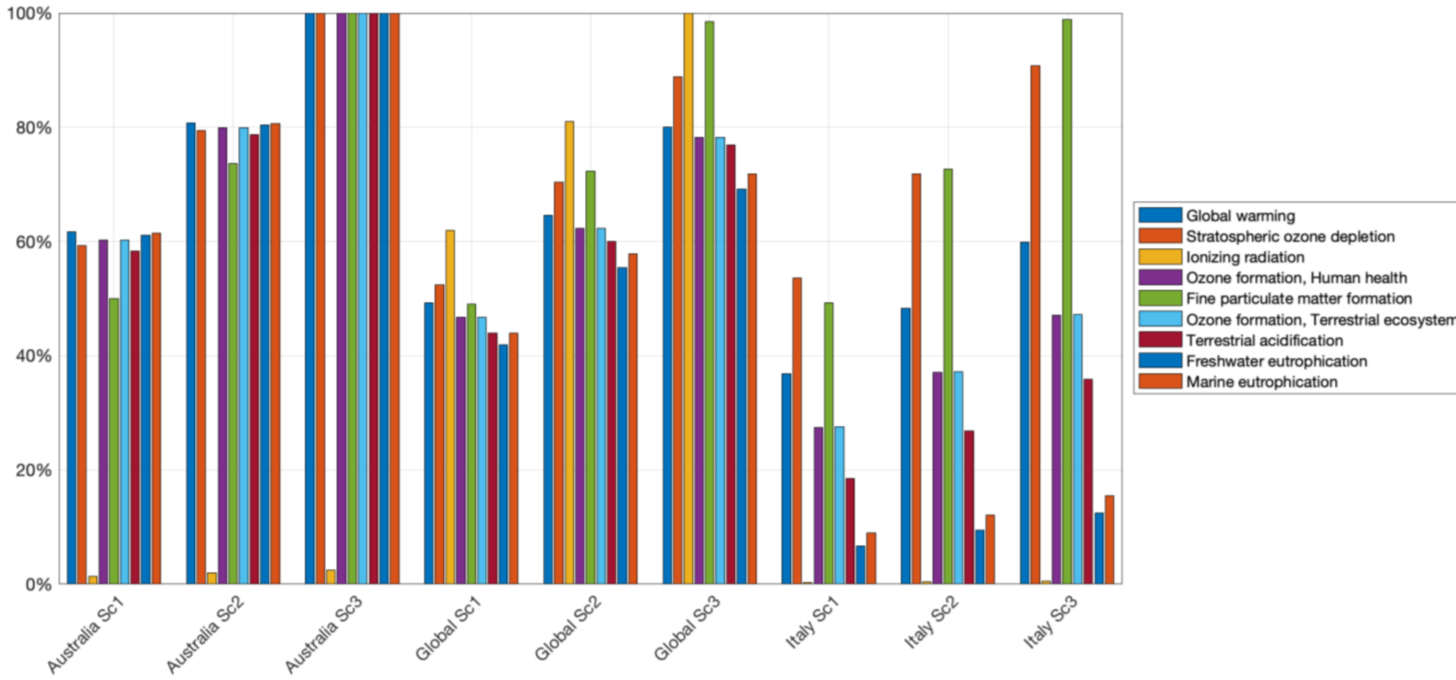

Figure 4. 2 Scaled relative LCIA of Global warming, stratospheric ozone depletion, ionizing radiation, Ozone formation, Human health, Fine particulate matter formation, Ozone formation, Terrestrial ecosystems, Terrestrial acidification, Freshwater eutrophication, Marine eutrophication indices.

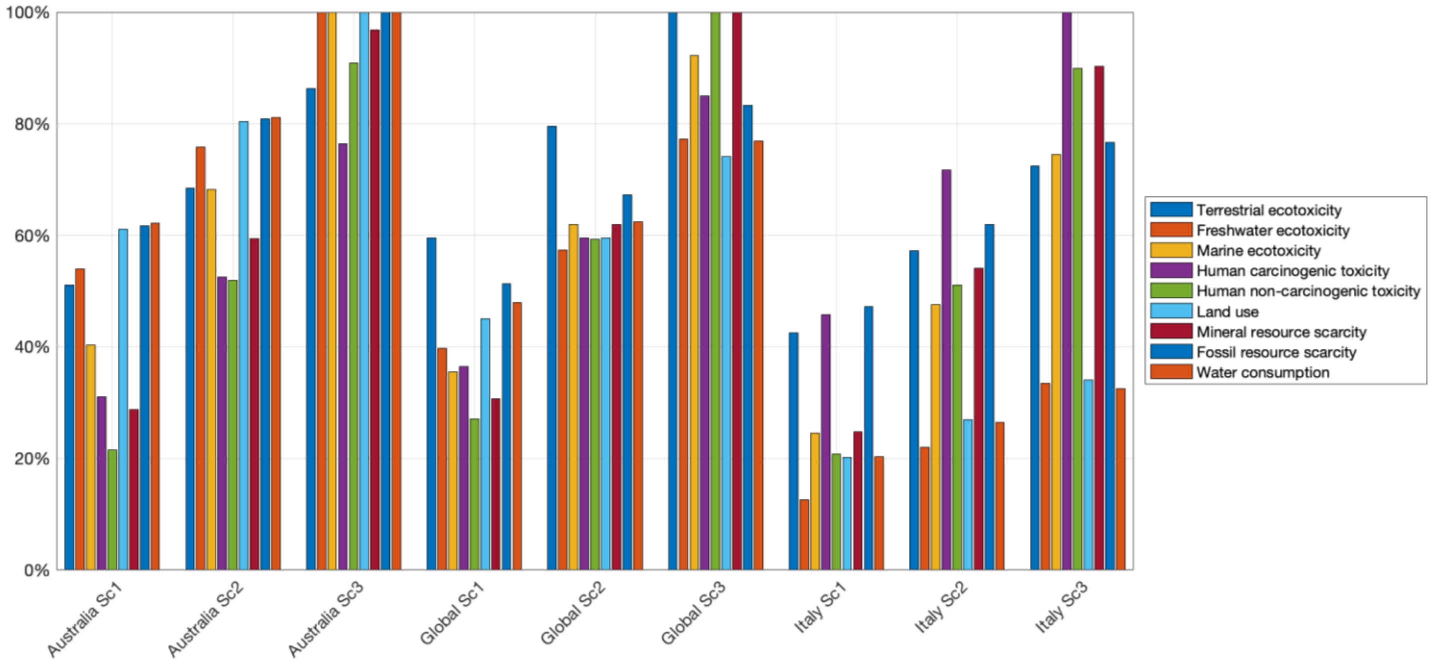

Figure 4. 3 Scaled relative LCIA of Terrestrial ecotoxicity, Freshwater ecotoxicity, Marine ecotoxicity, Human carcinogenic toxicity, Human non-carcinogenic toxicity, Land use, Mineral resource scarcity, Fossil resource scarcity, Water consumption indices.

It is seen in Figure 4. 2 and Figure 4. 3 that Australia-scenario 3 and Italy-scenario 1 represent the highest and lowest values, respectively. The second highest is related to Global-scenario 3 and the third highest quantities can be seen in Italy-scenario 3.

For a detailed comparison, including indices' values, several indices' quantities at the current situation are provided as examples in Figure 4. 4 to Figure 4. 8. These examples are chosen to cover various probable trends of indices. The other indices have almost similar trends to the examples and are provided in the appendix.

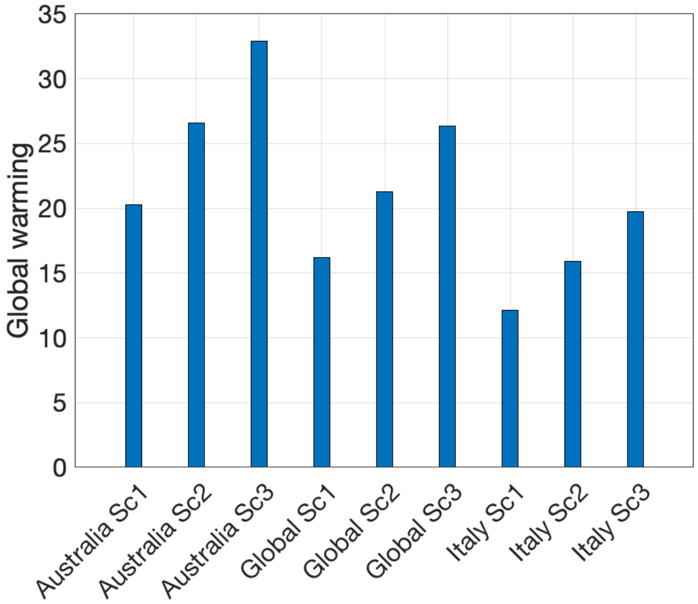

Figure 4. 4 Global warming (kg CO2 eq per kg of hydrogen) index

Carbon dioxide emission in PEM LCA is mainly related to electricity consumption and the type of fuel which is used to produce electricity. In Australia and global, the main contributor to electricity generation is coal, with a contribution of 52.8% and 36%, respectively. The main contributor in Italy is natural gas with 51% contribution. Coal has relatively high carbon dioxide emissions in comparison to other fuel sources, thus, the global warming index for Australia is higher than the global, and the global is greater than Italy. The global warming index ranges approximately 20-33, 16-26, and 12-20 kg CO_2, in Australia, the whole world, and Italy, respectively. In comparison to the result of Niklas Gerloff's [28] study, the global warming index of Sc3 for the whole world is almost similar to the result of PEM technology in 2019.

As can be seen in Figure 4. 5, the maximum value for ionizing radiation among the assessed activities is related to electricity generation via nuclear energy. Australia and Italy do not use nuclear power to generate electricity, therefore, ionizing index radiation in Australia and Italy is considerably lower than the world which has 9.8% contribution of nuclear energy in total electricity generation.

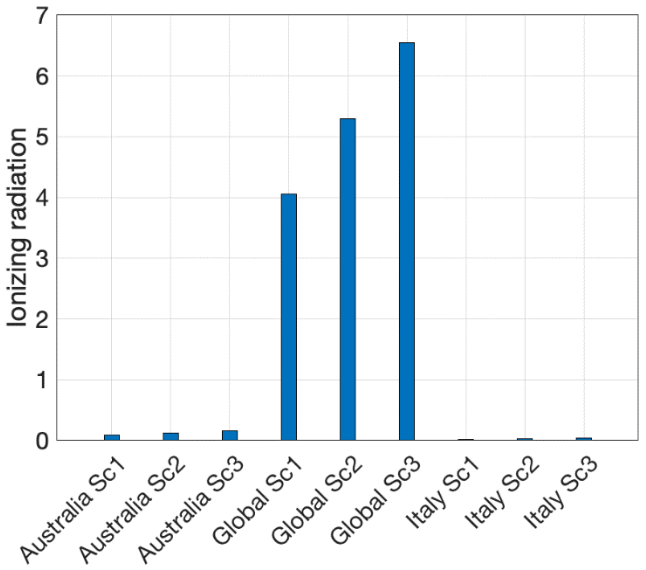

Figure 4. 5 Ionizing radiation (kBq Co-60 eq per kg of hydrogen) index

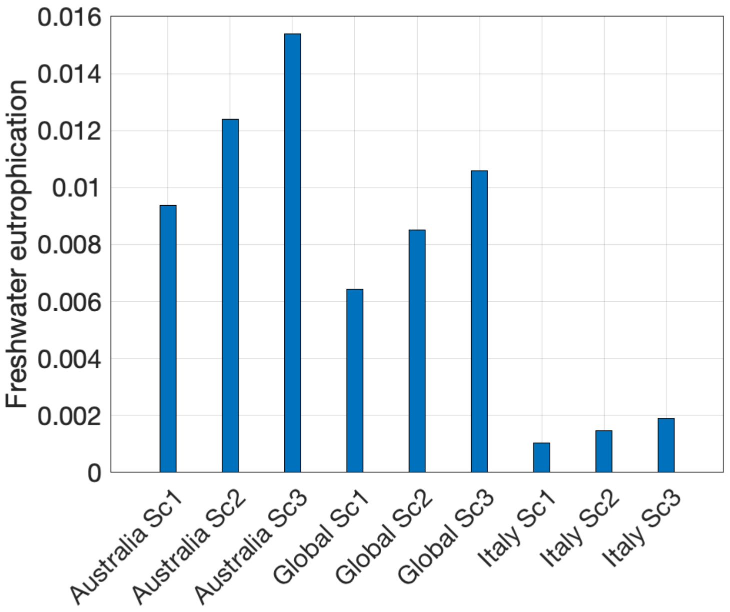

Figure 4. 6 freshwater eutrophication (kg P eq per kg of hydrogen) index

The main contributors to freshwater eutrophication are stack material and operational electricity consumption. Considering the assumption that the stack material is the same for all 3 scenarios, the reason for the difference is the electricity consumption. Coal has relatively higher phosphorus emissions in comparison to other fuel sources. Considering the contribution of electricity generation from coal in the assessed regions it is logical that Italy with 5% coal contribution indicates lower values of the freshwater eutrophication index.

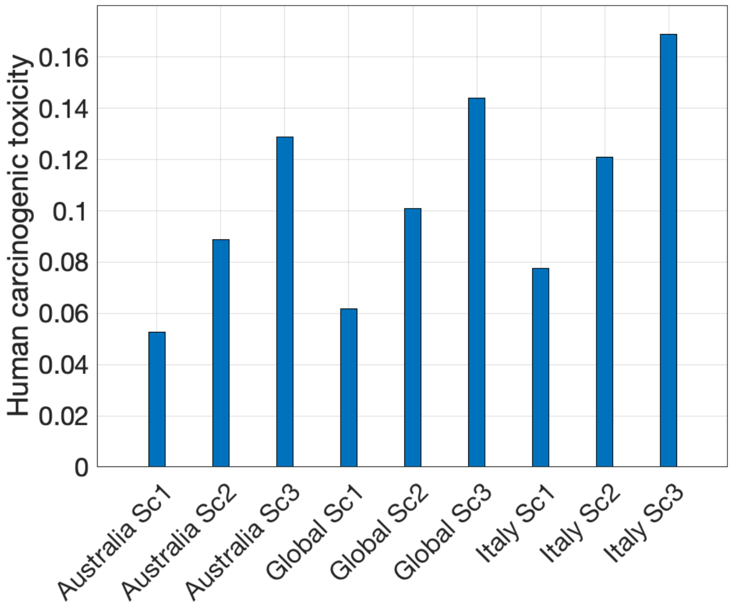

Figure 4. 7 Human carcinogenic toxicity (kg 1,4-DCB per kg of hydrogen) index

The main contributors to human carcinogenic toxicity are stack material and operational electricity consumption. Considering the assumption that the stack material is the same for all 3 scenarios, the reason for the difference is related to the electricity consumption. Human carcinogenic toxicity of oil, wind, gas and nuclear to produce 1kWh electricity is higher in comparison to other sources, 0.0055, 0.0038, 0.0024, and 0.0024 kg 1,4-DCB, respectively. Considering the contribution of these sources at the current situation of national grids the human carcinogenic toxicity index of Italy is the highest value among the assessed scenarios and Australia shows the lowest values.

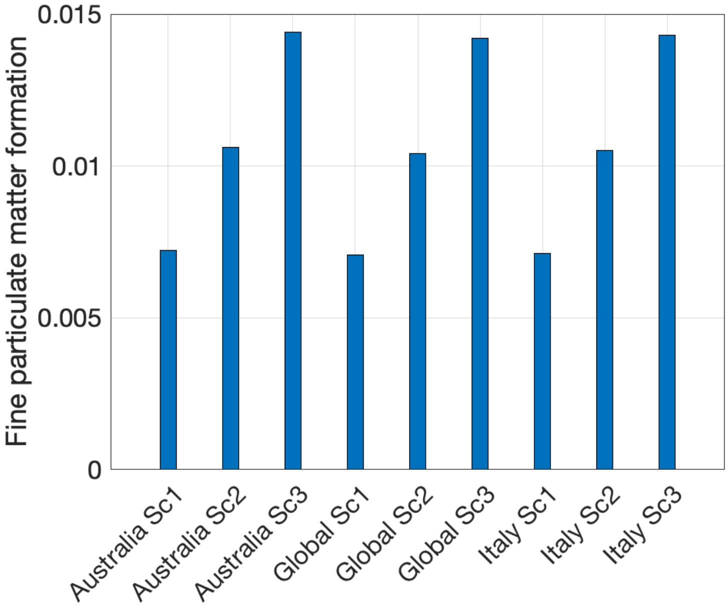

Figure 4. 8 Fine particulate matter formation (kg PM2.5 eq per kg of hydrogen) index

The main contributors to fine particulate matter formation are stack material and operational electricity consumption. It is seen that the values for each scenario in different regions are the same. Considering the assumption that the stack material is the same for all 3 scenarios it can be realized that the amount of PM2.5 eq for electricity consumption in all regions is the same. Despite the difference amount of PM2.5 eq for the different sources of electricity generation, the differences between contributions compensate for it, and the total result becomes almost equivalent.

According to the abovementioned environmental indices and information provided in supplementary data about the contribution of each section to the indices amount, it is verified, at the current condition, that the biggest contributor to environmental impact in hydrogen generation via PEM technology is electricity supply and the contribution of other parts is negligible.

The real amount of required water for water electrolysis to produce 1 kg hydrogen is more than 9 kg. Considering the low contribution of the water to environmental impact, according to the supplementary data, variation of the water amount does not have a significant impact on the LCIA results.

4.3.2 Sensitivity to stack material- current condition

The sensitivity of LCA to stack materials is investigated by fixing the quantities of other units and processes while changing the stack material from minimum mass to maximum mass according to the literature review. The variation of stack mass from the average mass is considered approximately -50 to 50%. The average operational energy is assumed for the energy consumption to produce 1 kg hydrogen. Table 4. 7 includes the result of LCIA for scenarios Sc2, Sc4, and Sc5. Figure 4. 9 illustrates the indices variation regarding Sc2 to show the range of variation of each index considering the variation of stack mass.

The contribution of electricity consumption to global warming at the current situation is more than 97% in all scenarios. This indicates that the variation in stack material does not have a considerable effect on carbon dioxide emission at the current condition. The contribution of each section is provided in supplementary data for different scenarios.

		Australia			Global			Italy		
	unit	Sc4	Sc2	Sc5	Sc4	Sc2	Sc5	Sc4	Sc2	Sc5
Global warming	kg CO2 eq	26.47	26.59	26.74	21.14	21.26	21.41	15.79	15.91	16.06
Stratospheric ozone depletion	kg CFC11 e	8.06E-06	8.28E-06	8.56E-06	7.11E-06	7.34E-06	7.62E-06	7.27E-06	7.50E-06	7.78E-06
Ionizing radiation	kBq Co-60	1.22E-01	1.27E-01	1.33E-01	5.30E+00	5.30E+00	5.31E+00	2.32E-02	2.81E-02	3.39E-02
Ozone formation, Human health	kg NOx eq	6.86E-02	6.99E-02	7.16E-02	5.31E-02	5.45E-02	5.62E-02	3.11E-02	3.24E-02	3.42E-02
Fine particulate matter formation	kg PM2.5 e	9.26E-03	1.06E-02	1.24E-02	9.08E-03	1.04E-02	1.22E-02	9.14E-03	1.05E-02	1.23E-02
Ozone formation, Terrestrial ecosystems	kg NOx eq	6.87E-02	7.00E-02	7.18E-02	5.32E-02	5.46E-02	5.63E-02	3.12E-02	3.26E-02	3.44E-02
Terrestrial acidification	kg SO2 eq	1.20E-01	1.25E-01	1.31E-01	9.06E-02	9.53E-02	1.01E-01	3.79E-02	4.25E-02	4.85E-02
Freshwater eutrophication	kg P eq	1.22E-02	1.24E-02	1.25E-02	8.38E-03	8.52E-03	8.69E-03	1.32E-03	1.46E-03	1.63E-03
Marine eutrophication	kg N eq	8.15E-04	8.20E-04	8.26E-04	5.83E-04	5.88E-04	5.94E-04	1.19E-04	1.24E-04	1.30E-04
Terrestrial ecotoxicity	kg 1,4-DCB	8.13E+00	8.41E+00	8.75E+00	9.49E+00	9.77E+00	1.01E+01	6.75E+00	7.03E+00	7.37E+00
Freshwater ecotoxicity	kg 1,4-DCB	4.37E-01	4.85E-01	5.48E-01	3.19E-01	3.67E-01	4.30E-01	9.21E-02	1.41E-01	2.03E-01
Marine ecotoxicity	kg 1,4-DCB	2.46E-01	3.59E-01	4.92E-01	2.13E-01	3.26E-01	4.59E-01	1.37E-01	2.50E-01	3.83E-01
Human carcinogenic toxicity	kg 1,4-DCB	6.40E-02	8.89E-02	1.18E-01	7.58E-02	1.01E-01	1.30E-01	9.64E-02	1.21E-01	1.50E-01
Human non-carcinogenic toxicity	kg 1,4-DCB	1.60E+00	3.55E+00	6.07E+00	2.10E+00	4.05E+00	6.57E+00	1.54E+00	3.49E+00	6.01E+00
Land use	m^2 crop eq	3.93E-01	3.97E-01	4.02E-01	2.89E-01	2.93E-01	2.99E-01	1.29E-01	1.33E-01	1.38E-01
Mineral resource scarcity	kg Cu eq	1.72E-02	2.94E-02	4.50E-02	1.84E-02	3.07E-02	4.63E-02	1.46E-02	2.68E-02	4.24E-02
Fossil resource scarcity	kg oil eq	9.17E+00	9.20E+00	9.25E+00	7.63E+00	7.66E+00	7.71E+00	7.01E+00	7.05E+00	7.09E+00
Water consumption	m^3	3.84E+00	3.84E+00	3.84E+00	2.95E+00	2.95E+00	2.95E+00	1.25E+00	1.25E+00	1.25E+00

Table 4. 7 LCIA for scenario Sc2, Sc4, and Sc5 in Australia, the whole world, and Italy

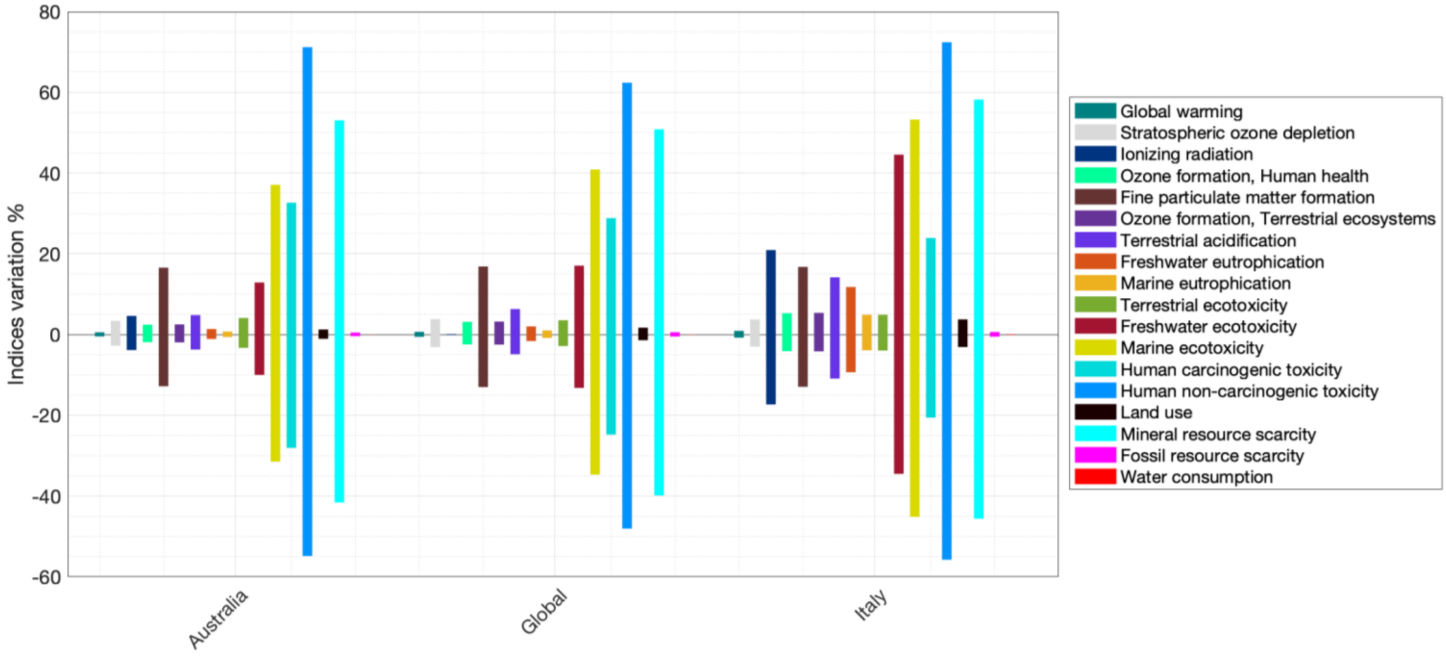

Figure 4. 9 Indices variation range regarding sc2

It is seen in Figure 4. 9 that fine particulate matter formation, freshwater ecotoxicity, marine ecotoxicity, human carcinogenic toxicity, human non-carcinogenic toxicity, and mineral resource scarcity indices are the most sensitive ones regarding the changes in stack material. The Human non-carcinogenic toxicity index shows the highest range of variation. For this index, the lower and upper limits are mainly associated with iridium and platinum variation, as in the freshwater ecotoxicity index. For mineral resource scarcity, iridium plays the most important role, at the current situation, for kg Cu eq emission. In the case of marine ecotoxicity, the variation is mainly related to Nafion and iridium. It is realized that the most effective elements on indices are iridium, platinum, and Nafion, and variation in other elements does not have a significant impact on the LCIA result. In addition, it is found that the lowest sensitivities are related to global warming, Fossil resource scarcity, and water consumption. The water consumption index has a range close to 0% which is not visible in Figure 4. 9 due to its small quantity.

4.3.3 Variation of electrical energy sources

The impact of increasing the contribution of RES on the LCIA is investigated and the results are provided in this section. For this purpose, changes are applied to electrical energy sources and the quantities of other units and processes are considered constant values. The assumed value for the stack mass is the average mass. Scenarios Sc2, Sc6, Sc7, Sc8, and Sc9 are assessed and compared to define the changes in indices. The values of indices for the mentioned scenarios in the three considered regions are provided in the supplementary data. To show a clearer impact of contribution, the increases of RES changes regarding scenario Sc2 are calculated. Figure 4. 10 to Figure 4. 16 are examples of index variation which are chosen to cover all probable trends. Figures of the remaining indices are provided in the appendix.

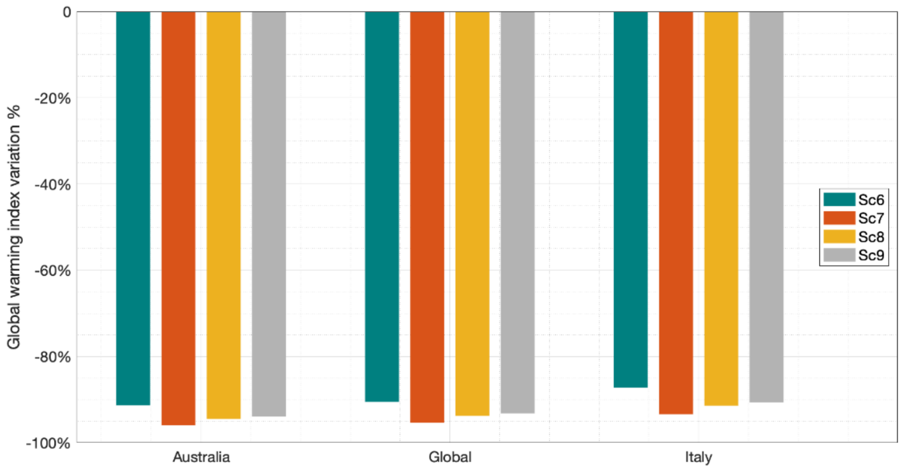

Figure 4. 10 Global warming index variation in Sc6, Sc7, Sc8, and Sc9 scenarios regarding sc2

Electricity consumption is the main contributor to the carbon dioxide emission of hydrogen generation via PEM technology at the current situation. The reason is related to the CO_2 emission of fossil fuels, thus, by complete transition from fossil fuels to RES the carbon dioxide emission of 1 kg hydrogen generation could reach the range of 1 to 2.3 kg. It is seen in Figure 4. 10 that the global warming index variations in all three regions for all scenarios are almost the same.

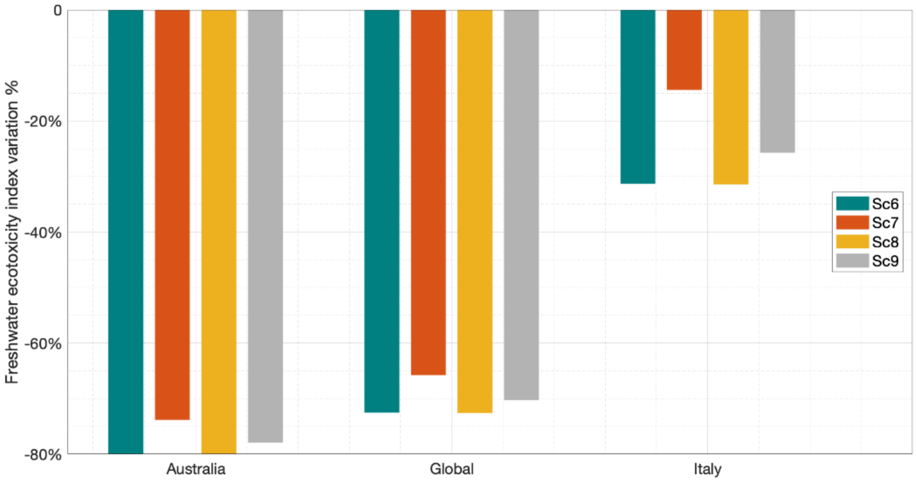

Figure 4. 11 Freshwater ecotoxicity index variation in Sc6, Sc7, Sc8, and Sc9 scenarios regarding sc2

The main contributor to freshwater ecotoxicity in electricity generation is the electricity production by coal. The contribution of coal at the current condition in Australia, the whole world, and Italy is 52.8, 36, and 5 %, respectively. Thus, the transition from fossil fuels to RES indicates much lower changes in the freshwater ecotoxicity index in Italy compared with Australia and the whole world. However, this index has considerable reduction by the complete transition to RES.

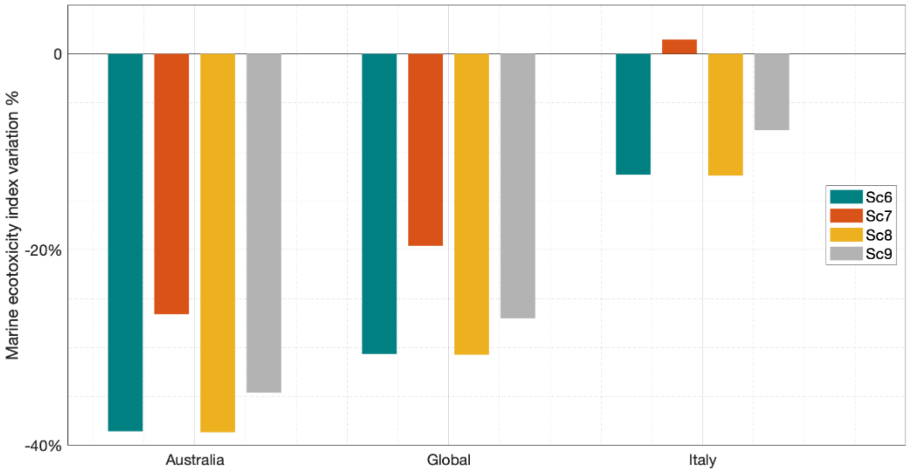

Figure 4. 12 Marine ecotoxicity index variation in Sc6, Sc7, Sc8, and Sc9 scenarios regarding sc2

It seems that with a complete transition from fossil fuels to RES, environmental impacts are decreasing, but it is not applicable to all indices. As can be seen in Figure 4. 12, scenario Sc7 which is related to the increase in wind contribution shows an increase in the marine ecotoxicity index in Italy. This increase originates from the difference between the marine ecotoxicity index of natural gas and wind electricity generation, 0.00046, and 0.0012 kg 1,4-DCB, respectively. The main current contributor to electricity generation in Italy is natural gas, 51%. Therefore, the marine ecotoxicity index increases with the transition from natural gas to wind. In the other two regions, Sc7 shows the lowest decrease, and it can be realized that it is not suitable to have a complete transition from fossil fuels to only wind energy.

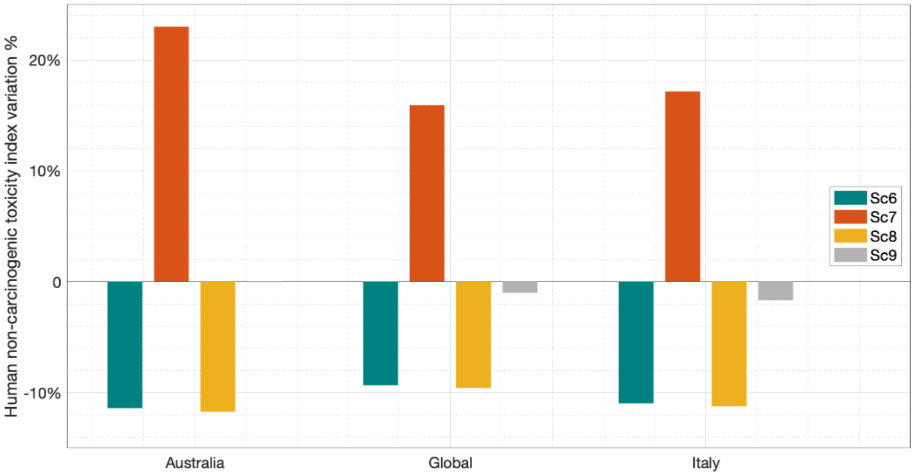

Figure 4. 13 Human non-carcinogenic toxicity index variation in Sc6, Sc7, Sc8, and Sc9 scenarios regarding sc2

The highest emission factor of human non-carcinogenic toxicity in electricity generation is related to nuclear energy. Nuclear energy contribution is considered constant, and it does not have an impact on this analysis, but in general, a solution to reduce this index is the transition from nuclear energy to other sources with lower emission factors. The highest emission factor of human non-carcinogenic toxicity among the other sources of energy considered in this study is related to wind energy. Thus, scenario Sc7 shows the increase of this index and Sc9 shows very low variation. It can be realized that it is not suitable to have a complete transition from fossil fuels to only wind energy. In addition, the partial transition to the wind should be investigated properly. It is seen that Sc6 and Sc8 and Sc9 do not show significant variation for this index in comparison to other indices' variation.

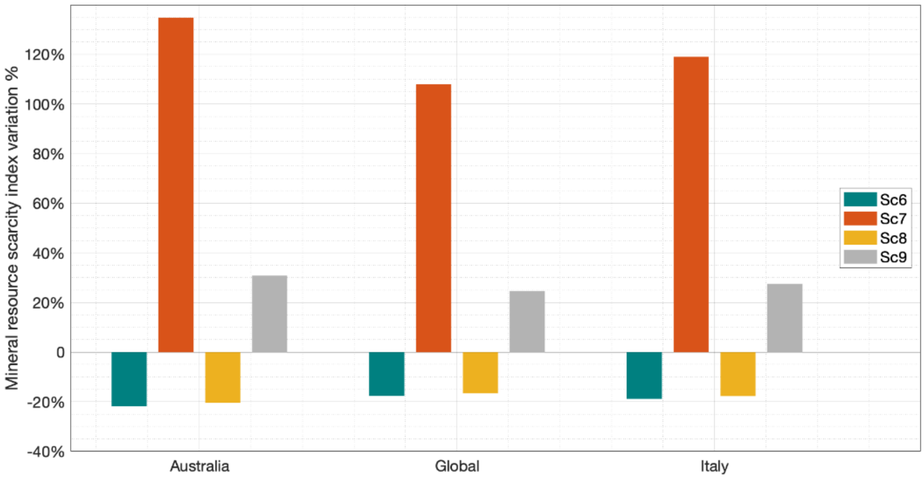

Figure 4. 14 Mineral resource scarcity index variation in Sc6, Sc7, Sc8, and Sc9 scenarios regarding sc2

The highest emission factor of mineral resources scarcity among the sources of energy considered in this study is related to wind energy, which is almost 10 times the main current contributor sources to electricity generation, coal, and natural gas. Thus, scenarios Sc7 and Sc9 show an increase in this index. It can be realized that it is not suitable to have a complete transition from fossil fuels to only wind energy. In addition, even a partial transition to wind has a negative impact on this index and should be investigated properly. It is seen that Sc6 and Sc8 do not show significant variation for this index.

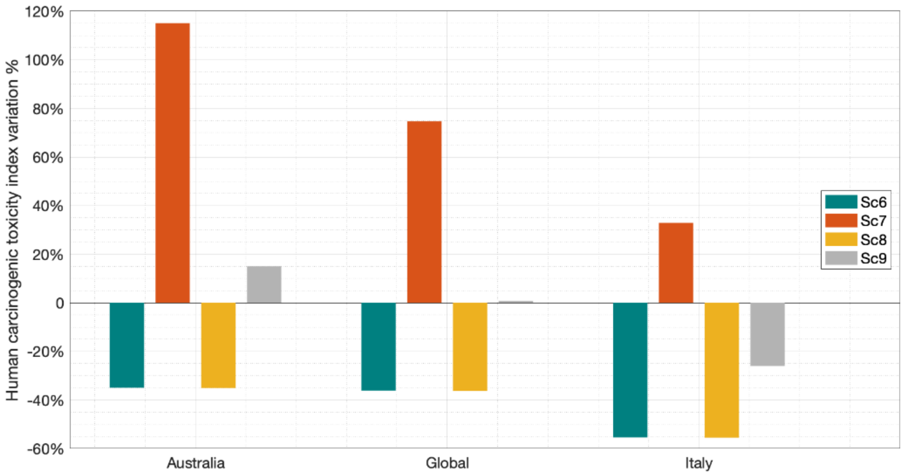

Figure 4. 15 Human carcinogenic toxicity index variation in Sc6, Sc7, Sc8, and Sc9 scenarios regarding sc2

Electricity generation by natural gas and coal have lower human carcinogenic toxicity emission factors in comparison to the wind. Considering the higher contribution of coal in Australia and the higher difference of wind with coal, the increase of this index is higher in Sc7 in Australia rather than in two other regions. Sc9 behaves differently in all regions which originates from the current contribution of coal and natural gas that transition is applied. It is realized that it is not proper to have a complete transition from fossil fuels to only wind energy. In addition, partial transition to the wind should be investigated properly considering the region of application.

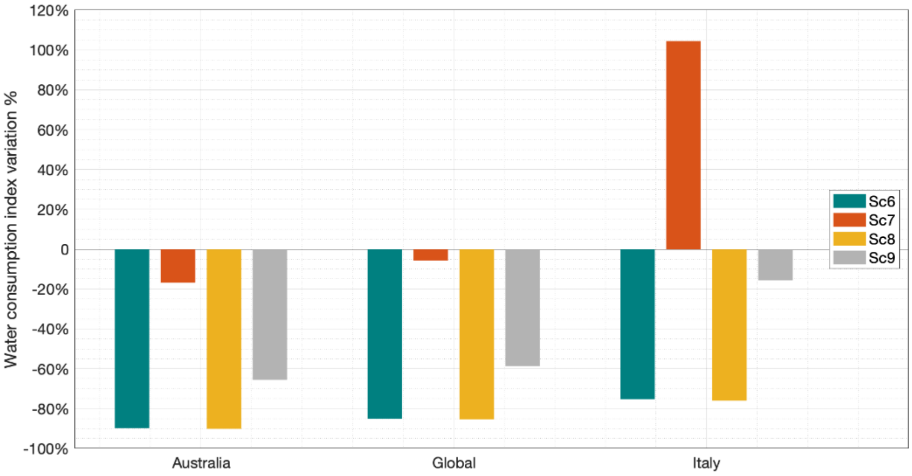

Figure 4. 16 Water consumption index variation in Sc6, Sc7, Sc8, and Sc9 scenarios regarding sc2

The water consumption emission factor of electricity generation by coal is higher than that of wind, almost 0.046 m^3, while this factor for natural gas is lower than wind, -0.06 m^3. Considering that Italy has a very low coal contribution the result is positive for this index in Sc7 of Italy. The low values of Sc7 in Australia and the whole world are related to the contribution of coal and natural gas at the current condition which positive and negative impacts compensate for each other.

It can be realized that by the transition to RES, some indices show the desirable result, such as global warming, while several indices, such as mineral resources scarcity show undesirable results. Therefore, a complete transition from fossil fuels to RES could be a proper solution for global warming mitigation but the scarcity of mineral resources and their cost will play important role in decision-making.

4.3.4 Sensitivity to stack material after increase in RES contribution

The sensitivity analysis of LCIA regarding the stack material in the “Sensitivity to stack material-current condition” section is assessed for the current situation. It is important to investigate LCIA changes regarding stack materials after the RES contribution increase. According to the comparison of scenarios Sc2, Sc6, Sc7, Sc8, and Sc9 which is provided in supplementary data, the contribution of stack material is considerable in all indices in all regions, except global warming and water consumption in all regions and Ionizing radiation for global values and Sc7 for Terrestrial ecotoxicity. Therefore, all indices except global warming and water consumption have high sensitivity to stack materials for future scenarios. By comparing with the sensitivity analysis at the current condition regarding stack materials it is seen that more indices become important for future scenarios. It shows the increase of stack importance by the transition from fossil fuels to RES.

According to the abovementioned environmental indices and information provided in supplementary data about the contribution of each section to the indices amount for the future RES scenarios, it is verified that the biggest contributor to environmental impact in hydrogen generation via PEM technology is stack material, not electricity consumption.

4.3.5 Comparison with SMR method

In this section, the results of 9 scenarios in the world region are compared with SMR environmental emission to make the indices' quantities clearer. The values related to SMR are extracted from Mehmeti et al. [29] study. SMR is considered as the reference since it is currently the most widely used method for hydrogen production. The results are summarized in Table 4. 8.

	Global warming	Stratospheric ozone depletion	Ionizing radiation	Ozone formation, Human health	Fine particulate matter formation	Ozone formation, Terrestrial ecosystems	Terrestrial acidification	Freshwater eutrophication	Marine eutrophication
	kg CO2 eq	kg CFC11 eq	kBq Co-60 ec	kg NOx eq	kg PM2.5 eq	kg NOx eq	kg SO2 eq	kg P eq	kg N eq
SMR	12.13	0.000003	0.501	0.0089	0.002	0.0085	0.0087	0.0007	Na
Sc1	16.22	0.0000055	4.056	0.0409	0.007	0.041	0.0698	0.0064	0.00045
Sc2	21.26	0.0000073	5.3	0.0545	0.01	0.0546	0.0953	0.0085	0.00059
Sc3	26.33	0.0000093	6.546	0.0684	0.014	0.0686	0.1221	0.0106	0.00073
Sc4	21.14	0.0000071	5.296	0.0531	0.009	0.0532	0.0906	0.0084	0.00058
Sc5	21.41	0.0000076	5.306	0.0562	0.012	0.0563	0.1013	0.0087	0.00059
Sc6	2.02	0.0000004	5.218	0.0027	0.002	0.0028	0.0069	0.0003	0.00002
Sc7	0.99	0.0000005	5.227	0.0036	0.003	0.0036	0.0083	0.0004	0.00004
Sc8	1.32	0.0000004	5.22	0.0029	0.002	0.0029	0.0069	0.0003	0.00002
Sc9	1.45	0.0000004	5.222	0.0031	0.002	0.0031	0.0074	0.0003	0.00003

	Terrestrial ecotoxicity	Freshwater ecotoxicity	Marine ecotoxicity	Human carcinogenic toxicity	Human non-carcinogenic toxicity	Land use	Mineral resource scarcity	Fossil resource scarcity	Water consumption
	kg 1,4-DCB	kg 1,4-DCB	kg 1,4-DCB	kg 1,4-DCB	kg 1,4-DCB	m^2a crop eq	kg Cu eq	kg oil eq	m^3
SMR	0.0005	0.0208	0.0423	0.0803	21.36	0.008272	0.00389	4.45	5.77
Sc1	7.3151	0.2546	0.1867	0.0617	1.85	0.222207	0.01521	5.85	2.27
Sc2	9.7666	0.3673	0.3257	0.1008	4.05	0.293496	0.03066	7.66	2.95
Sc3	12.2855	0.4941	0.485	0.1439	6.82	0.365672	0.04948	9.48	3.64
Sc4	9.4887	0.3188	0.2127	0.0758	2.1	0.289377	0.01844	7.63	2.95
Sc5	10.1119	0.4299	0.459	0.1298	6.57	0.298502	0.04625	7.71	2.95
Sc6	2.5422	0.101	0.2259	0.0643	3.67	0.012558	0.02526	0.11	0.44
Sc7	7.5467	0.1257	0.2618	0.176	4.69	0.038085	0.06376	0.18	2.79
Sc8	2.5607	0.1008	0.2256	0.0642	3.66	0.011611	0.02558	0.11	0.43
Sc9	4.217	0.1091	0.2378	0.1015	4.01	0.020754	0.0382	0.13	1.22

Table 4. 8 Summary of the indices' values for 9 scenarios and SMR (2 tables to cover all indices)

It is seen in this table that scenario Sc3 is the worst case with the highest values in almost all indices except Human carcinogenic toxicity, Human non-carcinogenic toxicity, Mineral resource scarcity, and Water consumption. However, Sc3 values are less than SMR only in Human non-carcinogenic toxicity, and Water consumption, in which SMR has the highest values in these two indices compared to other scenarios. The most considerable variations can be seen in Terrestrial ecotoxicity. By comparing the values in Table 4. 8, it can be recognized that Sc6 shows the best performance in terms of environmental impact reduction. By comparing scenarios Sc1 to Sc5, which are related to current electricity grid, and SMR, it can be realized that SMR has lower environmental impact in all indices except Human non-carcinogenic toxicity and water consumption. Therefore, at the current condition SMR is more sustainable, and to reach a sustainable PEM technology it is required to consider scenarios Sc5 to Sc9.

4.3.6 Contribution of materials on the global warming potential

The contribution of each material in stack and BOP should be investigated to determine the main contributors to environmental impact, without electricity emission consideration. In this section, global warming contribution, as the most known index, is considered to define the most important materials in terms of carbon dioxide emission. The result of this section can be used for research and development to reduce carbon dioxide emissions by focusing on the most contributors. The comparison of three scenarios, Sc4, Sc2, and Sc5, with the minimum, average, and maximum stack materials' weight is provided in Figure 4. 17. It can be seen that the main contributors to global warming, regarding the materials in stack and BOP, are titanium, iridium, and platinum from stack components. In addition, it is realized that the contribution of the BOP to global warming, in hydrogen generation through PEM technology, is almost negligible.

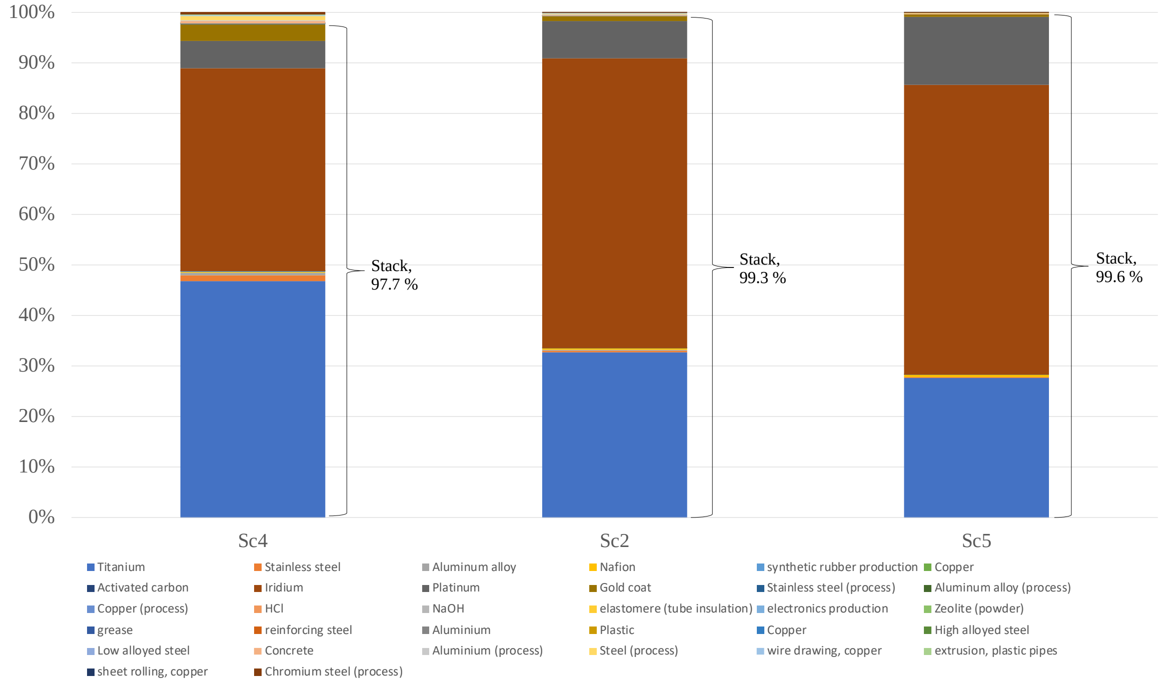

Figure 4. 17 Stack and BOP materials' contribution in global warming index

4.3.7 Contribution of electricity and material on GWP and reduction potential of using RES

The contribution comparison of materials, electricity, water consumption, and heat to global warming, in the global region, is performed in this section. The comparison is made between scenarios Sc2, Sc6, Sc7, Sc8, and Sc9 to investigate the impact of using RES on the contribution of each part to global warming. As mentioned in the previous sections, the amount of carbon dioxide emission reduces considerably by using RES as the energy source for hydrogen generation via PEM technology. While electricity (operation and pump) is still the main contributor to global warming potential, between 74% to 99% in all scenarios assessed in this section. Thus, if the objective of a plan is only reducing carbon dioxide emissions, without considering other environmental impacts, it can be recommended to focus only on electricity emission reduction and the optimum choice of electricity source.

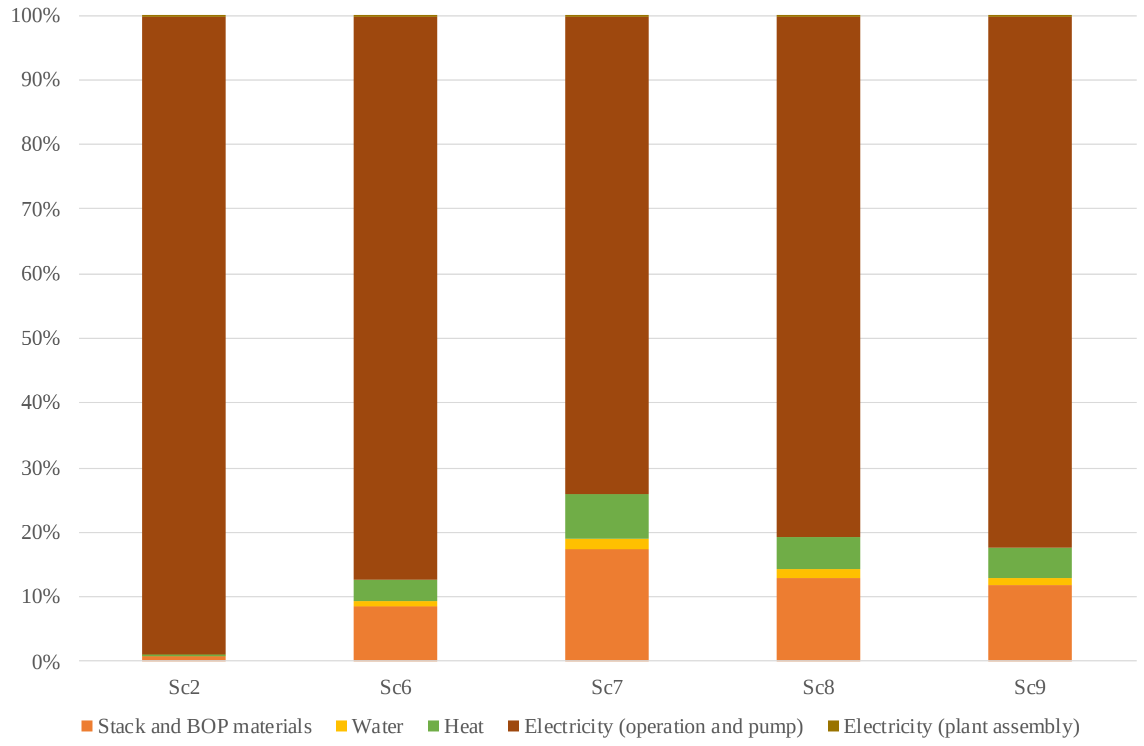

Figure 4. 18 contribution comparison of materials, electricity, water consumption, and heat to global warming, in global region

4.4 Conclusion

By comparing the water electrolysis technologies based on the maturity and efficiency of the systems, PEM technology is chosen to be assessed as the hydrogen generation technology to overcome the RES storage problem. Environmental impact indices of hydrogen generation by PEM electrolyser under nine energy and stack configuration scenarios in Australia, Italy, and the whole world are quantified and compared in this study. For the current condition, it is found that the biggest contributor to the environmental impact of hydrogen generation via PEM technology is the electricity supply and the contribution of the hydrogen production plant construction is negligible. while for the RES scenarios, it is found that the stack material is the main contributor with some exceptions. By comparing the result of scaled relative LCIA for the current condition, for Sc1, Sc2, and Sc3, in general, Australia represents the highest and Italy has the lowest values. The result of sensitivity analysis to the stack materials, at the current condition, indicates that the most sensitive indices are human non-carcinogenic toxicity, mineral resources scarcity, marine ecotoxicity, and freshwater ecotoxicity. By performing the sensitivity analysis of the environmental impact to stack material variation it is found that, at the current condition, the most effective elements on indices are iridium, platinum, and Nafion, and variation in other elements does not have a significant impact on the LCIA result.

The LCIA results of the transition from fossil fuels to RES indicate that indices such as global warming show desirable results, carbon dioxide emission of 1 kg hydrogen generation could reach the range of 1 to 2.3 kg from around 25 kg CO_2 emission. However, some indices, such as mineral resources scarcity show undesirable results. Thus, this transition could be a proper solution for global warming mitigation while the material intensity and their cost become more important in decision-making. Moreover, it is found that the transition to wind energy should be investigated properly since the result of several indices would be undesirable by this transition. By comparing the emission of the global region with the SMR method it is found that Sc3 and Sc6 have the worst and the best performance in environmental impact reduction, respectively. In addition, at the current condition SMR is more sustainable, and it is necessary to consider scenarios Sc5 to Sc9 to reach a sustainable PEM technology.

Global warming is one of the most interesting topics for researchers and the most known index for industries and investors, therefore, global warming potential is assessed in detail. By comparing the global warming potential regarding the stack and BOP materials, without the consideration of electricity emissions, it is found that titanium, iridium, and platinum are the main contributors. In addition, it is recognized that the BOP contribution is negligible in global warming potential. By comparing the contribution of materials, electricity, water consumption, and heat to global warming, in the global region, it is found that even with a complete transition from fossil fuels to RES, despite the fact that carbon dioxide emissions decrease significantly but still electricity consumption has the highest contribution to CO_2 emission, approximately more than 75% in scenarios Sc6 to Sc9.

4.5 Appendix

Table 4.A. 1 literature list

Row #	Ref No.	Year for estimation	Active area for 1MW (m^2)	Cell area (single cell format) [cm^2]	Experimental hydrogen yield for 1MW (m3/h)
1	[18]	2017	37	500	-
2	[30]	2018	16	17.64	-
3	[31]	2018	22	25	228.45
4	[31]	2018	31	25	240.56
5	[31]	2018	50	25	258.40
6	[31]	2018	110	25	282.48
7	[32]	2016	19.5	5	-
8	[33]	2018	20.5	25	190.73
9	[33]	2018	29.5	25	206.85
10	[33]	2018	49.5	25	228.10
11	[33]	2018	110	25	253.44
12	[34]	2010	53	250	-
13	[35]	2013	102	100	306.00
14	[36]	2010	91	100	242.67
15	[37]	2011	100	100	300.00

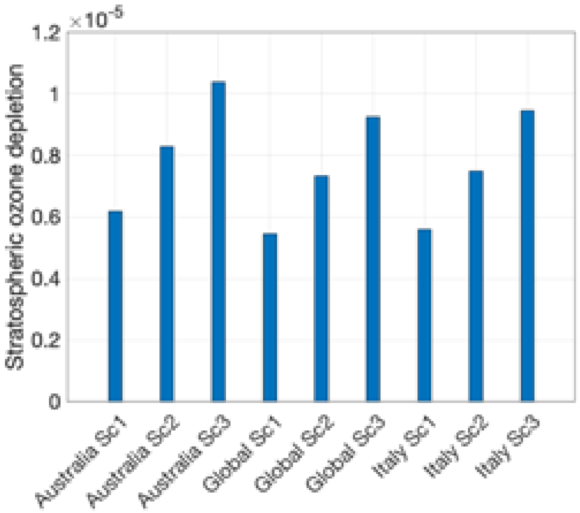
×10⁻⁵
Stratospheric ozone depletion
0
0.2
0.4
0.6
0.8
1
1.2
Australia Sc1
Australia Sc2
Australia Sc3
Global Sc1
Global Sc2
Global Sc3
Italy Sc1
Italy Sc2
Italy Sc3

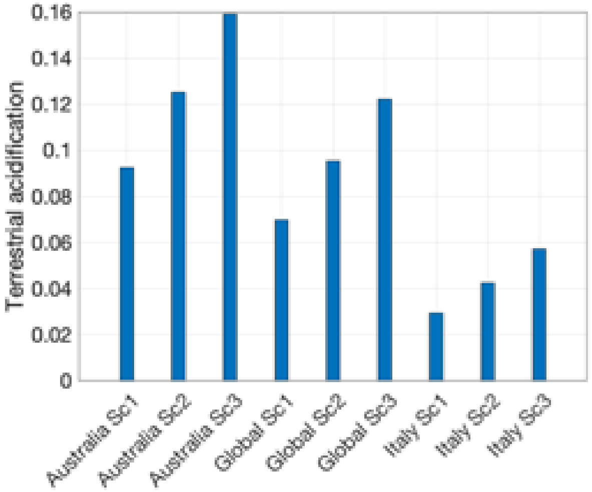
Terrestrial acidification
0
0.02
0.04
0.06
0.08
0.1
0.12
0.14
0.16
Australia Sc1
Australia Sc2
Australia Sc3
Global Sc1
Global Sc2
Global Sc3
Italy Sc1
Italy Sc2
Italy Sc3

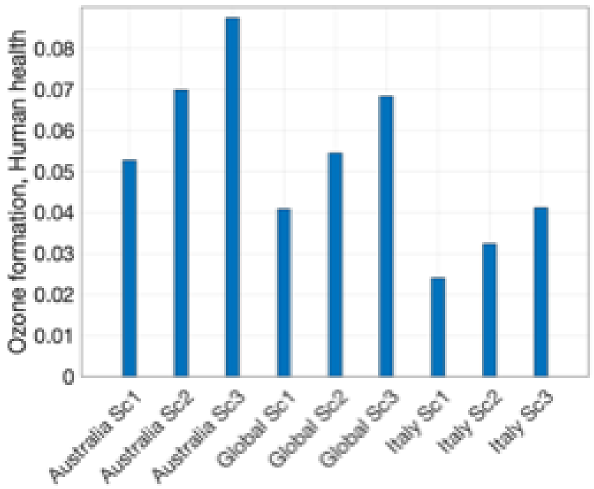
Ozone formation, Human health
0
0.01
0.02
0.03
0.04
0.05
0.06
0.07
0.08
Australia Sc1
Australia Sc2
Australia Sc3
Global Sc1
Global Sc2
Global Sc3
Italy Sc1
Italy Sc2
Italy Sc3

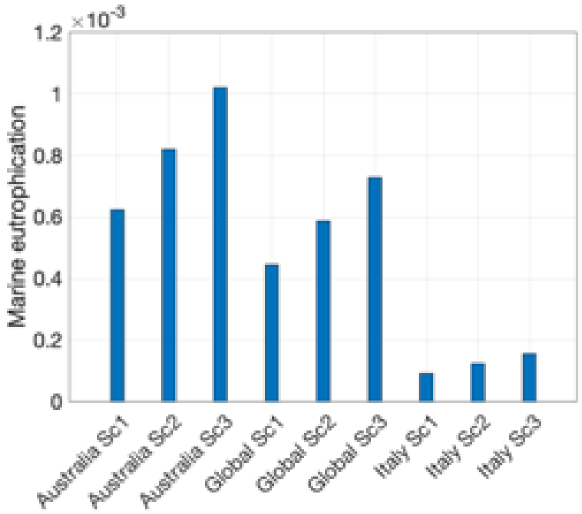
×10⁻³
Marine eutrophication
0
0.2
0.4
0.6
0.8
1
1.2
Australia Sc1
Australia Sc2
Australia Sc3
Global Sc1
Global Sc2
Global Sc3
Italy Sc1
Italy Sc2
Italy Sc3

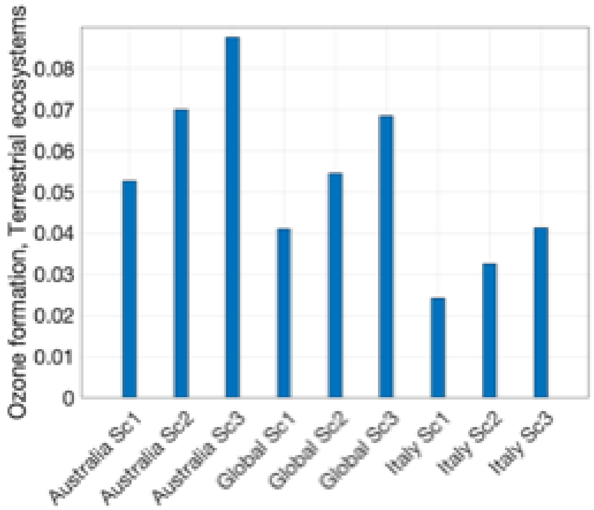
Ozone formation, Terrestrial ecosystems
0
0.01
0.02
0.03
0.04
0.05
0.06
0.07
0.08
Australia Sc1
Australia Sc2
Australia Sc3
Global Sc1
Global Sc2
Global Sc3
Italy Sc1
Italy Sc2
Italy Sc3

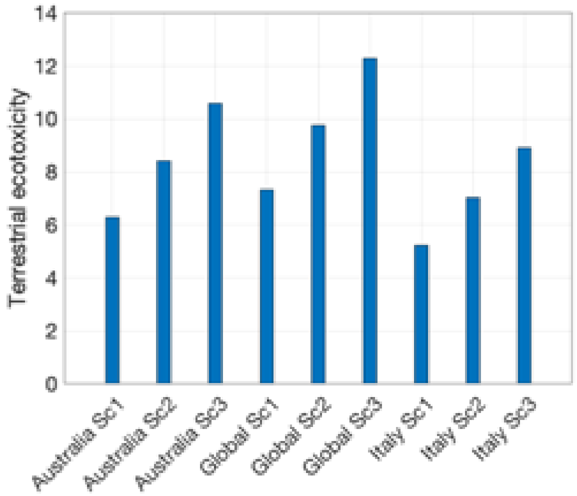
Terrestrial ecotoxicity
0
2
4
6
8
10
12
14
Australia Sc1
Australia Sc2
Australia Sc3
Global Sc1
Global Sc2
Global Sc3
Italy Sc1
Italy Sc2
Italy Sc3

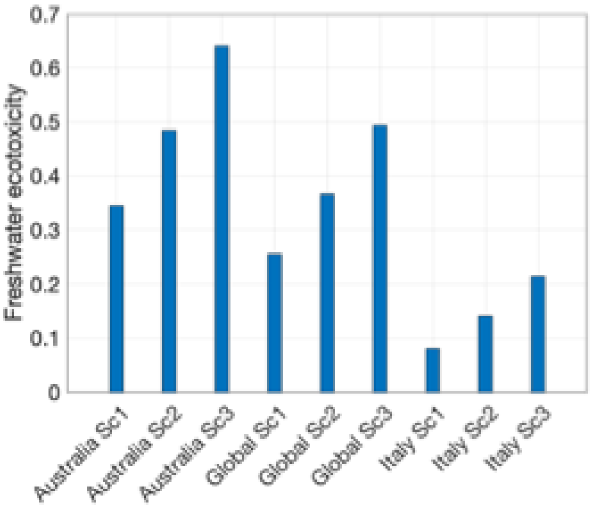
Freshwater ecotoxicity
0
0.1
0.2
0.3
0.4
0.5
0.6
0.7
Australia Sc1
Australia Sc2
Australia Sc3
Global Sc1
Global Sc2
Global Sc3
Italy Sc1
Italy Sc2
Italy Sc3

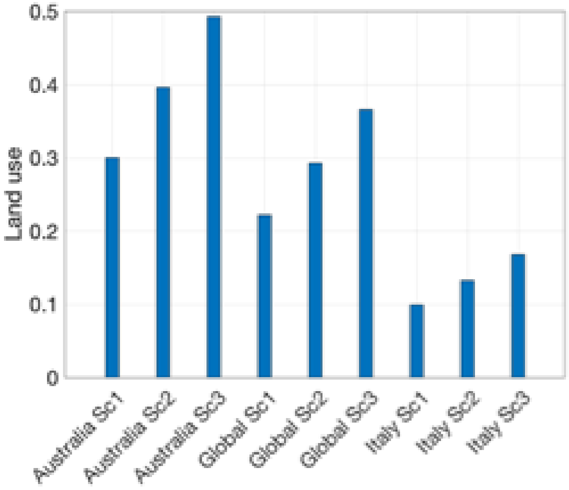
Land use
0
0.1
0.2
0.3
0.4
0.5
Australia Sc1
Australia Sc2
Australia Sc3
Global Sc1
Global Sc2
Global Sc3
Italy Sc1
Italy Sc2
Italy Sc3

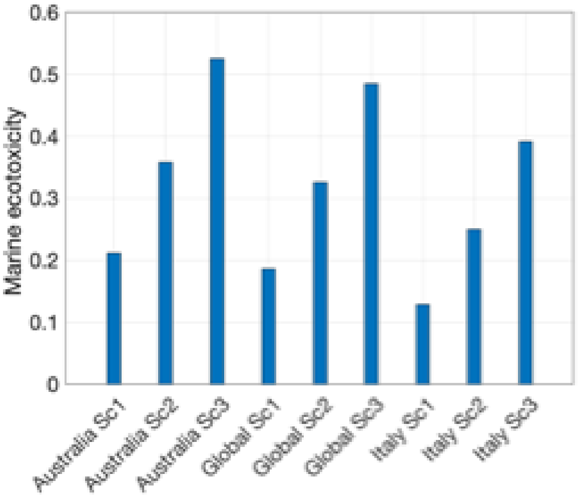
Marine ecotoxicity
0
0.1
0.2
0.3
0.4
0.5
0.6
Australia Sc1
Australia Sc2
Australia Sc3
Global Sc1
Global Sc2
Global Sc3
Italy Sc1
Italy Sc2
Italy Sc3

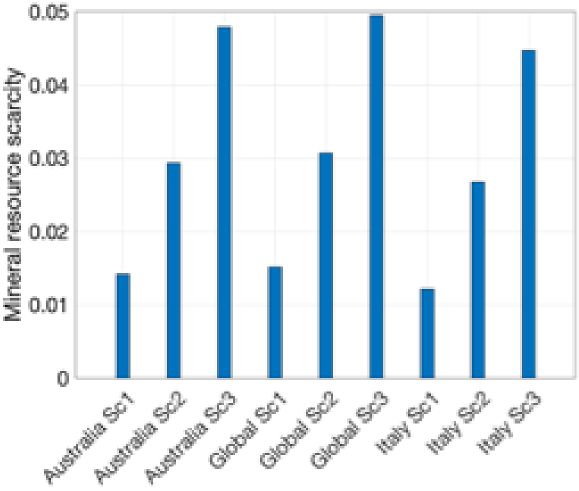
Mineral resource scarcity
0
0.01
0.02
0.03
0.04
0.05
Australia Sc1
Australia Sc2
Australia Sc3
Global Sc1
Global Sc2
Global Sc3
Italy Sc1
Italy Sc2
Italy Sc3

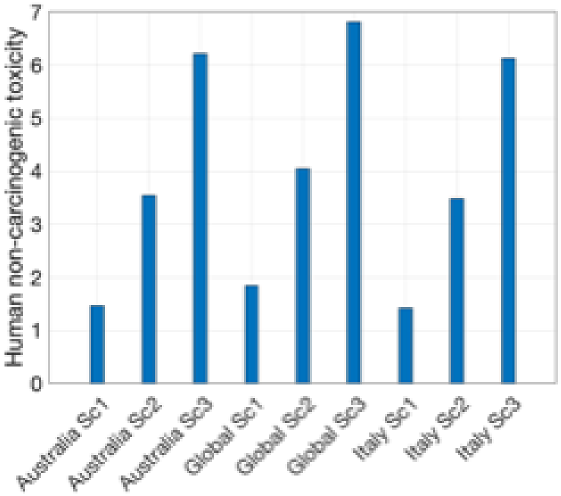
Human non-carcinogenic toxicity
0
1
2
3
4
5
6
7
Australia Sc1
Australia Sc2
Australia Sc3
Global Sc1
Global Sc2
Global Sc3
Italy Sc1
Italy Sc2
Italy Sc3

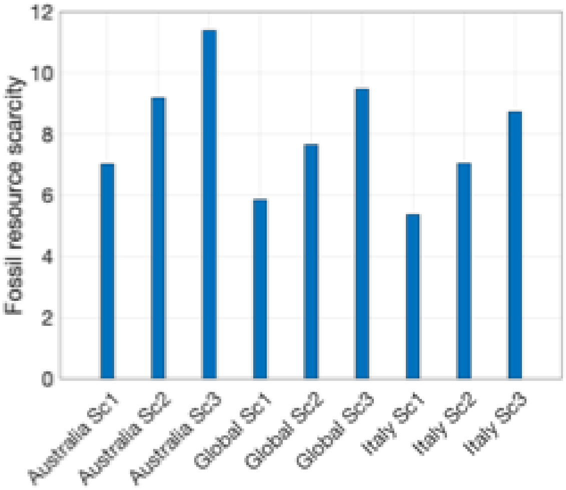
Fossil resource scarcity
0
2
4
6
8
10
12
Australia Sc1
Australia Sc2
Australia Sc3
Global Sc1
Global Sc2
Global Sc3
Italy Sc1
Italy Sc2
Italy Sc3

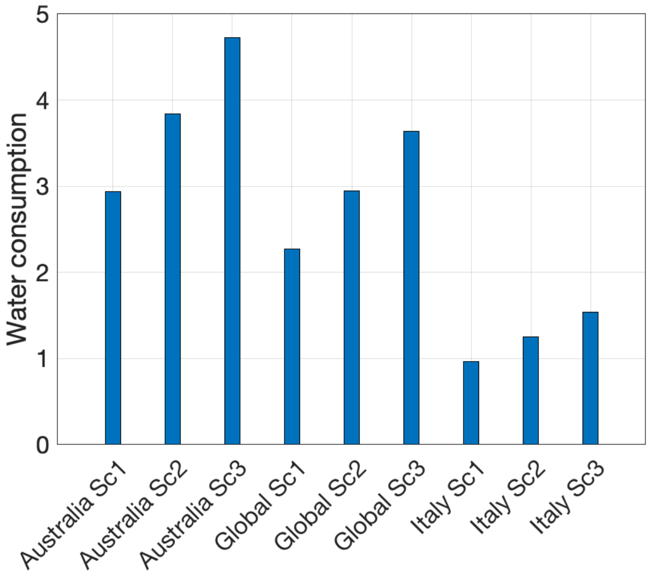

Figure 4.A. 1 LCIA results for the current condition (remaining indices), units are provided in Table 4. 7 per kg of hydrogen.

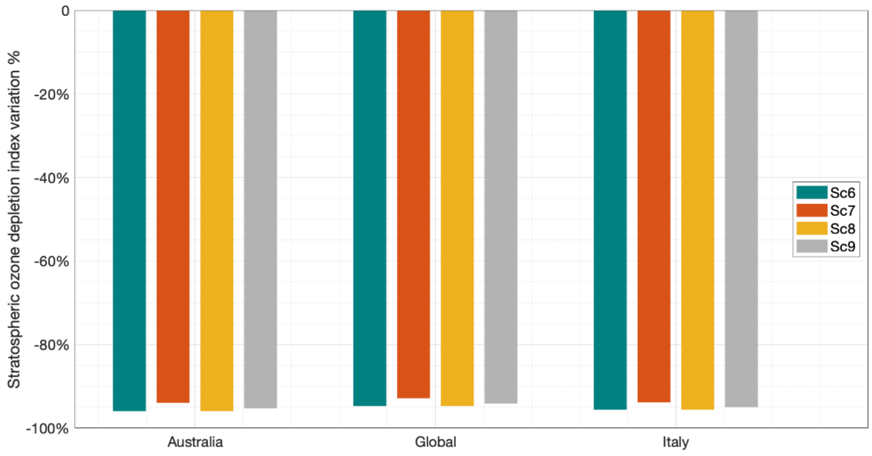
Stratospheric ozone depletion index variation %
0
-20%
-40%
-60%
-80%
-100%
Australia
Global
Italy
Sc6
Sc7
Sc8
Sc9

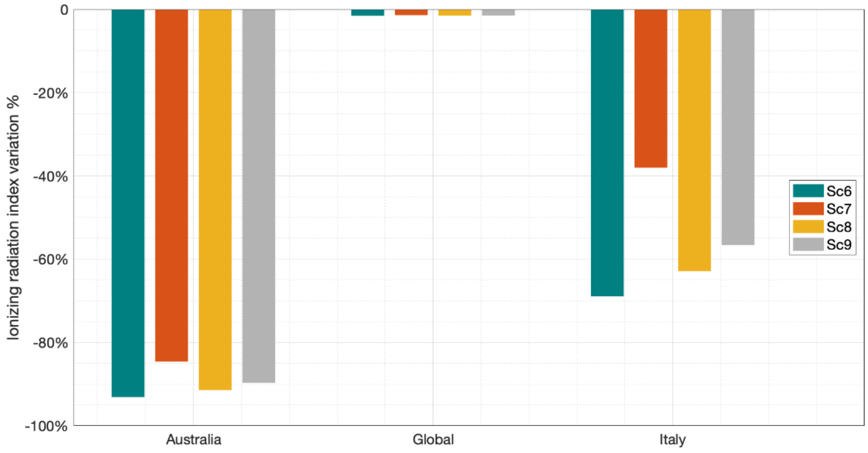
Ionizing radiation index variation %
0
-20%
-40%
-60%
-80%
-100%
Australia
Global
Italy
Sc6
Sc7
Sc8
Sc9

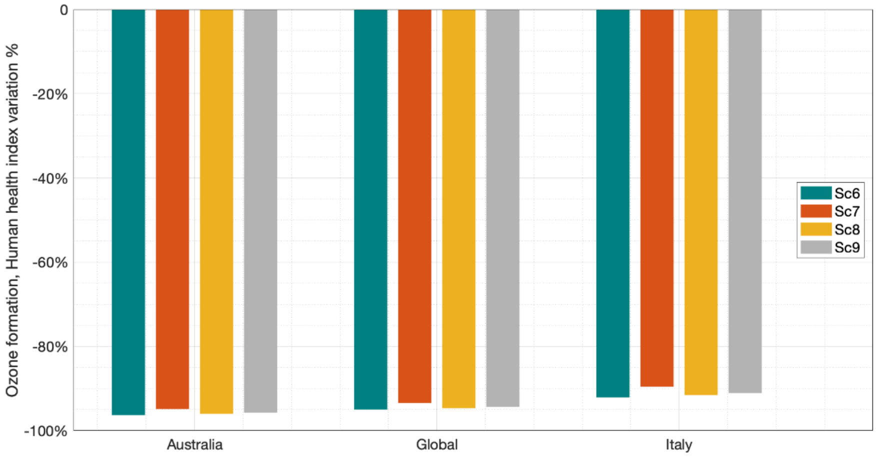
Ozone formation, Human health index variation %
0
-20%
-40%
-60%
-80%
-100%
Australia
Global
Italy
Sc6
Sc7
Sc8
Sc9

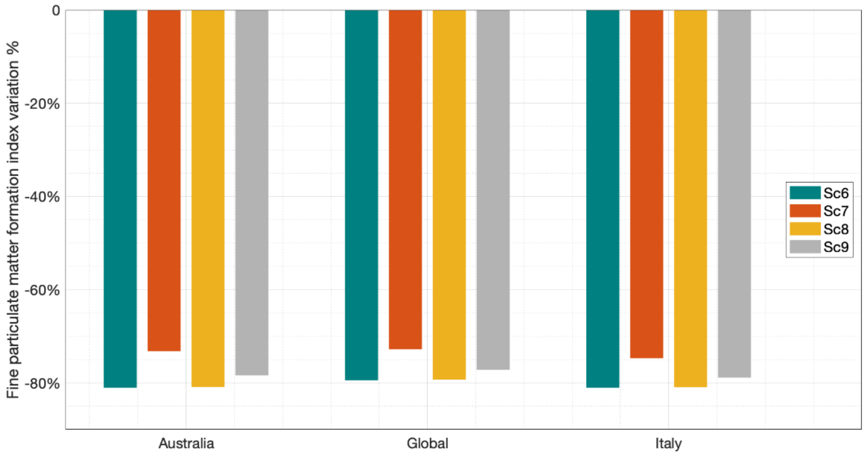
Fine particulate matter formation index variation %
0
-20%
-40%
-60%
-80%
Australia
Global
Italy
Sc6
Sc7
Sc8
Sc9

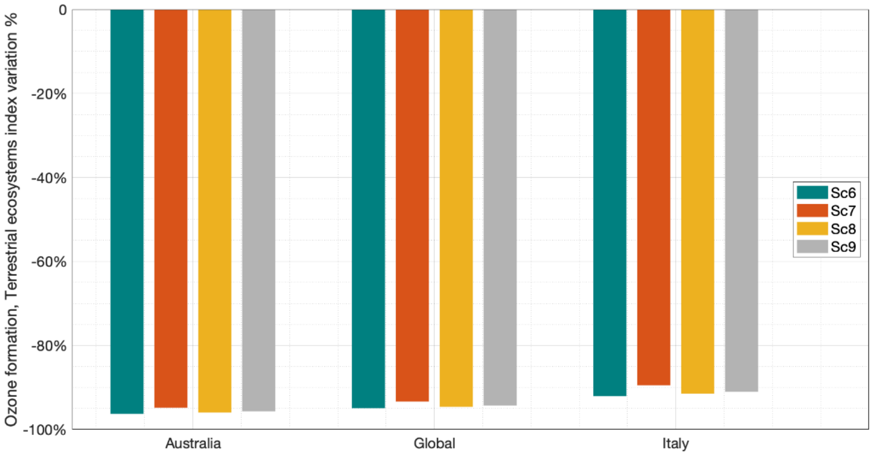
Ozone formation, Terrestrial ecosystems index variation %
0
-20%
-40%
-60%
-80%
-100%
Australia
Global
Italy
Sc6
Sc7
Sc8
Sc9

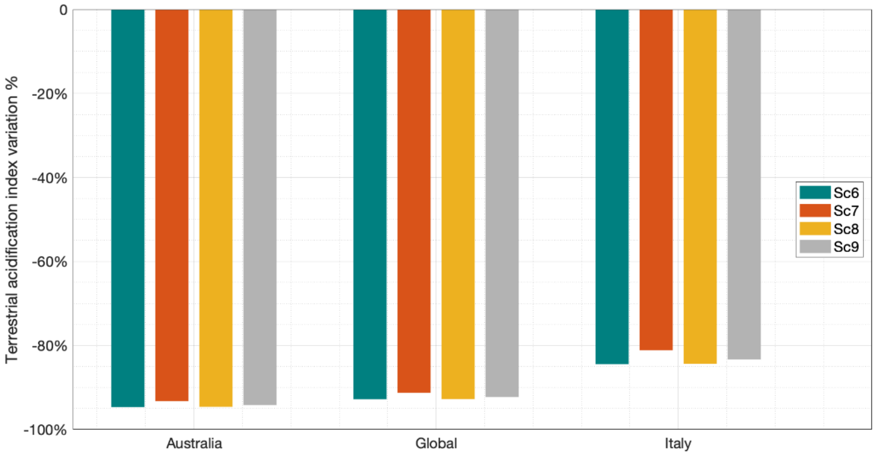
Terrestrial acidification index variation %
0
-20%
-40%
-60%
-80%
-100%
Australia
Global
Italy
Sc6
Sc7
Sc8
Sc9

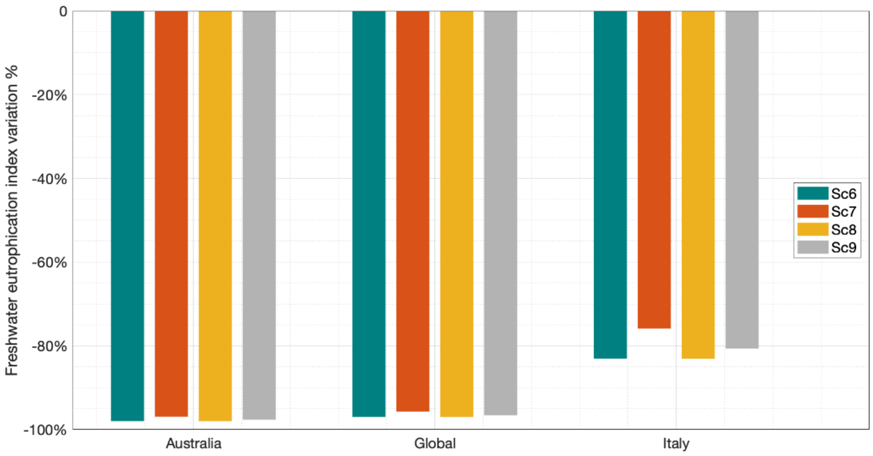
0
-20%
-40%
-60%
-80%
-100%
Freshwater eutrophication index variation %
Australia
Global
Italy
Sc6
Sc7
Sc8
Sc9

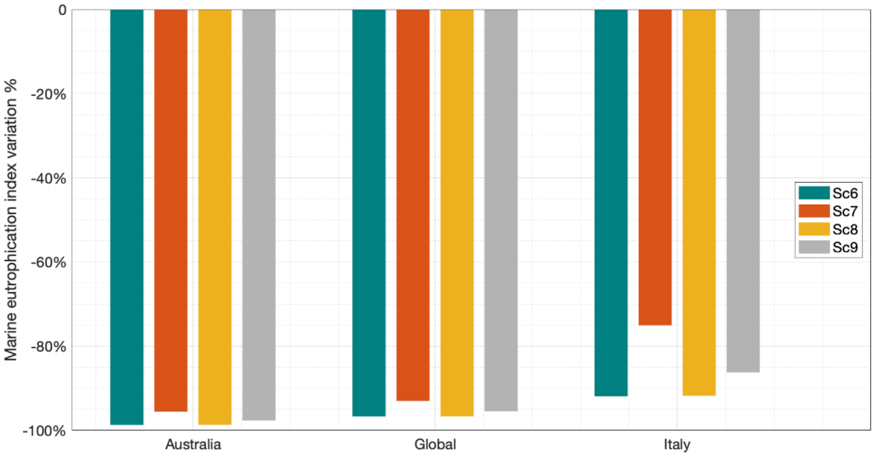
0
-20%
-40%
-60%
-80%
-100%
Marine eutrophication index variation %
Australia
Global
Italy
Sc6
Sc7
Sc8
Sc9

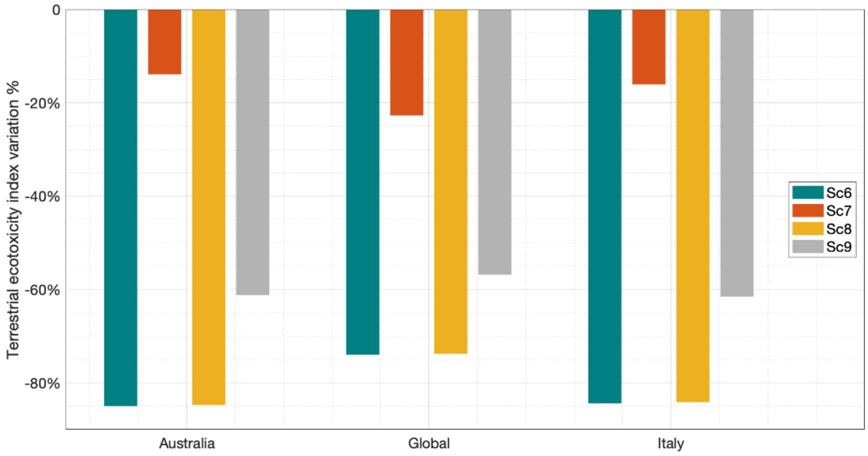
0
-20%
-40%
-60%
-80%
Terrestrial ecotoxicity index variation %
Australia
Global
Italy
Sc6
Sc7
Sc8
Sc9

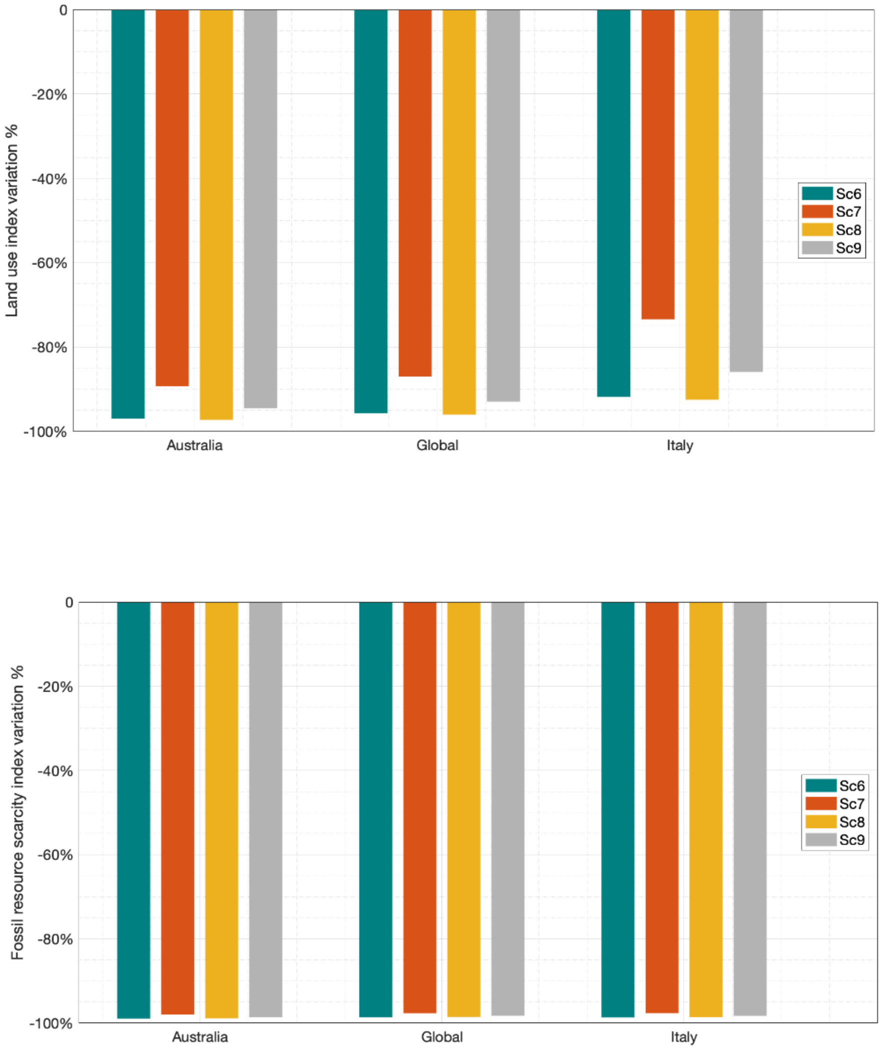

Figure 4.A. 2 Indices variation in Sc6, Sc7, Sc8, and Sc9 scenarios regarding sc2 (remaining indices)

In the following pages, supplementary data are provided.

Quantities (Sc1-Sc2-Sc3)-supplementary data

	Australia			Global			Italy		
Global Warming	Sc1	Sc2	Sc3	Sc1	Sc2	Sc3	Sc1	Sc2	Sc3
Stack material	5.20E-02	1.72E-01	3.19E-01	5.20E-02	1.72E-01	3.19E-01	5.20E-02	1.72E-01	3.19E-01
BOP material	1.21E-03	1.21E-03	1.21E-03	1.21E-03	1.21E-03	1.21E-03	1.21E-03	1.21E-03	1.21E-03
Electriciy-operation	1.99E+01	2.60E+01	3.22E+01	1.58E+01	2.08E+01	2.57E+01	1.18E+01	1.55E+01	1.91E+01
Electriciy-Stack assembly	6.08E-02	6.08E-02	6.08E-02	4.85E-02	4.85E-02	4.85E-02	3.61E-02	3.61E-02	3.61E-02
Electriciy-BOP assembly	9.76E-03	9.76E-03	9.76E-03	7.78E-03	7.78E-03	7.78E-03	5.80E-03	5.80E-03	5.80E-03
Electriciy-pump	2.44E-01	2.44E-01	2.44E-01	1.94E-01	1.94E-01	1.94E-01	1.45E-01	1.45E-01	1.45E-01
Water	1.61E-02	1.61E-02	1.61E-02	1.61E-02	1.61E-02	1.61E-02	1.61E-02	1.61E-02	1.61E-02
Heat	6.79E-02	6.79E-02	6.79E-02	6.79E-02	6.79E-02	6.79E-02	6.79E-02	6.79E-02	6.79E-02
Sum	2.03E+01	2.66E+01	3.29E+01	1.62E+01	2.13E+01	2.63E+01	1.21E+01	1.59E+01	1.97E+01

	Australia			Global			Italy		
Stratospheric ozone depletion	Sc1	Sc2	Sc3	Sc1	Sc2	Sc3	Sc1	Sc2	Sc3
Stack material	6.691E-08	2.929E-07	5.726E-07	6.691E-08	2.929E-07	5.726E-07	6.691E-08	2.929E-07	5.726E-07
BOP material	4.115E-10	4.115E-10	4.115E-10	4.115E-10	4.115E-10	4.115E-10	4.115E-10	4.115E-10	4.115E-10
Electriciy-operation	6.015E-06	7.884E-06	9.753E-06	5.302E-06	6.950E-06	8.597E-06	5.424E-06	7.110E-06	8.796E-06
Electriciy-Stack assembly	1.843E-08	1.843E-08	1.843E-08	1.624E-08	1.624E-08	1.624E-08	1.662E-08	1.662E-08	1.662E-08
Electriciy-BOP assembly	2.956E-09	2.956E-09	2.956E-09	2.606E-09	2.606E-09	2.606E-09	2.666E-09	2.666E-09	2.666E-09
Electriciy-pump	7.378E-08	7.378E-08	7.378E-08	6.504E-08	6.504E-08	6.504E-08	6.654E-08	6.654E-08	6.654E-08
Water	7.597E-09	7.597E-09	7.597E-09	7.597E-09	7.597E-09	7.597E-09	7.597E-09	7.597E-09	7.597E-09
Heat	2.411E-09	2.411E-09	2.411E-09	2.411E-09	2.411E-09	2.411E-09	2.411E-09	2.411E-09	2.411E-09
Sum	6.19E-06	8.28E-06	1.04E-05	5.46E-06	7.34E-06	9.26E-06	5.59E-06	7.50E-06	9.46E-06

	Australia			Global			Italy		
Ionizing radiation	Sc1	Sc2	Sc3	Sc1	Sc2	Sc3	Sc1	Sc2	Sc3
Stack material	2.245E-03	7.107E-03	1.299E-02	2.245E-03	7.107E-03	1.299E-02	2.245E-03	7.107E-03	1.299E-02
BOP material	9.759E-05	9.759E-05	9.759E-05	9.759E-05	9.759E-05	9.759E-05	9.759E-05	9.759E-05	9.759E-05
Electriciy-operation	9.022E-02	1.183E-01	1.463E-01	3.990E+00	5.230E+00	6.470E+00	1.571E-02	2.059E-02	2.547E-02
Electriciy-Stack assembly	2.764E-04	2.764E-04	2.764E-04	1.222E-02	1.222E-02	1.222E-02	4.813E-05	4.813E-05	4.813E-05
Electriciy-BOP assembly	4.434E-05	4.434E-05	4.434E-05	1.961E-03	1.961E-03	1.961E-03	7.721E-06	7.721E-06	7.721E-06
Electriciy-pump	1.107E-03	1.107E-03	1.107E-03	4.894E-02	4.894E-02	4.894E-02	1.927E-04	1.927E-04	1.927E-04
Water	1.738E-05	1.738E-05	1.738E-05	1.738E-05	1.738E-05	1.738E-05	1.738E-05	1.738E-05	1.738E-05
Heat	1.997E-06	1.997E-06	1.997E-06	1.997E-06	1.997E-06	1.997E-06	1.997E-06	1.997E-06	1.997E-06
Sum	9.40E-02	1.27E-01	1.61E-01	4.06E+00	5.30E+00	6.55E+00	1.83E-02	2.81E-02	3.88E-02

	Australia			Global			Italy		
Ozone formation, Human health	Sc1	Sc2	Sc3	Sc1	Sc2	Sc3	Sc1	Sc2	Sc3
Stack material	4.363E-04	1.767E-03	3.484E-03	4.363E-04	1.767E-03	3.484E-03	4.363E-04	1.767E-03	3.484E-03
BOP material	3.023E-06	3.023E-06	3.023E-06	3.023E-06	3.023E-06	3.023E-06	3.023E-06	3.023E-06	3.023E-06
Electriciy-operation	5.096E-02	6.680E-02	8.264E-02	3.931E-02	5.153E-02	6.374E-02	2.270E-02	2.975E-02	3.681E-02
Electriciy-Stack assembly	1.561E-04	1.561E-04	1.561E-04	1.204E-04	1.204E-04	1.204E-04	6.954E-05	6.954E-05	6.954E-05
Electriciy-BOP assembly	2.505E-05	2.505E-05	2.505E-05	1.932E-05	1.932E-05	1.932E-05	1.116E-05	1.116E-05	1.116E-05
Electriciy-pump	6.252E-04	6.252E-04	6.252E-04	4.822E-04	4.822E-04	4.822E-04	2.785E-04	2.785E-04	2.785E-04
Water	4.475E-05	4.475E-05	4.475E-05	4.475E-05	4.475E-05	4.475E-05	4.475E-05	4.475E-05	4.475E-05
Heat	5.075E-04	5.075E-04	5.075E-04	5.075E-04	5.075E-04	5.075E-04	5.075E-04	5.075E-04	5.075E-04
Sum	5.28E-02	6.99E-02	8.75E-02	4.09E-02	5.45E-02	6.84E-02	2.41E-02	3.24E-02	4.12E-02

	Australia			Global			Italy		
Fine particulate matter formation	Sc1	Sc2	Sc3	Sc1	Sc2	Sc3	Sc1	Sc2	Sc3
Stack material	4.161E-04	1.775E-03	3.535E-03	4.161E-04	1.775E-03	3.535E-03	4.161E-04	1.775E-03	3.535E-03
BOP material	1.768E-06	1.768E-06	1.768E-06	1.768E-06	1.768E-06	1.768E-06	1.768E-06	1.768E-06	1.768E-06
Electriciy-operation	6.606E-03	8.659E-03	1.071E-02	6.470E-03	8.481E-03	1.049E-02	6.509E-03	8.532E-03	1.056E-02
Electriciy-Stack assembly	2.024E-05	2.024E-05	2.024E-05	1.982E-05	1.982E-05	1.982E-05	1.994E-05	1.994E-05	1.994E-05
Electriciy-BOP assembly	3.247E-06	3.247E-06	3.247E-06	3.180E-06	3.180E-06	3.180E-06	3.199E-06	3.199E-06	3.199E-06
Electriciy-pump	8.104E-05	8.104E-05	8.104E-05	7.937E-05	7.937E-05	7.937E-05	7.985E-05	7.985E-05	7.985E-05
Water	2.485E-05	2.485E-05	2.485E-05	2.485E-05	2.485E-05	2.485E-05	2.485E-05	2.485E-05	2.485E-05
Heat	5.708E-05	5.708E-05	5.708E-05	5.708E-05	5.708E-05	5.708E-05	5.708E-05	5.708E-05	5.708E-05
Sum	7.21E-03	1.06E-02	1.44E-02	7.07E-03	1.04E-02	1.42E-02	7.11E-03	1.05E-02	1.43E-02

	Australia			Global			Italy		
Ozone formation, Terrestrial ecosystems	Sc1	Sc2	Sc3	Sc1	Sc2	Sc3	Sc1	Sc2	Sc3
Stack material	4.452E-04	1.804E-03	3.559E-03	4.452E-04	1.804E-03	3.559E-03	4.452E-04	1.804E-03	3.559E-03
BOP material	3.129E-06	3.129E-06	3.129E-06	3.129E-06	3.129E-06	3.129E-06	3.129E-06	3.129E-06	3.129E-06
Electriciy-operation	5.101E-02	6.687E-02	8.272E-02	3.937E-02	5.160E-02	6.383E-02	2.279E-02	2.988E-02	3.696E-02
Electriciy-Stack assembly	1.563E-04	1.563E-04	1.563E-04	1.206E-04	1.206E-04	1.206E-04	6.982E-05	6.982E-05	6.982E-05
Electriciy-BOP assembly	2.507E-05	2.507E-05	2.507E-05	1.935E-05	1.935E-05	1.935E-05	1.120E-05	1.120E-05	1.120E-05
Electriciy-pump	6.258E-04	6.258E-04	6.258E-04	4.829E-04	4.829E-04	4.829E-04	2.796E-04	2.796E-04	2.796E-04
Water	4.478E-05	4.478E-05	4.478E-05	4.478E-05	4.478E-05	4.478E-05	4.478E-05	4.478E-05	4.478E-05
Heat	5.076E-04	5.076E-04	5.076E-04	5.076E-04	5.076E-04	5.076E-04	5.076E-04	5.076E-04	5.076E-04
Sum	5.28E-02	7.00E-02	8.76E-02	4.10E-02	5.46E-02	6.86E-02	2.42E-02	3.26E-02	4.14E-02

	Australia			Global			Italy		
Terrestrial acidification	Sc1	Sc2	Sc3	Sc1	Sc2	Sc3	Sc1	Sc2	Sc3
Stack material	1.374E-03	6.008E-03	1.204E-02	1.374E-03	6.008E-03	1.204E-02	1.374E-03	6.008E-03	1.204E-02
BOP material	5.090E-06	5.090E-06	5.090E-06	5.090E-06	5.090E-06	5.090E-06	5.090E-06	5.090E-06	5.090E-06
Electriciy-operation	8.942E-02	1.172E-01	1.450E-01	6.707E-02	8.792E-02	1.088E-01	2.731E-02	3.580E-02	4.429E-02
Electriciy-Stack assembly	2.739E-04	2.739E-04	2.739E-04	2.055E-04	2.055E-04	2.055E-04	8.367E-05	8.367E-05	8.367E-05
Electriciy-BOP assembly	4.395E-05	4.395E-05	4.395E-05	3.296E-05	3.296E-05	3.296E-05	1.342E-05	1.342E-05	1.342E-05
Electriciy-pump	1.097E-03	1.097E-03	1.097E-03	8.227E-04	8.227E-04	8.227E-04	3.350E-04	3.350E-04	3.350E-04
Water	8.037E-05	8.037E-05	8.037E-05	8.037E-05	8.037E-05	8.037E-05	8.037E-05	8.037E-05	8.037E-05
Heat	1.868E-04	1.868E-04	1.868E-04	1.868E-04	1.868E-04	1.868E-04	1.868E-04	1.868E-04	1.868E-04
Sum	9.25E-02	1.25E-01	1.59E-01	6.98E-02	9.53E-02	1.22E-01	2.94E-02	4.25E-02	5.70E-02

	Australia			Global			Italy		
Freshwater eutrophication	Sc1	Sc2	Sc3	Sc1	Sc2	Sc3	Sc1	Sc2	Sc3
Stack material	9.560E-05	2.315E-04	4.033E-04	9.560E-05	2.315E-04	4.033E-04	9.560E-05	2.315E-04	4.033E-04
BOP material	6.968E-07	6.968E-07	6.968E-07	6.968E-07	6.968E-07	6.968E-07	6.968E-07	6.968E-07	6.968E-07
Electriciy-operation	9.140E-03	1.198E-02	1.482E-02	6.247E-03	8.189E-03	1.013E-02	9.214E-04	1.208E-03	1.494E-03
Electriciy-Stack assembly	2.800E-05	2.800E-05	2.800E-05	1.914E-05	1.914E-05	1.914E-05	2.823E-06	2.823E-06	2.823E-06
Electriciy-BOP assembly	4.492E-06	4.492E-06	4.492E-06	3.070E-06	3.070E-06	3.070E-06	4.528E-07	4.528E-07	4.528E-07
Electriciy-pump	1.121E-04	1.121E-04	1.121E-04	7.663E-05	7.663E-05	7.663E-05	1.130E-05	1.130E-05	1.130E-05
Water	8.096E-07	8.096E-07	8.096E-07	8.096E-07	8.096E-07	8.096E-07	8.096E-07	8.096E-07	8.096E-07
Heat	1.631E-08	1.631E-08	1.631E-08	1.631E-08	1.631E-08	1.631E-08	1.631E-08	1.631E-08	1.631E-08
Sum	9.38E-03	1.24E-02	1.54E-02	6.44E-03	8.52E-03	1.06E-02	1.03E-03	1.46E-03	1.91E-03

	Australia			Global			Italy		
Marine eutrophication	Sc1	Sc2	Sc3	Sc1	Sc2	Sc3	Sc1	Sc2	Sc3
Stack material	2.208E-06	7.023E-06	1.309E-05	2.208E-06	7.023E-06	1.309E-05	2.208E-06	7.023E-06	1.309E-05
BOP material	3.701E-08	3.701E-08	3.701E-08	3.701E-08	3.701E-08	3.701E-08	3.701E-08	3.701E-08	3.701E-08
Electriciy-operation	6.127E-04	8.031E-04	9.935E-04	4.375E-04	5.735E-04	7.095E-04	8.785E-05	1.152E-04	1.425E-04
Electriciy-Stack assembly	1.877E-06	1.877E-06	1.877E-06	1.340E-06	1.340E-06	1.340E-06	2.691E-07	2.691E-07	2.691E-07
Electriciy-BOP assembly	3.011E-07	3.011E-07	3.011E-07	2.150E-07	2.150E-07	2.150E-07	4.318E-08	4.318E-08	4.318E-08
Electriciy-pump	7.516E-06	7.516E-06	7.516E-06	5.367E-06	5.367E-06	5.367E-06	1.078E-06	1.078E-06	1.078E-06
Water	1.733E-07	1.733E-07	1.733E-07	1.733E-07	1.733E-07	1.733E-07	1.733E-07	1.733E-07	1.733E-07
Heat	1.556E-09	1.556E-09	1.556E-09	1.556E-09	1.556E-09	1.556E-09	1.556E-09	1.556E-09	1.556E-09
Sum	6.25E-04	8.20E-04	1.02E-03	4.47E-04	5.88E-04	7.30E-04	9.17E-05	1.24E-04	1.57E-04

	Australia			Global			Italy		
Terrestrial ecotoxicity	Sc1	Sc2	Sc3	Sc1	Sc2	Sc3	Sc1	Sc2	Sc3
Stack material	1.779E-01	4.558E-01	8.011E-01	1.779E-01	4.558E-01	8.011E-01	1.779E-01	4.558E-01	8.011E-01
BOP material	9.142E-03	9.142E-03	9.142E-03	9.142E-03	9.142E-03	9.142E-03	9.142E-03	9.142E-03	9.142E-03
Electriciy-operation	5.971E+00	7.827E+00	9.682E+00	6.994E+00	9.168E+00	1.134E+01	4.930E+00	6.463E+00	7.995E+00
Electriciy-Stack assembly	1.829E-02	1.829E-02	1.829E-02	2.143E-02	2.143E-02	2.143E-02	1.510E-02	1.510E-02	1.510E-02
Electriciy-BOP assembly	2.934E-03	2.934E-03	2.934E-03	3.437E-03	3.437E-03	3.437E-03	2.423E-03	2.423E-03	2.423E-03
Electriciy-pump	7.324E-02	7.324E-02	7.324E-02	8.579E-02	8.579E-02	8.579E-02	6.048E-02	6.048E-02	6.048E-02
Water	1.921E-02	1.921E-02	1.921E-02	1.921E-02	1.921E-02	1.921E-02	1.921E-02	1.921E-02	1.921E-02
Heat	4.283E-03	4.283E-03	4.283E-03	4.283E-03	4.283E-03	4.283E-03	4.283E-03	4.283E-03	4.283E-03
Sum	6.28E+00	8.41E+00	1.06E+01	7.32E+00	9.77E+00	1.23E+01	5.22E+00	7.03E+00	8.91E+00

	Australia			Global			Italy		
Freshwater ecotoxicity	Sc1	Sc2	Sc3	Sc1	Sc2	Sc3	Sc1	Sc2	Sc3
Stack material	4.445E-02	9.296E-02	1.556E-01	4.445E-02	9.296E-02	1.556E-01	4.445E-02	9.296E-02	1.556E-01
BOP material	2.157E-04	2.157E-04	2.157E-04	2.157E-04	2.157E-04	2.157E-04	2.157E-04	2.157E-04	2.157E-04
Electriciy-operation	2.955E-01	3.873E-01	4.791E-01	2.064E-01	2.706E-01	3.347E-01	3.556E-02	4.661E-02	5.766E-02
Electriciy-Stack assembly	9.051E-04	9.051E-04	9.051E-04	6.323E-04	6.323E-04	6.323E-04	1.089E-04	1.089E-04	1.089E-04
Electriciy-BOP assembly	1.452E-04	1.452E-04	1.452E-04	1.014E-04	1.014E-04	1.014E-04	1.748E-05	1.748E-05	1.748E-05
Electriciy-pump	3.624E-03	3.624E-03	3.624E-03	2.532E-03	2.532E-03	2.532E-03	4.362E-04	4.362E-04	4.362E-04
Water	2.461E-04	2.461E-04	2.461E-04	2.461E-04	2.461E-04	2.461E-04	2.461E-04	2.461E-04	2.461E-04
Heat	2.724E-06	2.724E-06	2.724E-06	2.724E-06	2.724E-06	2.724E-06	2.724E-06	2.724E-06	2.724E-06
Sum	3.45E-01	4.85E-01	6.40E-01	2.55E-01	3.67E-01	4.94E-01	8.10E-02	1.41E-01	2.14E-01

	Australia			Global			Italy		
Marine ecotoxicity	Sc1	Sc2	Sc3	Sc1	Sc2	Sc3	Sc1	Sc2	Sc3
Stack material	6.502E-02	1.780E-01	3.112E-01	6.502E-02	1.780E-01	3.112E-01	6.502E-02	1.780E-01	3.112E-01
BOP material	3.634E-02	3.634E-02	3.634E-02	3.634E-02	3.634E-02	3.634E-02	3.634E-02	3.634E-02	3.634E-02
Electriciy-operation	1.088E-01	1.426E-01	1.764E-01	8.369E-02	1.097E-01	1.357E-01	2.672E-02	3.502E-02	4.333E-02
Electriciy-Stack assembly	3.332E-04	3.332E-04	3.332E-04	2.564E-04	2.564E-04	2.564E-04	8.185E-05	8.185E-05	8.185E-05
Electriciy-BOP assembly	5.345E-05	5.345E-05	5.345E-05	4.113E-05	4.113E-05	4.113E-05	1.313E-05	1.313E-05	1.313E-05
Electriciy-pump	1.334E-03	1.334E-03	1.334E-03	1.027E-03	1.027E-03	1.027E-03	3.278E-04	3.278E-04	3.278E-04
Water	3.491E-04	3.491E-04	3.491E-04	3.491E-04	3.491E-04	3.491E-04	3.491E-04	3.491E-04	3.491E-04
Heat	1.129E-05	1.129E-05	1.129E-05	1.129E-05	1.129E-05	1.129E-05	1.129E-05	1.129E-05	1.129E-05
Sum	2.12E-01	3.59E-01	5.26E-01	1.87E-01	3.26E-01	4.85E-01	1.29E-01	2.50E-01	3.92E-01

	Australia			Global			Italy		
Human carcinogenic toxicity	Sc1	Sc2	Sc3	Sc1	Sc2	Sc3	Sc1	Sc2	Sc3
Stack material	1.479E-02	3.975E-02	6.879E-02	1.479E-02	3.975E-02	6.879E-02	1.479E-02	3.975E-02	6.879E-02
BOP material	6.604E-04	6.604E-04	6.604E-04	6.604E-04	6.604E-04	6.604E-04	6.604E-04	6.604E-04	6.604E-04
Electriciy-operation	3.633E-02	4.762E-02	5.891E-02	4.525E-02	5.932E-02	7.338E-02	6.077E-02	7.965E-02	9.853E-02
Electriciy-Stack assembly	1.113E-04	1.113E-04	1.113E-04	1.386E-04	1.386E-04	1.386E-04	1.861E-04	1.861E-04	1.861E-04
Electriciy-BOP assembly	1.785E-05	1.785E-05	1.785E-05	2.224E-05	2.224E-05	2.224E-05	2.986E-05	2.986E-05	2.986E-05
Electriciy-pump	4.456E-04	4.456E-04	4.456E-04	5.551E-04	5.551E-04	5.551E-04	7.454E-04	7.454E-04	7.454E-04
Water	2.932E-04	2.932E-04	2.932E-04	2.932E-04	2.932E-04	2.932E-04	2.932E-04	2.932E-04	2.932E-04
Heat	1.857E-05	1.857E-05	1.857E-05	1.857E-05	1.857E-05	1.857E-05	1.857E-05	1.857E-05	1.857E-05
Sum	5.27E-02	8.89E-02	1.29E-01	6.17E-02	1.01E-01	1.44E-01	7.75E-02	1.21E-01	1.69E-01

	Australia			Global			Italy		
Human non-carcinogenic toxicity	Sc1	Sc2	Sc3	Sc1	Sc2	Sc3	Sc1	Sc2	Sc3
Stack material	9.741E-01	2.919E+00	5.443E+00	9.741E-01	2.919E+00	5.443E+00	9.741E-01	2.919E+00	5.443E+00
BOP material	3.221E-02	3.221E-02	3.221E-02	3.221E-02	3.221E-02	3.221E-02	3.221E-02	3.221E-02	3.221E-02
Electriciy-operation	4.366E-01	5.723E-01	7.079E-01	8.138E-01	1.067E+00	1.320E+00	3.917E-01	5.134E-01	6.351E-01
Electriciy-Stack assembly	1.337E-03	1.337E-03	1.337E-03	2.493E-03	2.493E-03	2.493E-03	1.200E-03	1.200E-03	1.200E-03
Electriciy-BOP assembly	2.146E-04	2.146E-04	2.146E-04	4.000E-04	4.000E-04	4.000E-04	1.925E-04	1.925E-04	1.925E-04
Electriciy-pump	5.355E-03	5.355E-03	5.355E-03	9.983E-03	9.983E-03	9.983E-03	4.804E-03	4.804E-03	4.804E-03
Water	1.529E-02	1.529E-02	1.529E-02	1.529E-02	1.529E-02	1.529E-02	1.529E-02	1.529E-02	1.529E-02
Heat	3.321E-04	3.321E-04	3.321E-04	3.321E-04	3.321E-04	3.321E-04	3.321E-04	3.321E-04	3.321E-04
Sum	1.47E+00	3.55E+00	6.21E+00	1.85E+00	4.05E+00	6.82E+00	1.42E+00	3.49E+00	6.13E+00

	Australia			Global			Italy		
Land use	Sc1	Sc2	Sc3	Sc1	Sc2	Sc3	Sc1	Sc2	Sc3
Stack material	2.085E-03	6.204E-03	1.121E-02	2.085E-03	6.204E-03	1.121E-02	2.085E-03	6.204E-03	1.121E-02
BOP material	3.554E-05	3.554E-05	3.554E-05	3.554E-05	3.554E-05	3.554E-05	3.554E-05	3.554E-05	3.554E-05
Electriciy-operation	2.942E-01	3.856E-01	4.770E-01	2.161E-01	2.833E-01	3.505E-01	9.535E-02	1.250E-01	1.546E-01
Electriciy-Stack assembly	9.012E-04	9.012E-04	9.012E-04	6.621E-04	6.621E-04	6.621E-04	2.921E-04	2.921E-04	2.921E-04
Electriciy-BOP assembly	1.446E-04	1.446E-04	1.446E-04	1.062E-04	1.062E-04	1.062E-04	4.686E-05	4.686E-05	4.686E-05
Electriciy-pump	3.609E-03	3.609E-03	3.609E-03	2.651E-03	2.651E-03	2.651E-03	1.170E-03	1.170E-03	1.170E-03
Water	5.054E-04	5.054E-04	5.054E-04	5.054E-04	5.054E-04	5.054E-04	5.054E-04	5.054E-04	5.054E-04
Heat	2.321E-05	2.321E-05	2.321E-05	2.321E-05	2.321E-05	2.321E-05	2.321E-05	2.321E-05	2.321E-05
Sum	3.01E-01	3.97E-01	4.93E-01	2.22E-01	2.93E-01	3.66E-01	9.95E-02	1.33E-01	1.68E-01

	Australia			Global			Italy		
Mineral resource scarcity	Sc1	Sc2	Sc3	Sc1	Sc2	Sc3	Sc1	Sc2	Sc3
Stack material	4.591E-03	1.681E-02	3.240E-02	4.591E-03	1.681E-02	3.240E-02	4.591E-03	1.681E-02	3.240E-02
BOP material	2.169E-05	2.169E-05	2.169E-05	2.169E-05	2.169E-05	2.169E-05	2.169E-05	2.169E-05	2.169E-05
Electriciy-operation	9.423E-03	1.235E-02	1.528E-02	1.039E-02	1.362E-02	1.685E-02	7.469E-03	9.790E-03	1.211E-02
Electriciy-Stack assembly	2.887E-05	2.887E-05	2.887E-05	3.183E-05	3.183E-05	3.183E-05	2.288E-05	2.288E-05	2.288E-05
Electriciy-BOP assembly	4.631E-06	4.631E-06	4.631E-06	5.106E-06	5.106E-06	5.106E-06	3.670E-06	3.670E-06	3.670E-06
Electriciy-pump	1.156E-04	1.156E-04	1.156E-04	1.274E-04	1.274E-04	1.274E-04	9.161E-05	9.161E-05	9.161E-05
Water	4.323E-05	4.323E-05	4.323E-05	4.323E-05	4.323E-05	4.323E-05	4.323E-05	4.323E-05	4.323E-05
Heat	1.272E-06	1.272E-06	1.272E-06	1.272E-06	1.272E-06	1.272E-06	1.272E-06	1.272E-06	1.272E-06
Sum	1.42E-02	2.94E-02	4.79E-02	1.52E-02	3.07E-02	4.95E-02	1.22E-02	2.68E-02	4.47E-02

	Australia			Global			Italy		
Fossil resource scarcity	Sc1	Sc2	Sc3	Sc1	Sc2	Sc3	Sc1	Sc2	Sc3
Stack material	1.449E-02	5.083E-02	9.625E-02	1.449E-02	5.083E-02	9.625E-02	1.449E-02	5.083E-02	9.625E-02
BOP material	2.644E-04	2.644E-04	2.644E-04	2.644E-04	2.644E-04	2.644E-04	2.644E-04	2.644E-04	2.644E-04
Electriciy-operation	6.878E+00	9.015E+00	1.115E+01	5.716E+00	7.493E+00	9.269E+00	5.254E+00	6.887E+00	8.519E+00
Electriciy-Stack assembly	2.107E-02	2.107E-02	2.107E-02	1.751E-02	1.751E-02	1.751E-02	1.609E-02	1.609E-02	1.609E-02
Electriciy-BOP assembly	3.380E-03	3.380E-03	3.380E-03	2.809E-03	2.809E-03	2.809E-03	2.582E-03	2.582E-03	2.582E-03
Electriciy-pump	8.437E-02	8.437E-02	8.437E-02	7.012E-02	7.012E-02	7.012E-02	6.445E-02	6.445E-02	6.445E-02
Water	3.221E-03	3.221E-03	3.221E-03	3.221E-03	3.221E-03	3.221E-03	3.221E-03	3.221E-03	3.221E-03
Heat	2.489E-02	2.489E-02	2.489E-02	2.489E-02	2.489E-02	2.489E-02	2.489E-02	2.489E-02	2.489E-02
Sum	7.03E+00	9.20E+00	1.14E+01	5.85E+00	7.66E+00	9.48E+00	5.38E+00	7.05E+00	8.73E+00

	Australia			Global			Italy		
Water consumption	Sc1	Sc2	Sc3	Sc1	Sc2	Sc3	Sc1	Sc2	Sc3
Stack material	3.610E-04	1.117E-03	2.031E-03	3.610E-04	1.117E-03	2.031E-03	3.610E-04	1.117E-03	2.031E-03
BOP material	2.081E-05	2.081E-05	2.081E-05	2.081E-05	2.081E-05	2.081E-05	2.081E-05	2.081E-05	2.081E-05
Electriciy-operation	2.876E+00	3.769E+00	4.663E+00	2.209E+00	2.896E+00	3.582E+00	9.265E-01	1.214E+00	1.502E+00
Electriciy-Stack assembly	8.809E-03	8.809E-03	8.809E-03	6.768E-03	6.768E-03	6.768E-03	2.838E-03	2.838E-03	2.838E-03
Electriciy-BOP assembly	1.413E-03	1.413E-03	1.413E-03	1.086E-03	1.086E-03	1.086E-03	4.553E-04	4.553E-04	4.553E-04
Electriciy-pump	3.527E-02	3.527E-02	3.527E-02	2.710E-02	2.710E-02	2.710E-02	1.137E-02	1.137E-02	1.137E-02
Water	2.158E-02	2.158E-02	2.158E-02	2.158E-02	2.158E-02	2.158E-02	2.158E-02	2.158E-02	2.158E-02
Heat	1.530E-04	1.530E-04	1.530E-04	1.530E-04	1.530E-04	1.530E-04	1.530E-04	1.530E-04	1.530E-04
Sum	2.94E+00	3.84E+00	4.73E+00	2.27E+00	2.95E+00	3.64E+00	9.63E-01	1.25E+00	1.54E+00

Percentage (Sc1-Sc2-Sc3)-supplementary data

	Australia			Global			Italy		
Global Warming	Sc1	Sc2	Sc3	Sc1	Sc2	Sc3	Sc1	Sc2	Sc3
Stack material	0.26%	0.65%	0.97%	0.32%	0.81%	1.21%	0.43%	1.08%	1.62%
BOP material	0.01%	0.00%	0.00%	0.01%	0.01%	0.00%	0.01%	0.01%	0.01%
Electriciy-operation	97.78%	97.85%	97.82%	97.61%	97.61%	97.51%	97.33%	97.21%	97.01%
Electriciy-Stack assembly	0.30%	0.23%	0.18%	0.30%	0.23%	0.18%	0.30%	0.23%	0.18%
Electriciy-BOP assembly	0.05%	0.04%	0.03%	0.05%	0.04%	0.03%	0.05%	0.04%	0.03%
Electriciy-pump	1.20%	0.92%	0.74%	1.20%	0.91%	0.74%	1.19%	0.91%	0.73%
Water	0.08%	0.06%	0.05%	0.10%	0.08%	0.06%	0.13%	0.10%	0.08%
Heat	0.33%	0.26%	0.21%	0.42%	0.32%	0.26%	0.56%	0.43%	0.34%
Sum	1.00E+00	1.00E+00	1.00E+00	1.00E+00	1.00E+00	1.00E+00	1.00E+00	1.00E+00	1.00E+00

	Australia			Global			Italy		
Stratospheric ozone depletion	Sc1	Sc2	Sc3	Sc1	Sc2	Sc3	Sc1	Sc2	Sc3
Stack material	1.08%	3.54%	5.49%	1.22%	3.99%	6.18%	1.20%	3.91%	6.05%
BOP material	0.01%	0.00%	0.00%	0.01%	0.01%	0.00%	0.01%	0.01%	0.00%
Electriciy-operation	97.21%	95.19%	93.50%	97.05%	94.72%	92.80%	97.08%	94.81%	92.93%
Electriciy-Stack assembly	0.30%	0.22%	0.18%	0.30%	0.22%	0.18%	0.30%	0.22%	0.18%
Electriciy-BOP assembly	0.05%	0.04%	0.03%	0.05%	0.04%	0.03%	0.05%	0.04%	0.03%
Electriciy-pump	1.19%	0.89%	0.71%	1.19%	0.89%	0.70%	1.19%	0.89%	0.70%
Water	0.12%	0.09%	0.07%	0.14%	0.10%	0.08%	0.14%	0.10%	0.08%
Heat	0.04%	0.03%	0.02%	0.04%	0.03%	0.03%	0.04%	0.03%	0.03%
Sum	1.00E+00	1.00E+00	1.00E+00	1.00E+00	1.00E+00	1.00E+00	1.00E+00	1.00E+00	1.00E+00

	Australia			Global			Italy		
Ionizing radiation	Sc1	Sc2	Sc3	Sc1	Sc2	Sc3	Sc1	Sc2	Sc3
Stack material	2.39%	5.60%	8.07%	0.06%	0.13%	0.20%	12.25%	25.32%	33.45%
BOP material	0.10%	0.08%	0.06%	0.00%	0.00%	0.00%	0.53%	0.35%	0.25%
Electriciy-operation	95.97%	93.18%	90.97%	98.39%	98.67%	98.84%	85.75%	73.37%	65.61%
Electriciy-Stack assembly	0.29%	0.22%	0.17%	0.30%	0.23%	0.19%	0.26%	0.17%	0.12%
Electriciy-BOP assembly	0.05%	0.03%	0.03%	0.05%	0.04%	0.03%	0.04%	0.03%	0.02%
Electriciy-pump	1.18%	0.87%	0.69%	1.21%	0.92%	0.75%	1.05%	0.69%	0.50%
Water	0.02%	0.01%	0.01%	0.00%	0.00%	0.00%	0.09%	0.06%	0.04%
Heat	0.00%	0.00%	0.00%	0.00%	0.00%	0.00%	0.01%	0.01%	0.01%
Sum	1.00E+00	1.00E+00	1.00E+00	1.00E+00	1.00E+00	1.00E+00	1.00E+00	1.00E+00	1.00E+00

	Australia			Global			Italy		
Ozone formation, Human health	Sc1	Sc2	Sc3	Sc1	Sc2	Sc3	Sc1	Sc2	Sc3
Stack material	0.83%	2.53%	3.98%	1.07%	3.24%	5.09%	1.81%	5.45%	8.46%
BOP material	0.01%	0.00%	0.00%	0.01%	0.01%	0.00%	0.01%	0.01%	0.01%
Electriciy-operation	96.59%	95.53%	94.46%	96.06%	94.60%	93.19%	94.38%	91.73%	89.33%
Electriciy-Stack assembly	0.30%	0.22%	0.18%	0.29%	0.22%	0.18%	0.29%	0.21%	0.17%
Electriciy-BOP assembly	0.05%	0.04%	0.03%	0.05%	0.04%	0.03%	0.05%	0.03%	0.03%
Electriciy-pump	1.18%	0.89%	0.71%	1.18%	0.89%	0.70%	1.16%	0.86%	0.68%
Water	0.08%	0.06%	0.05%	0.11%	0.08%	0.07%	0.19%	0.14%	0.11%
Heat	0.96%	0.73%	0.58%	1.24%	0.93%	0.74%	2.11%	1.56%	1.23%
Sum	1.00E+00	1.00E+00	1.00E+00	1.00E+00	1.00E+00	1.00E+00	1.00E+00	1.00E+00	1.00E+00

	Australia			Global			Italy		
Fine particulate matter formation	Sc1	Sc2	Sc3	Sc1	Sc2	Sc3	Sc1	Sc2	Sc3
Stack material	5.77%	16.71%	24.49%	5.88%	17.00%	24.87%	5.85%	16.91%	24.76%
BOP material	0.02%	0.02%	0.01%	0.03%	0.02%	0.01%	0.02%	0.02%	0.01%
Electriciy-operation	91.62%	81.52%	74.21%	91.49%	81.22%	73.82%	91.53%	81.31%	73.93%
Electriciy-Stack assembly	0.28%	0.19%	0.14%	0.28%	0.19%	0.14%	0.28%	0.19%	0.14%
Electriciy-BOP assembly	0.05%	0.03%	0.02%	0.04%	0.03%	0.02%	0.04%	0.03%	0.02%
Electriciy-pump	1.12%	0.76%	0.56%	1.12%	0.76%	0.56%	1.12%	0.76%	0.56%
Water	0.34%	0.23%	0.17%	0.35%	0.24%	0.17%	0.35%	0.24%	0.17%
Heat	0.79%	0.54%	0.40%	0.81%	0.55%	0.40%	0.80%	0.54%	0.40%
Sum	1.00E+00	1.00E+00	1.00E+00	1.00E+00	1.00E+00	1.00E+00	1.00E+00	1.00E+00	1.00E+00

	Australia			Global			Italy		
Ozone formation, Terrestrial ecosystems	Sc1	Sc2	Sc3	Sc1	Sc2	Sc3	Sc1	Sc2	Sc3
Stack material	0.84%	2.58%	4.06%	1.09%	3.30%	5.19%	1.84%	5.53%	8.59%
BOP material	0.01%	0.00%	0.00%	0.01%	0.01%	0.00%	0.01%	0.01%	0.01%
Electriciy-operation	96.58%	95.48%	94.39%	96.04%	94.54%	93.09%	94.36%	91.66%	89.20%
Electriciy-Stack assembly	0.30%	0.22%	0.18%	0.29%	0.22%	0.18%	0.29%	0.21%	0.17%
Electriciy-BOP assembly	0.05%	0.04%	0.03%	0.05%	0.04%	0.03%	0.05%	0.03%	0.03%
Electriciy-pump	1.18%	0.89%	0.71%	1.18%	0.88%	0.70%	1.16%	0.86%	0.67%
Water	0.08%	0.06%	0.05%	0.11%	0.08%	0.07%	0.19%	0.14%	0.11%
Heat	0.96%	0.72%	0.58%	1.24%	0.93%	0.74%	2.10%	1.56%	1.23%
Sum	1.00E+00	1.00E+00	1.00E+00	1.00E+00	1.00E+00	1.00E+00	1.00E+00	1.00E+00	1.00E+00

	Australia			Global			Italy		
Terrestrial acidification	Sc1	Sc2	Sc3	Sc1	Sc2	Sc3	Sc1	Sc2	Sc3
Stack material	1.49%	4.81%	7.58%	1.97%	6.31%	9.85%	4.67%	14.13%	21.10%
BOP material	0.01%	0.00%	0.00%	0.01%	0.01%	0.00%	0.02%	0.01%	0.01%
Electriciy-operation	96.69%	93.84%	91.35%	96.12%	92.29%	89.05%	92.93%	84.21%	77.66%
Electriciy-Stack assembly	0.30%	0.22%	0.17%	0.29%	0.22%	0.17%	0.28%	0.20%	0.15%
Electriciy-BOP assembly	0.05%	0.04%	0.03%	0.05%	0.03%	0.03%	0.05%	0.03%	0.02%
Electriciy-pump	1.19%	0.88%	0.69%	1.18%	0.86%	0.67%	1.14%	0.79%	0.59%
Water	0.09%	0.06%	0.05%	0.12%	0.08%	0.07%	0.27%	0.19%	0.14%
Heat	0.20%	0.15%	0.12%	0.27%	0.20%	0.15%	0.64%	0.44%	0.33%
Sum	1.00E+00	1.00E+00	1.00E+00	1.00E+00	1.00E+00	1.00E+00	1.00E+00	1.00E+00	1.00E+00

	Australia			Global			Italy		
Freshwater eutrophication	Sc1	Sc2	Sc3	Sc1	Sc2	Sc3	Sc1	Sc2	Sc3
Stack material	1.02%	1.87%	2.62%	1.48%	2.72%	3.79%	9.25%	15.91%	21.08%
BOP material	0.01%	0.01%	0.00%	0.01%	0.01%	0.01%	0.07%	0.05%	0.04%
Electriciy-operation	97.42%	96.94%	96.43%	96.96%	96.10%	95.26%	89.19%	82.98%	78.08%
Electriciy-Stack assembly	0.30%	0.23%	0.18%	0.30%	0.22%	0.18%	0.27%	0.19%	0.15%
Electriciy-BOP assembly	0.05%	0.04%	0.03%	0.05%	0.04%	0.03%	0.04%	0.03%	0.02%
Electriciy-pump	1.20%	0.91%	0.73%	1.19%	0.90%	0.72%	1.09%	0.78%	0.59%
Water	0.01%	0.01%	0.01%	0.01%	0.01%	0.01%	0.08%	0.06%	0.04%
Heat	0.00%	0.00%	0.00%	0.00%	0.00%	0.00%	0.00%	0.00%	0.00%
Sum	1.00E+00	1.00E+00	1.00E+00	1.00E+00	1.00E+00	1.00E+00	1.00E+00	1.00E+00	1.00E+00

	Australia			Global			Italy		
Marine eutrophication	Sc1	Sc2	Sc3	Sc1	Sc2	Sc3	Sc1	Sc2	Sc3
Stack material	0.35%	0.86%	1.29%	0.49%	1.20%	1.79%	2.41%	5.67%	8.33%
BOP material	0.01%	0.00%	0.00%	0.01%	0.01%	0.01%	0.04%	0.03%	0.02%
Electriciy-operation	98.06%	97.94%	97.74%	97.91%	97.59%	97.23%	95.84%	93.03%	90.65%
Electriciy-Stack assembly	0.30%	0.23%	0.18%	0.30%	0.23%	0.18%	0.29%	0.22%	0.17%
Electriciy-BOP assembly	0.05%	0.04%	0.03%	0.05%	0.04%	0.03%	0.05%	0.03%	0.03%
Electriciy-pump	1.20%	0.92%	0.74%	1.20%	0.91%	0.74%	1.18%	0.87%	0.69%
Water	0.03%	0.02%	0.02%	0.04%	0.03%	0.02%	0.19%	0.14%	0.11%
Heat	0.00%	0.00%	0.00%	0.00%	0.00%	0.00%	0.00%	0.00%	0.00%
Sum	1.00E+00	1.00E+00	1.00E+00	1.00E+00	1.00E+00	1.00E+00	1.00E+00	1.00E+00	1.00E+00

	Australia			Global			Italy		
Terrestrial ecotoxicity	Sc1	Sc2	Sc3	Sc1	Sc2	Sc3	Sc1	Sc2	Sc3
Stack material	2.83%	5.42%	7.55%	2.43%	4.67%	6.52%	3.41%	6.48%	8.99%
BOP material	0.15%	0.11%	0.09%	0.12%	0.09%	0.07%	0.18%	0.13%	0.10%
Electriciy-operation	95.14%	93.07%	91.25%	95.61%	93.87%	92.31%	94.47%	91.94%	89.76%
Electriciy-Stack assembly	0.29%	0.22%	0.17%	0.29%	0.22%	0.17%	0.29%	0.21%	0.17%
Electriciy-BOP assembly	0.05%	0.03%	0.03%	0.05%	0.04%	0.03%	0.05%	0.03%	0.03%
Electriciy-pump	1.17%	0.87%	0.69%	1.17%	0.88%	0.70%	1.16%	0.86%	0.68%
Water	0.31%	0.23%	0.18%	0.26%	0.20%	0.16%	0.37%	0.27%	0.22%
Heat	0.07%	0.05%	0.04%	0.06%	0.04%	0.03%	0.08%	0.06%	0.05%
Sum	1.00E+00	1.00E+00	1.00E+00	1.00E+00	1.00E+00	1.00E+00	1.00E+00	1.00E+00	1.00E+00

	Australia			Global			Italy		
Freshwater ecotoxicity	Sc1	Sc2	Sc3	Sc1	Sc2	Sc3	Sc1	Sc2	Sc3
Stack material	12.88%	19.15%	24.32%	17.46%	25.31%	31.50%	54.85%	66.12%	72.62%
BOP material	0.06%	0.04%	0.03%	0.08%	0.06%	0.04%	0.27%	0.15%	0.10%
Electriciy-operation	85.63%	79.79%	74.88%	81.07%	73.67%	67.75%	43.88%	33.15%	26.90%
Electriciy-Stack assembly	0.26%	0.19%	0.14%	0.25%	0.17%	0.13%	0.13%	0.08%	0.05%
Electriciy-BOP assembly	0.04%	0.03%	0.02%	0.04%	0.03%	0.02%	0.02%	0.01%	0.01%
Electriciy-pump	1.05%	0.75%	0.57%	0.99%	0.69%	0.51%	0.54%	0.31%	0.20%
Water	0.07%	0.05%	0.04%	0.10%	0.07%	0.05%	0.30%	0.18%	0.11%
Heat	0.00%	0.00%	0.00%	0.00%	0.00%	0.00%	0.00%	0.00%	0.00%
Sum	1.00E+00	1.00E+00	1.00E+00	1.00E+00	1.00E+00	1.00E+00	1.00E+00	1.00E+00	1.00E+00

	Australia			Global			Italy		
Marine ecotoxicity	Sc1	Sc2	Sc3	Sc1	Sc2	Sc3	Sc1	Sc2	Sc3
Stack material	30.64%	49.58%	59.17%	34.82%	54.65%	64.18%	50.46%	71.16%	79.46%
BOP material	17.12%	10.12%	6.91%	19.46%	11.16%	7.49%	28.20%	14.53%	9.28%
Electriciy-operation	51.25%	39.71%	33.53%	44.82%	33.68%	27.98%	20.73%	14.00%	11.06%
Electriciy-Stack assembly	0.16%	0.09%	0.06%	0.14%	0.08%	0.05%	0.06%	0.03%	0.02%
Electriciy-BOP assembly	0.03%	0.01%	0.01%	0.02%	0.01%	0.01%	0.01%	0.01%	0.00%
Electriciy-pump	0.63%	0.37%	0.25%	0.55%	0.32%	0.21%	0.25%	0.13%	0.08%
Water	0.16%	0.10%	0.07%	0.19%	0.11%	0.07%	0.27%	0.14%	0.09%
Heat	0.01%	0.00%	0.00%	0.01%	0.00%	0.00%	0.01%	0.00%	0.00%
Sum	1.00E+00	1.00E+00	1.00E+00	1.00E+00	1.00E+00	1.00E+00	1.00E+00	1.00E+00	1.00E+00

	Australia			Global			Italy		
Human carcinogenic toxicity	Sc1	Sc2	Sc3	Sc1	Sc2	Sc3	Sc1	Sc2	Sc3
Stack material	28.08%	44.70%	53.22%	23.95%	39.45%	47.82%	19.08%	32.76%	40.64%
BOP material	1.25%	0.74%	0.51%	1.07%	0.66%	0.46%	0.85%	0.54%	0.39%
Electriciy-operation	68.98%	53.56%	45.58%	73.31%	58.88%	51.01%	78.42%	65.65%	58.22%
Electriciy-Stack assembly	0.21%	0.13%	0.09%	0.22%	0.14%	0.10%	0.24%	0.15%	0.11%
Electriciy-BOP assembly	0.03%	0.02%	0.01%	0.04%	0.02%	0.02%	0.04%	0.02%	0.02%
Electriciy-pump	0.85%	0.50%	0.34%	0.90%	0.55%	0.39%	0.96%	0.61%	0.44%
Water	0.56%	0.33%	0.23%	0.47%	0.29%	0.20%	0.38%	0.24%	0.17%
Heat	0.04%	0.02%	0.01%	0.03%	0.02%	0.01%	0.02%	0.02%	0.01%
Sum	1.00E+00	1.00E+00	1.00E+00	1.00E+00	1.00E+00	1.00E+00	1.00E+00	1.00E+00	1.00E+00

	Australia			Global			Italy		
Human non-carcinogenic toxicity	Sc1	Sc2	Sc3	Sc1	Sc2	Sc3	Sc1	Sc2	Sc3
Stack material	66.47%	82.32%	87.71%	52.69%	72.13%	79.77%	68.61%	83.72%	88.76%
BOP material	2.20%	0.91%	0.52%	1.74%	0.80%	0.47%	2.27%	0.92%	0.53%
Electriciy-operation	29.79%	16.14%	11.41%	44.02%	26.37%	19.34%	27.59%	14.73%	10.36%
Electriciy-Stack assembly	0.09%	0.04%	0.02%	0.13%	0.06%	0.04%	0.08%	0.03%	0.02%
Electriciy-BOP assembly	0.01%	0.01%	0.00%	0.02%	0.01%	0.01%	0.01%	0.01%	0.00%
Electriciy-pump	0.37%	0.15%	0.09%	0.54%	0.25%	0.15%	0.34%	0.14%	0.08%
Water	1.04%	0.43%	0.25%	0.83%	0.38%	0.22%	1.08%	0.44%	0.25%
Heat	0.02%	0.01%	0.01%	0.02%	0.01%	0.00%	0.02%	0.01%	0.01%
Sum	1.00E+00	1.00E+00	1.00E+00	1.00E+00	1.00E+00	1.00E+00	1.00E+00	1.00E+00	1.00E+00

	Australia			Global			Italy		
Land use	Sc1	Sc2	Sc3	Sc1	Sc2	Sc3	Sc1	Sc2	Sc3
Stack material	0.69%	1.56%	2.27%	0.94%	2.11%	3.07%	2.10%	4.66%	6.68%
BOP material	0.01%	0.01%	0.01%	0.02%	0.01%	0.01%	0.04%	0.03%	0.02%
Electriciy-operation	97.58%	97.12%	96.67%	97.27%	96.53%	95.84%	95.82%	93.79%	92.09%
Electriciy-Stack assembly	0.30%	0.23%	0.18%	0.30%	0.23%	0.18%	0.29%	0.22%	0.17%
Electriciy-BOP assembly	0.05%	0.04%	0.03%	0.05%	0.04%	0.03%	0.05%	0.04%	0.03%
Electriciy-pump	1.20%	0.91%	0.73%	1.19%	0.90%	0.73%	1.18%	0.88%	0.70%
Water	0.17%	0.13%	0.10%	0.23%	0.17%	0.14%	0.51%	0.38%	0.30%
Heat	0.01%	0.01%	0.00%	0.01%	0.01%	0.01%	0.02%	0.02%	0.01%

	Australia			Global			Italy		
Mineral resource scarcity	Sc1	Sc2	Sc3	Sc1	Sc2	Sc3	Sc1	Sc2	Sc3
Stack material	32.27%	57.22%	67.65%	30.18%	54.83%	65.49%	37.50%	62.76%	72.49%
BOP material	0.15%	0.07%	0.05%	0.14%	0.07%	0.04%	0.18%	0.08%	0.05%
Electriciy-operation	66.22%	42.04%	31.90%	68.30%	44.42%	34.05%	61.00%	36.55%	27.10%
Electriciy-Stack assembly	0.20%	0.10%	0.06%	0.21%	0.10%	0.06%	0.19%	0.09%	0.05%
Electriciy-BOP assembly	0.03%	0.02%	0.01%	0.03%	0.02%	0.01%	0.03%	0.01%	0.01%
Electriciy-pump	0.81%	0.39%	0.24%	0.84%	0.42%	0.26%	0.75%	0.34%	0.20%
Water	0.30%	0.15%	0.09%	0.28%	0.14%	0.09%	0.35%	0.16%	0.10%
Heat	0.01%	0.00%	0.00%	0.01%	0.00%	0.00%	0.01%	0.00%	0.00%
Sum	1.00E+00	1.00E+00	1.00E+00	1.00E+00	1.00E+00	1.00E+00	1.00E+00	1.00E+00	1.00E+00

	Australia			Global			Italy		
Fossil resource scarcity	Sc1	Sc2	Sc3	Sc1	Sc2	Sc3	Sc1	Sc2	Sc3
Stack material	0.21%	0.55%	0.85%	0.25%	0.66%	1.01%	0.27%	0.72%	1.10%
BOP material	0.00%	0.00%	0.00%	0.00%	0.00%	0.00%	0.00%	0.00%	0.00%
Electriciy-operation	97.84%	97.96%	97.95%	97.72%	97.79%	97.73%	97.66%	97.70%	97.62%
Electriciy-Stack assembly	0.30%	0.23%	0.19%	0.30%	0.23%	0.18%	0.30%	0.23%	0.18%
Electriciy-BOP assembly	0.05%	0.04%	0.03%	0.05%	0.04%	0.03%	0.05%	0.04%	0.03%
Electriciy-pump	1.20%	0.92%	0.74%	1.20%	0.92%	0.74%	1.20%	0.91%	0.74%
Water	0.05%	0.03%	0.03%	0.06%	0.04%	0.03%	0.06%	0.05%	0.04%
Heat	0.35%	0.27%	0.22%	0.43%	0.32%	0.26%	0.46%	0.35%	0.29%
Sum	1.00E+00	1.00E+00	1.00E+00	1.00E+00	1.00E+00	1.00E+00	1.00E+00	1.00E+00	1.00E+00

	Australia			Global			Italy		
Water consumption	Sc1	Sc2	Sc3	Sc1	Sc2	Sc3	Sc1	Sc2	Sc3
Stack material	0.01%	0.03%	0.04%	0.02%	0.04%	0.06%	0.04%	0.09%	0.13%
BOP material	0.00%	0.00%	0.00%	0.00%	0.00%	0.00%	0.00%	0.00%	0.00%
Electriciy-operation	97.70%	98.22%	98.54%	97.48%	98.04%	98.39%	96.18%	97.00%	97.50%
Electriciy-Stack assembly	0.30%	0.23%	0.19%	0.30%	0.23%	0.19%	0.29%	0.23%	0.18%
Electriciy-BOP assembly	0.05%	0.04%	0.03%	0.05%	0.04%	0.03%	0.05%	0.04%	0.03%
Electriciy-pump	1.20%	0.92%	0.75%	1.20%	0.92%	0.74%	1.18%	0.91%	0.74%
Water	0.73%	0.56%	0.46%	0.95%	0.73%	0.59%	2.24%	1.72%	1.40%
Heat	0.01%	0.00%	0.00%	0.01%	0.01%	0.00%	0.02%	0.01%	0.01%
Sum	1.00E+00	1.00E+00	1.00E+00	1.00E+00	1.00E+00	1.00E+00	1.00E+00	1.00E+00	1.00E+00

Quantities (Sc2-Sc4-Sc5)-supplementary data

	Australia			Global			Italy		
Global Warming	Sc4	Sc2	Sc5	Sc4	Sc2	Sc5	Sc4	Sc2	Sc5
Stack material	5.20E-02	1.72E-01	3.19E-01	5.20E-02	1.72E-01	3.19E-01	5.20E-02	1.72E-01	3.19E-01
BOP material	1.21E-03	1.21E-03	1.21E-03	1.21E-03	1.21E-03	1.21E-03	1.21E-03	1.21E-03	1.21E-03
Electriciy-operation	2.60E+01	2.60E+01	2.60E+01	2.08E+01	2.08E+01	2.08E+01	1.55E+01	1.55E+01	1.55E+01
Electriciy-Stack assembly	6.08E-02	6.08E-02	6.08E-02	4.85E-02	4.85E-02	4.85E-02	3.61E-02	3.61E-02	3.61E-02
Electriciy-BOP assembly	9.76E-03	9.76E-03	9.76E-03	7.78E-03	7.78E-03	7.78E-03	5.80E-03	5.80E-03	5.80E-03
Electriciy-pump	2.44E-01	2.44E-01	2.44E-01	1.94E-01	1.94E-01	1.94E-01	1.45E-01	1.45E-01	1.45E-01
Water	1.61E-02	1.61E-02	1.61E-02	1.61E-02	1.61E-02	1.61E-02	1.61E-02	1.61E-02	1.61E-02
Heat	6.79E-02	6.79E-02	6.79E-02	6.79E-02	6.79E-02	6.79E-02	6.79E-02	6.79E-02	6.79E-02
Sum	2.65E+01	2.66E+01	2.67E+01	2.11E+01	2.13E+01	2.14E+01	1.58E+01	1.59E+01	1.61E+01

	Australia			Global			Italy		
Stratospheric ozone depletion	Sc4	Sc2	Sc5	Sc4	Sc2	Sc5	Sc4	Sc2	Sc5
Stack material	6.691E-08	2.929E-07	5.726E-07	6.691E-08	2.929E-07	5.726E-07	6.691E-08	2.929E-07	5.726E-07
BOP material	4.115E-10	4.115E-10	4.115E-10	4.115E-10	4.115E-10	4.115E-10	4.115E-10	4.115E-10	4.115E-10
Electriciy-operation	7.884E-06	7.884E-06	7.884E-06	6.950E-06	6.950E-06	6.950E-06	7.110E-06	7.110E-06	7.110E-06
Electriciy-Stack assembly	1.843E-08	1.843E-08	1.843E-08	1.624E-08	1.624E-08	1.624E-08	1.662E-08	1.662E-08	1.662E-08
Electriciy-BOP assembly	2.956E-09	2.956E-09	2.956E-09	2.606E-09	2.606E-09	2.606E-09	2.666E-09	2.666E-09	2.666E-09
Electriciy-pump	7.378E-08	7.378E-08	7.378E-08	6.504E-08	6.504E-08	6.504E-08	6.654E-08	6.654E-08	6.654E-08
Water	7.597E-09	7.597E-09	7.597E-09	7.597E-09	7.597E-09	7.597E-09	7.597E-09	7.597E-09	7.597E-09
Heat	2.411E-09	2.411E-09	2.411E-09	2.411E-09	2.411E-09	2.411E-09	2.411E-09	2.411E-09	2.411E-09
Sum	8.06E-06	8.28E-06	8.56E-06	7.11E-06	7.34E-06	7.62E-06	7.27E-06	7.50E-06	7.78E-06

	Australia			Global			Italy		
Ionizing radiation	Sc4	Sc2	Sc5	Sc4	Sc2	Sc5	Sc4	Sc2	Sc5
Stack material	2.245E-03	7.107E-03	1.299E-02	2.245E-03	7.107E-03	1.299E-02	2.245E-03	7.107E-03	1.299E-02
BOP material	9.759E-05	9.759E-05	9.759E-05	9.759E-05	9.759E-05	9.759E-05	9.759E-05	9.759E-05	9.759E-05
Electriciy-operation	1.183E-01	1.183E-01	1.183E-01	5.230E+00	5.230E+00	5.230E+00	2.059E-02	2.059E-02	2.059E-02
Electriciy-Stack assembly	2.764E-04	2.764E-04	2.764E-04	1.222E-02	1.222E-02	1.222E-02	4.813E-05	4.813E-05	4.813E-05
Electriciy-BOP assembly	4.434E-05	4.434E-05	4.434E-05	1.961E-03	1.961E-03	1.961E-03	7.721E-06	7.721E-06	7.721E-06
Electriciy-pump	1.107E-03	1.107E-03	1.107E-03	4.894E-02	4.894E-02	4.894E-02	1.927E-04	1.927E-04	1.927E-04
Water	1.738E-05	1.738E-05	1.738E-05	1.738E-05	1.738E-05	1.738E-05	1.738E-05	1.738E-05	1.738E-05
Heat	1.997E-06	1.997E-06	1.997E-06	1.997E-06	1.997E-06	1.997E-06	1.997E-06	1.997E-06	1.997E-06
Sum	1.22E-01	1.27E-01	1.33E-01	5.30E+00	5.30E+00	5.31E+00	2.32E-02	2.81E-02	3.39E-02

	Australia			Global			Italy		
Ozone formation, Human health	Sc4	Sc2	Sc5	Sc4	Sc2	Sc5	Sc4	Sc2	Sc5
Stack material	4.363E-04	1.767E-03	3.484E-03	4.363E-04	1.767E-03	3.484E-03	4.363E-04	1.767E-03	3.484E-03
BOP material	3.023E-06	3.023E-06	3.023E-06	3.023E-06	3.023E-06	3.023E-06	3.023E-06	3.023E-06	3.023E-06
Electriciy-operation	6.680E-02	6.680E-02	6.680E-02	5.153E-02	5.153E-02	5.153E-02	2.975E-02	2.975E-02	2.975E-02
Electriciy-Stack assembly	1.561E-04	1.561E-04	1.561E-04	1.204E-04	1.204E-04	1.204E-04	6.954E-05	6.954E-05	6.954E-05
Electriciy-BOP assembly	2.505E-05	2.505E-05	2.505E-05	1.932E-05	1.932E-05	1.932E-05	1.116E-05	1.116E-05	1.116E-05
Electriciy-pump	6.252E-04	6.252E-04	6.252E-04	4.822E-04	4.822E-04	4.822E-04	2.785E-04	2.785E-04	2.785E-04
Water	4.475E-05	4.475E-05	4.475E-05	4.475E-05	4.475E-05	4.475E-05	4.475E-05	4.475E-05	4.475E-05
Heat	5.075E-04	5.075E-04	5.075E-04	5.075E-04	5.075E-04	5.075E-04	5.075E-04	5.075E-04	5.075E-04
Sum	6.86E-02	6.99E-02	7.16E-02	5.31E-02	5.45E-02	5.62E-02	3.11E-02	3.24E-02	3.42E-02

	Australia			Global			Italy		
Fine particulate matter formation	Sc4	Sc2	Sc5	Sc4	Sc2	Sc5	Sc4	Sc2	Sc5
Stack material	4.161E-04	1.775E-03	3.535E-03	4.161E-04	1.775E-03	3.535E-03	4.161E-04	1.775E-03	3.535E-03
BOP material	1.768E-06	1.768E-06	1.768E-06	1.768E-06	1.768E-06	1.768E-06	1.768E-06	1.768E-06	1.768E-06
Electriciy-operation	8.659E-03	8.659E-03	8.659E-03	8.481E-03	8.481E-03	8.481E-03	8.532E-03	8.532E-03	8.532E-03
Electriciy-Stack assembly	2.024E-05	2.024E-05	2.024E-05	1.982E-05	1.982E-05	1.982E-05	1.994E-05	1.994E-05	1.994E-05
Electriciy-BOP assembly	3.247E-06	3.247E-06	3.247E-06	3.180E-06	3.180E-06	3.180E-06	3.199E-06	3.199E-06	3.199E-06
Electriciy-pump	8.104E-05	8.104E-05	8.104E-05	7.937E-05	7.937E-05	7.937E-05	7.985E-05	7.985E-05	7.985E-05
Water	2.485E-05	2.485E-05	2.485E-05	2.485E-05	2.485E-05	2.485E-05	2.485E-05	2.485E-05	2.485E-05
Heat	5.708E-05	5.708E-05	5.708E-05	5.708E-05	5.708E-05	5.708E-05	5.708E-05	5.708E-05	5.708E-05
Sum	9.26E-03	1.06E-02	1.24E-02	9.08E-03	1.04E-02	1.22E-02	9.14E-03	1.05E-02	1.23E-02

	Australia			Global			Italy		
Ozone formation, Terrestrial ecosystems	Sc4	Sc2	Sc5	Sc4	Sc2	Sc5	Sc4	Sc2	Sc5
Stack material	4.452E-04	1.804E-03	3.559E-03	4.452E-04	1.804E-03	3.559E-03	4.452E-04	1.804E-03	3.559E-03
BOP material	3.129E-06	3.129E-06	3.129E-06	3.129E-06	3.129E-06	3.129E-06	3.129E-06	3.129E-06	3.129E-06
Electriciy-operation	6.687E-02	6.687E-02	6.687E-02	5.160E-02	5.160E-02	5.160E-02	2.988E-02	2.988E-02	2.988E-02
Electriciy-Stack assembly	1.563E-04	1.563E-04	1.563E-04	1.206E-04	1.206E-04	1.206E-04	6.982E-05	6.982E-05	6.982E-05
Electriciy-BOP assembly	2.507E-05	2.507E-05	2.507E-05	1.935E-05	1.935E-05	1.935E-05	1.120E-05	1.120E-05	1.120E-05
Electriciy-pump	6.258E-04	6.258E-04	6.258E-04	4.829E-04	4.829E-04	4.829E-04	2.796E-04	2.796E-04	2.796E-04
Water	4.478E-05	4.478E-05	4.478E-05	4.478E-05	4.478E-05	4.478E-05	4.478E-05	4.478E-05	4.478E-05
Heat	5.076E-04	5.076E-04	5.076E-04	5.076E-04	5.076E-04	5.076E-04	5.076E-04	5.076E-04	5.076E-04
Sum	6.87E-02	7.00E-02	7.18E-02	5.32E-02	5.46E-02	5.63E-02	3.12E-02	3.26E-02	3.44E-02

	Australia			Global			Italy		
Terrestrial acidification	Sc4	Sc2	Sc5	Sc4	Sc2	Sc5	Sc4	Sc2	Sc5
Stack material	1.374E-03	6.008E-03	1.204E-02	1.374E-03	6.008E-03	1.204E-02	1.374E-03	6.008E-03	1.204E-02
BOP material	5.090E-06	5.090E-06	5.090E-06	5.090E-06	5.090E-06	5.090E-06	5.090E-06	5.090E-06	5.090E-06
Electriciy-operation	1.172E-01	1.172E-01	1.172E-01	8.792E-02	8.792E-02	8.792E-02	3.580E-02	3.580E-02	3.580E-02
Electriciy-Stack assembly	2.739E-04	2.739E-04	2.739E-04	2.055E-04	2.055E-04	2.055E-04	8.367E-05	8.367E-05	8.367E-05
Electriciy-BOP assembly	4.395E-05	4.395E-05	4.395E-05	3.296E-05	3.296E-05	3.296E-05	1.342E-05	1.342E-05	1.342E-05
Electriciy-pump	1.097E-03	1.097E-03	1.097E-03	8.227E-04	8.227E-04	8.227E-04	3.350E-04	3.350E-04	3.350E-04
Water	8.037E-05	8.037E-05	8.037E-05	8.037E-05	8.037E-05	8.037E-05	8.037E-05	8.037E-05	8.037E-05
Heat	1.868E-04	1.868E-04	1.868E-04	1.868E-04	1.868E-04	1.868E-04	1.868E-04	1.868E-04	1.868E-04
Sum	1.20E-01	1.25E-01	1.31E-01	9.06E-02	9.53E-02	1.01E-01	3.79E-02	4.25E-02	4.85E-02

	Australia			Global			Italy		
Freshwater eutrophication	Sc4	Sc2	Sc5	Sc4	Sc2	Sc5	Sc4	Sc2	Sc5
Stack material	9.560E-05	2.315E-04	4.033E-04	9.560E-05	2.315E-04	4.033E-04	9.560E-05	2.315E-04	4.033E-04
BOP material	6.968E-07	6.968E-07	6.968E-07	6.968E-07	6.968E-07	6.968E-07	6.968E-07	6.968E-07	6.968E-07
Electriciy-operation	1.198E-02	1.198E-02	1.198E-02	8.189E-03	8.189E-03	8.189E-03	1.208E-03	1.208E-03	1.208E-03
Electriciy-Stack assembly	2.800E-05	2.800E-05	2.800E-05	1.914E-05	1.914E-05	1.914E-05	2.823E-06	2.823E-06	2.823E-06
Electriciy-BOP assembly	4.492E-06	4.492E-06	4.492E-06	3.070E-06	3.070E-06	3.070E-06	4.528E-07	4.528E-07	4.528E-07
Electriciy-pump	1.121E-04	1.121E-04	1.121E-04	7.663E-05	7.663E-05	7.663E-05	1.130E-05	1.130E-05	1.130E-05
Water	8.096E-07	8.096E-07	8.096E-07	8.096E-07	8.096E-07	8.096E-07	8.096E-07	8.096E-07	8.096E-07
Heat	1.631E-08	1.631E-08	1.631E-08	1.631E-08	1.631E-08	1.631E-08	1.631E-08	1.631E-08	1.631E-08
Sum	1.22E-02	1.24E-02	1.25E-02	8.38E-03	8.52E-03	8.69E-03	1.32E-03	1.46E-03	1.63E-03

	Australia			Global			Italy		
Marine eutrophication	Sc4	Sc2	Sc5	Sc4	Sc2	Sc5	Sc4	Sc2	Sc5
Stack material	2.208E-06	7.023E-06	1.309E-05	2.208E-06	7.023E-06	1.309E-05	2.208E-06	7.023E-06	1.309E-05
BOP material	3.701E-08	3.701E-08	3.701E-08	3.701E-08	3.701E-08	3.701E-08	3.701E-08	3.701E-08	3.701E-08
Electriciy-operation	8.031E-04	8.031E-04	8.031E-04	5.735E-04	5.735E-04	5.735E-04	1.152E-04	1.152E-04	1.152E-04
Electriciy-Stack assembly	1.877E-06	1.877E-06	1.877E-06	1.340E-06	1.340E-06	1.340E-06	2.691E-07	2.691E-07	2.691E-07
Electriciy-BOP assembly	3.011E-07	3.011E-07	3.011E-07	2.150E-07	2.150E-07	2.150E-07	4.318E-08	4.318E-08	4.318E-08
Electriciy-pump	7.516E-06	7.516E-06	7.516E-06	5.367E-06	5.367E-06	5.367E-06	1.078E-06	1.078E-06	1.078E-06
Water	1.733E-07	1.733E-07	1.733E-07	1.733E-07	1.733E-07	1.733E-07	1.733E-07	1.733E-07	1.733E-07
Heat	1.556E-09	1.556E-09	1.556E-09	1.556E-09	1.556E-09	1.556E-09	1.556E-09	1.556E-09	1.556E-09
Sum	8.15E-04	8.20E-04	8.26E-04	5.83E-04	5.88E-04	5.94E-04	1.19E-04	1.24E-04	1.30E-04

	Australia			Global			Italy		
Terrestrial ecotoxicity	Sc4	Sc2	Sc5	Sc4	Sc2	Sc5	Sc4	Sc2	Sc5
Stack material	1.779E-01	4.558E-01	8.011E-01	1.779E-01	4.558E-01	8.011E-01	1.779E-01	4.558E-01	8.011E-01
BOP material	9.142E-03	9.142E-03	9.142E-03	9.142E-03	9.142E-03	9.142E-03	9.142E-03	9.142E-03	9.142E-03
Electriciy-operation	7.827E+00	7.827E+00	7.827E+00	9.168E+00	9.168E+00	9.168E+00	6.463E+00	6.463E+00	6.463E+00
Electriciy-Stack assembly	1.829E-02	1.829E-02	1.829E-02	2.143E-02	2.143E-02	2.143E-02	1.510E-02	1.510E-02	1.510E-02
Electriciy-BOP assembly	2.934E-03	2.934E-03	2.934E-03	3.437E-03	3.437E-03	3.437E-03	2.423E-03	2.423E-03	2.423E-03
Electriciy-pump	7.324E-02	7.324E-02	7.324E-02	8.579E-02	8.579E-02	8.579E-02	6.048E-02	6.048E-02	6.048E-02
Water	1.921E-02	1.921E-02	1.921E-02	1.921E-02	1.921E-02	1.921E-02	1.921E-02	1.921E-02	1.921E-02
Heat	4.283E-03	4.283E-03	4.283E-03	4.283E-03	4.283E-03	4.283E-03	4.283E-03	4.283E-03	4.283E-03
Sum	8.13E+00	8.41E+00	8.75E+00	9.49E+00	9.77E+00	1.01E+01	6.75E+00	7.03E+00	7.37E+00

	Australia			Global			Italy		
Freshwater ecotoxicity	Sc4	Sc2	Sc5	Sc4	Sc2	Sc5	Sc4	Sc2	Sc5
Stack material	4.445E-02	9.296E-02	1.556E-01	4.445E-02	9.296E-02	1.556E-01	4.445E-02	9.296E-02	1.556E-01
BOP material	2.157E-04	2.157E-04	2.157E-04	2.157E-04	2.157E-04	2.157E-04	2.157E-04	2.157E-04	2.157E-04
Electriciy-operation	3.873E-01	3.873E-01	3.873E-01	2.706E-01	2.706E-01	2.706E-01	4.661E-02	4.661E-02	4.661E-02
Electriciy-Stack assembly	9.051E-04	9.051E-04	9.051E-04	6.323E-04	6.323E-04	6.323E-04	1.089E-04	1.089E-04	1.089E-04
Electriciy-BOP assembly	1.452E-04	1.452E-04	1.452E-04	1.014E-04	1.014E-04	1.014E-04	1.748E-05	1.748E-05	1.748E-05
Electriciy-pump	3.624E-03	3.624E-03	3.624E-03	2.532E-03	2.532E-03	2.532E-03	4.362E-04	4.362E-04	4.362E-04
Water	2.461E-04	2.461E-04	2.461E-04	2.461E-04	2.461E-04	2.461E-04	2.461E-04	2.461E-04	2.461E-04
Heat	2.724E-06	2.724E-06	2.724E-06	2.724E-06	2.724E-06	2.724E-06	2.724E-06	2.724E-06	2.724E-06
Sum	4.37E-01	4.85E-01	5.48E-01	3.19E-01	3.67E-01	4.30E-01	9.21E-02	1.41E-01	2.03E-01

	Australia			Global			Italy		
Marine ecotoxicity	Sc4	Sc2	Sc5	Sc4	Sc2	Sc5	Sc4	Sc2	Sc5
Stack material	6.502E-02	1.780E-01	3.112E-01	6.502E-02	1.780E-01	3.112E-01	6.502E-02	1.780E-01	3.112E-01
BOP material	3.634E-02	3.634E-02	3.634E-02	3.634E-02	3.634E-02	3.634E-02	3.634E-02	3.634E-02	3.634E-02
Electriciy-operation	1.426E-01	1.426E-01	1.426E-01	1.097E-01	1.097E-01	1.097E-01	3.502E-02	3.502E-02	3.502E-02
Electriciy-Stack assembly	3.332E-04	3.332E-04	3.332E-04	2.564E-04	2.564E-04	2.564E-04	8.185E-05	8.185E-05	8.185E-05
Electriciy-BOP assembly	5.345E-05	5.345E-05	5.345E-05	4.113E-05	4.113E-05	4.113E-05	1.313E-05	1.313E-05	1.313E-05
Electriciy-pump	1.334E-03	1.334E-03	1.334E-03	1.027E-03	1.027E-03	1.027E-03	3.278E-04	3.278E-04	3.278E-04
Water	3.491E-04	3.491E-04	3.491E-04	3.491E-04	3.491E-04	3.491E-04	3.491E-04	3.491E-04	3.491E-04
Heat	1.129E-05	1.129E-05	1.129E-05	1.129E-05	1.129E-05	1.129E-05	1.129E-05	1.129E-05	1.129E-05
Sum	2.46E-01	3.59E-01	4.92E-01	2.13E-01	3.26E-01	4.59E-01	1.37E-01	2.50E-01	3.83E-01

	Australia			Global			Italy		
Human carcinogenic toxicity	Sc4	Sc2	Sc5	Sc4	Sc2	Sc5	Sc4	Sc2	Sc5
Stack material	1.479E-02	3.975E-02	6.879E-02	1.479E-02	3.975E-02	6.879E-02	1.479E-02	3.975E-02	6.879E-02
BOP material	6.604E-04	6.604E-04	6.604E-04	6.604E-04	6.604E-04	6.604E-04	6.604E-04	6.604E-04	6.604E-04
Electriciy-operation	4.762E-02	4.762E-02	4.762E-02	5.932E-02	5.932E-02	5.932E-02	7.965E-02	7.965E-02	7.965E-02
Electriciy-Stack assembly	1.113E-04	1.113E-04	1.113E-04	1.386E-04	1.386E-04	1.386E-04	1.861E-04	1.861E-04	1.861E-04
Electriciy-BOP assembly	1.785E-05	1.785E-05	1.785E-05	2.224E-05	2.224E-05	2.224E-05	2.986E-05	2.986E-05	2.986E-05
Electriciy-pump	4.456E-04	4.456E-04	4.456E-04	5.551E-04	5.551E-04	5.551E-04	7.454E-04	7.454E-04	7.454E-04
Water	2.932E-04	2.932E-04	2.932E-04	2.932E-04	2.932E-04	2.932E-04	2.932E-04	2.932E-04	2.932E-04
Heat	1.857E-05	1.857E-05	1.857E-05	1.857E-05	1.857E-05	1.857E-05	1.857E-05	1.857E-05	1.857E-05
Sum	6.40E-02	8.89E-02	1.18E-01	7.58E-02	1.01E-01	1.30E-01	9.64E-02	1.21E-01	1.50E-01

	Australia			Global			Italy		
Human non-carcinogenic toxicity	Sc4	Sc2	Sc5	Sc4	Sc2	Sc5	Sc4	Sc2	Sc5
Stack material	9.741E-01	2.919E+00	5.443E+00	9.741E-01	2.919E+00	5.443E+00	9.741E-01	2.919E+00	5.443E+00
BOP material	3.221E-02	3.221E-02	3.221E-02	3.221E-02	3.221E-02	3.221E-02	3.221E-02	3.221E-02	3.221E-02
Electriciy-operation	5.723E-01	5.723E-01	5.723E-01	1.067E+00	1.067E+00	1.067E+00	5.134E-01	5.134E-01	5.134E-01
Electriciy-Stack assembly	1.337E-03	1.337E-03	1.337E-03	2.493E-03	2.493E-03	2.493E-03	1.200E-03	1.200E-03	1.200E-03
Electriciy-BOP assembly	2.146E-04	2.146E-04	2.146E-04	4.000E-04	4.000E-04	4.000E-04	1.925E-04	1.925E-04	1.925E-04
Electriciy-pump	5.355E-03	5.355E-03	5.355E-03	9.983E-03	9.983E-03	9.983E-03	4.804E-03	4.804E-03	4.804E-03
Water	1.529E-02	1.529E-02	1.529E-02	1.529E-02	1.529E-02	1.529E-02	1.529E-02	1.529E-02	1.529E-02
Heat	3.321E-04	3.321E-04	3.321E-04	3.321E-04	3.321E-04	3.321E-04	3.321E-04	3.321E-04	3.321E-04
Sum	1.60E+00	3.55E+00	6.07E+00	2.10E+00	4.05E+00	6.57E+00	1.54E+00	3.49E+00	6.01E+00

	Australia			Global			Italy		
Land use	Sc4	Sc2	Sc5	Sc4	Sc2	Sc5	Sc4	Sc2	Sc5
Stack material	2.085E-03	6.204E-03	1.121E-02	2.085E-03	6.204E-03	1.121E-02	2.085E-03	6.204E-03	1.121E-02
BOP material	3.554E-05	3.554E-05	3.554E-05	3.554E-05	3.554E-05	3.554E-05	3.554E-05	3.554E-05	3.554E-05
Electriciy-operation	3.856E-01	3.856E-01	3.856E-01	2.833E-01	2.833E-01	2.833E-01	1.250E-01	1.250E-01	1.250E-01
Electriciy-Stack assembly	9.012E-04	9.012E-04	9.012E-04	6.621E-04	6.621E-04	6.621E-04	2.921E-04	2.921E-04	2.921E-04
Electriciy-BOP assembly	1.446E-04	1.446E-04	1.446E-04	1.062E-04	1.062E-04	1.062E-04	4.686E-05	4.686E-05	4.686E-05
Electriciy-pump	3.609E-03	3.609E-03	3.609E-03	2.651E-03	2.651E-03	2.651E-03	1.170E-03	1.170E-03	1.170E-03
Water	5.054E-04	5.054E-04	5.054E-04	5.054E-04	5.054E-04	5.054E-04	5.054E-04	5.054E-04	5.054E-04
Heat	2.321E-05	2.321E-05	2.321E-05	2.321E-05	2.321E-05	2.321E-05	2.321E-05	2.321E-05	2.321E-05
Sum	3.93E-01	3.97E-01	4.02E-01	2.89E-01	2.93E-01	2.99E-01	1.29E-01	1.33E-01	1.38E-01

	Australia			Global			Italy		
Mineral resource scarcity	Sc4	Sc2	Sc5	Sc4	Sc2	Sc5	Sc4	Sc2	Sc5
Stack material	4.591E-03	1.681E-02	3.240E-02	4.591E-03	1.681E-02	3.240E-02	4.591E-03	1.681E-02	3.240E-02
BOP material	2.169E-05	2.169E-05	2.169E-05	2.169E-05	2.169E-05	2.169E-05	2.169E-05	2.169E-05	2.169E-05
Electriciy-operation	1.235E-02	1.235E-02	1.235E-02	1.362E-02	1.362E-02	1.362E-02	9.790E-03	9.790E-03	9.790E-03
Electriciy-Stack assembly	2.887E-05	2.887E-05	2.887E-05	3.183E-05	3.183E-05	3.183E-05	2.288E-05	2.288E-05	2.288E-05
Electriciy-BOP assembly	4.631E-06	4.631E-06	4.631E-06	5.106E-06	5.106E-06	5.106E-06	3.670E-06	3.670E-06	3.670E-06
Electriciy-pump	1.156E-04	1.156E-04	1.156E-04	1.274E-04	1.274E-04	1.274E-04	9.161E-05	9.161E-05	9.161E-05
Water	4.323E-05	4.323E-05	4.323E-05	4.323E-05	4.323E-05	4.323E-05	4.323E-05	4.323E-05	4.323E-05
Heat	1.272E-06	1.272E-06	1.272E-06	1.272E-06	1.272E-06	1.272E-06	1.272E-06	1.272E-06	1.272E-06
Sum	1.72E-02	2.94E-02	4.50E-02	1.84E-02	3.07E-02	4.63E-02	1.46E-02	2.68E-02	4.24E-02

	Australia			Global			Italy		
Fossil resource scarcity	Sc4	Sc2	Sc5	Sc4	Sc2	Sc5	Sc4	Sc2	Sc5
Stack material	1.449E-02	5.083E-02	9.625E-02	1.449E-02	5.083E-02	9.625E-02	1.449E-02	5.083E-02	9.625E-02
BOP material	2.644E-04	2.644E-04	2.644E-04	2.644E-04	2.644E-04	2.644E-04	2.644E-04	2.644E-04	2.644E-04
Electriciy-operation	9.015E+00	9.015E+00	9.015E+00	7.493E+00	7.493E+00	7.493E+00	6.887E+00	6.887E+00	6.887E+00
Electriciy-Stack assembly	2.107E-02	2.107E-02	2.107E-02	1.751E-02	1.751E-02	1.751E-02	1.609E-02	1.609E-02	1.609E-02
Electriciy-BOP assembly	3.380E-03	3.380E-03	3.380E-03	2.809E-03	2.809E-03	2.809E-03	2.582E-03	2.582E-03	2.582E-03
Electriciy-pump	8.437E-02	8.437E-02	8.437E-02	7.012E-02	7.012E-02	7.012E-02	6.445E-02	6.445E-02	6.445E-02
Water	3.221E-03	3.221E-03	3.221E-03	3.221E-03	3.221E-03	3.221E-03	3.221E-03	3.221E-03	3.221E-03
Heat	2.489E-02	2.489E-02	2.489E-02	2.489E-02	2.489E-02	2.489E-02	2.489E-02	2.489E-02	2.489E-02
Sum	9.17E+00	9.20E+00	9.25E+00	7.63E+00	7.66E+00	7.71E+00	7.01E+00	7.05E+00	7.09E+00

	Australia			Global			Italy		
Water consumption	Sc4	Sc2	Sc5	Sc4	Sc2	Sc5	Sc4	Sc2	Sc5
Stack material	3.610E-04	1.117E-03	2.031E-03	3.610E-04	1.117E-03	2.031E-03	3.610E-04	1.117E-03	2.031E-03
BOP material	2.081E-05	2.081E-05	2.081E-05	2.081E-05	2.081E-05	2.081E-05	2.081E-05	2.081E-05	2.081E-05
Electriciy-operation	3.769E+00	3.769E+00	3.769E+00	2.896E+00	2.896E+00	2.896E+00	1.214E+00	1.214E+00	1.214E+00
Electriciy-Stack assembly	8.809E-03	8.809E-03	8.809E-03	6.768E-03	6.768E-03	6.768E-03	2.838E-03	2.838E-03	2.838E-03
Electriciy-BOP assembly	1.413E-03	1.413E-03	1.413E-03	1.086E-03	1.086E-03	1.086E-03	4.553E-04	4.553E-04	4.553E-04
Electriciy-pump	3.527E-02	3.527E-02	3.527E-02	2.710E-02	2.710E-02	2.710E-02	1.137E-02	1.137E-02	1.137E-02
Water	2.158E-02	2.158E-02	2.158E-02	2.158E-02	2.158E-02	2.158E-02	2.158E-02	2.158E-02	2.158E-02
Heat	1.530E-04	1.530E-04	1.530E-04	1.530E-04	1.530E-04	1.530E-04	1.530E-04	1.530E-04	1.530E-04
Sum	3.84E+00	3.84E+00	3.84E+00	2.95E+00	2.95E+00	2.95E+00	1.25E+00	1.25E+00	1.25E+00

Percentage (Sc2-Sc4-Sc5)-supplementary data

	Australia			Global			Italy		
Global Warming	Sc4	Sc2	Sc5	Sc4	Sc2	Sc5	Sc4	Sc2	Sc5
Stack material	0.20%	0.65%	1.19%	0.25%	0.81%	1.49%	0.33%	1.08%	1.98%
BOP material	0.00%	0.00%	0.00%	0.01%	0.01%	0.01%	0.01%	0.01%	0.01%
Electriciy-operation	98.30%	97.85%	97.32%	98.17%	97.61%	96.94%	97.95%	97.21%	96.32%
Electriciy-Stack assembly	0.23%	0.23%	0.23%	0.23%	0.23%	0.23%	0.23%	0.23%	0.23%
Electriciy-BOP assembly	0.04%	0.04%	0.04%	0.04%	0.04%	0.04%	0.04%	0.04%	0.04%
Electriciy-pump	0.92%	0.92%	0.91%	0.92%	0.91%	0.91%	0.92%	0.91%	0.90%
Water	0.06%	0.06%	0.06%	0.08%	0.08%	0.08%	0.10%	0.10%	0.10%
Heat	0.26%	0.26%	0.25%	0.32%	0.32%	0.32%	0.43%	0.43%	0.42%
Sum	1.00E+00	1.00E+00	1.00E+00	1.00E+00	1.00E+00	1.00E+00	1.00E+00	1.00E+00	1.00E+00

	Australia			Global			Italy		
Stratospheric ozone depletion	Sc4	Sc2	Sc5	Sc4	Sc2	Sc5	Sc4	Sc2	Sc5
Stack material	0.83%	3.54%	6.69%	0.94%	3.99%	7.52%	0.92%	3.91%	7.36%
BOP material	0.01%	0.00%	0.00%	0.01%	0.01%	0.01%	0.01%	0.01%	0.01%
Electriciy-operation	97.86%	95.19%	92.08%	97.73%	94.72%	91.24%	97.76%	94.81%	91.40%
Electriciy-Stack assembly	0.23%	0.22%	0.22%	0.23%	0.22%	0.21%	0.23%	0.22%	0.21%
Electriciy-BOP assembly	0.04%	0.04%	0.03%	0.04%	0.04%	0.03%	0.04%	0.04%	0.03%
Electriciy-pump	0.92%	0.89%	0.86%	0.91%	0.89%	0.85%	0.91%	0.89%	0.86%
Water	0.09%	0.09%	0.09%	0.11%	0.10%	0.10%	0.10%	0.10%	0.10%
Heat	0.03%	0.03%	0.03%	0.03%	0.03%	0.03%	0.03%	0.03%	0.03%
Sum	1.00E+00	1.00E+00	1.00E+00	1.00E+00	1.00E+00	1.00E+00	1.00E+00	1.00E+00	1.00E+00

	Australia			Global			Italy		
Ionizing radiation	Sc4	Sc2	Sc5	Sc4	Sc2	Sc5	Sc4	Sc2	Sc5
Stack material	1.84%	5.60%	9.78%	0.04%	0.13%	0.24%	9.67%	25.32%	38.26%
BOP material	0.08%	0.08%	0.07%	0.00%	0.00%	0.00%	0.42%	0.35%	0.29%
Electriciy-operation	96.90%	93.18%	89.06%	98.76%	98.67%	98.56%	88.75%	73.37%	60.67%
Electriciy-Stack assembly	0.23%	0.22%	0.21%	0.23%	0.23%	0.23%	0.21%	0.17%	0.14%
Electriciy-BOP assembly	0.04%	0.03%	0.03%	0.04%	0.04%	0.04%	0.03%	0.03%	0.02%
Electriciy-pump	0.91%	0.87%	0.83%	0.92%	0.92%	0.92%	0.83%	0.69%	0.57%
Water	0.01%	0.01%	0.01%	0.00%	0.00%	0.00%	0.07%	0.06%	0.05%
Heat	0.00%	0.00%	0.00%	0.00%	0.00%	0.00%	0.01%	0.01%	0.01%
Sum	1.00E+00	1.00E+00	1.00E+00	1.00E+00	1.00E+00	1.00E+00	1.00E+00	1.00E+00	1.00E+00

	Australia			Global			Italy		
Ozone formation, Human health	Sc4	Sc2	Sc5	Sc4	Sc2	Sc5	Sc4	Sc2	Sc5
Stack material	0.64%	2.53%	4.86%	0.82%	3.24%	6.20%	1.40%	5.45%	10.20%
BOP material	0.00%	0.00%	0.00%	0.01%	0.01%	0.01%	0.01%	0.01%	0.01%
Electriciy-operation	97.38%	95.53%	93.24%	96.96%	94.60%	91.70%	95.66%	91.73%	87.12%
Electriciy-Stack assembly	0.23%	0.22%	0.22%	0.23%	0.22%	0.21%	0.22%	0.21%	0.20%
Electriciy-BOP assembly	0.04%	0.04%	0.03%	0.04%	0.04%	0.03%	0.04%	0.03%	0.03%
Electriciy-pump	0.91%	0.89%	0.87%	0.91%	0.89%	0.86%	0.90%	0.86%	0.82%
Water	0.07%	0.06%	0.06%	0.08%	0.08%	0.08%	0.14%	0.14%	0.13%
Heat	0.74%	0.73%	0.71%	0.95%	0.93%	0.90%	1.63%	1.56%	1.49%
Sum	1.00E+00	1.00E+00	1.00E+00	1.00E+00	1.00E+00	1.00E+00	1.00E+00	1.00E+00	1.00E+00

	Australia			Global			Italy		
Fine particulate matter formation	Sc4	Sc2	Sc5	Sc4	Sc2	Sc5	Sc4	Sc2	Sc5
Stack material	4.49%	16.71%	28.55%	4.58%	17.00%	28.97%	4.55%	16.91%	28.85%
BOP material	0.02%	0.02%	0.01%	0.02%	0.02%	0.01%	0.02%	0.02%	0.01%
Electriciy-operation	93.48%	81.52%	69.93%	93.37%	81.22%	69.50%	93.40%	81.31%	69.63%
Electriciy-Stack assembly	0.22%	0.19%	0.16%	0.22%	0.19%	0.16%	0.22%	0.19%	0.16%
Electriciy-BOP assembly	0.04%	0.03%	0.03%	0.04%	0.03%	0.03%	0.04%	0.03%	0.03%
Electriciy-pump	0.87%	0.76%	0.65%	0.87%	0.76%	0.65%	0.87%	0.76%	0.65%
Water	0.27%	0.23%	0.20%	0.27%	0.24%	0.20%	0.27%	0.24%	0.20%
Heat	0.62%	0.54%	0.46%	0.63%	0.55%	0.47%	0.62%	0.54%	0.47%
Sum	1.00E+00	1.00E+00	1.00E+00	1.00E+00	1.00E+00	1.00E+00	1.00E+00	1.00E+00	1.00E+00

	Australia			Global			Italy		
Ozone formation, Terrestrial ecosystems	Sc4	Sc2	Sc5	Sc4	Sc2	Sc5	Sc4	Sc2	Sc5
Stack material	0.65%	2.58%	4.96%	0.84%	3.30%	6.32%	1.43%	5.53%	10.36%
BOP material	0.00%	0.00%	0.00%	0.01%	0.01%	0.01%	0.01%	0.01%	0.01%
Electriciy-operation	97.37%	95.48%	93.15%	96.95%	94.54%	91.59%	95.64%	91.66%	86.97%
Electriciy-Stack assembly	0.23%	0.22%	0.22%	0.23%	0.22%	0.21%	0.22%	0.21%	0.20%
Electriciy-BOP assembly	0.04%	0.04%	0.03%	0.04%	0.04%	0.03%	0.04%	0.03%	0.03%
Electriciy-pump	0.91%	0.89%	0.87%	0.91%	0.88%	0.86%	0.90%	0.86%	0.81%
Water	0.07%	0.06%	0.06%	0.08%	0.08%	0.08%	0.14%	0.14%	0.13%
Heat	0.74%	0.72%	0.71%	0.95%	0.93%	0.90%	1.62%	1.56%	1.48%
Sum	1.00E+00	1.00E+00	1.00E+00	1.00E+00	1.00E+00	1.00E+00	1.00E+00	1.00E+00	1.00E+00

	Australia			Global			Italy		
Terrestrial acidification	Sc4	Sc2	Sc5	Sc4	Sc2	Sc5	Sc4	Sc2	Sc5
Stack material	1.14%	4.81%	9.19%	1.52%	6.31%	11.88%	3.63%	14.13%	24.79%
BOP material	0.00%	0.00%	0.00%	0.01%	0.01%	0.01%	0.01%	0.01%	0.01%
Electriciy-operation	97.46%	93.84%	89.52%	97.01%	92.29%	86.80%	94.51%	84.21%	73.76%
Electriciy-Stack assembly	0.23%	0.22%	0.21%	0.23%	0.22%	0.20%	0.22%	0.20%	0.17%
Electriciy-BOP assembly	0.04%	0.04%	0.03%	0.04%	0.03%	0.03%	0.04%	0.03%	0.03%
Electriciy-pump	0.91%	0.88%	0.84%	0.91%	0.86%	0.81%	0.88%	0.79%	0.69%
Water	0.07%	0.06%	0.06%	0.09%	0.08%	0.08%	0.21%	0.19%	0.17%
Heat	0.16%	0.15%	0.14%	0.21%	0.20%	0.18%	0.49%	0.44%	0.38%
Sum	1.00E+00	1.00E+00	1.00E+00	1.00E+00	1.00E+00	1.00E+00	1.00E+00	1.00E+00	1.00E+00

	Australia			Global			Italy		
Freshwater eutrophication	Sc4	Sc2	Sc5	Sc4	Sc2	Sc5	Sc4	Sc2	Sc5
Stack material	0.78%	1.87%	3.22%	1.14%	2.72%	4.64%	7.25%	15.91%	24.79%
BOP material	0.01%	0.01%	0.01%	0.01%	0.01%	0.01%	0.05%	0.05%	0.04%
Electriciy-operation	98.02%	96.94%	95.62%	97.66%	96.10%	94.21%	91.53%	82.98%	74.23%
Electriciy-Stack assembly	0.23%	0.23%	0.22%	0.23%	0.22%	0.22%	0.21%	0.19%	0.17%
Electriciy-BOP assembly	0.04%	0.04%	0.04%	0.04%	0.04%	0.04%	0.03%	0.03%	0.03%
Electriciy-pump	0.92%	0.91%	0.89%	0.91%	0.90%	0.88%	0.86%	0.78%	0.69%
Water	0.01%	0.01%	0.01%	0.01%	0.01%	0.01%	0.06%	0.06%	0.05%
Heat	0.00%	0.00%	0.00%	0.00%	0.00%	0.00%	0.00%	0.00%	0.00%
Sum	1.00E+00	1.00E+00	1.00E+00	1.00E+00	1.00E+00	1.00E+00	1.00E+00	1.00E+00	1.00E+00

	Australia			Global			Italy		
Marine eutrophication	Sc4	Sc2	Sc5	Sc4	Sc2	Sc5	Sc4	Sc2	Sc5
Stack material	0.27%	0.86%	1.58%	0.38%	1.20%	2.20%	1.86%	5.67%	10.08%
BOP material	0.00%	0.00%	0.00%	0.01%	0.01%	0.01%	0.03%	0.03%	0.03%
Electriciy-operation	98.51%	97.94%	97.22%	98.40%	97.59%	96.59%	96.80%	93.03%	88.69%
Electriciy-Stack assembly	0.23%	0.23%	0.23%	0.23%	0.23%	0.23%	0.23%	0.22%	0.21%
Electriciy-BOP assembly	0.04%	0.04%	0.04%	0.04%	0.04%	0.04%	0.04%	0.03%	0.03%
Electriciy-pump	0.92%	0.92%	0.91%	0.92%	0.91%	0.90%	0.91%	0.87%	0.83%
Water	0.02%	0.02%	0.02%	0.03%	0.03%	0.03%	0.15%	0.14%	0.13%
Heat	0.00%	0.00%	0.00%	0.00%	0.00%	0.00%	0.00%	0.00%	0.00%
Sum	1.00E+00	1.00E+00	1.00E+00	1.00E+00	1.00E+00	1.00E+00	1.00E+00	1.00E+00	1.00E+00

	Australia			Global			Italy		
Terrestrial ecotoxicity	Sc4	Sc2	Sc5	Sc4	Sc2	Sc5	Sc4	Sc2	Sc5
Stack material	2.19%	5.42%	9.15%	1.87%	4.67%	7.92%	2.63%	6.48%	10.86%
BOP material	0.11%	0.11%	0.10%	0.10%	0.09%	0.09%	0.14%	0.13%	0.12%
Electriciy-operation	96.25%	93.07%	89.40%	96.62%	93.87%	90.66%	95.73%	91.94%	87.64%
Electriciy-Stack assembly	0.22%	0.22%	0.21%	0.23%	0.22%	0.21%	0.22%	0.21%	0.20%
Electriciy-BOP assembly	0.04%	0.03%	0.03%	0.04%	0.04%	0.03%	0.04%	0.03%	0.03%
Electriciy-pump	0.90%	0.87%	0.84%	0.90%	0.88%	0.85%	0.90%	0.86%	0.82%
Water	0.24%	0.23%	0.22%	0.20%	0.20%	0.19%	0.28%	0.27%	0.26%
Heat	0.05%	0.05%	0.05%	0.05%	0.04%	0.04%	0.06%	0.06%	0.06%
Sum	1.00E+00	1.00E+00	1.00E+00	1.00E+00	1.00E+00	1.00E+00	1.00E+00	1.00E+00	1.00E+00

	Australia			Global			Italy		
Freshwater ecotoxicity	Sc4	Sc2	Sc5	Sc4	Sc2	Sc5	Sc4	Sc2	Sc5
Stack material	10.18%	19.15%	28.40%	13.95%	25.31%	36.20%	48.27%	66.12%	76.56%
BOP material	0.05%	0.04%	0.04%	0.07%	0.06%	0.05%	0.23%	0.15%	0.11%
Electriciy-operation	88.65%	79.79%	70.67%	84.88%	73.67%	62.93%	50.61%	33.15%	22.93%
Electriciy-Stack assembly	0.21%	0.19%	0.17%	0.20%	0.17%	0.15%	0.12%	0.08%	0.05%
Electriciy-BOP assembly	0.03%	0.03%	0.03%	0.03%	0.03%	0.02%	0.02%	0.01%	0.01%
Electriciy-pump	0.83%	0.75%	0.66%	0.79%	0.69%	0.59%	0.47%	0.31%	0.21%
Water	0.06%	0.05%	0.04%	0.08%	0.07%	0.06%	0.27%	0.18%	0.12%
Heat	0.00%	0.00%	0.00%	0.00%	0.00%	0.00%	0.00%	0.00%	0.00%
Sum	1.00E+00	1.00E+00	1.00E+00	1.00E+00	1.00E+00	1.00E+00	1.00E+00	1.00E+00	1.00E+00

	Australia			Global			Italy		
Marine ecotoxicity	Sc4	Sc2	Sc5	Sc4	Sc2	Sc5	Sc4	Sc2	Sc5
Stack material	26.43%	49.58%	63.23%	30.56%	54.65%	67.81%	47.40%	71.16%	81.18%
BOP material	14.77%	10.12%	7.38%	17.08%	11.16%	7.92%	26.49%	14.53%	9.48%
Electriciy-operation	57.95%	39.71%	28.96%	51.56%	33.68%	23.90%	25.53%	14.00%	9.14%
Electriciy-Stack assembly	0.14%	0.09%	0.07%	0.12%	0.08%	0.06%	0.06%	0.03%	0.02%
Electriciy-BOP assembly	0.02%	0.01%	0.01%	0.02%	0.01%	0.01%	0.01%	0.01%	0.00%
Electriciy-pump	0.54%	0.37%	0.27%	0.48%	0.32%	0.22%	0.24%	0.13%	0.09%
Water	0.14%	0.10%	0.07%	0.16%	0.11%	0.08%	0.25%	0.14%	0.09%
Heat	0.00%	0.00%	0.00%	0.01%	0.00%	0.00%	0.01%	0.00%	0.00%
Sum	1.00E+00	1.00E+00	1.00E+00	1.00E+00	1.00E+00	1.00E+00	1.00E+00	1.00E+00	1.00E+00

	Australia			Global			Italy		
Human carcinogenic toxicity	Sc4	Sc2	Sc5	Sc4	Sc2	Sc5	Sc4	Sc2	Sc5
Stack material	23.12%	44.70%	58.32%	19.51%	39.45%	53.00%	15.34%	32.76%	45.75%
BOP material	1.03%	0.74%	0.56%	0.87%	0.66%	0.51%	0.69%	0.54%	0.44%
Electriciy-operation	74.46%	53.56%	40.37%	78.26%	58.88%	45.70%	82.65%	65.65%	52.97%
Electriciy-Stack assembly	0.17%	0.13%	0.09%	0.18%	0.14%	0.11%	0.19%	0.15%	0.12%
Electriciy-BOP assembly	0.03%	0.02%	0.02%	0.03%	0.02%	0.02%	0.03%	0.02%	0.02%
Electriciy-pump	0.70%	0.50%	0.38%	0.73%	0.55%	0.43%	0.77%	0.61%	0.50%
Water	0.46%	0.33%	0.25%	0.39%	0.29%	0.23%	0.30%	0.24%	0.19%
Heat	0.03%	0.02%	0.02%	0.02%	0.02%	0.01%	0.02%	0.02%	0.01%
Sum	1.00E+00	1.00E+00	1.00E+00	1.00E+00	1.00E+00	1.00E+00	1.00E+00	1.00E+00	1.00E+00

	Australia			Global			Italy		
Human non-carcinogenic toxicity	Sc4	Sc2	Sc5	Sc4	Sc2	Sc5	Sc4	Sc2	Sc5
Stack material	60.84%	82.32%	89.67%	46.35%	72.13%	82.84%	63.19%	83.72%	90.56%
BOP material	2.01%	0.91%	0.53%	1.53%	0.80%	0.49%	2.09%	0.92%	0.54%
Electriciy-operation	35.74%	16.14%	9.43%	50.76%	26.37%	16.24%	33.30%	14.73%	8.54%
Electriciy-Stack assembly	0.08%	0.04%	0.02%	0.12%	0.06%	0.04%	0.08%	0.03%	0.02%
Electriciy-BOP assembly	0.01%	0.01%	0.00%	0.02%	0.01%	0.01%	0.01%	0.01%	0.00%
Electriciy-pump	0.33%	0.15%	0.09%	0.48%	0.25%	0.15%	0.31%	0.14%	0.08%
Water	0.95%	0.43%	0.25%	0.73%	0.38%	0.23%	0.99%	0.44%	0.25%
Heat	0.02%	0.01%	0.01%	0.02%	0.01%	0.01%	0.02%	0.01%	0.01%
Sum	1.00E+00	1.00E+00	1.00E+00	1.00E+00	1.00E+00	1.00E+00	1.00E+00	1.00E+00	1.00E+00

	Australia			Global			Italy		
Land use	Sc4	Sc2	Sc5	Sc4	Sc2	Sc5	Sc4	Sc2	Sc5
Stack material	0.53%	1.56%	2.79%	0.72%	2.11%	3.76%	1.61%	4.66%	8.11%
BOP material	0.01%	0.01%	0.01%	0.01%	0.01%	0.01%	0.03%	0.03%	0.03%
Electriciy-operation	98.14%	97.12%	95.91%	97.90%	96.53%	94.91%	96.78%	93.79%	90.39%
Electriciy-Stack assembly	0.23%	0.23%	0.22%	0.23%	0.23%	0.22%	0.23%	0.22%	0.21%
Electriciy-BOP assembly	0.04%	0.04%	0.04%	0.04%	0.04%	0.04%	0.04%	0.04%	0.03%
Electriciy-pump	0.92%	0.91%	0.90%	0.92%	0.90%	0.89%	0.91%	0.88%	0.85%
Water	0.13%	0.13%	0.13%	0.17%	0.17%	0.17%	0.39%	0.38%	0.37%
Heat	0.01%	0.01%	0.01%	0.01%	0.01%	0.01%	0.02%	0.02%	0.02%
Sum	1.00E+00	1.00E+00	1.00E+00	1.00E+00	1.00E+00	1.00E+00	1.00E+00	1.00E+00	1.00E+00

	Australia			Global			Italy		
Mineral resource scarcity	Sc4	Sc2	Sc5	Sc4	Sc2	Sc5	Sc4	Sc2	Sc5
Stack material	26.76%	57.22%	72.05%	24.90%	54.83%	70.06%	31.52%	62.76%	76.46%
BOP material	0.13%	0.07%	0.05%	0.12%	0.07%	0.05%	0.15%	0.08%	0.05%
Electriciy-operation	71.99%	42.04%	27.47%	73.85%	44.42%	29.44%	67.21%	36.55%	23.10%
Electriciy-Stack assembly	0.17%	0.10%	0.06%	0.17%	0.10%	0.07%	0.16%	0.09%	0.05%
Electriciy-BOP assembly	0.03%	0.02%	0.01%	0.03%	0.02%	0.01%	0.03%	0.01%	0.01%
Electriciy-pump	0.67%	0.39%	0.26%	0.69%	0.42%	0.28%	0.63%	0.34%	0.22%
Water	0.25%	0.15%	0.10%	0.23%	0.14%	0.09%	0.30%	0.16%	0.10%
Heat	0.01%	0.00%	0.00%	0.01%	0.00%	0.00%	0.01%	0.00%	0.00%
Sum	1.00E+00	1.00E+00	1.00E+00	1.00E+00	1.00E+00	1.00E+00	1.00E+00	1.00E+00	1.00E+00

	Australia			Global			Italy		
Fossil resource scarcity	Sc4	Sc2	Sc5	Sc4	Sc2	Sc5	Sc4	Sc2	Sc5
Stack material	0.16%	0.55%	1.04%	0.19%	0.66%	1.25%	0.21%	0.72%	1.36%
BOP material	0.00%	0.00%	0.00%	0.00%	0.00%	0.00%	0.00%	0.00%	0.00%
Electriciy-operation	98.35%	97.96%	97.48%	98.25%	97.79%	97.21%	98.20%	97.70%	97.07%
Electriciy-Stack assembly	0.23%	0.23%	0.23%	0.23%	0.23%	0.23%	0.23%	0.23%	0.23%
Electriciy-BOP assembly	0.04%	0.04%	0.04%	0.04%	0.04%	0.04%	0.04%	0.04%	0.04%
Electriciy-pump	0.92%	0.92%	0.91%	0.92%	0.92%	0.91%	0.92%	0.91%	0.91%
Water	0.04%	0.03%	0.03%	0.04%	0.04%	0.04%	0.05%	0.05%	0.05%
Heat	0.27%	0.27%	0.27%	0.33%	0.32%	0.32%	0.35%	0.35%	0.35%
Sum	1.00E+00	1.00E+00	1.00E+00	1.00E+00	1.00E+00	1.00E+00	1.00E+00	1.00E+00	1.00E+00

	Australia			Global			Italy		
Water consumption	Sc4	Sc2	Sc5	Sc4	Sc2	Sc5	Sc4	Sc2	Sc5
Stack material	0.01%	0.03%	0.05%	0.01%	0.04%	0.07%	0.03%	0.09%	0.16%
BOP material	0.00%	0.00%	0.00%	0.00%	0.00%	0.00%	0.00%	0.00%	0.00%
Electriciy-operation	98.24%	98.22%	98.20%	98.07%	98.04%	98.01%	97.06%	97.00%	96.93%
Electriciy-Stack assembly	0.23%	0.23%	0.23%	0.23%	0.23%	0.23%	0.23%	0.23%	0.23%
Electriciy-BOP assembly	0.04%	0.04%	0.04%	0.04%	0.04%	0.04%	0.04%	0.04%	0.04%
Electriciy-pump	0.92%	0.92%	0.92%	0.92%	0.92%	0.92%	0.91%	0.91%	0.91%
Water	0.56%	0.56%	0.56%	0.73%	0.73%	0.73%	1.72%	1.72%	1.72%
Heat	0.00%	0.00%	0.00%	0.01%	0.01%	0.01%	0.01%	0.01%	0.01%
Sum	1.00E+00	1.00E+00	1.00E+00	1.00E+00	1.00E+00	1.00E+00	1.00E+00	1.00E+00	1.00E+00

Quantities (Sc6-Sc7-Sc8-Sc9)-supplementary data

	Australia					Global					Italy				
Global Warming	Sc2	Sc6	Sc7	Sc8	Sc9	Sc2	Sc6	Sc7	Sc8	Sc9	Sc2	Sc6	Sc7	Sc8	Sc9
Stack material	1.72E-01	1.72E-01	1.72E-01	1.72E-01	1.72E-01	1.72E-01	1.72E-01	1.72E-01	1.72E-01	1.72E-01	1.72E-01	1.72E-01	1.72E-01	1.72E-01	1.72E-01
BOP material	1.21E-03	1.21E-03	1.21E-03	1.21E-03	1.21E-03	1.21E-03	1.21E-03	1.21E-03	1.21E-03	1.21E-03	1.21E-03	1.21E-03	1.21E-03	1.21E-03	1.21E-03
Electriciy-operation	2.60E+01	2.03E+00	8.20E-01	1.21E+00	1.35E+00	2.08E+01	1.74E+00	7.29E-01	1.06E+00	1.18E+00	1.55E+01	1.76E+00	7.87E-01	1.10E+00	1.22E+00
Electriciy-Stack assembly	6.08E-02	4.74E-03	1.92E-03	2.83E-03	3.16E-03	4.85E-02	4.07E-03	1.70E-03	2.47E-03	2.75E-03	3.61E-02	4.11E-03	1.84E-03	2.57E-03	2.84E-03
Electriciy-BOP assembly	9.76E-03	7.61E-04	3.08E-04	4.54E-04	5.07E-04	7.78E-03	6.53E-04	2.73E-04	3.96E-04	4.41E-04	5.80E-03	6.60E-04	2.95E-04	4.13E-04	4.56E-04
Electriciy-pump	2.44E-01	1.90E-02	7.68E-03	1.13E-02	1.27E-02	1.94E-01	1.63E-02	6.82E-03	9.87E-03	1.10E-02	1.45E-01	1.65E-02	7.37E-03	1.03E-02	1.14E-02
Water	1.61E-02	1.61E-02	1.61E-02	1.61E-02	1.61E-02	1.61E-02	1.61E-02	1.61E-02	1.61E-02	1.61E-02	1.61E-02	1.61E-02	1.61E-02	1.61E-02	1.61E-02
Heat	6.79E-02	6.79E-02	6.79E-02	6.79E-02	6.79E-02	6.79E-02	6.79E-02	6.79E-02	6.79E-02	6.79E-02	6.79E-02	6.79E-02	6.79E-02	6.79E-02	6.79E-02
Sum	2.66E+01	2.31E+00	1.09E+00	1.48E+00	1.63E+00	2.13E+01	2.02E+00	9.94E-01	1.32E+00	1.45E+00	1.59E+01	2.04E+00	1.05E+00	1.37E+00	1.49E+00

	Australia					Global					Italy				
Stratospheric ozone depletion	Sc2	Sc6	Sc7	Sc8	Sc9	Sc2	Sc6	Sc7	Sc8	Sc9	Sc2	Sc6	Sc7	Sc8	Sc9
Stack material	2.929E-07	2.929E-07	2.929E-07	2.93E-07	2.93E-07	2.929E-07	2.929E-07	2.929E-07	2.93E-07	2.93E-07	2.929E-07	2.929E-07	2.929E-07	2.93E-07	2.93E-07
BOP material	4.115E-10	4.115E-10	4.115E-10	4.12E-10	4.12E-10	4.115E-10	4.115E-10	4.115E-10	4.12E-10	4.12E-10	4.115E-10	4.115E-10	4.115E-10	4.12E-10	4.12E-10
Electriciy-operation	7.884E-06	3.449E-08	1.959E-07	3.43E-08	8.82E-08	6.950E-06	8.314E-08	2.183E-07	8.30E-08	1.28E-07	7.110E-06	2.872E-08	1.584E-07	2.86E-08	7.19E-08
Electriciy-Stack assembly	1.843E-08	8.060E-11	4.578E-10	8.02E-11	2.06E-10	1.624E-08	1.943E-10	5.102E-10	1.94E-10	3.00E-10	1.662E-08	6.713E-11	3.702E-10	6.68E-11	1.68E-10
Electriciy-BOP assembly	2.956E-09	1.293E-11	7.344E-11	1.29E-11	3.31E-11	2.606E-09	3.117E-11	8.185E-11	3.11E-11	4.81E-11	2.666E-09	1.077E-11	5.939E-11	1.07E-11	2.70E-11
Electriciy-pump	7.378E-08	3.227E-10	1.833E-09	3.21E-10	8.26E-10	6.504E-08	7.781E-10	2.043E-09	7.77E-10	1.20E-09	6.654E-08	2.688E-10	1.482E-09	2.68E-10	6.73E-10
Water	7.597E-09	7.597E-09	7.597E-09	7.60E-09	7.60E-09	7.597E-09	7.597E-09	7.597E-09	7.60E-09	7.60E-09	7.597E-09	7.597E-09	7.597E-09	7.60E-09	7.60E-09
Heat	2.411E-09	2.411E-09	2.411E-09	2.41E-09	2.41E-09	2.411E-09	2.411E-09	2.411E-09	2.41E-09	2.41E-09	2.411E-09	2.411E-09	2.411E-09	2.41E-09	2.41E-09
Sum	8.28E-06	3.38E-07	5.02E-07	3.38E-07	3.93E-07	7.34E-06	3.87E-07	5.24E-07	3.87E-07	4.33E-07	7.50E-06	3.32E-07	4.64E-07	3.32E-07	3.76E-07

	Australia					Global					Italy				
Ionizing radiation	Sc2	Sc6	Sc7	Sc8	Sc9	Sc2	Sc6	Sc7	Sc8	Sc9	Sc2	Sc6	Sc7	Sc8	Sc9
Stack material	7.107E-03	7.107E-03	7.107E-03	7.11E-03	7.11E-03	7.107E-03	7.107E-03	7.107E-03	7.11E-03	7.11E-03	7.107E-03	7.107E-03	7.107E-03	7.11E-03	7.11E-03
BOP material	9.759E-05	9.759E-05	9.759E-05	9.76E-05	9.76E-05	9.759E-05	9.759E-05	9.759E-05	9.76E-05	9.76E-05	9.759E-05	9.759E-05	9.759E-05	9.76E-05	9.76E-05
Electriciy-operation	1.183E-01	1.511E-03	1.218E-02	3.60E-03	5.76E-03	5.230E+00	5.149E+00	5.158E+00	5.15E+00	5.15E+00	2.059E-02	1.479E-03	1.005E-02	3.16E-03	4.90E-03
Electriciy-Stack assembly	2.764E-04	3.531E-06	2.846E-05	8.41E-06	1.35E-05	1.222E-02	1.203E-02	1.205E-02	1.20E-02	1.20E-02	4.813E-05	3.457E-06	2.349E-05	7.37E-06	1.14E-05
Electriciy-BOP assembly	4.434E-05	5.665E-07	4.566E-06	1.35E-06	2.16E-06	1.961E-03	1.930E-03	1.934E-03	1.93E-03	1.93E-03	7.721E-06	5.546E-07	3.768E-06	1.18E-06	1.84E-06
Electriciy-pump	1.107E-03	1.414E-05	1.140E-04	3.37E-05	5.39E-05	4.894E-02	4.818E-02	4.827E-02	4.82E-02	4.82E-02	1.927E-04	1.384E-05	9.406E-05	2.95E-05	4.58E-05
Water	1.738E-05	1.738E-05	1.738E-05	1.74E-05	1.74E-05	1.738E-05	1.738E-05	1.738E-05	1.74E-05	1.74E-05	1.738E-05	1.738E-05	1.738E-05	1.74E-05	1.74E-05
Heat	1.997E-06	1.997E-06	1.997E-06	2.00E-06	2.00E-06	1.997E-06	1.997E-06	1.997E-06	2.00E-06	2.00E-06	1.997E-06	1.997E-06	1.997E-06	2.00E-06	2.00E-06
Sum	1.27E-01	8.75E-03	1.96E-02	1.09E-02	1.31E-02	5.30E+00	5.22E+00	5.23E+00	5.22E+00	5.22E+00	2.81E-02	8.72E-03	1.74E-02	1.04E-02	1.22E-02

	Australia					Global					Italy				
Ozone formation, Human health	Sc2	Sc6	Sc7	Sc8	Sc9	Sc2	Sc6	Sc7	Sc8	Sc9	Sc2	Sc6	Sc7	Sc8	Sc9
Stack material	1.767E-03	1.767E-03	1.767E-03	1.77E-03	1.77E-03	1.767E-03	1.767E-03	1.767E-03	1.77E-03	1.77E-03	1.767E-03	1.767E-03	1.767E-03	1.77E-03	1.77E-03
BOP material	3.023E-06	3.023E-06	3.023E-06	3.02E-06	3.02E-06	3.023E-06	3.023E-06	3.023E-06	3.02E-06	3.02E-06	3.023E-06	3.023E-06	3.023E-06	3.02E-06	3.02E-06
Electriciy-operation	6.680E-02	2.453E-04	1.266E-03	4.60E-04	6.57E-04	5.153E-02	3.975E-04	1.252E-03	5.78E-04	7.43E-04	2.975E-02	2.354E-04	1.055E-03	4.08E-04	5.66E-04
Electriciy-Stack assembly	1.561E-04	5.733E-07	2.959E-06	1.08E-06	1.54E-06	1.204E-04	9.289E-07	2.927E-06	1.35E-06	1.74E-06	6.954E-05	5.501E-07	2.467E-06	9.54E-07	1.32E-06
Electriciy-BOP assembly	2.505E-05	9.197E-08	4.747E-07	1.73E-07	2.46E-07	1.932E-05	1.490E-07	4.695E-07	2.17E-07	2.78E-07	1.116E-05	8.825E-08	3.957E-07	1.53E-07	2.12E-07
Electriciy-pump	6.252E-04	2.296E-06	1.185E-05	4.31E-06	6.15E-06	4.822E-04	3.719E-06	1.172E-05	5.41E-06	6.95E-06	2.785E-04	2.203E-06	9.878E-06	3.82E-06	5.30E-06
Water	4.475E-05	4.475E-05	4.475E-05	4.47E-05	4.47E-05	4.475E-05	4.475E-05	4.475E-05	4.47E-05	4.47E-05	4.475E-05	4.475E-05	4.475E-05	4.47E-05	4.47E-05
Heat	5.075E-04	5.075E-04	5.075E-04	5.07E-04	5.07E-04	5.075E-04	5.075E-04	5.075E-04	5.07E-04	5.07E-04	5.075E-04	5.075E-04	5.075E-04	5.07E-04	5.07E-04
Sum	6.99E-02	2.57E-03	3.60E-03	2.79E-03	2.99E-03	5.45E-02	2.72E-03	3.59E-03	2.91E-03	3.07E-03	3.24E-02	2.56E-03	3.39E-03	2.73E-03	2.90E-03

	Australia					Global					Italy				
Fine particulate matter formation	Sc2	Sc6	Sc7	Sc8	Sc9	Sc2	Sc6	Sc7	Sc8	Sc9	Sc2	Sc6	Sc7	Sc8	Sc9
Stack material	1.775E-03	1.775E-03	1.775E-03	1.77E-03	1.77E-03	1.775E-03	1.775E-03	1.775E-03	1.77E-03	1.77E-03	1.775E-03	1.775E-03	1.775E-03	1.77E-03	1.77E-03
BOP material	1.768E-06	1.768E-06	1.768E-06	1.77E-06	1.77E-06	1.768E-06	1.768E-06	1.768E-06	1.77E-06	1.77E-06	1.768E-06	1.768E-06	1.768E-06	1.77E-06	1.77E-06
Electriciy-operation	8.659E-03	1.515E-04	9.740E-04	1.71E-04	4.32E-04	8.481E-03	2.836E-04	9.723E-04	3.00E-04	5.19E-04	8.532E-03	1.271E-04	7.879E-04	1.43E-04	3.53E-04
Electriciy-Stack assembly	2.024E-05	3.542E-07	2.276E-06	4.01E-07	1.01E-06	1.982E-05	6.628E-07	2.272E-06	7.02E-07	1.21E-06	1.994E-05	2.971E-07	1.841E-06	3.35E-07	8.24E-07
Electriciy-BOP assembly	3.247E-06	5.682E-08	3.652E-07	6.43E-08	1.62E-07	3.180E-06	1.063E-07	3.645E-07	1.13E-07	1.95E-07	3.199E-06	4.766E-08	2.954E-07	5.37E-08	1.32E-07
Electriciy-pump	8.104E-05	1.418E-06	9.115E-06	1.60E-06	4.05E-06	7.937E-05	2.654E-06	9.099E-06	2.81E-06	4.86E-06	7.985E-05	1.190E-06	7.374E-06	1.34E-06	3.30E-06
Water	2.485E-05	2.485E-05	2.485E-05	2.48E-05	2.48E-05	2.485E-05	2.485E-05	2.485E-05	2.48E-05	2.48E-05	2.485E-05	2.485E-05	2.485E-05	2.48E-05	2.48E-05
Heat	5.708E-05	5.708E-05	5.708E-05	5.71E-05	5.71E-05	5.708E-05	5.708E-05	5.708E-05	5.71E-05	5.71E-05	5.708E-05	5.708E-05	5.708E-05	5.71E-05	5.71E-05
Sum	1.06E-02	2.01E-03	2.84E-03	2.03E-03	2.30E-03	1.04E-02	2.15E-03	2.84E-03	2.16E-03	2.38E-03	1.05E-02	1.99E-03	2.66E-03	2.00E-03	2.22E-03

	Australia					Global					Italy				
Ozone formation, Terrestrial ecosystems	Sc2	Sc6	Sc7	Sc8	Sc9	Sc2	Sc6	Sc7	Sc8	Sc9	Sc2	Sc6	Sc7	Sc8	Sc9
Stack material	1.804E-03	1.804E-03	1.804E-03	1.80E-03	1.80E-03	1.804E-03	1.804E-03	1.804E-03	1.80E-03	1.80E-03	1.804E-03	1.804E-03	1.804E-03	1.80E-03	1.80E-03
BOP material	3.129E-06	3.129E-06	3.129E-06	3.13E-06	3.13E-06	3.129E-06	3.129E-06	3.129E-06	3.13E-06	3.13E-06	3.129E-06	3.129E-06	3.129E-06	3.13E-06	3.13E-06
Electriciy-operation	6.687E-02	2.456E-04	1.268E-03	4.61E-04	6.58E-04	5.160E-02	3.980E-04	1.254E-03	5.78E-04	7.44E-04	2.988E-02	2.356E-04	1.057E-03	4.09E-04	5.67E-04
Electriciy-Stack assembly	1.563E-04	5.740E-07	2.964E-06	1.08E-06	1.54E-06	1.206E-04	9.302E-07	2.931E-06	1.35E-06	1.74E-06	6.982E-05	5.507E-07	2.471E-06	9.55E-07	1.33E-06
Electriciy-BOP assembly	2.507E-05	9.208E-08	4.755E-07	1.73E-07	2.47E-07	1.935E-05	1.492E-07	4.703E-07	2.17E-07	2.79E-07	1.120E-05	8.834E-08	3.964E-07	1.53E-07	2.13E-07
Electriciy-pump	6.258E-04	2.298E-06	1.187E-05	4.31E-06	6.16E-06	4.829E-04	3.725E-06	1.174E-05	5.41E-06	6.96E-06	2.796E-04	2.205E-06	9.893E-06	3.82E-06	5.31E-06
Water	4.478E-05	4.478E-05	4.478E-05	4.48E-05	4.48E-05	4.478E-05	4.478E-05	4.478E-05	4.48E-05	4.48E-05	4.478E-05	4.478E-05	4.478E-05	4.48E-05	4.48E-05
Heat	5.076E-04	5.076E-04	5.076E-04	5.08E-04	5.08E-04	5.076E-04	5.076E-04	5.076E-04	5.08E-04	5.08E-04	5.076E-04	5.076E-04	5.076E-04	5.08E-04	5.08E-04
Sum	7.00E-02	2.61E-03	3.64E-03	2.83E-03	3.03E-03	5.46E-02	2.76E-03	3.63E-03	2.94E-03	3.11E-03	3.26E-02	2.60E-03	3.43E-03	2.77E-03	2.93E-03

	Australia					Global					Italy				
Terrestrial acidification	Sc2	Sc6	Sc7	Sc8	Sc9	Sc2	Sc6	Sc7	Sc8	Sc9	Sc2	Sc6	Sc7	Sc8	Sc9
Stack material	6.008E-03	6.008E-03	6.008E-03	6.01E-03	6.01E-03	6.008E-03	6.008E-03	6.008E-03	6.01E-03	6.01E-03	6.008E-03	6.008E-03	6.008E-03	6.01E-03	6.01E-03
BOP material	5.090E-06	5.090E-06	5.090E-06	5.09E-06	5.09E-06	5.090E-06	5.090E-06	5.090E-06	5.09E-06	5.09E-06	5.090E-06	5.090E-06	5.090E-06	5.09E-06	5.09E-06
Electriciy-operation	1.172E-01	3.782E-04	2.122E-03	4.39E-04	9.80E-04	8.792E-02	5.662E-04	2.027E-03	6.17E-04	1.07E-03	3.580E-02	3.239E-04	1.725E-03	3.73E-04	8.07E-04
Electriciy-Stack assembly	2.739E-04	8.840E-07	4.960E-06	1.03E-06	2.29E-06	2.055E-04	1.323E-06	4.736E-06	1.44E-06	2.50E-06	8.367E-05	7.570E-07	4.032E-06	8.72E-07	1.89E-06
Electriciy-BOP assembly	4.395E-05	1.418E-07	7.957E-07	1.65E-07	3.67E-07	3.296E-05	2.123E-07	7.598E-07	2.31E-07	4.01E-07	1.342E-05	1.214E-07	6.468E-07	1.40E-07	3.03E-07
Electriciy-pump	1.097E-03	3.540E-06	1.986E-05	4.11E-06	9.17E-06	8.227E-04	5.298E-06	1.897E-05	5.78E-06	1.00E-05	3.350E-04	3.031E-06	1.614E-05	3.49E-06	7.56E-06
Water	8.037E-05	8.037E-05	8.037E-05	8.04E-05	8.04E-05	8.037E-05	8.037E-05	8.037E-05	8.04E-05	8.04E-05	8.037E-05	8.037E-05	8.037E-05	8.04E-05	8.04E-05
Heat	1.868E-04	1.868E-04	1.868E-04	1.87E-04	1.87E-04	1.868E-04	1.868E-04	1.868E-04	1.87E-04	1.87E-04	1.868E-04	1.868E-04	1.868E-04	1.87E-04	1.87E-04
Sum	1.25E-01	6.66E-03	8.43E-03	6.73E-03	7.27E-03	9.53E-02	6.85E-03	8.33E-03	6.91E-03	7.36E-03	4.25E-02	6.61E-03	8.03E-03	6.66E-03	7.10E-03

	Australia					Global					Italy				
Freshwater eutrophication	Sc2	Sc6	Sc7	Sc8	Sc9	Sc2	Sc6	Sc7	Sc8	Sc9	Sc2	Sc6	Sc7	Sc8	Sc9
Stack material	2.315E-04	2.315E-04	2.315E-04	2.32E-04	2.32E-04	2.315E-04	2.315E-04	2.315E-04	2.32E-04	2.32E-04	2.315E-04	2.315E-04	2.315E-04	2.32E-04	2.32E-04
BOP material	6.968E-07	6.968E-07	6.968E-07	6.97E-07	6.97E-07	6.968E-07	6.968E-07	6.968E-07	6.97E-07	6.97E-07	6.968E-07	6.968E-07	6.968E-07	6.97E-07	6.97E-07
Electriciy-operation	1.198E-02	1.698E-05	1.454E-04	1.63E-05	5.96E-05	8.189E-03	2.334E-05	1.309E-04	2.28E-05	5.90E-05	1.208E-03	1.326E-05	1.164E-04	1.27E-05	4.75E-05
Electriciy-Stack assembly	2.800E-05	3.968E-08	3.398E-07	3.82E-08	1.39E-07	1.914E-05	5.456E-08	3.058E-07	5.33E-08	1.38E-07	2.823E-06	3.099E-08	2.721E-07	2.98E-08	1.11E-07
Electriciy-BOP assembly	4.492E-06	6.366E-09	5.451E-08	6.12E-09	2.23E-08	3.070E-06	8.752E-09	4.907E-08	8.55E-09	2.21E-08	4.528E-07	4.971E-09	4.365E-08	4.78E-09	1.78E-08
Electriciy-pump	1.121E-04	1.589E-07	1.360E-06	1.53E-07	5.57E-07	7.663E-05	2.185E-07	1.225E-06	2.13E-07	5.52E-07	1.130E-05	1.241E-07	1.090E-06	1.19E-07	4.44E-07
Water	8.096E-07	8.096E-07	8.096E-07	8.10E-07	8.10E-07	8.096E-07	8.096E-07	8.096E-07	8.10E-07	8.10E-07	8.096E-07	8.096E-07	8.096E-07	8.10E-07	8.10E-07
Heat	1.631E-08	1.631E-08	1.631E-08	1.63E-08	1.63E-08	1.631E-08	1.631E-08	1.631E-08	1.63E-08	1.63E-08	1.631E-08	1.631E-08	1.631E-08	1.63E-08	1.63E-08
Sum	1.24E-02	2.50E-04	3.80E-04	2.50E-04	2.93E-04	8.52E-03	2.57E-04	3.66E-04	2.56E-04	2.93E-04	1.46E-03	2.46E-04	3.51E-04	2.46E-04	2.81E-04

	Australia					Global					Italy				
Marine eutrophication	Sc2	Sc6	Sc7	Sc8	Sc9	Sc2	Sc6	Sc7	Sc8	Sc9	Sc2	Sc6	Sc7	Sc8	Sc9
Stack material	7.023E-06	7.023E-06	7.023E-06	7.02E-06	7.02E-06	7.023E-06	7.023E-06	7.023E-06	7.02E-06	7.02E-06	7.023E-06	7.023E-06	7.023E-06	7.02E-06	7.02E-06
BOP material	3.701E-08	3.701E-08	3.701E-08	3.70E-08	3.70E-08	3.701E-08	3.701E-08	3.701E-08	3.70E-08	3.70E-08	3.701E-08	3.701E-08	3.701E-08	3.70E-08	3.70E-08
Electriciy-operation	8.031E-04	3.465E-06	2.912E-05	3.66E-06	1.21E-05	5.735E-04	1.203E-05	3.352E-05	1.22E-05	1.92E-05	1.152E-04	2.759E-06	2.337E-05	2.92E-06	9.68E-06
Electriciy-Stack assembly	1.877E-06	8.098E-09	6.807E-08	8.56E-09	2.82E-08	1.340E-06	2.812E-08	7.833E-08	2.85E-08	4.50E-08	2.691E-07	6.448E-09	5.463E-08	6.82E-09	2.26E-08
Electriciy-BOP assembly	3.011E-07	1.299E-09	1.092E-08	1.37E-09	4.53E-09	2.150E-07	4.510E-09	1.257E-08	4.57E-09	7.22E-09	4.318E-08	1.034E-09	8.764E-09	1.09E-09	3.63E-09
Electriciy-pump	7.516E-06	3.243E-08	2.726E-07	3.43E-08	1.13E-07	5.367E-06	1.126E-07	3.137E-07	1.14E-07	1.80E-07	1.078E-06	2.582E-08	2.187E-07	2.73E-08	9.06E-08
Water	1.733E-07	1.733E-07	1.733E-07	1.73E-07	1.73E-07	1.733E-07	1.733E-07	1.733E-07	1.73E-07	1.73E-07	1.733E-07	1.733E-07	1.733E-07	1.73E-07	1.73E-07
Heat	1.556E-09	1.556E-09	1.556E-09	1.56E-09	1.56E-09	1.556E-09	1.556E-09	1.556E-09	1.56E-09	1.56E-09	1.556E-09	1.556E-09	1.556E-09	1.56E-09	1.56E-09
Sum	8.20E-04	1.07E-05	3.67E-05	1.09E-05	1.95E-05	5.88E-04	1.94E-05	4.12E-05	1.96E-05	2.67E-05	1.24E-04	1.00E-05	3.09E-05	1.02E-05	1.70E-05

	Australia					Global					Italy				
Terrestrial ecotoxicity	Sc2	Sc6	Sc7	Sc8	Sc9	Sc2	Sc6	Sc7	Sc8	Sc9	Sc2	Sc6	Sc7	Sc8	Sc9
Stack material	4.558E-01	4.558E-01	4.558E-01	4.56E-01	4.56E-01	4.558E-01	4.558E-01	4.558E-01	4.56E-01	4.56E-01	4.558E-01	4.558E-01	4.558E-01	4.56E-01	4.56E-01
BOP material	9.142E-03	9.142E-03	9.142E-03	9.14E-03	9.14E-03	9.142E-03	9.142E-03	9.142E-03	9.14E-03	9.14E-03	9.142E-03	9.142E-03	9.142E-03	9.14E-03	9.14E-03
Electriciy-operation	7.827E+00	7.653E-01	6.670E+00	7.87E-01	2.74E+00	9.168E+00	2.029E+00	6.974E+00	2.05E+00	3.68E+00	6.463E+00	6.025E-01	5.347E+00	6.20E-01	2.19E+00
Electriciy-Stack assembly	1.829E-02	1.789E-03	1.559E-02	1.84E-03	6.41E-03	2.143E-02	4.743E-03	1.630E-02	4.79E-03	8.61E-03	1.510E-02	1.408E-03	1.250E-02	1.45E-03	5.12E-03
Electriciy-BOP assembly	2.934E-03	2.869E-04	2.501E-03	2.95E-04	1.03E-03	3.437E-03	7.609E-04	2.615E-03	7.68E-04	1.38E-03	2.423E-03	2.259E-04	2.005E-03	2.32E-04	8.21E-04
Electriciy-pump	7.324E-02	7.162E-03	6.242E-02	7.37E-03	2.56E-02	8.579E-02	1.899E-02	6.527E-02	1.92E-02	3.45E-02	6.048E-02	5.639E-03	5.004E-02	5.80E-03	2.05E-02
Water	1.921E-02	1.921E-02	1.921E-02	1.92E-02	1.92E-02	1.921E-02	1.921E-02	1.921E-02	1.92E-02	1.92E-02	1.921E-02	1.921E-02	1.921E-02	1.92E-02	1.92E-02
Heat	4.283E-03	4.283E-03	4.283E-03	4.28E-03	4.28E-03	4.283E-03	4.283E-03	4.283E-03	4.28E-03	4.28E-03	4.283E-03	4.283E-03	4.283E-03	4.28E-03	4.28E-03
Sum	8.41E+00	1.26E+00	7.24E+00	1.28E+00	3.26E+00	9.77E+00	2.54E+00	7.55E+00	2.56E+00	4.22E+00	7.03E+00	1.10E+00	5.90E+00	1.12E+00	2.70E+00

	Australia					Global					Italy				
Freshwater ecotoxicity	Sc2	Sc6	Sc7	Sc8	Sc9	Sc2	Sc6	Sc7	Sc8	Sc9	Sc2	Sc6	Sc7	Sc8	Sc9
Stack material	9.296E-02	9.296E-02	9.296E-02	9.30E-02	9.30E-02	9.296E-02	9.296E-02	9.296E-02	9.30E-02	9.30E-02	9.296E-02	9.296E-02	9.296E-02	9.30E-02	9.30E-02
BOP material	2.157E-04	2.157E-04	2.157E-04	2.16E-04	2.16E-04	2.157E-04	2.157E-04	2.157E-04	2.16E-04	2.16E-04	2.157E-04	2.157E-04	2.157E-04	2.16E-04	2.16E-04
Electriciy-operation	3.873E-01	3.990E-03	3.318E-02	3.74E-03	1.36E-02	2.706E-01	7.450E-03	3.189E-02	7.24E-03	1.55E-02	4.661E-02	3.120E-03	2.657E-02	2.92E-03	1.09E-02
Electriciy-Stack assembly	9.051E-04	9.325E-06	7.755E-05	8.75E-06	3.19E-05	6.323E-04	1.741E-05	7.454E-05	1.69E-05	3.63E-05	1.089E-04	7.291E-06	6.211E-05	6.83E-06	2.54E-05
Electriciy-BOP assembly	1.452E-04	1.496E-06	1.244E-05	1.40E-06	5.11E-06	1.014E-04	2.793E-06	1.196E-05	2.72E-06	5.82E-06	1.748E-05	1.170E-06	9.963E-06	1.10E-06	4.08E-06
Electriciy-pump	3.624E-03	3.734E-05	3.105E-04	3.50E-05	1.28E-04	2.532E-03	6.972E-05	2.985E-04	6.78E-05	1.45E-04	4.362E-04	2.919E-05	2.487E-04	2.73E-05	1.02E-04
Water	2.461E-04	2.461E-04	2.461E-04	2.46E-04	2.46E-04	2.461E-04	2.461E-04	2.461E-04	2.46E-04	2.46E-04	2.461E-04	2.461E-04	2.461E-04	2.46E-04	2.46E-04
Heat	2.724E-06	2.724E-06	2.724E-06	2.72E-06	2.72E-06	2.724E-06	2.724E-06	2.724E-06	2.72E-06	2.72E-06	2.724E-06	2.724E-06	2.724E-06	2.72E-06	2.72E-06
Sum	4.85E-01	9.75E-02	1.27E-01	9.72E-02	1.07E-01	3.67E-01	1.01E-01	1.26E-01	1.01E-01	1.09E-01	1.41E-01	9.66E-02	1.20E-01	9.64E-02	1.04E-01

	Australia					Global					Italy				
Marine ecotoxicity	Sc2	Sc6	Sc7	Sc8	Sc9	Sc2	Sc6	Sc7	Sc8	Sc9	Sc2	Sc6	Sc7	Sc8	Sc9
Stack material	1.780E-01	1.780E-01	1.780E-01	1.78E-01	1.78E-01	1.780E-01	1.780E-01	1.780E-01	1.78E-01	1.78E-01	1.780E-01	1.780E-01	1.780E-01	1.78E-01	1.78E-01
BOP material	3.634E-02	3.634E-02	3.634E-02	3.63E-02	3.63E-02	3.634E-02	3.634E-02	3.634E-02	3.63E-02	3.63E-02	3.634E-02	3.634E-02	3.634E-02	3.63E-02	3.63E-02
Electriciy-operation	1.426E-01	5.785E-03	4.821E-02	5.45E-03	1.98E-02	1.097E-01	1.102E-02	4.655E-02	1.07E-02	2.28E-02	3.502E-02	4.525E-03	3.861E-02	4.26E-03	1.58E-02
Electriciy-Stack assembly	3.332E-04	1.352E-05	1.127E-04	1.27E-05	4.63E-05	2.564E-04	2.576E-05	1.088E-04	2.51E-05	5.32E-05	8.185E-05	1.058E-05	9.024E-05	9.96E-06	3.69E-05
Electriciy-BOP assembly	5.345E-05	2.169E-06	1.808E-05	2.05E-06	7.43E-06	4.113E-05	4.133E-06	1.745E-05	4.03E-06	8.54E-06	1.313E-05	1.697E-06	1.448E-05	1.60E-06	5.92E-06
Electriciy-pump	1.334E-03	5.414E-05	4.512E-04	5.10E-05	1.85E-04	1.027E-03	1.032E-04	4.356E-04	1.01E-04	2.13E-04	3.278E-04	4.235E-05	3.614E-04	3.99E-05	1.48E-04
Water	3.491E-04	3.491E-04	3.491E-04	3.49E-04	3.49E-04	3.491E-04	3.491E-04	3.491E-04	3.49E-04	3.49E-04	3.491E-04	3.491E-04	3.491E-04	3.49E-04	3.49E-04
Heat	1.129E-05	1.129E-05	1.129E-05	1.13E-05	1.13E-05	1.129E-05	1.129E-05	1.129E-05	1.13E-05	1.13E-05	1.129E-05	1.129E-05	1.129E-05	1.13E-05	1.13E-05
Sum	3.59E-01	2.21E-01	2.63E-01	2.20E-01	2.35E-01	3.26E-01	2.26E-01	2.62E-01	2.26E-01	2.38E-01	2.50E-01	2.19E-01	2.54E-01	2.19E-01	2.31E-01

	Australia					Global					Italy				
Human carcinogenic toxicity	Sc2	Sc6	Sc7	Sc8	Sc9	Sc2	Sc6	Sc7	Sc8	Sc9	Sc2	Sc6	Sc7	Sc8	Sc9
Stack material	3.975E-02	3.975E-02	3.975E-02	3.97E-02	3.97E-02	3.975E-02	3.975E-02	3.975E-02	3.97E-02	3.97E-02	3.975E-02	3.975E-02	3.975E-02	3.97E-02	3.97E-02
BOP material	6.604E-04	6.604E-04	6.604E-04	6.60E-04	6.60E-04	6.604E-04	6.604E-04	6.604E-04	6.60E-04	6.60E-04	6.604E-04	6.604E-04	6.604E-04	6.60E-04	6.60E-04
Electriciy-operation	4.762E-02	1.690E-02	1.487E-01	1.68E-02	6.08E-02	5.932E-02	2.330E-02	1.337E-01	2.32E-02	6.01E-02	7.965E-02	1.320E-02	1.191E-01	1.31E-02	4.85E-02
Electriciy-Stack assembly	1.113E-04	3.949E-05	3.476E-04	3.92E-05	1.42E-04	1.386E-04	5.445E-05	3.125E-04	5.42E-05	1.40E-04	1.861E-04	3.085E-05	2.784E-04	3.06E-05	1.13E-04
Electriciy-BOP assembly	1.785E-05	6.336E-06	5.576E-05	6.29E-06	2.28E-05	2.224E-05	8.736E-06	5.013E-05	8.70E-06	2.25E-05	2.986E-05	4.950E-06	4.466E-05	4.92E-06	1.82E-05
Electriciy-pump	4.456E-04	1.581E-04	1.392E-03	1.57E-04	5.69E-04	5.551E-04	2.180E-04	1.251E-03	2.17E-04	5.62E-04	7.454E-04	1.235E-04	1.115E-03	1.23E-04	4.54E-04
Water	2.932E-04	2.932E-04	2.932E-04	2.93E-04	2.93E-04	2.932E-04	2.932E-04	2.932E-04	2.93E-04	2.93E-04	2.932E-04	2.932E-04	2.932E-04	2.93E-04	2.93E-04
Heat	1.857E-05	1.857E-05	1.857E-05	1.86E-05	1.86E-05	1.857E-05	1.857E-05	1.857E-05	1.86E-05	1.86E-05	1.857E-05	1.857E-05	1.857E-05	1.86E-05	1.86E-05
Sum	8.89E-02	5.78E-02	1.91E-01	5.77E-02	1.02E-01	1.01E-01	6.43E-02	1.76E-01	6.42E-02	1.02E-01	1.21E-01	5.41E-02	1.61E-01	5.40E-02	8.98E-02

	Australia					Global					Italy				
Human non-carcinogenic toxicity	Sc2	Sc6	Sc7	Sc8	Sc9	Sc2	Sc6	Sc7	Sc8	Sc9	Sc2	Sc6	Sc7	Sc8	Sc9
Stack material	2.919E+00	2.919E+00	2.919E+00	2.92E+00	2.92E+00	2.919E+00	2.919E+00	2.919E+00	2.92E+00	2.92E+00	2.919E+00	2.919E+00	2.919E+00	2.92E+00	2.92E+00
BOP material	3.221E-02	3.221E-02	3.221E-02	3.22E-02	3.22E-02	3.221E-02	3.221E-02	3.221E-02	3.22E-02	3.22E-02	3.221E-02	3.221E-02	3.221E-02	3.22E-02	3.22E-02
Electriciy-operation	5.723E-01	1.733E-01	1.378E+00	1.62E-01	5.71E-01	1.067E+00	6.941E-01	1.703E+00	6.85E-01	1.03E+00	5.134E-01	1.364E-01	1.104E+00	1.27E-01	4.56E-01
Electriciy-Stack assembly	1.337E-03	4.050E-04	3.220E-03	3.78E-04	1.33E-03	2.493E-03	1.622E-03	3.980E-03	1.60E-03	2.40E-03	1.200E-03	3.188E-04	2.581E-03	2.97E-04	1.07E-03
Electriciy-BOP assembly	2.146E-04	6.497E-05	5.166E-04	6.07E-05	2.14E-04	4.000E-04	2.602E-04	6.385E-04	2.57E-04	3.85E-04	1.925E-04	5.115E-05	4.141E-04	4.77E-05	1.71E-04
Electriciy-pump	5.355E-03	1.622E-03	1.290E-02	1.51E-03	5.34E-03	9.983E-03	6.496E-03	1.594E-02	6.41E-03	9.61E-03	4.804E-03	1.277E-03	1.033E-02	1.19E-03	4.27E-03
Water	1.529E-02	1.529E-02	1.529E-02	1.53E-02	1.53E-02	1.529E-02	1.529E-02	1.529E-02	1.53E-02	1.53E-02	1.529E-02	1.529E-02	1.529E-02	1.53E-02	1.53E-02
Heat	3.321E-04	3.321E-04	3.321E-04	3.32E-04	3.32E-04	3.321E-04	3.321E-04	3.321E-04	3.32E-04	3.32E-04	3.321E-04	3.321E-04	3.321E-04	3.32E-04	3.32E-04
Sum	3.55E+00	3.14E+00	4.36E+00	3.13E+00	3.54E+00	4.05E+00	3.67E+00	4.69E+00	3.66E+00	4.01E+00	3.49E+00	3.10E+00	4.08E+00	3.10E+00	3.43E+00

	Australia					Global					Italy				
Land use	Sc2	Sc6	Sc7	Sc8	Sc9	Sc2	Sc6	Sc7	Sc8	Sc9	Sc2	Sc6	Sc7	Sc8	Sc9
Stack material	6.204E-03	6.204E-03	6.204E-03	6.20E-03	6.20E-03	6.204E-03	6.204E-03	6.204E-03	6.20E-03	6.20E-03	6.204E-03	6.204E-03	6.204E-03	6.20E-03	6.20E-03
BOP material	3.554E-05	3.554E-05	3.554E-05	3.55E-05	3.55E-05	3.554E-05	3.554E-05	3.554E-05	3.55E-05	3.55E-05	3.554E-05	3.554E-05	3.554E-05	3.55E-05	3.55E-05
Electriciy-operation	3.856E-01	5.197E-03	3.532E-02	4.08E-03	1.49E-02	2.833E-01	5.721E-03	3.094E-02	4.79E-03	1.38E-02	1.250E-01	4.087E-03	2.829E-02	3.19E-03	1.19E-02
Electriciy-Stack assembly	9.012E-04	1.215E-05	8.254E-05	9.53E-06	3.47E-05	6.621E-04	1.337E-05	7.232E-05	1.12E-05	3.23E-05	2.921E-04	9.551E-06	6.611E-05	7.45E-06	2.77E-05
Electriciy-BOP assembly	1.446E-04	1.948E-06	1.324E-05	1.53E-06	5.57E-06	1.062E-04	2.145E-06	1.160E-05	1.79E-06	5.18E-06	4.686E-05	1.532E-06	1.061E-05	1.20E-06	4.44E-06
Electriciy-pump	3.609E-03	4.863E-05	3.305E-04	3.82E-05	1.39E-04	2.651E-03	5.354E-05	2.896E-04	4.48E-05	1.29E-04	1.170E-03	3.824E-05	2.647E-04	2.98E-05	1.11E-04
Water	5.054E-04	5.054E-04	5.054E-04	5.05E-04	5.05E-04	5.054E-04	5.054E-04	5.054E-04	5.05E-04	5.05E-04	5.054E-04	5.054E-04	5.054E-04	5.05E-04	5.05E-04
Heat	2.321E-05	2.321E-05	2.321E-05	2.32E-05	2.32E-05	2.321E-05	2.321E-05	2.321E-05	2.32E-05	2.32E-05	2.321E-05	2.321E-05	2.321E-05	2.32E-05	2.32E-05
Sum	3.97E-01	1.20E-02	4.25E-02	1.09E-02	2.18E-02	2.93E-01	1.26E-02	3.81E-02	1.16E-02	2.08E-02	1.33E-01	1.09E-02	3.54E-02	1.00E-02	1.88E-02

	Australia					Global					Italy				
Mineral resource scarcity	Sc2	Sc6	Sc7	Sc8	Sc9	Sc2	Sc6	Sc7	Sc8	Sc9	Sc2	Sc6	Sc7	Sc8	Sc9
Stack material	1.681E-02	1.681E-02	1.681E-02	1.68E-02	1.68E-02	1.681E-02	1.681E-02	1.681E-02	1.68E-02	1.68E-02	1.681E-02	1.681E-02	1.681E-02	1.68E-02	1.68E-02
BOP material	2.169E-05	2.169E-05	2.169E-05	2.17E-05	2.17E-05	2.169E-05	2.169E-05	2.169E-05	2.17E-05	2.17E-05	2.169E-05	2.169E-05	2.169E-05	2.17E-05	2.17E-05
Electriciy-operation	1.235E-02	6.027E-03	5.146E-02	6.41E-03	2.13E-02	1.362E-02	8.279E-03	4.633E-02	8.60E-03	2.11E-02	9.790E-03	4.791E-03	4.130E-02	5.09E-03	1.71E-02
Electriciy-Stack assembly	2.887E-05	1.409E-05	1.203E-04	1.50E-05	4.98E-05	3.183E-05	1.935E-05	1.083E-04	2.01E-05	4.92E-05	2.288E-05	1.120E-05	9.652E-05	1.19E-05	3.99E-05
Electriciy-BOP assembly	4.631E-06	2.260E-06	1.930E-05	2.40E-06	7.99E-06	5.106E-06	3.104E-06	1.737E-05	3.22E-06	7.90E-06	3.670E-06	1.796E-06	1.548E-05	1.91E-06	6.40E-06
Electriciy-pump	1.156E-04	5.640E-05	4.816E-04	5.99E-05	1.99E-04	1.274E-04	7.747E-05	4.335E-04	8.04E-05	1.97E-04	9.161E-05	4.483E-05	3.865E-04	4.77E-05	1.60E-04
Water	4.323E-05	4.323E-05	4.323E-05	4.32E-05	4.32E-05	4.323E-05	4.323E-05	4.323E-05	4.32E-05	4.32E-05	4.323E-05	4.323E-05	4.323E-05	4.32E-05	4.32E-05
Heat	1.272E-06	1.272E-06	1.272E-06	1.27E-06	1.27E-06	1.272E-06	1.272E-06	1.272E-06	1.27E-06	1.27E-06	1.272E-06	1.272E-06	1.272E-06	1.27E-06	1.27E-06
Sum	2.94E-02	2.30E-02	6.90E-02	2.34E-02	3.84E-02	3.07E-02	2.53E-02	6.38E-02	2.56E-02	3.82E-02	2.68E-02	2.17E-02	5.87E-02	2.20E-02	3.41E-02

	Australia					Global					Italy				
Fossil resource scarcity	Sc2	Sc6	Sc7	Sc8	Sc9	Sc2	Sc6	Sc7	Sc8	Sc9	Sc2	Sc6	Sc7	Sc8	Sc9
Stack material	5.083E-02	5.083E-02	5.083E-02	5.08E-02	5.08E-02	5.083E-02	5.083E-02	5.083E-02	5.08E-02	5.08E-02	5.083E-02	5.083E-02	5.083E-02	5.08E-02	5.08E-02
BOP material	2.644E-04	2.644E-04	2.644E-04	2.64E-04	2.64E-04	2.644E-04	2.644E-04	2.644E-04	2.64E-04	2.64E-04	2.644E-04	2.644E-04	2.644E-04	2.64E-04	2.64E-04
Electriciy-operation	9.015E+00	1.889E-02	1.045E-01	2.37E-02	4.90E-02	7.493E+00	2.657E-02	9.821E-02	3.06E-02	5.18E-02	6.887E+00	1.644E-02	8.519E-02	2.03E-02	4.07E-02
Electriciy-Stack assembly	2.107E-02	4.415E-05	2.441E-04	5.55E-05	1.15E-04	1.751E-02	6.209E-05	2.295E-04	7.16E-05	1.21E-04	1.609E-02	3.843E-05	1.991E-04	4.75E-05	9.50E-05
Electriciy-BOP assembly	3.380E-03	7.082E-06	3.916E-05	8.90E-06	1.84E-05	2.809E-03	9.960E-06	3.682E-05	1.15E-05	1.94E-05	2.582E-03	6.164E-06	3.194E-05	7.63E-06	1.52E-05
Electriciy-pump	8.437E-02	1.768E-04	9.775E-04	2.22E-04	4.59E-04	7.012E-02	2.486E-04	9.191E-04	2.87E-04	4.85E-04	6.445E-02	1.539E-04	7.972E-04	1.90E-04	3.80E-04
Water	3.221E-03	3.221E-03	3.221E-03	3.22E-03	3.22E-03	3.221E-03	3.221E-03	3.221E-03	3.22E-03	3.22E-03	3.221E-03	3.221E-03	3.221E-03	3.22E-03	3.22E-03
Heat	2.489E-02	2.489E-02	2.489E-02	2.49E-02	2.49E-02	2.489E-02	2.489E-02	2.489E-02	2.49E-02	2.49E-02	2.489E-02	2.489E-02	2.489E-02	2.49E-02	2.49E-02
Sum	9.20E+00	9.83E-02	1.85E-01	1.03E-01	1.29E-01	7.66E+00	1.06E-01	1.79E-01	1.10E-01	1.32E-01	7.05E+00	9.58E-02	1.65E-01	9.98E-02	1.20E-01

	Australia					Global					Italy				
Water consumption	Sc2	Sc6	Sc7	Sc8	Sc9	Sc2	Sc6	Sc7	Sc8	Sc9	Sc2	Sc6	Sc7	Sc8	Sc9
Stack material	1.117E-03	1.117E-03	1.117E-03	1.12E-03	1.12E-03	1.117E-03	1.117E-03	1.117E-03	1.12E-03	1.12E-03	1.117E-03	1.117E-03	1.117E-03	1.12E-03	1.12E-03
BOP material	2.081E-05	2.081E-05	2.081E-05	2.08E-05	2.08E-05	2.081E-05	2.081E-05	2.081E-05	2.08E-05	2.08E-05	2.081E-05	2.081E-05	2.081E-05	2.08E-05	2.08E-05
Electriciy-operation	3.769E+00	3.627E-01	3.130E+00	3.51E-01	1.28E+00	2.896E+00	4.135E-01	2.731E+00	4.04E-01	1.18E+00	1.214E+00	2.832E-01	2.506E+00	2.74E-01	1.02E+00
Electriciy-Stack assembly	8.809E-03	8.476E-04	7.315E-03	8.21E-04	2.99E-03	6.768E-03	9.663E-04	6.382E-03	9.44E-04	2.76E-03	2.838E-03	6.618E-04	5.858E-03	6.41E-04	2.39E-03
Electriciy-BOP assembly	1.413E-03	1.360E-04	1.173E-03	1.32E-04	4.80E-04	1.086E-03	1.550E-04	1.024E-03	1.51E-04	4.44E-04	4.553E-04	1.062E-04	9.397E-04	1.03E-04	3.83E-04
Electriciy-pump	3.527E-02	3.394E-03	2.929E-02	3.29E-03	1.20E-02	2.710E-02	3.869E-03	2.555E-02	3.78E-03	1.11E-02	1.137E-02	2.650E-03	2.346E-02	2.57E-03	9.56E-03
Water	2.158E-02	2.158E-02	2.158E-02	2.16E-02	2.16E-02	2.158E-02	2.158E-02	2.158E-02	2.16E-02	2.16E-02	2.158E-02	2.158E-02	2.158E-02	2.16E-02	2.16E-02
Heat	1.530E-04	1.530E-04	1.530E-04	1.53E-04	1.53E-04	1.530E-04	1.530E-04	1.530E-04	1.53E-04	1.53E-04	1.530E-04	1.530E-04	1.530E-04	1.53E-04	1.53E-04
Sum	3.84E+00	3.90E-01	3.19E+00	3.79E-01	1.32E+00	2.95E+00	4.41E-01	2.79E+00	4.32E-01	1.22E+00	1.25E+00	3.09E-01	2.56E+00	3.00E-01	1.06E+00

Percentage (Sc6-Sc7-Sc8-Sc9)-supplementary data

	Australia					Global					Italy				
Global Warming	Sc2	Sc6	Sc7	Sc8	Sc9	Sc2	Sc6	Sc7	Sc8	Sc9	Sc2	Sc6	Sc7	Sc8	Sc9
Stack material	0.65%	7.42%	15.78%	11.58%	10.55%	0.81%	8.49%	17.25%	12.95%	11.86%	1.08%	8.42%	16.28%	12.52%	11.53%
BOP material	0.00%	0.05%	0.11%	0.08%	0.07%	0.01%	0.06%	0.12%	0.09%	0.08%	0.01%	0.06%	0.12%	0.09%	0.08%
Electriciy-operation	97.85%	87.83%	75.47%	81.68%	83.21%	97.61%	86.25%	73.29%	79.65%	81.27%	97.21%	86.35%	74.73%	80.29%	81.75%
Electriciy-Stack assembly	0.23%	0.21%	0.18%	0.19%	0.19%	0.23%	0.20%	0.17%	0.19%	0.19%	0.23%	0.20%	0.17%	0.19%	0.19%
Electriciy-BOP assembly	0.04%	0.03%	0.03%	0.03%	0.03%	0.04%	0.03%	0.03%	0.03%	0.03%	0.04%	0.03%	0.03%	0.03%	0.03%
Electriciy-pump	0.92%	0.82%	0.71%	0.76%	0.78%	0.91%	0.81%	0.69%	0.75%	0.76%	0.91%	0.81%	0.70%	0.75%	0.77%
Water	0.06%	0.70%	1.48%	1.09%	0.99%	0.08%	0.80%	1.62%	1.21%	1.11%	0.10%	0.79%	1.53%	1.17%	1.08%
Heat	0.26%	2.94%	6.25%	4.59%	4.18%	0.32%	3.36%	6.83%	5.13%	4.70%	0.43%	3.33%	6.45%	4.96%	4.57%
Sum	1.00E+00	1.00E+00	1.00E+00	1.00E+00	1.00E+00	1.00E+00	1.00E+00	1.00E+00	1.00E+00	1.00E+00	1.00E+00	1.00E+00	1.00E+00	1.00E+00	1.00E+00

	Australia					Global					Italy				
Stratospheric ozone depletion	Sc2	Sc6	Sc7	Sc8	Sc9	Sc2	Sc6	Sc7	Sc8	Sc9	Sc2	Sc6	Sc7	Sc8	Sc9
Stack material	3.54%	86.60%	58.39%	86.64%	74.60%	3.99%	75.59%	55.87%	75.62%	67.64%	3.91%	88.12%	63.17%	88.15%	77.88%
BOP material	0.00%	0.12%	0.08%	0.12%	0.10%	0.01%	0.11%	0.08%	0.11%	0.10%	0.01%	0.12%	0.09%	0.12%	0.11%
Electriciy-operation	95.19%	10.20%	39.06%	10.15%	22.47%	94.72%	21.46%	41.64%	21.43%	29.60%	94.81%	8.64%	34.17%	8.61%	19.12%
Electriciy-Stack assembly	0.22%	0.02%	0.09%	0.02%	0.05%	0.22%	0.05%	0.10%	0.05%	0.07%	0.22%	0.02%	0.08%	0.02%	0.04%
Electriciy-BOP assembly	0.04%	0.00%	0.01%	0.00%	0.01%	0.04%	0.01%	0.02%	0.01%	0.01%	0.04%	0.00%	0.01%	0.00%	0.01%
Electriciy-pump	0.89%	0.10%	0.37%	0.10%	0.21%	0.89%	0.20%	0.39%	0.20%	0.28%	0.89%	0.08%	0.32%	0.08%	0.18%
Water	0.09%	2.25%	1.51%	2.25%	1.94%	0.10%	1.96%	1.45%	1.96%	1.75%	0.10%	2.29%	1.64%	2.29%	2.02%
Heat	0.03%	0.71%	0.48%	0.71%	0.61%	0.03%	0.62%	0.46%	0.62%	0.56%	0.03%	0.73%	0.52%	0.73%	0.64%
Sum	1.00E+00	1.00E+00	1.00E+00	1.00E+00	1.00E+00	1.00E+00	1.00E+00	1.00E+00	1.00E+00	1.00E+00	1.00E+00	1.00E+00	1.00E+00	1.00E+00	1.00E+00

	Australia					Global					Italy				
Ionizing radiation	Sc2	Sc6	Sc7	Sc8	Sc9	Sc2	Sc6	Sc7	Sc8	Sc9	Sc2	Sc6	Sc7	Sc8	Sc9
Stack material	5.60%	81.19%	36.35%	65.41%	54.43%	0.13%	0.14%	0.14%	0.14%	0.14%	25.32%	81.49%	40.85%	68.22%	58.36%
BOP material	0.08%	1.11%	0.50%	0.90%	0.75%	0.00%	0.00%	0.00%	0.00%	0.00%	0.35%	1.12%	0.56%	0.94%	0.80%
Electriciy-operation	93.18%	17.26%	62.30%	33.11%	44.14%	98.67%	98.67%	98.67%	98.67%	98.67%	73.37%	16.96%	57.78%	30.29%	40.20%
Electriciy-Stack assembly	0.22%	0.04%	0.15%	0.08%	0.10%	0.23%	0.23%	0.23%	0.23%	0.23%	0.17%	0.04%	0.14%	0.07%	0.09%
Electriciy-BOP assembly	0.03%	0.01%	0.02%	0.01%	0.02%	0.04%	0.04%	0.04%	0.04%	0.04%	0.03%	0.01%	0.02%	0.01%	0.02%
Electriciy-pump	0.87%	0.16%	0.58%	0.31%	0.41%	0.92%	0.92%	0.92%	0.92%	0.92%	0.69%	0.16%	0.54%	0.28%	0.38%
Water	0.01%	0.20%	0.09%	0.16%	0.13%	0.00%	0.00%	0.00%	0.00%	0.00%	0.06%	0.20%	0.10%	0.17%	0.14%
Heat	0.00%	0.02%	0.01%	0.02%	0.02%	0.00%	0.00%	0.00%	0.00%	0.00%	0.01%	0.02%	0.01%	0.02%	0.02%
Sum	1.00E+00	1.00E+00	1.00E+00	1.00E+00	1.00E+00	1.00E+00	1.00E+00	1.00E+00	1.00E+00	1.00E+00	1.00E+00	1.00E+00	1.00E+00	1.00E+00	1.00E+00

	Australia					Global					Italy				
Ozone formation, Human health	Sc2	Sc6	Sc7	Sc8	Sc9	Sc2	Sc6	Sc7	Sc8	Sc9	Sc2	Sc6	Sc7	Sc8	Sc9
Stack material	2.53%	68.73%	49.03%	63.37%	59.14%	3.24%	64.85%	49.22%	60.78%	57.48%	5.45%	69.00%	52.11%	64.59%	61.02%
BOP material	0.00%	0.12%	0.08%	0.11%	0.10%	0.01%	0.11%	0.08%	0.10%	0.10%	0.01%	0.12%	0.09%	0.11%	0.10%
Electriciy-operation	95.53%	9.54%	35.14%	16.52%	22.00%	94.60%	14.59%	34.89%	19.87%	24.16%	91.73%	9.19%	31.14%	14.93%	19.56%
Electriciy-Stack assembly	0.22%	0.02%	0.08%	0.04%	0.05%	0.22%	0.03%	0.08%	0.05%	0.06%	0.21%	0.02%	0.07%	0.03%	0.05%
Electriciy-BOP assembly	0.04%	0.00%	0.01%	0.01%	0.01%	0.04%	0.01%	0.01%	0.01%	0.01%	0.03%	0.00%	0.01%	0.01%	0.01%
Electriciy-pump	0.89%	0.09%	0.33%	0.15%	0.21%	0.89%	0.14%	0.33%	0.19%	0.23%	0.86%	0.09%	0.29%	0.14%	0.18%
Water	0.06%	1.74%	1.24%	1.61%	1.50%	0.08%	1.64%	1.25%	1.54%	1.46%	0.14%	1.75%	1.32%	1.64%	1.55%
Heat	0.73%	19.75%	14.08%	18.20%	16.99%	0.93%	18.63%	14.14%	17.46%	16.51%	1.56%	19.82%	14.97%	18.56%	17.53%
Sum	1.00E+00	1.00E+00	1.00E+00	1.00E+00	1.00E+00	1.00E+00	1.00E+00	1.00E+00	1.00E+00	1.00E+00	1.00E+00	1.00E+00	1.00E+00	1.00E+00	1.00E+00

	Australia					Global					Italy				
Fine particulate matter formation	Sc2	Sc6	Sc7	Sc8	Sc9	Sc2	Sc6	Sc7	Sc8	Sc9	Sc2	Sc6	Sc7	Sc8	Sc9
Stack material	16.71%	88.22%	62.40%	87.34%	77.30%	17.00%	82.72%	62.44%	82.08%	74.46%	16.91%	89.31%	66.83%	88.59%	80.11%
BOP material	0.02%	0.09%	0.06%	0.09%	0.08%	0.02%	0.08%	0.06%	0.08%	0.07%	0.02%	0.09%	0.07%	0.09%	0.08%
Electriciy-operation	81.52%	7.53%	34.24%	8.44%	18.83%	81.22%	13.22%	34.20%	13.89%	21.76%	81.31%	6.40%	29.66%	7.14%	15.92%
Electriciy-Stack assembly	0.19%	0.02%	0.08%	0.02%	0.04%	0.19%	0.03%	0.08%	0.03%	0.05%	0.19%	0.01%	0.07%	0.02%	0.04%
Electriciy-BOP assembly	0.03%	0.00%	0.01%	0.00%	0.01%	0.03%	0.00%	0.01%	0.01%	0.01%	0.03%	0.00%	0.01%	0.00%	0.01%
Electriciy-pump	0.76%	0.07%	0.32%	0.08%	0.18%	0.76%	0.12%	0.32%	0.13%	0.20%	0.76%	0.06%	0.28%	0.07%	0.15%
Water	0.23%	1.23%	0.87%	1.22%	1.08%	0.24%	1.16%	0.87%	1.15%	1.04%	0.24%	1.25%	0.94%	1.24%	1.12%
Heat	0.54%	2.84%	2.01%	2.81%	2.49%	0.55%	2.66%	2.01%	2.64%	2.39%	0.54%	2.87%	2.15%	2.85%	2.58%
Sum	1.00E+00	1.00E+00	1.00E+00	1.00E+00	1.00E+00	1.00E+00	1.00E+00	1.00E+00	1.00E+00	1.00E+00	1.00E+00	1.00E+00	1.00E+00	1.00E+00	1.00E+00

	Australia					Global					Italy				
Ozone formation, Terrestrial ecosystems	Sc2	Sc6	Sc7	Sc8	Sc9	Sc2	Sc6	Sc7	Sc8	Sc9	Sc2	Sc6	Sc7	Sc8	Sc9
Stack material	2.58%	69.17%	49.52%	63.84%	59.62%	3.30%	65.30%	49.71%	61.26%	57.96%	5.53%	69.44%	52.60%	65.05%	61.49%
BOP material	0.00%	0.12%	0.09%	0.11%	0.10%	0.01%	0.11%	0.09%	0.11%	0.10%	0.01%	0.12%	0.09%	0.11%	0.11%
Electriciy-operation	95.48%	9.42%	34.81%	16.31%	21.76%	94.54%	14.41%	34.57%	19.64%	23.90%	91.66%	9.07%	30.83%	14.73%	19.34%
Electriciy-Stack assembly	0.22%	0.02%	0.08%	0.04%	0.05%	0.22%	0.03%	0.08%	0.05%	0.06%	0.21%	0.02%	0.07%	0.03%	0.05%
Electriciy-BOP assembly	0.04%	0.00%	0.01%	0.01%	0.01%	0.04%	0.01%	0.01%	0.01%	0.01%	0.03%	0.00%	0.01%	0.01%	0.01%
Electriciy-pump	0.89%	0.09%	0.33%	0.15%	0.20%	0.88%	0.13%	0.32%	0.18%	0.22%	0.86%	0.08%	0.29%	0.14%	0.18%
Water	0.06%	1.72%	1.23%	1.58%	1.48%	0.08%	1.62%	1.23%	1.52%	1.44%	0.14%	1.72%	1.31%	1.61%	1.53%
Heat	0.72%	19.46%	13.93%	17.96%	16.78%	0.93%	18.38%	13.99%	17.24%	16.31%	1.56%	19.54%	14.80%	18.31%	17.30%
Sum	1.00E+00	1.00E+00	1.00E+00	1.00E+00	1.00E+00	1.00E+00	1.00E+00	1.00E+00	1.00E+00	1.00E+00	1.00E+00	1.00E+00	1.00E+00	1.00E+00	1.00E+00

	Australia					Global					Italy				
Terrestrial acidification	Sc2	Sc6	Sc7	Sc8	Sc9	Sc2	Sc6	Sc7	Sc8	Sc9	Sc2	Sc6	Sc7	Sc8	Sc9
Stack material	4.81%	90.17%	71.29%	89.34%	82.62%	6.31%	87.67%	72.11%	87.01%	81.59%	14.13%	90.92%	74.86%	90.24%	84.65%
BOP material	0.00%	0.08%	0.06%	0.08%	0.07%	0.01%	0.07%	0.06%	0.07%	0.07%	0.01%	0.08%	0.06%	0.08%	0.07%
Electriciy-operation	93.84%	5.68%	25.18%	6.53%	13.48%	92.29%	8.26%	24.32%	8.94%	14.53%	84.21%	4.90%	21.49%	5.60%	11.38%
Electriciy-Stack assembly	0.22%	0.01%	0.06%	0.02%	0.03%	0.22%	0.02%	0.06%	0.02%	0.03%	0.20%	0.01%	0.05%	0.01%	0.03%
Electriciy-BOP assembly	0.04%	0.00%	0.01%	0.00%	0.01%	0.03%	0.00%	0.01%	0.00%	0.01%	0.03%	0.00%	0.01%	0.00%	0.00%
Electriciy-pump	0.88%	0.05%	0.24%	0.06%	0.13%	0.86%	0.08%	0.23%	0.08%	0.14%	0.79%	0.05%	0.20%	0.05%	0.11%
Water	0.06%	1.21%	0.95%	1.19%	1.11%	0.08%	1.17%	0.96%	1.16%	1.09%	0.19%	1.22%	1.00%	1.21%	1.13%
Heat	0.15%	2.80%	2.22%	2.78%	2.57%	0.20%	2.73%	2.24%	2.71%	2.54%	0.44%	2.83%	2.33%	2.81%	2.63%
Sum	1.00E+00	1.00E+00	1.00E+00	1.00E+00	1.00E+00	1.00E+00	1.00E+00	1.00E+00	1.00E+00	1.00E+00	1.00E+00	1.00E+00	1.00E+00	1.00E+00	1.00E+00

	Australia					Global					Italy				
Freshwater eutrophication	Sc2	Sc6	Sc7	Sc8	Sc9	Sc2	Sc6	Sc7	Sc8	Sc9	Sc2	Sc6	Sc7	Sc8	Sc9
Stack material	1.87%	92.53%	60.90%	92.77%	78.93%	2.72%	90.20%	63.35%	90.40%	79.08%	15.91%	93.94%	65.99%	94.14%	82.37%
BOP material	0.01%	0.28%	0.18%	0.28%	0.24%	0.01%	0.27%	0.19%	0.27%	0.24%	0.05%	0.28%	0.20%	0.28%	0.25%
Electriciy-operation	96.94%	6.78%	38.24%	6.54%	20.30%	96.10%	9.09%	35.80%	8.90%	20.16%	82.98%	5.38%	33.18%	5.18%	16.89%
Electriciy-Stack assembly	0.23%	0.02%	0.09%	0.02%	0.05%	0.22%	0.02%	0.08%	0.02%	0.05%	0.19%	0.01%	0.08%	0.01%	0.04%
Electriciy-BOP assembly	0.04%	0.00%	0.01%	0.00%	0.01%	0.04%	0.00%	0.01%	0.00%	0.01%	0.03%	0.00%	0.01%	0.00%	0.01%
Electriciy-pump	0.91%	0.06%	0.36%	0.06%	0.19%	0.90%	0.09%	0.34%	0.08%	0.19%	0.78%	0.05%	0.31%	0.05%	0.16%
Water	0.01%	0.32%	0.21%	0.32%	0.28%	0.01%	0.32%	0.22%	0.32%	0.28%	0.06%	0.33%	0.23%	0.33%	0.29%
Heat	0.00%	0.01%	0.00%	0.01%	0.01%	0.00%	0.01%	0.00%	0.01%	0.01%	0.00%	0.01%	0.00%	0.01%	0.01%
Sum	1.00E+00	1.00E+00	1.00E+00	1.00E+00	1.00E+00	1.00E+00	1.00E+00	1.00E+00	1.00E+00	1.00E+00	1.00E+00	1.00E+00	1.00E+00	1.00E+00	1.00E+00

	Australia					Global					Italy				
Marine eutrophication	Sc2	Sc6	Sc7	Sc8	Sc9	Sc2	Sc6	Sc7	Sc8	Sc9	Sc2	Sc6	Sc7	Sc8	Sc9
Stack material	0.86%	65.38%	19.13%	64.19%	36.08%	1.20%	36.18%	17.06%	35.87%	26.29%	5.67%	70.04%	22.73%	68.93%	41.22%
BOP material	0.00%	0.34%	0.10%	0.34%	0.19%	0.01%	0.19%	0.09%	0.19%	0.14%	0.03%	0.37%	0.12%	0.36%	0.22%
Electriciy-operation	97.94%	32.26%	79.34%	33.47%	62.08%	97.59%	61.98%	81.44%	62.29%	72.05%	93.03%	27.52%	75.67%	28.64%	56.85%
Electriciy-Stack assembly	0.23%	0.08%	0.19%	0.08%	0.15%	0.23%	0.14%	0.19%	0.15%	0.17%	0.22%	0.06%	0.18%	0.07%	0.13%
Electriciy-BOP assembly	0.04%	0.01%	0.03%	0.01%	0.02%	0.04%	0.02%	0.03%	0.02%	0.03%	0.03%	0.01%	0.03%	0.01%	0.02%
Electriciy-pump	0.92%	0.30%	0.74%	0.31%	0.58%	0.91%	0.58%	0.76%	0.58%	0.67%	0.87%	0.26%	0.71%	0.27%	0.53%
Water	0.02%	1.61%	0.47%	1.58%	0.89%	0.03%	0.89%	0.42%	0.89%	0.65%	0.14%	1.73%	0.56%	1.70%	1.02%
Heat	0.00%	0.01%	0.00%	0.01%	0.01%	0.00%	0.01%	0.00%	0.01%	0.01%	0.00%	0.02%	0.01%	0.02%	0.01%
Sum	1.00E+00	1.00E+00	1.00E+00	1.00E+00	1.00E+00	1.00E+00	1.00E+00	1.00E+00	1.00E+00	1.00E+00	1.00E+00	1.00E+00	1.00E+00	1.00E+00	1.00E+00

	Australia					Global					Italy				
Terrestrial ecotoxicity	Sc2	Sc6	Sc7	Sc8	Sc9	Sc2	Sc6	Sc7	Sc8	Sc9	Sc2	Sc6	Sc7	Sc8	Sc9
Stack material	5.42%	36.09%	6.30%	35.47%	13.97%	4.67%	17.93%	6.04%	17.80%	10.81%	6.48%	41.50%	7.72%	40.84%	16.85%
BOP material	0.11%	0.72%	0.13%	0.71%	0.28%	0.09%	0.36%	0.12%	0.36%	0.22%	0.13%	0.83%	0.15%	0.82%	0.34%
Electriciy-operation	93.07%	60.60%	92.14%	61.25%	84.02%	93.87%	79.83%	92.41%	79.96%	87.36%	91.94%	54.87%	90.63%	55.56%	80.97%
Electriciy-Stack assembly	0.22%	0.14%	0.22%	0.14%	0.20%	0.22%	0.19%	0.22%	0.19%	0.20%	0.21%	0.13%	0.21%	0.13%	0.19%
Electriciy-BOP assembly	0.03%	0.02%	0.03%	0.02%	0.03%	0.04%	0.03%	0.03%	0.03%	0.03%	0.03%	0.02%	0.03%	0.02%	0.03%
Electriciy-pump	0.87%	0.57%	0.86%	0.57%	0.79%	0.88%	0.75%	0.86%	0.75%	0.82%	0.86%	0.51%	0.85%	0.52%	0.76%
Water	0.23%	1.52%	0.27%	1.49%	0.59%	0.20%	0.76%	0.25%	0.75%	0.46%	0.27%	1.75%	0.33%	1.72%	0.71%
Heat	0.05%	0.34%	0.06%	0.33%	0.13%	0.04%	0.17%	0.06%	0.17%	0.10%	0.06%	0.39%	0.07%	0.38%	0.16%
Sum	1.00E+00	1.00E+00	1.00E+00	1.00E+00	1.00E+00	1.00E+00	1.00E+00	1.00E+00	1.00E+00	1.00E+00	1.00E+00	1.00E+00	1.00E+00	1.00E+00	1.00E+00

	Australia					Global					Italy				
Freshwater ecotoxicity	Sc2	Sc6	Sc7	Sc8	Sc9	Sc2	Sc6	Sc7	Sc8	Sc9	Sc2	Sc6	Sc7	Sc8	Sc9
Stack material	19.15%	95.38%	73.19%	95.63%	86.69%	25.31%	92.07%	73.95%	92.26%	85.17%	66.12%	96.25%	77.26%	96.45%	89.02%
BOP material	0.04%	0.22%	0.17%	0.22%	0.20%	0.06%	0.21%	0.17%	0.21%	0.20%	0.15%	0.22%	0.18%	0.22%	0.21%
Electriciy-operation	79.79%	4.09%	26.13%	3.85%	12.72%	73.67%	7.38%	25.37%	7.19%	14.23%	33.15%	3.23%	22.09%	3.03%	10.41%
Electriciy-Stack assembly	0.19%	0.01%	0.06%	0.01%	0.03%	0.17%	0.02%	0.06%	0.02%	0.03%	0.08%	0.01%	0.05%	0.01%	0.02%
Electriciy-BOP assembly	0.03%	0.00%	0.01%	0.00%	0.00%	0.03%	0.00%	0.01%	0.00%	0.01%	0.01%	0.00%	0.01%	0.00%	0.00%
Electriciy-pump	0.75%	0.04%	0.24%	0.04%	0.12%	0.69%	0.07%	0.24%	0.07%	0.13%	0.31%	0.03%	0.21%	0.03%	0.10%
Water	0.05%	0.25%	0.19%	0.25%	0.23%	0.07%	0.24%	0.20%	0.24%	0.23%	0.18%	0.25%	0.20%	0.26%	0.24%
Heat	0.00%	0.00%	0.00%	0.00%	0.00%	0.00%	0.00%	0.00%	0.00%	0.00%	0.00%	0.00%	0.00%	0.00%	0.00%
Sum	1.00E+00	1.00E+00	1.00E+00	1.00E+00	1.00E+00	1.00E+00	1.00E+00	1.00E+00	1.00E+00	1.00E+00	1.00E+00	1.00E+00	1.00E+00	1.00E+00	1.00E+00

	Australia					Global					Italy				
Marine ecotoxicity	Sc2	Sc6	Sc7	Sc8	Sc9	Sc2	Sc6	Sc7	Sc8	Sc9	Sc2	Sc6	Sc7	Sc8	Sc9
Stack material	49.58%	80.71%	67.55%	80.83%	75.82%	54.65%	78.81%	67.99%	78.91%	74.87%	71.16%	81.17%	70.14%	81.27%	77.16%
BOP material	10.12%	16.48%	13.79%	16.50%	15.48%	11.16%	16.09%	13.88%	16.11%	15.28%	14.53%	16.57%	14.32%	16.59%	15.75%
Electriciy-operation	39.71%	2.62%	18.30%	2.48%	8.44%	33.68%	4.88%	17.78%	4.76%	9.58%	14.00%	2.06%	15.22%	1.94%	6.85%
Electriciy-Stack assembly	0.09%	0.01%	0.04%	0.01%	0.02%	0.08%	0.01%	0.04%	0.01%	0.02%	0.03%	0.00%	0.04%	0.00%	0.02%
Electriciy-BOP assembly	0.01%	0.00%	0.01%	0.00%	0.00%	0.01%	0.00%	0.01%	0.00%	0.00%	0.01%	0.00%	0.01%	0.00%	0.00%
Electriciy-pump	0.37%	0.02%	0.17%	0.02%	0.08%	0.32%	0.05%	0.17%	0.04%	0.09%	0.13%	0.02%	0.14%	0.02%	0.06%
Water	0.10%	0.16%	0.13%	0.16%	0.15%	0.11%	0.15%	0.13%	0.15%	0.15%	0.14%	0.16%	0.14%	0.16%	0.15%
Heat	0.00%	0.01%	0.00%	0.01%	0.00%	0.00%	0.00%	0.00%	0.01%	0.00%	0.00%	0.01%	0.00%	0.01%	0.00%
Sum	1.00E+00	1.00E+00	1.00E+00	1.00E+00	1.00E+00	1.00E+00	1.00E+00	1.00E+00	1.00E+00	1.00E+00	1.00E+00	1.00E+00	1.00E+00	1.00E+00	1.00E+00

	Australia					Global					Italy				
Human carcinogenic toxicity	Sc2	Sc6	Sc7	Sc8	Sc9	Sc2	Sc6	Sc7	Sc8	Sc9	Sc2	Sc6	Sc7	Sc8	Sc9
Stack material	44.70%	68.74%	20.78%	68.88%	38.87%	39.45%	61.81%	22.58%	61.91%	39.15%	32.76%	73.50%	24.64%	73.62%	44.27%
BOP material	0.74%	1.14%	0.35%	1.14%	0.65%	0.66%	1.03%	0.38%	1.03%	0.65%	0.54%	1.22%	0.41%	1.22%	0.74%
Electriciy-operation	53.56%	29.23%	77.77%	29.09%	59.46%	58.88%	36.24%	75.95%	36.14%	59.18%	65.65%	24.41%	73.86%	24.28%	54.00%
Electriciy-Stack assembly	0.13%	0.07%	0.18%	0.07%	0.14%	0.14%	0.08%	0.18%	0.08%	0.14%	0.15%	0.06%	0.17%	0.06%	0.13%
Electriciy-BOP assembly	0.02%	0.01%	0.03%	0.01%	0.02%	0.02%	0.01%	0.03%	0.01%	0.02%	0.02%	0.01%	0.03%	0.01%	0.02%
Electriciy-pump	0.50%	0.27%	0.73%	0.27%	0.56%	0.55%	0.34%	0.71%	0.34%	0.55%	0.61%	0.23%	0.69%	0.23%	0.51%
Water	0.33%	0.51%	0.15%	0.51%	0.29%	0.29%	0.46%	0.17%	0.46%	0.29%	0.24%	0.54%	0.18%	0.54%	0.33%
Heat	0.02%	0.03%	0.01%	0.03%	0.02%	0.02%	0.03%	0.01%	0.03%	0.02%	0.02%	0.03%	0.01%	0.03%	0.02%
Sum	1.00E+00	1.00E+00	1.00E+00	1.00E+00	1.00E+00	1.00E+00	1.00E+00	1.00E+00	1.00E+00	1.00E+00	1.00E+00	1.00E+00	1.00E+00	1.00E+00	1.00E+00

	Australia					Global					Italy				
Human non-carcinogenic toxicity	Sc2	Sc6	Sc7	Sc8	Sc9	Sc2	Sc6	Sc7	Sc8	Sc9	Sc2	Sc6	Sc7	Sc8	Sc9
Stack material	82.32%	92.90%	66.92%	93.24%	82.34%	72.13%	79.55%	62.23%	79.76%	72.85%	83.72%	94.01%	71.46%	94.29%	85.14%
BOP material	0.91%	1.03%	0.74%	1.03%	0.91%	0.80%	0.88%	0.69%	0.88%	0.80%	0.92%	1.04%	0.79%	1.04%	0.94%
Electriciy-operation	16.14%	5.52%	31.60%	5.17%	16.11%	26.37%	18.92%	36.31%	18.71%	25.64%	14.73%	4.39%	27.04%	4.11%	13.30%
Electriciy-Stack assembly	0.04%	0.01%	0.07%	0.01%	0.04%	0.06%	0.04%	0.08%	0.04%	0.06%	0.03%	0.01%	0.06%	0.01%	0.03%
Electriciy-BOP assembly	0.01%	0.00%	0.01%	0.00%	0.01%	0.01%	0.01%	0.01%	0.01%	0.01%	0.01%	0.00%	0.01%	0.00%	0.00%
Electriciy-pump	0.15%	0.05%	0.30%	0.05%	0.15%	0.25%	0.18%	0.34%	0.18%	0.24%	0.14%	0.04%	0.25%	0.04%	0.12%
Water	0.43%	0.49%	0.35%	0.49%	0.43%	0.38%	0.42%	0.33%	0.42%	0.38%	0.44%	0.49%	0.37%	0.49%	0.45%
Heat	0.01%	0.01%	0.01%	0.01%	0.01%	0.01%	0.01%	0.01%	0.01%	0.01%	0.01%	0.01%	0.01%	0.01%	0.01%
Sum	1.00E+00	1.00E+00	1.00E+00	1.00E+00	1.00E+00	1.00E+00	1.00E+00	1.00E+00	1.00E+00	1.00E+00	1.00E+00	1.00E+00	1.00E+00	1.00E+00	1.00E+00

	Australia					Global					Italy				
Land use	Sc2	Sc6	Sc7	Sc8	Sc9	Sc2	Sc6	Sc7	Sc8	Sc9	Sc2	Sc6	Sc7	Sc8	Sc9
Stack material	1.56%	51.58%	14.59%	56.93%	28.44%	2.11%	49.40%	16.29%	53.43%	29.89%	4.66%	56.89%	17.53%	62.07%	33.06%
BOP material	0.01%	0.30%	0.08%	0.33%	0.16%	0.01%	0.28%	0.09%	0.31%	0.17%	0.03%	0.33%	0.10%	0.36%	0.19%
Electriciy-operation	97.12%	43.21%	83.08%	37.44%	68.15%	96.53%	45.56%	81.25%	41.21%	66.59%	93.79%	37.48%	79.92%	31.90%	63.17%
Electriciy-Stack assembly	0.23%	0.10%	0.19%	0.09%	0.16%	0.23%	0.11%	0.19%	0.10%	0.16%	0.22%	0.09%	0.19%	0.07%	0.15%
Electriciy-BOP assembly	0.04%	0.02%	0.03%	0.01%	0.03%	0.04%	0.02%	0.03%	0.02%	0.02%	0.04%	0.01%	0.03%	0.01%	0.02%
Electriciy-pump	0.91%	0.40%	0.78%	0.35%	0.64%	0.90%	0.43%	0.76%	0.39%	0.62%	0.88%	0.35%	0.75%	0.30%	0.59%
Water	0.13%	4.20%	1.19%	4.64%	2.32%	0.17%	4.02%	1.33%	4.35%	2.44%	0.38%	4.64%	1.43%	5.06%	2.69%
Heat	0.01%	0.19%	0.05%	0.21%	0.11%	0.01%	0.18%	0.06%	0.20%	0.11%	0.02%	0.21%	0.07%	0.23%	0.12%
Sum	1.00E+00	1.00E+00	1.00E+00	1.00E+00	1.00E+00	1.00E+00	1.00E+00	1.00E+00	1.00E+00	1.00E+00	1.00E+00	1.00E+00	1.00E+00	1.00E+00	1.00E+00

	Australia					Global					Italy				
Mineral resource scarcity	Sc2	Sc6	Sc7	Sc8	Sc9	Sc2	Sc6	Sc7	Sc8	Sc9	Sc2	Sc6	Sc7	Sc8	Sc9
Stack material	57.22%	73.16%	24.38%	71.96%	43.74%	54.83%	66.56%	26.36%	65.73%	44.00%	62.76%	77.38%	28.65%	76.30%	49.23%
BOP material	0.07%	0.09%	0.03%	0.09%	0.06%	0.07%	0.09%	0.03%	0.08%	0.06%	0.08%	0.10%	0.04%	0.10%	0.06%
Electriciy-operation	42.04%	26.23%	74.63%	27.42%	55.42%	44.42%	32.78%	72.65%	33.61%	55.16%	36.55%	22.05%	70.39%	23.12%	49.97%
Electriciy-Stack assembly	0.10%	0.06%	0.17%	0.06%	0.13%	0.10%	0.08%	0.17%	0.08%	0.13%	0.09%	0.05%	0.16%	0.05%	0.12%
Electriciy-BOP assembly	0.02%	0.01%	0.03%	0.01%	0.02%	0.02%	0.01%	0.03%	0.01%	0.02%	0.01%	0.01%	0.03%	0.01%	0.02%
Electriciy-pump	0.39%	0.25%	0.70%	0.26%	0.52%	0.42%	0.31%	0.68%	0.31%	0.52%	0.34%	0.21%	0.66%	0.22%	0.47%
Water	0.15%	0.19%	0.06%	0.19%	0.11%	0.14%	0.17%	0.07%	0.17%	0.11%	0.16%	0.20%	0.07%	0.20%	0.13%
Heat	0.00%	0.01%	0.00%	0.01%	0.00%	0.00%	0.01%	0.00%	0.00%	0.00%	0.00%	0.01%	0.00%	0.01%	0.00%
Sum	1.00E+00	1.00E+00	1.00E+00	1.00E+00	1.00E+00	1.00E+00	1.00E+00	1.00E+00	1.00E+00	1.00E+00	1.00E+00	1.00E+00	1.00E+00	1.00E+00	1.00E+00

	Australia					Global					Italy				
Fossil resource scarcity	Sc2	Sc6	Sc7	Sc8	Sc9	Sc2	Sc6	Sc7	Sc8	Sc9	Sc2	Sc6	Sc7	Sc8	Sc9
Stack material	0.55%	51.70%	27.49%	49.24%	39.46%	0.66%	47.91%	28.46%	46.13%	38.61%	0.72%	53.04%	30.73%	50.94%	42.24%
BOP material	0.00%	0.27%	0.14%	0.26%	0.21%	0.00%	0.25%	0.15%	0.24%	0.20%	0.00%	0.28%	0.16%	0.26%	0.22%
Electriciy-operation	97.96%	19.21%	56.49%	23.00%	38.06%	97.79%	25.04%	54.99%	27.79%	39.36%	97.70%	17.15%	51.50%	20.38%	33.78%
Electriciy-Stack assembly	0.23%	0.04%	0.13%	0.05%	0.09%	0.23%	0.06%	0.13%	0.06%	0.09%	0.23%	0.04%	0.12%	0.05%	0.08%
Electriciy-BOP assembly	0.04%	0.01%	0.02%	0.01%	0.01%	0.04%	0.01%	0.02%	0.01%	0.01%	0.04%	0.01%	0.02%	0.01%	0.01%
Electriciy-pump	0.92%	0.18%	0.53%	0.22%	0.36%	0.92%	0.23%	0.51%	0.26%	0.37%	0.91%	0.16%	0.48%	0.19%	0.32%
Water	0.03%	3.28%	1.74%	3.12%	2.50%	0.04%	3.04%	1.80%	2.92%	2.45%	0.05%	3.36%	1.95%	3.23%	2.68%
Heat	0.27%	25.31%	13.46%	24.11%	19.32%	0.32%	23.46%	13.93%	22.58%	18.90%	0.35%	25.97%	15.04%	24.94%	20.68%
Sum	1.00E+00	1.00E+00	1.00E+00	1.00E+00	1.00E+00	1.00E+00	1.00E+00	1.00E+00	1.00E+00	1.00E+00	1.00E+00	1.00E+00	1.00E+00	1.00E+00	1.00E+00

	Australia					Global					Italy				
Water consumption	Sc2	Sc6	Sc7	Sc8	Sc9	Sc2	Sc6	Sc7	Sc8	Sc9	Sc2	Sc6	Sc7	Sc8	Sc9
Stack material	0.03%	0.29%	0.04%	0.30%	0.08%	0.04%	0.25%	0.04%	0.26%	0.09%	0.09%	0.36%	0.04%	0.37%	0.11%
BOP material	0.00%	0.01%	0.00%	0.01%	0.00%	0.00%	0.00%	0.00%	0.00%	0.00%	0.00%	0.01%	0.00%	0.01%	0.00%
Electriciy-operation	98.22%	93.01%	98.10%	92.84%	97.09%	98.04%	93.69%	98.00%	93.57%	96.96%	97.00%	91.50%	97.92%	91.28%	96.67%
Electriciy-Stack assembly	0.23%	0.22%	0.23%	0.22%	0.23%	0.23%	0.22%	0.23%	0.22%	0.23%	0.23%	0.21%	0.23%	0.21%	0.23%
Electriciy-BOP assembly	0.04%	0.03%	0.04%	0.03%	0.04%	0.04%	0.04%	0.04%	0.04%	0.04%	0.04%	0.03%	0.04%	0.03%	0.04%
Electriciy-pump	0.92%	0.87%	0.92%	0.87%	0.91%	0.92%	0.88%	0.92%	0.88%	0.91%	0.91%	0.86%	0.92%	0.85%	0.90%
Water	0.56%	5.54%	0.68%	5.70%	1.64%	0.73%	4.89%	0.77%	5.00%	1.77%	1.72%	6.97%	0.84%	7.19%	2.04%
Heat	0.00%	0.04%	0.00%	0.04%	0.01%	0.01%	0.03%	0.01%	0.04%	0.01%	0.01%	0.05%	0.01%	0.05%	0.01%
Sum	1.00E+00	1.00E+00	1.00E+00	1.00E+00	1.00E+00	1.00E+00	1.00E+00	1.00E+00	1.00E+00	1.00E+00	1.00E+00	1.00E+00	1.00E+00	1.00E+00	1.00E+00

4.6 References

[1] A. Aghakhani, N. Haque, C. Saccani, M. Pellegrini and A. Guzzini, “Direct carbon footprint of hydrogen generation via PEM and Alkaline electrolysers using various electrical energy sources and considering cell characteristics, unpublished,” 2023.

[2] A. P. Pavlos Nikolaidis, “A comparative overview of hydrogen production processes,” *Renewable and Sustainable Energy Reviews,* vol. 67, pp. 597-611, 2017.

[3] K. G. d. Santos, C. T. Eckerta, E. D. Rossi, R. A. Bariccatti, E. P. Frigo, C. A. Lindino and H. J. Alves, “Hydrogen production in the electrolysis of water in Brazil, a review,” *Renewable and Sustainable Energy Reviews,* vol. 68, pp. 563-571, 2017.

[4] “Products and Markets-Hydrogen,” Gulf Cryo, [Online]. Available: https://www.gulfcryo.com/gas_hydrogen.html. [Accessed 12 January 2023].

[5] O. Faye, J. Szpunar and U. Eduok, “A critical review on the current technologies for the generation, storage, and transportation of hydrogen,” *International Journal of Hydrogen Energy,* vol. 47, no. 29, pp. 13771-13802, 2022.

[6] I. Gondal and M. Sahir, “Prospects of natural gas pipeline infrastructure in hydrogen transportation,” *International Journal of Energy Research,* vol. 36, no. 15, pp. 1338-1345, 2012.

[7] M. Pellegrini, A. Guzzini and C. Saccani, “A Preliminary Assessment of the Potential of Low Percentage Green Hydrogen Blending in the Italian Natural Gas Network,” *energies,* vol. 13, p. 5570, 2020.

[8] J. Bard, N. Gerhardt, P. Selzam, M. Beil, D. M. Wiemer and M. Buddensiek, “THE LIMITATIONS OF HYDROGEN BLENDING IN THE EUROPEAN GAS GRID A study on the use, limitations and cost of hydrogen blending in the European gas grid at the transport and distribution level,” January 2022. [Online]. Available: https://www.iee.fraunhofer.de/content/dam/iee/energiesystemtechnik/en/documents/Studies-Reports/FINAL_FraunhoferIEE_ShortStudy_H2_Blending_EU_ECF_Jan22.pdf. [Accessed 29 August 2022].

[9] L. M.Romeo, M. Cavana, M. Bailera, P. Leone, B. Peña and P. Lisbona, “Non-stoichiometric methanation as strategy to overcome the limitations of green hydrogen injection into the natural gas grid,” *Applied Energy,* vol. 309, p. 118462, 2022.

[10] B. Hurtubia and E. Sauma, “Economic and environmental analysis of hydrogen production when complementing renewable energy generation with grid electricity,” *Applied Energy,* vol. 304, p. 117739, 2021.

[11] M. Delpierre, J. Quist, J. Mertens, A. Prieur-Vernat and S. Cucurachi, “Assessing the environmental impacts of wind-based hydrogen production in the Netherlands using ex-ante LCA and scenarios analysis,” *Journal of Cleaner Production,* vol. 299, p. 126866, 2021.

[12] IEA, “Electrolysers,” IEA, [Online]. Available: https://www.iea.org/reports/electrolysers. [Accessed 12 January 2023].

[13] S. Kumar and V.Himabindu, “Hydrogen production by PEM water electrolysis – A review,” *Materials Science for Energy Technologies,* vol. 2, no. 3, pp. 442-454 , 2019.

[14] M. Algren, W. Fisher and A. E. Landis, “Chapter 8 - Machine learning in life cycle assessment,” in *Data Science Applied to Sustainability Analysis,* Elsevier, 2021 , pp. 167-190.

[15] E. Schropp, G. Naumann and a. M. Gaderer, “Life Cycle Assessment of a Polymer Electrolyte Membrane Water Electrolysis,” in *In Progress in Life Cycle Assessment,* Springer, 2019, pp. 53-66.

[16] G. Zhao, M. R. Kraglund, H. L. Frandsen, A. C. Wulff, S. H. Jensen, M. Chen and a. C. R. Graves, “Life cycle assessment of H2O electrolysis technologies.,” *International Journal of Hydrogen Energy,* vol. 45, no. 43, pp. 23765-23781, 2020.

[17] X. Zhang, C. Bauer, C. L. Mutel and a. K. Volkart, “Life Cycle Assessment of Power-to-Gas: Approaches, system variations and their environmental implications,” *Applied Energy,* vol. 190, pp. 326-338, 2017.

[18] K. Bareiß, C. d. l. Rua, M. Möckl and T. Hamacher, “Life cycle assessment of hydrogen from proton exchange membrane water electrolysis in future energy systems,” *Applied Energy,* vol. 237, pp. 862-872, 2019.

[19] M. Delpierre, J. Quist, J. Mertens, A. Prieur-Vernat and a. S. Cucurachi, “Assessing the environmental impacts of wind-based hydrogen production in the Netherlands using ex-ante LCA and scenarios analysis,” *Journal of Cleaner Production,* vol. 299, p. 126866, 2021.

[20] G. Zhao and a. A. S. Pedersen, “Life cycle assessment of hydrogen production and consumption in an isolated territory,” *Procedia CIRP,* vol. 69, pp. 529-533, 2018.

[21] J. Zhang, B. Ling, Y. He, Y. Zhu and a. Z. Wang, “Life cycle assessment of three types of hydrogen production methods using solar energy,” *International Journal of Hydrogen Energy,* vol. 47, no. 30, pp. 14158-14168, 2022.

[22] A. Lozanovski, O. Schuller and M. Faltenbacher, “ Guidance Document for performing LCAs on Fuel Cells and H2 Technologies,” 2011. [Online]. Available: http://hytechcycling.eu/wp-content/uploads/HY-Guidance-Document.pdf. [Accessed 7 November 2022].

[23] C. Wulf and a. M. Kaltschmitt, “Hydrogen supply chains for mobility—environmental and economic assessment.,” *Sustainability,* vol. 10, no. 6, p. 1699, 2018.

[24] E. W. Technology, “Mixed Bed Ion Exchange,” EWT Water Technology, 2018. [Online]. Available: http://www.ewt-wasser.de/en/product/mixed-bed.html. [Accessed 10 November 2022].

[25] S. Energy, “Alkaline Water Electrolysis and Refueling Equipment,” SinoHy Energy, [Online]. Available: https://www.sinohyenergy.com/alkaline-water-electrolysis-and-refueling-equipment/?utm_campaignid=14164801656&utm_adgroupid=127184701882&utm_creative=537473751324&utm_network=g&utm_matchtype=p&utm_device=c&utm_term=hydrogen%20production%20plant&utm_placeme. [Accessed 11 November 2022].

[26] H. company, “Plate Heat Exchanger,” [Online]. Available: https://www.hisaka.co.jp/english/phe/cgi-other/catalog/96/file.pdf. [Accessed 15 November 2022].

[27] M. Lehner, R. Tichler, H. Steinmüller and a. M. Koppe, Power-to-gas: technology and business models, Springer, 2014.

[28] N. Gerloff, “Comparative Life-Cycle-Assessment analysis of three major water electrolysis technologies while applying various energy scenarios for a greener hydrogen production,” *Journal of Energy Storage,* vol. 43, p. 102759, 2021.

[29] A. Mehmeti, A. Angelis-Dimakis, G. Arampatzis, S. J. McPhail and a. S. Ulgiati, “Life cycle assessment and water footprint of hydrogen production methods: from conventional to emerging technologies.,” *Environments,* vol. 5, no. 2, p. 24, 2018.

[30] C. Rakousky, G. P. Keeley, K. Wippermann, M. Carmo and a. D. Stolten., “The stability challenge on the pathway to high-current-density polymer electrolyte membrane water electrolyzers.,” *Electrochimica acta* , vol. 278, pp. 324-331, 2018.

[31] S. S. Kumar, S. U. B. Ramakrishna, B. R. Devi and a. V. Himabindu, “Phosphorus-doped carbon nanoparticles supported palladium electrocatalyst for the hydrogen evolution reaction (HER) in PEM water electrolysis.,” *Ionics,* vol. 24, no. 10, pp. 3113-3121, 2018.

[32] M. Bernt and a. H. A. Gasteiger, “Influence of ionomer content in IrO2/TiO2 electrodes on PEM water electrolyzer performance,” *Journal of The Electrochemical Society,* vol. 163, no. 11, p. F3179, 2016.

[33] S. S. Kumar, S. U. B. Ramakrishna, D. Bhagawan and a. V. Himabindu., “Preparation of RuxPd1-xO2 electrocatalysts for the oxygen evolution reaction (OER) in PEM water electrolysis.,” *Ionics,* vol. 24, no. 8, pp. 2411-2419, 2018.

[34] P. Millet, R. Ngameni, S. A. Grigoriev, N. Mbemba, F. Brisset, A. Ranjbari and a. C. Etiévant, “PEM water electrolyzers: From electrocatalysis to stack development,” *International Journal of hydrogen energy,* vol. 35, no. 10, pp. 5043-5052, 2010.

[35] A. D. Blasi, L. Andaloro, S. Siracusano, N. Briguglio, G. Brunaccini, A. Stassi, A. S. Arico and a. V. Antonucci, “Evaluation of materials and components degradation of a PEM electrolyzer for marine applications,” *International journal of hydrogen energy,* vol. 38, no. 18, pp. 7612-7615, 2013.

[36] S. Siracusano, V. Baglio, A. D. Blasi, N. Briguglio, A. Stassi, R. Ornelas, E. Trifoni, V. Antonucci and a. A. S. Arico, “Electrochemical characterization of single cell and short stack PEM electrolyzers based on a nanosized IrO2 anode electrocatalyst,” *International journal of hydrogen energy,* vol. 35, no. 11, pp. 5558-5568, 2010.

[37] S. Siracusano, A. D. Blasi, V. Baglio, G. Brunaccini, N. Briguglio, A. Stassi, R. Ornelas, E. Trifoni, V. Antonucci and a. A. S. Aricò, “Optimization of components and assembling in a PEM electrolyzer stack,” *International Journal of Hydrogen Energy,* vol. 36, no. 5, pp. 3333-3339, 2011.

5 CHAPTER 5: Hydrogen delivery

ABSTRACT

Hydrogen should be transported and distributed by a reliable delivery infrastructure from the hydrogen generation plant to end-users such as hydrogen refuelling stations. The infrastructure capacity must be proportional to the demand. There are three main delivery methods for hydrogen delivery, tube trailers, pipelines, and cryogenic tankers. Tube trailers and pipelines are mainly used for the gaseous form of hydrogen, and cryogenic tankers are used for the liquid form. Pipelines are mostly used to supply high-demand districts and for users such as large industrial users, while tube-trailers and medium cryogenic tankers are used for smaller regions and located at closer distances. Large cryogenic tankers can be used for sea transport which is more affordable compared to pipeline instalment in the marine environment for general export. To reach a sustainable and affordable delivery method several challenges for each pathway must be addressed. Pipeline pathway challenges are its high cost, probability of leakage, hydrogen embrittlement of steel pipelines, issues with the geological storage such as contamination and leak, selection of preferred pipeline route, and monitoring and maintenance. Tube-trailers pathway challenges are the need for high-resistance tubes and reliable compressors to reach desired high loading pressure and high storage cost. Cryogenic tanker pathway challenges are cost, specialised liquid hydrogen ship, boil-off at tank wall and during unloading at the refuelling station, and high cost to reach very low temperature. Carrier materials are another hydrogen delivery method that is not mature and needs more research and development. These are synthetic chemicals such as methanation, ammonia, liquid organic hydrogen carriers (LOHC), and metal hydrides. The safety issue is an integral part of all delivery methods that is associated with the physical and chemical properties of hydrogen. Issues related to untrained people for refuelling cars and domestic consumption should be taken into account for safety considerations. The pipeline is likely to be the safest and most economical way of hydrogen distribution. The reason could be the lower likelihood of accidents and exposure to humans. In this chapter, in addition to providing general information about various pathways, environmental impact, cost, policies, and safety issues, a comparison of the hydrogen content of carriers is provided. In addition, a hydrogen transportation model is proposed that can be used to optimize the total cost of hydrogen delivery from several hydrogen production plants to end-users. Furthermore, the proposed model can be used for the determination of the location and capacity of the new hydrogen generation plant.

Keywords:

Hydrogen, Hydrogen delivery, transportation, distribution, pipeline, transport model

5.1 Hydrogen Delivery infrastructures

Hydrogen generation system as a large socio-technical system requires an appropriate infrastructure to operate properly [1]. Hydrogen delivery plays an important role in energy consumption, emissions, and hydrogen fuel economy. It is possible to increase the market penetration of hydrogen technology by a suitable hydrogen delivery method. The focus of this chapter is the hydrogen delivery infrastructures, from production facilities to the end consumers. Hydrogen production can be divided into two categories regarding the hydrogen generation facilities' location, centralized and decentralized. Centralized is referred to the hydrogen generation in large-scale plants which is called off-site. Decentralized is related to the generation on the spot, called on-site production [2]. Proper hydrogen delivery infrastructure including transmission and distribution is needed for centralized hydrogen production to be able to supply the hydrogen demand. Transmission is associated with the hydrogen delivery from the production sites to the city gates or the areas of consumption, and distribution is referred to the delivery from the city gates to the fuelling stations or end users [3].

The specific cost of centralized hydrogen generation is less than decentralized one because of the economy of scale [2]. Although on-site hydrogen production is expensive, in districts without considerable hydrogen demand and in cases where end users are located on islands or a far distance from production plants, decentralized hydrogen is a suitable choice due to less delivery and distribution cost. For remote users, on-site natural gas steam reforming or electrolysis is the preferred choice for hydrogen production [4].Delivery of hydrogen as an integral part of hydrogen technology arises several questions as follow:

-What are the possible current and future hydrogen delivery pathways?
-What are the environmental impact and cost of hydrogen delivery pathways?
-How is it possible to optimize the hydrogen delivery?

Hydrogen demand is an important parameter for the determination of the transport infrastructure scale. It can be predicted that hydrogen transport will be developed as a result of the expansion of the hydrogen market and the increase in hydrogen fuel acceptance in society. Delivery of green hydrogen requires longer delivery distances [5] because of the geographical location of the suitable regions with the potential for renewable energy generation which are usually far from city gates.

There are three primary methods for hydrogen delivery from generation sites to the end users: 1) tube-trailer or pressurized tank delivery, 2) pipeline delivery, and 3) cryogenic tankers or liquid delivery [5, 6]. These means of hydrogen delivery can be used either for the transmission or distribution of hydrogen. It provides the opportunity to combine pathways for transporting hydrogen to the end users and hydrogen refuelling stations (HRS) [5]. Examples of pathways combination assessment are provided in Elgowainy et al. [5] study, pipeline and liquid delivery pathway, pipeline and tube-trailer delivery pathway. Similar methods to trucks are possible such as barge or rail transportation, the problem is their lower geographic availability [7]. Variations of the pressure and temperature can change the hydrogen form from liquid to gaseous or vice versa. This change in the form could affect the means of transportation. To optimize the cost of hydrogen storage and delivery, it is desired to reduce the large hydrogen gas volume. Hydrogen gas has very low volumetric energy density under standard condition, almost more than three orders of magnitude less than gasoline. *It should be noted that standard condition is associated with the* standard temperature and atmospheric pressure. The volume of 1 kg of hydrogen is 11 m^3 under standard condition [8, 9].

It is possible to deliver hydrogen in gaseous form, liquid form, or by means of carrier chemicals. Gaseous delivery could be via truck (tube trailer) or pipeline, the liquid form can be delivered by means of tank truck and the delivery of carriers can be done via tank trucks or pipeline [7].

Various parameters affect the choice of the delivery pathway such as the regional sources, geographical characteristics, forecasted demand, district population, consuming behaviours, population density, size of HRS, and market penetration of hydrogen-consuming units such as fuel cell vehicles [1, 3]. Furthermore, industries’ decision in terms of the type of fuel is a critical aspect of the hydrogen pathway options. The pipeline pathway is the most favourable method in regions with high market penetration, high population density, and large HRS. In regions with low population, low population density, low demand, low market penetration, and small HRS, compressed gas trucks can be the main pathway. For areas with a large population with low population density and small HRS, liquid hydrogen could be the desired pathway for hydrogen delivery [10].

Currently, the most used method for hydrogen delivery to stations is trucks, while delivery by means of the pipeline is not used a lot [11]. According to the predictions for 2050, approximately all stationary hydrogen consumers, such as industries, households, and services, will be joined to regional pipeline networks and liquefied hydrogen will be consumed to supply HRS demand [4]. An example of accelerating decarbonisation via hydrogen infrastructure is European Hydrogen Backbone (EHB) project. The objective of this project is decarbonisation acceleration in Europe based on existing and new pipelines. According to the EHB report, 53,000 km pipeline is needed by 2040, 60% of repurposed natural gas pipelines, and 40% of new pipeline extension, which could cost around € 80-143 billion [12].

HRS can be considered as the final destination of hydrogen delivery If the produced hydrogen is used as fuel in a hydrogen vehicle (HV). HRS type varies depending on the delivery mode regarding the hydrogen form: (i) HRS relied on compressed gas, which further compression from the station delivery pressure to the desired hydrogen vehicle storage pressure is required, (ii) HRS relied on liquid hydrogen delivery [9]. Therefore, the delivery method should include several major stages and units or elements such as liquefiers, pipelines, trucks, terminals, and HRS [5]. In this case, the system units included in the delivery pathway considering the hydrogen form and pathway type could be as follow [9]:

- Gas pipeline: Compression and storage at hydrogen plant, gas pipelines, HRS, compressor, high-pressure storage, dispensers
- Compressed gas trucks: Compression and storage at hydrogen plant, compressed gas trucks, HRS, compressor, high-pressure storage, dispensers
- Liquid H_2 trucks: liquefaction and storage at hydrogen plant, liquid hydrogen trucks, HRS, liquid hydrogen storage, liquid hydrogen pump, high-pressure storage, dispensers

For compressed gas delivery by pipeline or truck, compression and storage at the hydrogen plant are needed, while in liquid hydrogen delivery, liquefaction, storage at the central plant, and liquid hydrogen storage tanks are required.

It is recognized from the system components that storage is one of the most essential parts of hydrogen delivery which is required to overcome the demand and supply imbalances. Storage is provided at HRS and the hydrogen generation plant to respond properly to the time variations in hydrogen demand and to provide a satisfactory and reliable hydrogen supply [9]. Hydrogen storage is a relatively expensive part of hydrogen delivery infrastructure [7]. Variations in demand and production can be used to determine the storage characteristics such as size and pressure. Two types of storage for hydrogen delivery associated with the temporal variation in demand are short-term and long-term. Short-term covers hourly variations in demand and long-term are related to seasonal variations in demand and outages in the schedule of the hydrogen production plant [5]. Based on the economic optimization of gaseous hydrogen pipeline methods, Elgowainy et al. [5] found that compressed gas storage in geologic formation is desirable for long-term storage if suitable geologic storage is available. Furthermore, they summarized that liquid storage can be used for short-term storage. If the system comprises HRS the desired storage is low-pressure (∼170 bar) compressed gas storage at the HRS.

To optimize the economics and environmental aspects of the hydrogen delivery infrastructure it is possible to mix various delivery methods and storage types. Examples of combination are provided by Elgowainy et. al [5], as follows:

- Liquid delivery method with liquid long-term storage: in this combination liquid H2 terminal is co-located with the hydrogen generation plant, and storage tanks are used for transmission and delivery to HRS.

- Mixed-mode pipeline and liquid delivery pathway with long-term geologic storage: in this combination, generated hydrogen at the central plant is stored in a geological storage system, and transmission is performed via the pipeline to the city gate in which the liquid hydrogen terminal is located, at the liquid hydrogen terminal tankers are filled and the distribution is done by the tankers.

- Mixed-mode pipeline and liquid delivery method with liquid long-term storage: this combination is similar to the previous one except for long-term storage which is replaced by compressor and storage tank.
- Mixed-mode pipeline and tube-trailer delivery pathway with long-term geologic storage: in this combination, generated hydrogen at the central plant is compressed and stored for long-term in geologic storage, the pipeline is used for transmission to the city gate, gaseous hydrogen terminal is located at the city gate which tube-trailer deliver hydrogen as distribution section.
- Mixed-mode pipeline and tube-trailer delivery pathway with liquid long-term storage: this combination is the same as the previous one, the difference is the first stage after hydrogen generation and before transmission via pipeline, this stage is allocated to liquefaction and liquid storage
- Tube-trailer delivery method with long-term geologic storage: in this combination geologic storage is used for long-term storage, gaseous hydrogen terminal is located before transmission and the tube-trailer delivers hydrogen from the terminal to HRS, distribution and transmission in this method are performed by means of tube-trailer.
- Tube-trailer delivery pathway with long-term liquid storage: this combination is like the previous combination, except for the storage type, which is liquid storage, thus, the liquefaction stage is required.
- Pipeline delivery method with long-term geologic storage: both transmission and distribution are performed by means of pipeline, compression is needed, and compressed hydrogen is stored in geologic storage.

- Pipeline delivery pathway with long-term liquid storage: this combination is the same as the previous combination, except for the storage type, which is liquid storage, therefore, a liquefaction stage is required.

5.1.1 Tube-trailers

The compressor is used to reduce the hydrogen volume, which increases the total performance efficiency of the hydrogen delivery system. High-pressure gas can be delivered via tube trailers. A stationary compressor at the central plant can be used to provide the opportunity for the tube trailers to be filled under their specified pressure. Tube trailers' structure includes several tubes which are designed to resist specific pressure [5]. The tube trailer is carried by means of a truck cab (tractor) to the HRS [9]. In commercial tube trailers, 12 to 20 long steel cylinders mounted on a truck trailer bed are used. However, for each country government sector regulations should be considered [9]. In addition, for safe delivery, tubes are protected inside a protective frame [8]. In the USA, gas pressure on the truck is limited to 160 atm [9]. The medium amount of compressed gaseous hydrogen is delivered by truck in tubes with a pressure range of 200 to 500 bars or in gas cylinders. For example, the capacity of a tube trailer with steel cylinders is around 25,000 L of compressed hydrogen at 200 bars, which is equal to 420 kg of hydrogen [8]. It is not possible to completely discharge the tube trailer, therefore, the delivered capacity is less than the nominal one. If the end users of hydrogen are vehicles, because of the difference between the pressure of hydrogen delivered by tube-trailer and the desired pressure for vehicles, an extra compression phase at the HRS might be required [9]. Tube loading is relatively a time-consuming step of this pathway. It could take approximately 6 to 10 hours which varies based on the characteristics of the tubes and compressors such as the temperature limit of the tube and compressor capacity [5]. The number of trailers required for the delivery depends on the demand; to meet the demand properly and overcome the long loading time in the HRS, the number of tube trailers can be determined as the number of truck cabs plus the number of HRS, which the tube trailer can be left at the station, Therefore, drivers and trucks would not wait for loading and unloading [9].

Materials with higher resistance can be used to increase the capacity of this pathway. For example, lighter tank materials such as composite materials for gas tubes and gas cylinders, these materials have the capacity to work under higher pressure [8]. Examples of composite materials are carbon fibre and glass fibre which affect the efficiency of the delivery method. Tubes made of these materials have low weight and can operate at higher pressure [5]. Tube trailer capacity made of carbon fibre composite with high-density polyethylene liners can be around 39,600 l of hydrogen [8]. *This capacity could be increased to approximately 1000 kg by cooling the compressed gas* [5]. *Weisberg* *et al.* [10] suggested hydrogen delivery in glass fibre vessels by truck and tube trailers, carrying hydrogen at approximately 70 MPa and 200 K to improve the efficiency of the hydrogen delivery pathway and reduce the cost. They claimed that by hydrogen cooling down to 200 K, it will be 35% more compact. In addition, glass fibres, at this temperature, are almost 50% stronger which increases the capacity of the delivery method without using carbon fibre composite which is more expensive. Moreover, the refuelling step can be faster without overtemperatures and overpressures by cooling down the hydrogen [10].

Tube trailers have several benefits. It is the simplest delivery method in terms of infrastructure requirement. Furthermore, compression costs and hydrogen loss are low at refuelling stations. However, this pathway has several disadvantages, the high manufacturing cost of composite overwrapped pressure vessels which can be around 70% of the total cost, tank dimension limitation, pressure capacity limitation, and low storage capacity of the tube trailer [3].

5.1.2 Pipelines

The pipeline delivery method can be the best option to deliver hydrogen when large quantities of hydrogen are needed for several stationary consumers [4]. This method can be considered an affordable pathway for long-term hydrogen delivery and large hydrogen quantities [7]. Two performances can be considered for the pipeline pathway: i) supplying energy to the consumers considering the demand by connecting the hydrogen generation sites to the distribution network and end users. ii) storage, which can store significant quantities of hydrogen depending on the capacity of the pipeline and the supply and demand difference [13, 4]. The current pipeline networks, solely allocated for hydrogen delivery, are not proportional to the hydrogen demand. Approximately 2600 km of hydrogen pipelines are operating in the United States which are located in regions with high demand such as chemical plants and petroleum refineries [14]. Figure 5. 1 provides information about the length of the existing pipelines for hydrogen delivery in various countries including the U.S., Europe, and the rest of the world by location. The world total length of hydrogen pipelines is estimated around 4550 km Based on a study in 2016 by the Pacific Northwest National Laboratory [15], among the total length, 2600 km is operating in the US and 1600 km is associated with Europe.

According to the projection for 2050 by Tzimas et. al [4] in Europe, approximately 35,000 km of high-pressure transmission pipelines, 400 000 km of medium-pressure sub-transmission pipelines, and 1-4 km distribution pipeline might be required. This development of the infrastructure could cost approximately 700 to 2200 thousand million euros and the main expenses are associated with the distribution network development. Like tube trailers, lightweight materials can be used to reduce the pathway cost in pipeline pathway. Glass fibre reinforced polymer (GFRP) could be considered as an alternative to the low-alloy steel which is used in hydrogen delivery; GFRP can provide a better lifecycle performance, in addition, it has a lower capital cost compared to steel pipelines [16].

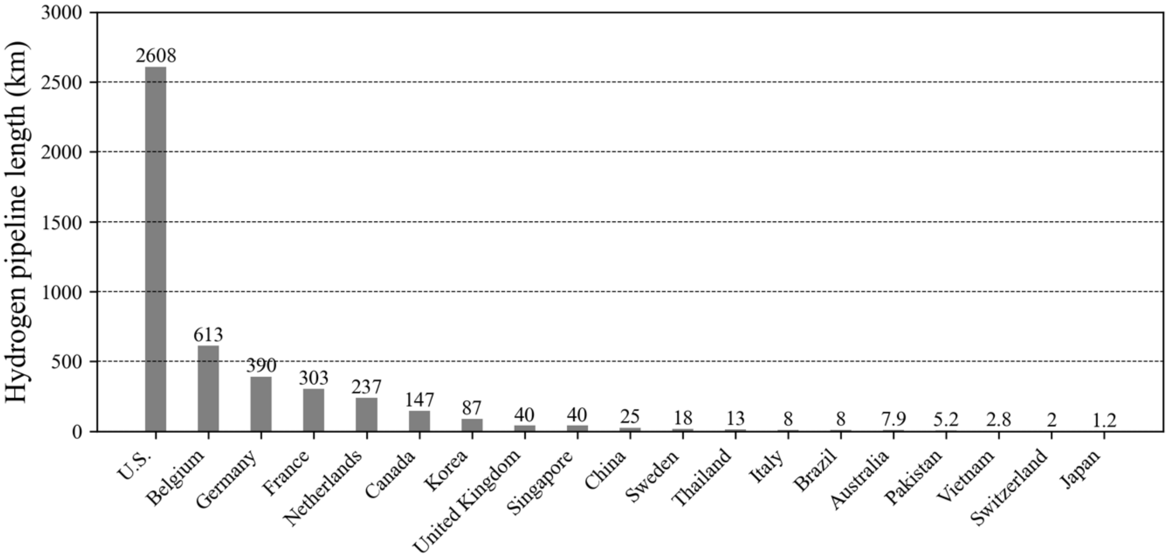

Figure 5. 1 Existing hydrogen pipelines length, 2016

It is possible to integrate electricity and natural gas (NG) by blending hydrogen with natural gas. Which is an option to decrease the pipeline delivery cost. The existing natural gas infrastructure can be used for hydrogen delivery by blending hydrogen and NG. The estimated length of the needed pipeline for hydrogen delivery without blending with NG in the US is around hundreds of thousands of kilometres which lead researchers and policymakers to assess the blending option for hydrogen transmission and distribution [3]. Two main reasons for the blending of hydrogen with natural gas are i) using the existing natural gas network for hydrogen delivery, therefore, reducing the cost of new infrastructure construction, and ii) improving the renewable content of natural gas [17]. Hydrogen can react with pipeline and other components material. It is a challenging issue in blending hydrogen with natural gas and delivering with existing pipelines. The level of blending concentration is different in various countries and researchers reported different ranges in their studies. Faye et al. [8] *claimed that concentrations in the range of 5 to 15% volumetric mixture of hydrogen with natural gas result in minor issues. It is associated with the composition of natural gas and the characteristics of the existing infrastructure. This range is limited to 17% by Gondal et al.* [13]. *It is worth mentioning that high quantities of blended hydrogen lead to the upgrade of household appliances and enhanced compression capacity for industrial users along the delivery pathway* [8]. *Pellegrini et al.* [18] *recommended up to 10% hydrogen blending to the Italian natural gas network. The proposed amount by the European Commission for EU-wide, by 2030, is 5%* [19]. A stochastic model to optimize the concentration of hydrogen in the natural gas pipeline and minimize the capital and operating cost by optimizing the location of power-to-gas (PtG) units is proposed by Ogbe et al. [17].

In the pipeline design procedure, the temporal demand and flow variation should be considered. In addition, network expansion consideration is essential to reduce future costs while supplying the demand. Therefore, the capacity of the network is usually designed higher than the average flow rate based on studies on demand and demand variation [10]. Pipelines might be designed underground and aboveground. In the case of aboveground, pipelines should be protected by paint to resist atmospheric corrosion [20].

5.1.2.1 Specifications and characteristics

5.1.2.1.1 Advantages

pipeline infrastructure is considered the most environmentally friendly option for hydrogen delivery due to the emission of fuel burning in tube trailers and cryogenic tankers pathways and the lengthy lifetime of large-scale pipeline infrastructures [8]. Furthermore, pipelines are mostly buried underground and there is less probability of incidents or accidents and human exposure. Therefore, this pathway is safer and more reliable compared to other delivery pathways.

5.1.2.2 Challenges

There are several challenging issues in pipeline delivery that should be addressed to make this pathway more reliable. The pipeline has high capital expenditure considering the hydrogen demand initially, which is associated with the cost of installation including civil work, pipes, and equipment costs. Furthermore, hydrogen losses along the delivery pipeline are higher than the other fuels. Therefore, it is required to properly design the network’s components to prevent gas leakage from seals, gaskets, and valves to eliminate safety hazards [8], *either in the blending mode with natural gas or in pipelines specifically allocated to hydrogen delivery*. Hydrogen has a very low density which is approximately 1/8th of NG, which results in hydrogen compression requirement to the pressure of approximately 10 to 20 bars to increase the delivery rate [8]. Standard reciprocating compressors are not completely satisfying for hydrogen compression, and standard centrifugal ones are not sufficiently efficient due to the small size of the hydrogen molecule [7].

The environment in which the pipeline would be installed is important in the performance of the infrastructure. Carbon steel pipelines are susceptible to the hydrogen embrittlement (HE) phenomenon. To predict the hydrogen embrittlement, pipeline history, including the frequency and intensity of pressure change, could be used [13]. Cohesive forces in steel structure and deformation mechanisms of steel might be changed by hydrogen delivery. It could be in the form of ductility and toughness reduction of steel under specific conditions such as specific loading. Moreover, due to probable cyclic variation in pressure because of demand variation cracks growth might be sensitive under fatigue loads [7]. Thus, the pipeline should have the capacity to resist the acidic soil environment and hydrogen inside the pipeline. In addition, materials that are used in the pipeline should be capable of bearing hydrogen pressure, operating temperature, and other loadings such as backfill soil, and also be able to resist freezing. In urban areas that are highly populated and there is a dense network of infrastructures it is not possible to construct a new pipeline network for hydrogen. For the underground pipelines, the damage would be probable because of lightning strikes and ground fault conditions, therefore, electrical continuity to the surface should be avoided [20].

Existing NG networks are quite old in some cases; therefore, it might not be possible to use them as the infrastructure for hydrogen delivery by hydrogen blending to NG. The old pipelines that were designed and installed based on the criteria are probably not suitable for the combination of hydrogen and NG. criteria could be related to allowable defect sizes, inspection techniques, carbon steel weld, and grad of carbon steel. In addition, the pipeline network has likely been influenced by damages during its service time, such as deterioration and wall thinning because of corrosion, third-party damage, and soil movement. Furthermore, during the pipeline lifespan, there might be replacement and repair. Polymer materials have high porosity and hydrogen has a higher diffusion coefficient in comparison to natural gas since it is the smallest element in the periodic table, therefore, they are not the appropriate infrastructure choice for mixing hydrogen with natural gas [8]. Thus, substantial uncertainty in pipeline conditions is inevitable, which makes it challenging to blend hydrogen into the existing natural gas networks [7]. Therefore, using the existing natural gas pipelines needs performing intensive testing of pipes, welds, and joints to control the suitability for hydrogen blending [13].

5.1.3 Cryogenic tankers

In this pathway, gaseous hydrogen is liquefied by reducing temperature below −253 °C through the liquefaction stage, then it can be stored in large tanks at the liquefaction plant. Compared to the compressed gas in containers, the hydrogen is denser, and this pathway can deliver significantly more hydrogen quantities [8]. This pathway could be proper for moderate to high demands, above 500 kg/day, and medium to long distances [3, 10]. There are three main steps in hydrogen delivery by cryogenic tankers pathway: i) liquefaction, ii) storage and iii) delivery by cryogenic tankers to the end users [3].

Cryogenic liquid trucks' capacity is around 65 m^3, and a nominal capacity of 4,600 kg hydrogen [5], which is almost greater than 10 times the amount of hydrogen that can be delivered via the tube trailer pathway. It decreases the number of trucks, drivers, and trips that are needed to supply the demand

and reduces fuel consumption for truck transport. A cryogenic liquid hydrogen truck comprises a truck cab and a large single liquid hydrogen tank which is mounted on a trailer. It is not possible to leave the liquid hydrogen trailers at the HRS, thus, the assumptions for the optimization of the number of trucks in the tube trailer are not applicable here, and the number of liquid hydrogen tank trailers is always equal to the number of truck cabs [10].

5.1.3.1 Advantages and disadvantages

Liquefaction capital cost and energy consumption are significantly greater than the cost and energy of compression [10]. The liquefaction process has high energy loss, around 40% of energy is lost, in addition, there would be loss through evaporation, boil-off of liquid hydrogen, and unloading procedure at HRS, which might be approximately 6% of the total capacity of the truck. Thus, it is recommended to minimize the number of HRS that each truck should serve on each trip to reduce high losses. In addition, liquefied hydrogen is unlikely to be used for stationary applications, it is associated with the high and constant demand that makes the delivery of liquified hydrogen impractical by using trucks because it needs large cryogenic storage facilities and also a huge number of trucks is required to supply the demand without any interruption [4]. Tanker filling time is faster compared to gaseous hydrogen, around 2 to 3 hours, resulting in less time waiting for drivers and trucks [8, 5]. To decrease heat transfer and reduce boil-off, the ratio of volume to the surface of the tank should be greater. When the diameter increases the raise of volume is faster than the surface area, therefore, spherical and cylindrical tanks are suitable for this pathway. It should be noted that cylindrical tanks are cheaper and easier to construct compared to spherical ones with the same volume-to-surface ratio. The evaporated hydrogen could be vented or stays in the tank up to the tank design pressure, then it should be vented. The time at which the gas pressure reaches the design pressure is called lock-up time. The evaporated hydrogen could be used in the process in which gaseous hydrogen is required. If the storage time which is required to use gaseous hydrogen is shorter than the lock-up time, hydrogen loss due to boil-off will be zero, because gaseous hydrogen is used before venting into the atmosphere. The amount of vented hydrogen does not have significant safety issues because it diffuses rapidly in the air. If the liquid hydrogen is stored at the same site of liquefaction, it is possible to pull out the hydrogen gas from the storage vessel and re-liquify it [21].

5.1.4 Under development pathways

In addition to the abovementioned pathways, there are several delivery methods that are not mature and are under development, such as chemical reactions or physisorption with a material [6]. Liquid organic hydrogen carriers (LOHCs) could be a long-term storage and can be used for long-distance hydrogen delivery. In this delivery method, organic molecules are hydrogenated by loading liquid hydrogen molecules into organic molecules, and they will be dehydrogenated, and hydrogen molecules will be unloaded to consume. LOHC provides the opportunity to deliver them under ambient conditions and using existing crude oil infrastructures [22]. An example of LOHCs could be toluene-methylcyclohexane, in which Carvalho et al. [22] economically analysed it and stated that the break-even price of hydrogen loading and release could be around 1.9 $/kg of hydrogen. Brigljević et al. [23] performed a techno-economic analysis, and market performance assessment of a large-scale dehydrogenation system with a capacity of 1000 m^3/h hydrogen without CO_2 emission. Four LOHCs were investigated in this study, Eutectic biphenyl/diphenylmethane mixture (EUT), 2-(N-Methylbenzyl) pyridine (MBP), N-phenylcarbazole (NPC), and N-ethylcarbazole (NEC), and a case including all four LOHCs in a temperature-cascade process. They realized that LOHCs' price and shipping costs are the main expenses. In addition, they found that the total capital investment for this size of the plant could be around 24-44 million USD. By the assessment of the market performance, they stated that for the hydrogen which can be sold at 3.5 USD per kilogram of hydrogen the purchase prices of LOHC chemicals should be 5.44, 4.74, 4.01, 4.12 USD/kg for EUT, MBP, NPC, and NEC, respectively. Ammonia is another hydrogen carrier that is studied by Malenkov et al. [24]. They stated that ammonia consumption as a hydrogen carrier in industrial quantities could be rational when using sea or trail delivery for distances over 2000-3000 km. liquid ammonia, at 10 bars, can store around 123kg hydrogen in one m^3, approximately 17.7% (wt.) [25]. An ammonia cracking plant is required to extract hydrogen from ammonia to use hydrogen [26]. Methanol is another hydrogen carrier, the problem with methanol is its carbon dioxide emission after combustion, in addition, the direct carbon capture from the air to make methanol increases the cost.

Another opportunity is metal hydride, which is bonding hydrogen chemically to metals and alloys. Hydrides are capable of storing hydrogen at the range of around 2 to 6% of the weight of hydrides, but as they have high volumetric storage density, they can be considered a suitable option for hydrogen delivery. The advantage of this delivery method is related to the procedure pressure, in which hydrogen can bond to some metals at or below atmospheric pressure and could be released at higher pressures after heating (thermolysis), higher pressures could be achieved by the application of higher temperature. The heating breaks the bond between metal and hydrogen. Hydrogen can bond to the metal up to approximately 90% of metal capacity under low pressure, the rest of the capacity can be achieved at higher pressures. It is worth mentioning that the reaction of hydrogen with metal is an exothermic reaction, and to prevent hydride from heating up the released heat should be removed. Hydrogen extraction of up to 90% can be obtained by applying heat, while the remaining 10% is related to the strong bond of hydrogen and metal which is not simply breakable [21]. In addition to thermolysis which is an endothermic reaction, hydrogen could be released from hydride through hydrolysis (reaction with water), which is an exothermic reaction. A good example of metal hydride for hydrolysis is sodium borohydride ($NaBH_4$). The most suitable metals for the large-scale storage of hydrogen are magnesium hydride (MgH_2) and aluminium hydride (AlH_3). Magnesium has a high theoretical capacity of hydrogen storage, approximately 7.6% (wt.). In addition, magnesium is cheap and widely available. The issue with magnesium hydride is the strong bond that requires higher energy for dehydrogenation. The benefit of aluminium hydride is its weak bond, which the dehydrogenation is simpler compared to magnesium hydride, but the problem with aluminium hydride is the reaction of aluminium and hydrogen gas which can be done under extreme pressures [25].

5.2 Environmental impact

Environmental impact is one of the most important factors for the market penetration and acceptance of technology. Frank et al. [27] investigated a life-cycle analysis of greenhouse gas (GHG) emissions from hydrogen delivery for various pathways with different distances, the result is depicted in Figure 5. 2. These results show the emission due to liquefaction, pipeline, terminal for tube trailer, trucking, and HRS. It is seen that the pipeline delivery mode has the lowest amount of GHG emission for 1kg hydrogen delivery compared to others. Furthermore, the Tube trailer is the most sensitive pathway to distance, as can be seen in this figure the changes in the GHG emission by increasing the distance is more considerable.

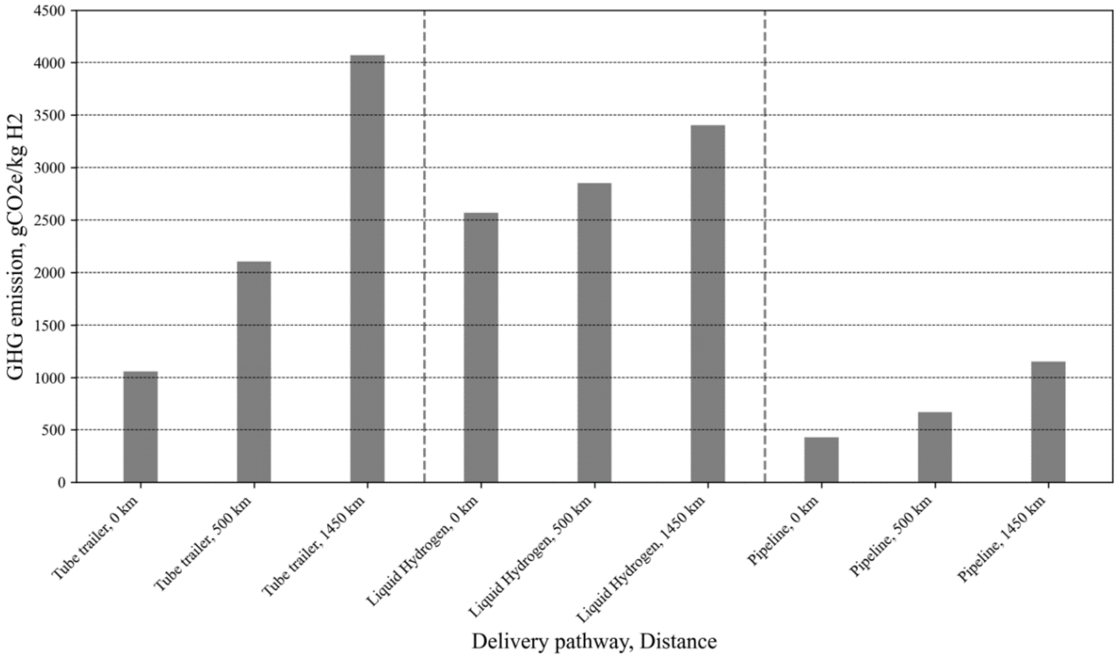

Figure 5. 2 Life-cycle GHG emissions for delivery by tube trailer for gaseous H2, by tanker for liquid H2, or by pipelines in various delivery distances (Modified figure from Frank et al. *[27]*)

The energy consumption of pipelines, among the three main delivery methods, is significantly less than the others. The only energy type which is consumed in the pipeline method is electricity while in tube-trailer and cryogenic tankers pathways diesel fuel is used in addition to electricity as fuel for the truck. Electricity is consumed for gas compression and liquefaction. Tube-trailer and cryogenic tanker trucks use considerable diesel fuel by the increase of delivery distance due to their limited capacity. Compared to compressed gas trucks, pipeline pressure is lower and less energy is needed to overcome the friction losses along the pipeline if the network is sized adequately. Furthermore, in the pipeline delivery, the energy loss change at a wide range of flow, 2 to 100 tonne/day, is almost negligible, and the main energy consumption is related to hydrogen gas compression at the pipeline inlet [10]. Energy consumption for hydrogen gas compression is high in tube trailer and pipeline pathways, it can be around 40% of the delivered hydrogen energy content, lower heating value (LHV). The total energy which is used in the cryogenic tankers' pathway is higher in comparison to the tube-trailer pathway, mostly because of the energy quantity that is consumed for liquefaction which is greater than the required energy for hydrogen gas compression [5, 10]. However, the estimated quantity is different in Weisberg et al. [10] study. They indicated that in the pipeline pathway, the required energy for hydrogen gas compression to approximately 1000psi equals 2 - 3% of the energy content of hydrogen which is much less than 40% which is stated by Elgowainy et al. [5]. Moreover, they reported the liquefaction energy consumption as around 33% of the hydrogen energy content. These differences can be a result of the scale of the experimental test, the efficiency of the technologies for compression and liquefaction, and conditions such as temperature and pressure. Furthermore, improper calibration could result in incorrect results. According to the Department of Energy, U.S., report [28], the theoretical energy to isothermally compress hydrogen from 20 bar to 350 bar, which is around 5000 psi, is 1.05 kWh/kg H_2, while to reach 700 bar (around 10,000 psi), the theoretical energy is 1.36 kWh/kg H_2. The theoretical energy to isothermally compress hydrogen could be approximately 3-4% of Hydrogen energy content (considering the LHV of hydrogen which is 33.33 kWh/kg). In this report, the theoretical energy to liquefy hydrogen from the standard condition is 3.9 kWh/ kg LH_2, which is around 10% of the hydrogen energy content. The theoretical one required energy is much lower than the practical one, the practical hydrogen compression of generated hydrogen on-site could be around 5-20% of hydrogen LHV, and for liquefaction, it can be 30-40% of LHV.

5.3 Cost of hydrogen transportation and distribution

In addition to low environmental impact, the cost is important for the penetration of hydrogen fuel into the market. An important issue in the market penetration of a fuel is its price, thus, the oil price compared to hydrogen price plays an important role in the acceptance of hydrogen technology.

Hydrogen delivery is one of the main contributors to the total hydrogen fuel economy. Zero-emission technologies become more competitive considering the world's concern about global warming and carbon price. But to stay in the competition cost reduction is needed. The initial investment in hydrogen infrastructure is high which long time is needed to reach the break-even point, it is related to the uncertainty of demand and reliability by society. Therefore, investors are sensitive to investment risk in hydrogen technology. Consumers are an integral part of an infrastructure success because if there is not any demand for hydrogen there would not be any investment interest by companies in it [1]. Growth in hydrogen demand leads to an increase in generation, therefore, cost reduction. Cost reduction could increase the demand. This loop continues until reaching a stable condition. It should be noted that supplying the increased demand requires larger infrastructures for delivery which increase the cost.

5.3.1 Pipeline

The Pipeline pathway is the most affordable mode for hydrogen delivery for large quantities and long distances [29]. The cost of hydrogen pipeline infrastructure varies project by project. This cost includes initial investment, operational costs, and maintenance costs. However, the maintenance and operational costs of pipeline networks are relatively low compared to the initial investment [8]. The pipeline pathway expenses are related to the geography of the terrain in which the network should be constructed, the diameter of the pipeline, the equipment along the network, the labour and material cost in each region, the choice of material, and the operating condition [4]. Weisberg et al. [10] stated that the total cost per unit length of a pipeline at a large pipe diameter network is sensitive to the pipe diameter (while at a smaller diameter pipelines diameter is less effective, due to a small portion of materials in the total cost in small-dimeter networks). In addition, they reported that the installation and rights of way costs are the main contributors to the overall cost [10]. Lee et al. [30], made a comparison of hydrogen delivery costs in gaseous and liquid forms in Seoul, Korea, based on a techno-economic analysis. They realized that the gaseous form delivery is cheaper, however, cost varies due to changes in the capacity of the station and the market penetration, especially when these factors are small.

The hydrogen delivery cost target by the year 2017 was less than 1 dollar per 1 kg hydrogen [7], which is not achieved. Pawel et al. [7] reported that the pipeline cost for hydrogen delivery could be \$2M/mile or more for larger diameters. They evaluated that to reach the goal of less than 1kg hydrogen delivery it is needed to decrease the pipeline cost to around \$0.5 M/mile. The main contributors to initial costs are materials and labour for the network construction, around 70% of the total pipeline cost, which is almost constant over time. The remaining 30% of costs are related to regulatory fees, right-of-way purchase, engineering, surveying, equipment, management, and administration [7]. It is not possible to reduce the costs related to the remaining 30% by research and development (R&D), therefore, the main focus is on material and labour to obtain the desired cost. Pawel et al. [7] claimed that for more than 50% cost reduction per mile, it is required to reduce the costs of labour and materials by around 80% or more, which is almost unlikely to be obtained. Polymer pipelines could be an option for the material with improvement in their characteristics such as preventing hydrogen loss due to the high porosity of polymers. As mentioned in the previous sections, fibre-reinforced polymer (FRP) pipelines are an alternative to steel pipelines which can be installed in extended lengths, depending on the diameter, which decreases the number of joints/weld per unit length of the pipeline, which reduces costs related to handling, fit-up, and joining by labourer and inspection costs, such as leak-checking and non-destructive tests. Furthermore, FRP pipelines need less corrosion protection such as painting for buried steel and cathodic protection [7]. These benefits in cost reduction suggest the development of FRP pipeline infrastructure as an area for research and development.

Based on the research in Fraunhofer Institute [19] the increase in the blending percentage of hydrogen to the NG causes an increase in the end-user price, especially for industrial customers. They estimated by blending 5 %, 10%, and 20% of hydrogen to NG the price growth for the end-users in the European Union could be 1.3%, 9.9%, and 23.8%, respectively. This price rocket at higher percentages is more significant.

Penev et al. [11] proposed a system which is called the Hyline system, to decrease the cost of hydrogen delivery. This system produces hydrogen at urban industrial or commercial power plants. In this system, hydrogen is compressed to 15,000 psi and stored at the generation site, then delivered via a high-pressure pipeline to HRS. They considered 6 scenarios for pipeline delivery. The total length of the pipeline was around 61.15 km. The difference between scenarios is related to the pipeline pressure, hydrogen production rate, and number of HRS. The result of the cost assessment is shown in Table 5. 1.

Table 5. 1 Cost analysis of pipeline delivery *[11]*, total cost includes production, terminal, delivery, and retail.

Hydrogen production rate (kg/day)	Number of HRS	Pipeline pressure (bar)	Total cost $/kg	Delivery cost $/kg	Delivery cost $/kg.km
400	8	40	21.6	7.79	0.13
400	8	1000	17.1	7.83	0.13
950	16	40	10.7	1.75	0.03
950	16	1000	7.1	1.75	0.03
1500	24	40	8.5	0.69	0.01
1500	24	1000	5.3	0.69	0.01

Transportation distance and the hydrogen demand amount determine the transmission costs while distribution stage costs are defined based on the demand volume and the size of the targeted district. However, these costs are dependent on the geography of the delivery route and infrastructure complexity [2]. For small cities, remote districts, and rural areas where the demand is low and the market is at the early stages, it is not economically logical to deliver hydrogen through the pipeline to the end-users. For large power plants, with a demand of more than 1000 tonnes/day, the pipeline pathway is the most cost-effective option, the result could be around $2.73 per Kg of hydrogen delivery [8, 6]. *This cost is based on the pipeline pressure of 1000 psi, transmission length of 100 km, 80 HRS, 2 trunk pipelines each 112.6 km for distribution, and average demand of 80,000 kg/day. Assuming the delivery to the furthest consumer, the total length of the pipeline would be 212.6 km, therefore, the hydrogen delivery cost could be around 0.01* $/kg.km.

5.3.2 Tube trailer

The main parameters to determine the hydrogen delivery cost utilizing the tube-trailer pathway are the initial investment in truck cabs, tubes, and tube trailers, and operation costs such as driver cost, fuel consumption, and maintenance [10]. The cost of hydrogen delivery by tube-trailer pathway can be formulated as a function of transported capacity and distance, which consists of other costs such as compression, storage, and road transportation, this term is called the Levelized cost of transporting hydrogen (LCOTH). LCOTH should be minimized by optimizing the capacity of each compressed gas truck. LCOTH can be decreased by increasing the transport capacity and increased by increasing the truck trip distance. LCOTH ranges between 0.5 to 3.02 \$/kg [31] depending on the amount of delivery and distance. For the daily demand of 50 tons per day, the cost for 20, 75, 250, 350, and 400 km distance delivery were evaluated at approximately 0.006, 0.004, 0.003, 0.004, 0.004 \$/kg.km, respectively. According to the analysis performed by Weisberg et al. [10], in 2019, based on information extracted from the US Department of Energy the hydrogen delivery cost via the tube-trailer pathway can be less than \$1/kg H_2. Faye et al. [8] *stated that the hydrogen delivery cost by means of a tube-trailer in a small-scale power plant could be around* \$2.86 per kg of hydrogen; considering 100 km round-trip distance, the cost would be 0.03 \$/kg.km. Moreno-Blanco et al. [32] made a comparison of the delivery cost of hydrogen gas compressed to 875 bar (high pressure) and at the temperature of 200 K with a 350 bar trailer. For this purpose, the high-pressure hydrogen was assumed to be delivered in a thermally insulated trailer and dispensing was performed directly from the trailer. It can result in the elimination of several units such as the station compressor, cascade, and refrigerator, which leads to cost and complexity reduction. They estimated that the total delivery cost at 875 bars can be \$0.58/kg hydrogen less than 350 bar, \$2.96, and 2.38/kg hydrogen for 350 bar and 875 bar, respectively. Assuming a 100 km distance from the generation site and city gate and 50 km for distribution, the total roundtrip is 300 km which results in around 0.008 to 0.01 \$/kg.km. Lahnaoui et al. [33] investigated tube trailer costs for different forms of hydrogen, compressed gas (CGH), LOHC, and liquid hydrogen (LH) at different pressures. The result is shown in Table 5. 2. It is worth mentioning that the reported values for tube trailer cost are related to the trailer cost (vehicle), not the hydrogen delivery cost.

Table 5. 2 Tube trailer (vehicle) cost based on Lahnaoui et al. *[33]* study, 2021.

	CGH					LOHC	LH
Storage pressure (bar)	180	250	350	500	540	1	1
Net truck capacity (kg)	350	668	885	1100	1230	1500	3600
Tube trailer cost in K\$	455	621	815	1250	1416	67	2049

5.3.3 Cryogenic liquid trucks

Although the liquid hydrogen tank trailers cost higher than tube trailers because of the liquefaction process cost, the overall hydrogen delivery cost can be lower considering that the cost of delivery, including truck fuel, and driver labour cost, per unit of hydrogen can be lower. The high cost of liquefaction is related to two main factors, high energy consumption for liquefaction, and the high capital cost of liquefaction equipment [7]. Hydrogen delivery through this pathway and dispensing at the fuel station can cost around \$1.40 to \$2.42 /kg of hydrogen [8]. Thermal insulation is a method that can be used to reduce the cost of cryogenic tankers' pathway by reducing losses. It is possible to decrease the costs by reducing the losses as a result of evaporation, and liquid hydrogen boil-off. Penev et al. [11] performed a cost analysis of 3 scenarios for liquid hydrogen delivery at three different production rates and different numbers of HRS. The results are shown in Table 5. 3.

Table 5. 3 Cost analysis of liquid trucks delivery *[11]*, total cost includes production, liquefaction, terminal, delivery, and retail. Total distance is considered 2*61.15 km for roundtrip

Hydrogen production rate (kg/day)	Number of HRS	Total cost \$/kg	Delivery cost \$/kg	Delivery cost \$/kg.km
400	8	16.4	0.22	0.002
950	16	13.3	0.22	0.002
1500	24	12.7	0.22	0.002

5.3.4 Comparison of pathways

One of the most important parameters for choosing the right pathway for hydrogen delivery is the hydrogen quantity that can be delivered via each pathway. Figure 5. 3 shows the hydrogen mass which can be delivered in 1 m^3 of materials. Various delivery types are considered such as 100% hydrogen in the pipeline, 5% and 15% blending with natural gas, tube trailer, cryogenic liquid tanker, and hydrogen carrier materials. This figure is based on the information provided in the appendix. It is seen that magnesium hydride and methanol can deliver the highest quantities of hydrogen in the same volume of delivery compared to other delivery modes, 110.20 and 99 kg, respectively. This high capacity indicates their potential to reduce the delivery cost.

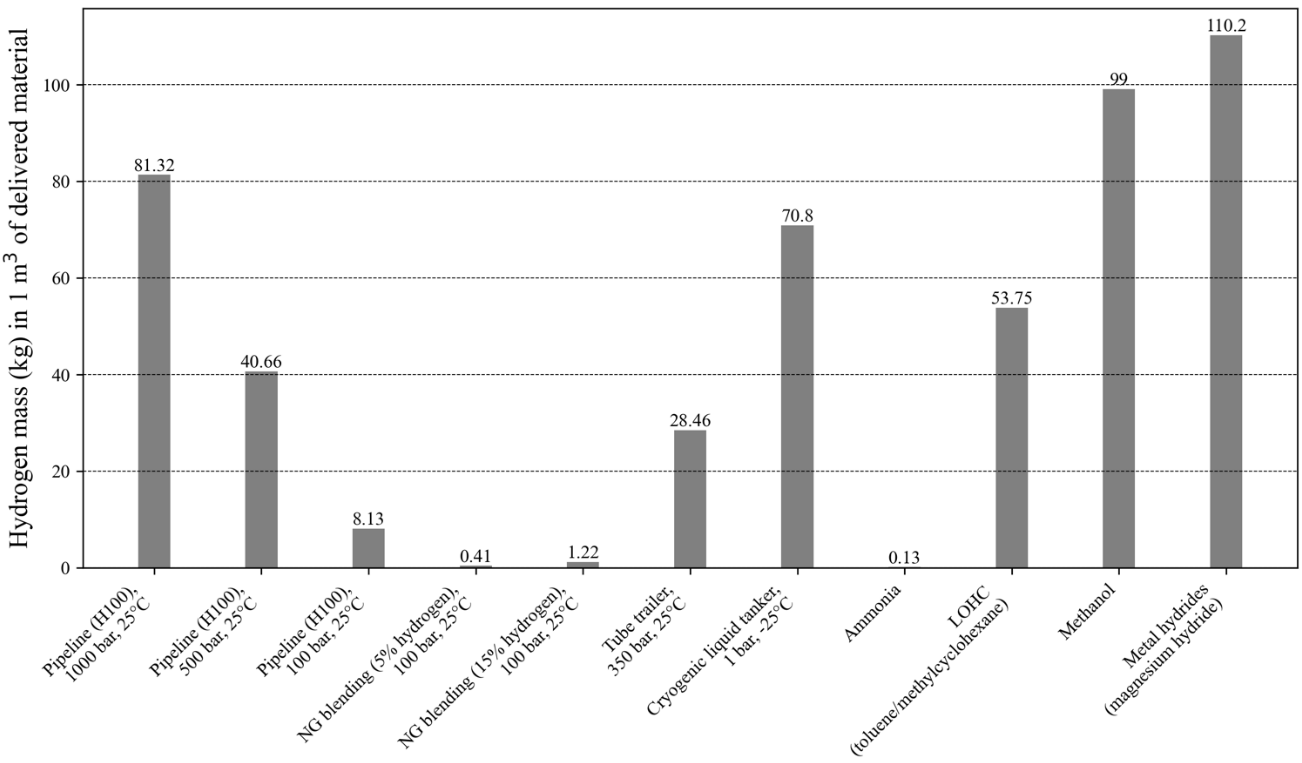

Figure 5. 3 Mass of delivered hydrogen in 1 m^3 of delivered material. H100 refers to 100% hydrogen.

Several parameters affect the pathway choice among the main three mentioned pathways, such as the geography of the delivery route and market characteristics including city population and size, population density, and end-user type (e.g., size and number of HRS, and fuel cell vehicles market penetration). Weisberg et al. [10] indicated that the pipeline delivery method is suitable for dense areas with high hydrogen demand, the compressed gas truck pathway is suitable for small stations with very low demand, and liquid delivery is suitable for long distances and moderate hydrogen demand.

Tzimas et al. [4], in 2007, performed an economic assessment of two scenarios, hydrogen delivery to a vehicle as the end-user when hydrogen is generated in a large-scale steam reforming plant, then liquefied and delivered by truck to a HRS which is located at a distance of 100 km, and the second scenario is hydrogen generation in small scale on-site infrastructure using steam reforming technology and compressed to 700 bar. They concluded that the cost difference is not significant [4].

Demir et al. [6] made an economical comparison of three hydrogen delivery scenarios, i) transmission via pipeline to the city gate, distribution by liquid tanker, ii) using geological storage, transmission, and distribution by hydrogen tube trailers, iii) using geological storage, transmission, and distribution via pipeline. They stated that the lowest Levelized cost of delivery is achieved by the third scenario, 2.73 $/kg hydrogen, and the highest cost is related to the first scenario, 8.02 $/kg hydrogen. It should be noted that the Levelized cost is the lifetime costs divided by energy production.

The liquid hydrogen storage cost is significantly lower than high-pressure hydrogen. The amount of delivered hydrogen can be increased by liquefaction, thus, the reliability of the system to supply the variation of the demand can be obtained with a relatively lower cost compared to compressed hydrogen. However, it is worth mentioning that the liquefaction cost is a crucial factor for the determination of the pathway with the lowest cost and liquid hydrogen is preferred when it is needed to store a large quantity of hydrogen [10].

In the report published by the European Union [26], two hydrogen production rates and delivery distance scenarios, named case "A" and case "B", were assessed considering various pathways for each scenario which the results are shown in Table 5. 4 and Table 5. 5. Values reported in these table are hydrogen delivery costs in USD per kg of hydrogen, including transport, storage, compression, liquefaction, process of bonding in a carrier, and the reversing procedure to have gaseous hydrogen at the desired pressure and purity. Case "A" is assumed an industrial use of hydrogen with a generation rate of 1 Mt hydrogen per year and case “B” has a lower capacity, with a production rate of 100kt hydrogen per year. The delivery distance in case “A” is assumed 2500 km. while the delivery distance in case "B" is assumed 3000 km (including 2500 km shipping, and 500 km train and truck). Furthermore, two electricity cost scenarios were considered in their report, low price (Lo) and high price (Hi). In Lo, the generation costs at the production site and consumption site were considered \$11.83/MWh and \$59.15/MWh, respectively. In Hi, the generation costs at the production site and consumption site were considered \$59.15/MWh and \$153.79/MWh, respectively. In addition, waste heat was considered in case “A” at \$23.66/MWh.

Table 5. 4 Hydrogen delivery cost comparison via different pathways in case “A”, numbers are extracted from diagrams in the European Union report *[26]*. All deliveries are considered via shipping except pipeline.

Case A, total cost of delivery and preparation processes for delivery and reverse processes	H2 pipeline		Compressed H2		Liquefied H2		LOHC		Ammonia	
	Hi	Lo	Hi	Lo	Hi	Lo	Hi	Lo	Hi	Lo
	0.85	0.73	1.04	0.86	1.27	0.89	2.25	1.12	3.11	1.53
contribution of transport and storage	90%	95%	67%	81%	30%	36%	12%	24%	7%	14%

Table 5. 5 Hydrogen delivery cost comparison via different pathways in case “B”, numbers are extracted from diagrams in the European Union report *[26]*.

Case B, total cost of delivery and preparation processes for delivery and reverse processes	Compressed H2		Liquefied H2		LOHC		Ammonia	
	Hi	Lo	Hi	Lo	Hi	Lo	Hi	Lo
	5.21	4.42	3.73	2.67	5.17	3.94	6.83	4.84
contribution of transport and storage	72%	83%	58%	58%	14%	19%	37%	51%

It is seen that in the case “A”, although the ammonia carrier (Hi) has the minimum contribution of transport and storage, the maximum cost is related to this delivery method. H2 pipeline (Lo) shows the maximum contribution of transport and storage in the case “A”, while it has the lowest total cost. In case “B”, the maximum cost is associated with ammonia carrier (Hi), like in case “A”, and the minimum cost is associated with the liquefied H2 (Lo). The minimum and the maximum contribution of transport and storage in case “B” are associated with LOHC (Hi) and LOHC (Lo), respectively. These results show the importance of the required processes for the preparation of hydrogen for delivery and the reverse procedure to obtain gaseous hydrogen at the desired pressure and purity.

Figure 5. 4 illustrates the guide for a suitable choice of pathway regarding demand and distance. This figure is summarized based on the abovementioned sections. It should be noted that for a more accurate choice, a techno-economic assessment is necessary for every project.

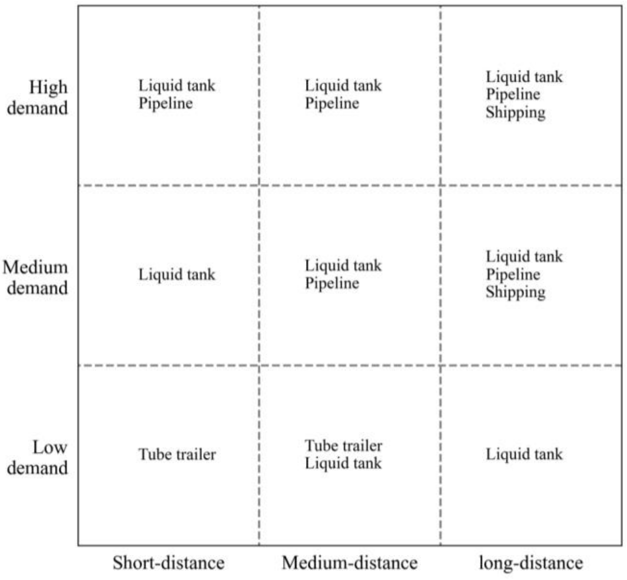

Figure 5. 4 Pathway choice regarding distance and demand.

5.3.5 HRS

The total cost of hydrogen delivery can be affected by the size of the HRS. The smaller the station size the higher the station cost per unit of hydrogen, therefore, the greater the total cost of hydrogen delivery. Liquid storage costs less than gas storage, furthermore, the cost of compressors for gas compression is more than the cost of liquid hydrogen pumping [10]. The components which are usually needed in HRS are a hydrogen generation unit, hydrogen compressor, hydrogen storage, purification unit, hydrogen gas booster, cooling unit, safety equipment, and dispenser. Components and units vary regarding the delivery and production method. The HRS cost is related to the components which are used in the station. The most contributor to the HRS cost is the compressor [34]. As reported by Apostolou et al. [34], the HRS cost in 2018 ranged between €1.2 and €2 million, and the expected cost for 2023 is €0.6 to €1.6 million.

5.4 Safety in hydrogen transportation and distribution

Hydrogen has a higher level of safety hazards in comparison to NG. It is related to the higher risk of hydrogen leakage from valves, seals, and gaskets due to the small size of the hydrogen molecule. This small size causes higher diffusion of hydrogen in comparison to NG, around five times. The annual loss of hydrogen due to leakage can be around 0.0005 to 0.001% of the total volume of delivered hydrogen. Among the pipelines’ materials, cast iron and fibrous cement pipelines have a higher leakage risk. Polyethylene pipelines are Currently the most widely used for the NG network [13]. However, there is an issue related to the high porosity of this material. Gondal et al. [13] indicated that although the leakage of hydrogen is much higher than NG, due to its high energetic content the leakage is negligibly small. It should be noted that because of the flammability range and the small amount of energy that is needed for hydrogen ignition, the leakage can lead to problems [8]. Deformation mechanisms and cohesive forces of steel pipelines could vary considerably because of the hydrogen presence, which under specific loading reduces ductility and toughness [7]. That might lead pipeline damage and uncontrollable release of hydrogen might happens which is potentially hazardous for humans, other species, and surroundings properties [29].

Mouli-Castillo et al. [35] investigated the risk of hydrogen release upstream and downstream of the domestic gas meter in a proposed H100 network (H100 means pipelines include 100% hydrogen, without blending with natural gas). They realized that the risk of release for the proposed H100 network is lower than the existing NG network by a factor of 88%. Lee et al. [30], compared the safety of hydrogen delivery in gaseous and liquid form in Seoul, Korea, based on a quantitative risk analysis. They stated that liquid form shows a better safety performance, however, risk changes due to variations in the capacity of the station and the market penetration, especially for small values of these factors.

Hazardous conditions could be faced during the lifetime of hydrogen pipelines due to the following matters [20]:

- Use of unsuitable materials and equipment under all operating conditions
- Hydrogen embrittlement
- External corrosion due to inappropriate cathodic protection
- Damage by third parties
- Pipeline improper operation and maintenance of the pipeline
- Leaks at valve packing, gaskets, and other components
- Pipeline over pressurisation
- Unsuitable inerting procedure
- The radiation of a vent fire or a flare
- Uncommon applied loads due to natural happenings such as landslides, floods, earthquakes, or non-natural, e.g., the crossing of roads, railways
- Other structures impact, such as high-power electrical grids, electrical railways

Several aspects of design, construction, and maintenance procedures are required to mitigate the risk of the abovementioned hazardous conditions [20]:

- pipeline thickness increment
- pipelines route alteration based on safety issues
- Reducing pipeline operating pressure
- using proper pipeline materials
- Deepen the pipeline
- Physical protections, such as concrete coating
- Control of third-party interference
- valves and other components isolation
- Regular maintenance
- performing non-destructive tests on welds
- Pipeline inerting
- Pipeline marking
- monitoring and performing mass balance for leak detection

To increase the public acceptance of hydrogen it is needed to improve safety. To achieve this objective, standards and codes are required for the construction and performance of the hydrogen delivery infrastructure. Odorants can be used which help the identification of gas leakage and reduce the risk of leakage. Mouli-Castillo et al. [36], in a case study for gas escape detection of hydrogen and natural gas, found that the untrained test participants can recognize the escaping gas which is odorized with New Blend (78% tert-Butylthiol, 22% Dimethyl Sulfide), and Standby Odorant 2 (34% Odorant NB, 64% Hexane) when the concentration is 1% of the air.

5.5 Policies

GHG emissions would be significant if fossil fuels are used for hydrogen delivery in a large-scale hydrogen delivery chain, therefore, certification and labelling of renewable hydrogen should also be used for the full delivery chain, not only hydrogen generation. [26]. Cost-effective, environmentally friendly, and easy-operating hydrogen delivery infrastructures affect the investment risks of stakeholders [6], therefore, proper policies should be considered for stakeholders' confidence. Demand is an integral part of defining public policies since it affects the economy of technology. The transition from fossil fuels to hydrogen is not straightforward and public support is needed to be successful in this transition. Hydrogen technology is relatively new and rapid growth is predicted in the early stages, therefore, hydrogen end-users such as hydrogen car users can expect cheaper and better technologies, e.g., better, and more affordable hydrogen cars and more available HRS. The lack of proper infrastructure is an important problem in hydrogen delivery. Investors in hydrogen infrastructures can be infrastructure promoters such as oil companies whose current main investment is in the field of conventional energy. They might want to make benefit from conventional energy as much as possible. It is unlikely to have private investors in an infrastructure that has high initial costs with an unclear demand quantity [1]. Carbon taxes and trading schemes which are related to controlling carbon emissions could affect the choice of delivery pathway [10].

Blending hydrogen into the NG network would increase costs for end users, by around 16% for households and 43% for industrial users at the blending level of 20 Vol-%, which indicates the pricing policies' impact [19].

5.6 Hydrogen transportation model

The focus of this section is the design of a hydrogen transportation model. For this purpose, different kinds of information are required to fully address all contributors to the delivery cost. This information includes temporal and spatial demand variation, demand growth over time considering social, economic, technological, and policy alteration, city characteristics (such as city radius, number of HRS, and their distribution), population, and population density. The model should be able to satisfy the consumers' needs. If a hydrogen car is considered as the end-user the following factors should be taken into account to make hydrogen consumption convenient for consumers: i) minimizing the average distance that consumers must travel to reach a HRS, ii) the distance which the trucks should travel from the city gate to the HRS or the length of the pipeline if pipeline pathway is used as the delivery mode for distribution, iii) the distribution of demand considering the distribution of HRS in the city [10]. It should be noted that in addition to delivery cost other parameters such as hydrogen generation price and capacity of the hydrogen generation site should be taken into account since the optimization of the total cost of hydrogen production and delivery is the final aim, not only delivery cost minimization.

The Hydrogen Delivery Scenario Analysis Model (HDSAM) is a model which was designed to analyse different hydrogen delivery scenarios. This model was developed under the hydrogen analysis (H2A) project, by the US Department of Energy. The hydrogen delivery in this model is considered from the central generation site to vehicles. This model includes each delivery system component with related performance characteristics and cost. Furthermore, this model included a scenario model which made it possible to assess the system’s effectiveness under various market supply and demand conditions. Inputs to define the scenarios included pathway or pathways combination, number of HRS and their distribution, number of hydrogen vehicles, urban population, and expected revenue [7, 37].

In another study, Gim et al. [2] built a cost-effective central hydrogen generation using a transportation model in Korea. They used a window-based software developed by Scharge, which is called LINGO. They determined the optimal hydrogen delivery volumes for supply and demand sites. Eq 5. 1 is the general equation which is recommended by Gim et al. [2]. In their study hydrogen plants and HRS are assumed as the hydrogen sources are hydrogen destinations, respectively. To solve the problem, the “z” value should be minimized. z is the total transportation cost.

$$z = \sum_{i=1}^{m}\sum_{j=1}^{n} c_{ij}x_{ij} \qquad \text{Eq 5. 1}$$

$$\sum_{j=1}^{n} x_{ij} = a_i, i = 1, 2, \dots, m \qquad \text{Eq 5. 2}$$

$$\sum_{i=1}^{m} x_{ij} = b_j, j = 1, 2, \dots, n \qquad \text{Eq 5. 3}$$

$$x_{ij} \geq 0, all\ i\ and\ j \qquad \text{Eq 5. 4}$$

Where:

x_{ij} = delivery volume from hydrogen plant i to end-user j,

c_{ij} = unit delivery cost from hydrogen plant i to end-user j,

m = number of hydrogen plants,

n = number of location of end-users

a_i = hydrogen supply from plant i,

b_j = hydrogen demand at end-user j

The hydrogen supply from each production site can be calculated by Eq 5. 2 and the result of Eq 5. 3 should be equal to hydrogen demand at the destination. They assumed that the total supply is equal to the total demand, and there is no excess or lack of hydrogen, which means the model is balanced.

Demand prediction is a challenging parameter in Gim's model. Thus, they used the diffusion model. The diffusion model is a method to predict the demand for new products which are not mature and have not had enough market penetration. The diffusion model which is considered by Gim et al. [2] is Lawrence–Lawton's diffusion model for the estimation of the number of fuel cell vehicles and the amount of hydrogen. The general form of Lawrence-Lawton's diffusion model is shown in Eq 5. 5:

$$S_t = \frac{1+P}{1+\left(\frac{1}{P}\right)e^{-RV}} - P \qquad \text{Eq 5. 5}$$

Where:

S_t = accumulated rate time,
P = initial market parameter,
R = diffusion rate parameter,
V = current year + degree of maturity base year.

The “initial market parameter” is related to the market share of the product in the base year, which is very low for the new products, it is considered 0.1% to 1.0%. The “diffusion rate parameter” is associated with product characteristics and is considered the measurement unit of market diffusion. Maturity is related to the duration in which a product exists in the market. The more the duration in the market the higher value of maturity. Products with subsidies and incentives have lower maturity value or they are assumed as new products. Based on Eq 5. 5 and the survey, Gim et al. [2] calculated the demand in Korea as 12,000 tons, 330,000 tons, and 3,545,000 tons in 2020, 2030, and 2040, respectively. Based on the information about the hydrogen destinations and production sites’ location, and using the diffusion model for the demand forecast, Gim et al. [2] calculated the delivery volumes from hydrogen plant “i” to end-user “j” in 2040 in various regions in Korea to optimize the delivery cost.

Hydrogen demand for future scenarios should include market penetration, population growth, and hydrogen vehicle and appliance technologies development. Furthermore, the growing number of hydrogen vehicles in public transport, such as hydrogen-powered buses, increases the number of people who use hydrogen for daily transport. These considerations could be only predictions because unpredicted situations might occur such as COVID-19 which can limit the use of public transport or reduce the travel distance due to lockdown.

In this section, Gim et al. [2] model is modified by considering other parameters such as hydrogen price, and carbon tax. More than one hydrogen generation site is considered and the price of hydrogen in different districts varies depending on the method and technology to generate hydrogen, the authority pricing policies of each district, the source of energy for hydrogen generation, gas compression, and liquefaction. For example, hydrogen generation through a PEM electrolyser is more expensive compared to an alkaline electrolyser [33]. Thus, it is important to add the price of hydrogen to Gim’s formula. Hydrogen generation cost also includes the energy consumption for hydrogen production and any other units such as compression and liquefaction, therefore, the energy price difference is already considered implicitly by the hydrogen generation cost. Hydrogen production cost information can be collected based on surveys, price inquiries, and empirical equations. The example of empirical equations is used by Lahnaoui et al. [33]. This equation is based on the National Renewable Energy Laboratory (NREL) model for hydrogen generation to define the hydrogen production cost.

$$LCOPH = \begin{cases} \dfrac{55P_e + 1.6}{100}(174 - 13.11\, ln(Tp_d)) & for\ Tp_d \in [1,10] ton\ per\ day \\ \dfrac{55P_e + 1.6}{100}(67 - 1.74\, ln(Tp_d)) & for\ Tp_d \in [10,200] ton\ per\ day \end{cases}$$

Where:

LCOPH = levelized cost of hydrogen production,
P_e = electricity price,
Tp_d = plant capacity

For future scenarios, hydrogen cost can be predicted by a sensitivity analysis of the parameters that define the hydrogen price. However, unpredictable conditions could occur which make a considerable difference between anticipated and actual prices, such as war and energy crises.

The amount of carbon dioxide emission for hydrogen production could be different due to different sources of electricity generation and hydrogen generation technology. Carbon dioxide emission from different modes of hydrogen delivery should be considered in the total cost because in some countries there is a carbon tax. The carbon tax could be different because of different approaches taken by the authorities' policies of each district. It is assumed that the carbon tax is considered based on the location of the hydrogen generation site. There could be a hydrogen generation plant with huge emissions within a short distance from the HRS which the total cost of hydrogen production, carbon tax, and delivery becomes higher compared to the hydrogen production plant located at a longer distance using renewable energy as the energy source.

The proposed model in this chapter to cover the hydrogen production cost and the carbon tax is shown in Eq 5. 6. By minimizing the parameter "T" the optimized delivery cost can be obtained. The next step after optimization is removing the hydrogen generation cost and the carbon tax related to hydrogen production to define the total cost of hydrogen delivery in the whole network or for each destination or production plant. It is worth mentioning that in this equation the mass of hydrogen is used instead of the volume of hydrogen, thus, this equation can be used for various pathways with different hydrogen forms, e.g., gaseous hydrogen, liquid hydrogen, or carriers in which the hydrogen content should be considered in this equation.

$$T = \sum_{i=1}^{m} \sum_{j=1}^{n} (c_{dij} + c_{ctpij} + c_{ctdij} + c_{Hpij}) M_{ij} \qquad \text{Eq 5. 6}$$

$$\sum_{j=1}^{n} M_{ij} = A_i, i = 1, 2, \dots, m \qquad \text{Eq 5. 7}$$

$$\sum_{i=1}^{m} M_{ij} = B_j, j = 1, 2, \dots, n \qquad \text{Eq 5. 8}$$

$$M_{ij} \geq 0, all\ i\ and\ j \qquad \text{Eq 5. 9}$$

Where:

T = total cost of hydrogen production, carbon tax and delivery

M_{ij} = delivery mass from hydrogen plant i to end-user j,

c_{dij} = unit delivery cost from hydrogen plant i to end-user j,

c_{ctpij} = unit carbon tax for hydrogen produced at plant i which is delivered to end-user j,

c_{ctdij} = unit carbon tax for hydrogen delivery from plant i to end-user j,

c_{Hpij} = unit hydrogen production cost at hydrogen plant i which is delivered to end-user j,

m = number of hydrogen plants,

n = number of location of end-users

A_i = Mass of hydrogen supply from plant i,

B_j = Mass of hydrogen demand at end-user j

After optimization of the total hydrogen production, delivery, and carbon tax cost, the hydrogen amounts which are supplied from each hydrogen production plant to each end user are defined and could be used in Eq 5. 10 to estimate the whole delivery cost.

$$D = \sum_{i=1}^{m} \sum_{j=1}^{n} (c_{dij} + c_{ctdij}) M_{ij} \qquad \text{Eq 5. 10}$$

Where:

D = total cost of hydrogen delivery and carbon tax associated with the delivery

The network representation of the hydrogen production sources and destinations to determine the total cost of hydrogen production, hydrogen delivery, and carbon tax is shown in Figure 5. 5.

The storage capacity can be considered as the limiting quantity for both hydrogen plants and HRS (hydrogen destination in this model). For system development, this model is applicable by applying the increase in storage size by assuming a higher limit for the storage and rerunning the model. Furthermore, using this model provides the opportunity to decide on the location of the new hydrogen production plant and HRS. In addition, it is possible to apply this model to the NG pipeline considering various possible percentages of Hydrogen. Hydrogen should be separated from the NG-hydrogen mixture to use in HV, therefore, a scenario for combining pathways could be combining hydrogen with NG, delivery by a transmission line, then separating hydrogen for distribution. By this method appliances in the domestic sector do not need adaptability to hydrogen, but other infrastructures for the distribution of hydrogen and hydrogen separation from NG are required. In addition, it is possible to do sensitivity analysis based on Eq 5. 6 regarding various parameters such as storage size, the capacity of tankers, pipeline capacity, and other parameters to find the optimum values.

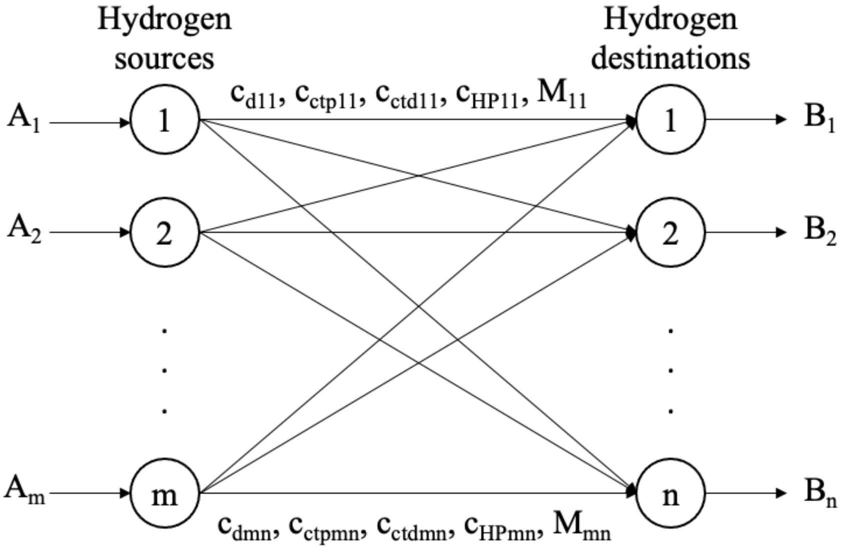

Figure 5. 5 network representation of the total hydrogen production, delivery, and carbon tax model

5.7 Conclusion

Hydrogen delivery is one of the most important stages of hydrogen supply. There are three main pathways for hydrogen delivery, tube trailers, pipelines, and cryogenic tankers. Pipelines are used to supply high-demand regions, while tube trailers and medium cryogenic tankers are mainly used for smaller districts. Several issues are mentioned in this chapter that should be addressed for the cost and environmental impact reduction of hydrogen delivery. These issues are associated with the cost, required hydrogen pressure, hydrogen losses, storage, the reaction between hydrogen and delivery infrastructure materials, geography of the delivery route, maintenance, and monitoring. The pipeline delivery mode has the lowest GHG emission in comparison to the other two main hydrogen delivery methods, while the lower emission between the tube trailer and the cryogenic tank is determined based on the delivery distance. The cost of delivery is related to several parameters such as the distance and density of consumers in a region. Therefore, for each project, it is needed to perform a techno-economic analysis to find the most suitable pathway. The pipeline delivery mode is likely to be the safest and most economical way of hydrogen distribution due to the lower likelihood of accidents and exposure to humans. A transport model is proposed in this chapter to minimize the cost of hydrogen delivery, which includes the cost of hydrogen production, carbon tax for hydrogen production, and carbon tax for hydrogen delivery.

5.8 Appendix

Mass of delivered hydrogen in 1 m^3 of delivered materials.

Density of gaseous hydrogen is estimated based on the ideal gas equation. Cryogenic liquid tanker information is extracted from [38].

	Pressure (bar)	temperature, °C	hydrogen content-volume	Hydrogen content-mass	Density (kg/m^3)	Mass of delivered hydrogen (kg) in 1 m^3 of the whole
Pipeline (H100, 100% hydrogen)-1000 bar	1000	25	100%	100.00%	81.32	81.32
Pipeline (H100, 100% hydrogen)-500 bar	500	25	100%	100.00%	40.66	40.66
Pipeline (H100, 100% hydrogen)-100 bar	100	25	100%	100.00%	8.13	8.13
Pipeline-NG blending (5% hydrogen)	100	25	5%	0.51%	79.89	0.41
Pipeline-NG blending (15% hydrogen)	100	25	15%	1.69%	72.34	1.22
Tube trailer	350	25	100%	100.00%	28.46	28.46
Cryogenic liquid tanker	1	-252	100%	100.00%	70.8	70.80
Ammonia	ambient	ambient	-	17.65%	0.73	0.13
LOHC (toluene/methylcyclohexane)	ambient	ambient	-	6.20%	867	53.75
Methanol	ambient	ambient	-	12.50%	792	99.00
Metal hydrides (magnesium hydride)	ambient	ambient	-	7.60%	1450	110.20

Hydrogen mass content in NG blending 5% volumetric

	Hydrogen	Natural gas
percentage (volumetric)	5	95
density(kg/m3)	8.13	83.672
volume in 1 m3 mix (m3)	0.05	0.95
mass in 1 m^3 mix (kg)	0.40	79.49
mixed density(kg/m^3)	79.89	
mass content	0.51%	

Hydrogen mass content in NG blending 15% volumetric

	Hydrogen	Natural gas
percentage (volumetric)	15	85
density(kg/m3)	8.13	83.672
volume in 1 m^3 mix (m3)	0.15	0.85
mass in 1 m3 mix (kg)	1.22	71.12
mixed density(kg/m^3)	72.34	
mass content	1.69%	

5.9 References

[1] N. Bento, “Investing in the hydrogen delivery infrastructure: methodology for a public policy.,” *Energy Studies Review,* vol. 17, no. 2, 2010.

[2] B. Gim, K. Boo and S. Cho, “A transportation model approach for constructing the cost effective central hydrogen supply system in Korea,” *International journal of hydrogen energy,* vol. 37, no. 2, pp. 1162-1172, 2012.

[3] R. Moradi and a. K. Groth, “Hydrogen storage and delivery: Review of the state of the art technologies and risk and reliability analysis.,” *International Journal of Hydrogen Energy,* vol. 44, no. 23, pp. 12254-12269, 2019.

[4] E. Tzimas, P. Castello and a. S. Peteves., “The evolution of size and cost of a hydrogen delivery infrastructure in Europe in the medium and long term.,” *International Journal of Hydrogen Energy.,* vol. 32, no. 10-11, pp. 1369-80, 2007.

[5] A. Elgowainy, M. Mintz and M. Gardiner, “Distribution networking,” in *Handbook of hydrogen energy,* 2014, pp. 935-956.

[6] M. Demir and I. Dincer, “Cost assessment and evaluation of various hydrogen delivery scenarios,” *International Journal of Hydrogen Energy,* vol. 43, no. 22, pp. 10420-10430, 2018.

[7] S. P. a. M. Gardiner, “HYDROGEN DELIVERY: INFRASTRUCTURE, CHALLENGES, AND MATERIALS NEEDS ...,” in *In Effects of Hydrogen on Materials: Proceedings of the 2008 International Hydrogen Conference,* vol. 1, Jackson Lake Lodge, Grand Teton National Park, Wyoming, USA, ASM International, 2008, p. 316.

[8] O. Faye, J. Szpunar and U. Eduok, “A critical review on the current technologies for the generation, storage, and transportation of hydrogen,” *International Journal of Hydrogen Energy,* vol. 47, no. 29, pp. 13771-13802, 2022.

[9] C. Yang and J. Ogden, “Determining the lowest-cost hydrogen delivery mode,” *International Journal of Hydrogen Energy,* vol. 32, no. 2, pp. 268-286, 2007.

[10] A. H. Weisberg, S. M. Aceves, F. Espinosa-Loza, E. Ledesma-Orozco and a. B. Myers., “Delivery of cold hydrogen in glass fiber composite pressure vessels,” *International journal of hydrogen energy,* vol. 34, no. 24, pp. 9773-9780, 2009.

[11] M. Penev, J. Zuboy and C. Hunter, “Economic analysis of a high-pressure urban pipeline concept (HyLine) for delivering hydrogen to retail fueling stations.,” *Transportation Research Part D: Transport and Environment.,* vol. 77, pp. 92-105, 2019.

[12] E. H. Backbone, “Estimated Investment & Cost,” European Hydrogen Backbone, [Online]. Available: https://ehb.eu/page/estimated-investment-cost. [Accessed 19 09 2022].

[13] I. Gondal and M. Sahir, “Prospects of natural gas pipeline infrastructure in hydrogen transportation,” *International Journal of Energy Research,* vol. 36, no. 15, pp. 1338-1345, 2012.

[14] O. O. E. E. &. R. ENERGY, “Hydrogen Pipelines,” United States Hydrogen and Fuel Cell Technologies Office, [Online]. Available: https://www.energy.gov/eere/fuelcells/hydrogen-pipelines. [Accessed 29 August 2022].

[15] P. N. N. Laboratory, “Hydrogen Tools,” Pacific Northwest National Laboratory, September 2016. [Online]. Available: https://h2tools.org/hyarc/hydrogen-data/hydrogen-pipelines. [Accessed 29 August 2022].

[16] D. B. Smith, B. J. Frame, L. M. Anovitz and a. C. Makselon., “Feasibility of Using Glass-Fiber-Reinforced Polymer Pipelines for Hydrogen Delivery,” *InPressure Vessels and Piping Conference,* vol. 50435, p. V06BT06A036, 2016.

[17] E. Ogbe, U. Mukherjee, M. Fowler, A. Almansoori and a. A. Elkamel., “Integrated Design and Operation Optimization of Hydrogen Commingled with Natural Gas in Pipeline Networks.,” *Industrial & Engineering Chemistry Research,* vol. 59, no. 4, pp. 1584-1595, 2019.

[18] M. Pellegrini, A. Guzzini and C. Saccani, “A Preliminary Assessment of the Potential of Low Percentage Green Hydrogen Blending in the Italian Natural Gas Network,” *energies*, vol. 13, p. 5570, 2020.

[19] J. Bard, N. Gerhardt, P. Selzam, M. Beil, D. M. Wiemer and M. Buddensiek, “THE LIMITATIONS OF HYDROGEN BLENDING IN THE EUROPEAN GAS GRID A study on the use, limitations and cost of hydrogen blending in the European gas grid at the transport and distribution level,” January 2022. [Online]. Available: https://www.iee.fraunhofer.de/content/dam/iee/energiesystemtechnik/en/documents/Studies-Reports/FINAL_FraunhoferIEE_ShortStudy_H2_Blending_EU_ECF_Jan22.pdf. [Accessed 29 August 2022].

[20] E. I. G. ASSOCIATION, “HYDROGEN TRANSPORTATION PIPELINES, IGC Doc 121/04/E GLOBALLY HARMONISED DOCUMENT,” 2004. [Online]. Available: https://h2tools.org/sites/default/files/Doc121_04%20H2TransportationPipelines.pdf. [Accessed 29 August 2022].

[21] W. Amos, “Costs of storing and transporting hydrogen,” National Renewable Energy Laboratory, Golden, Colorado, 1999.

[22] M. C. Carvalho, J. Marques, H. A. Matos and a. J. F. Granjo, “Long-distance hydrogen delivery using a toluene-based liquid organic hydrogen carrier system.,” *In Computer Aided Chemical Engineering*, vol. 50, pp. 1647-1652, 2021.

[23] B. Brigljević, M. Byun and a. H. Lim, “Design, economic evaluation, and market uncertainty analysis of LOHC-based, CO2 free, hydrogen delivery systems,” *Applied Energy*, vol. 274, p. 115314, 2020.

[24] A. S. Malenkov, V. Y. Naumov, S. I. Shabalova and a. D. M. Kharlamova, “Economic Feasibility Assessment of Using Ammonia for Hydrogen Transportation.,” in *SMART Automatics and Energy*, Springer, 2022, pp. 89-98.

[25] J. Andersson and S. Grönkvist, “Large-scale storage of hydrogen,” *International Journal of Hydrogen Energy*, vol. 44, no. 23, pp. 11901-11919, 2019.

[26] E. commision, “Assessment of Hydrogen Delivery Options- science for policy briefs,” 2021 – JRC124206. [Online]. Available: https://joint-research-centre.ec.europa.eu/system/files/2021-06/jrc124206_assessment_of_hydrogen_delivery_options.pdf. [Accessed 26 08 2022].

[27] E. D. Frank, A. Elgowainy, K. Reddi and a. A. Bafana, “Life-cycle analysis of greenhouse gas emissions from hydrogen delivery: A cost-guided analysis,” *International Journal of Hydrogen Energy*, vol. 46, no. 43, pp. 22670-22683, 2021.

[28] D. o. E. U. Monterey Gardiner, “Energy requirements for hydrogen gas compression and liquefaction as related to vehicle storage needs,” July 2009. [Online]. Available: https://www.hydrogen.energy.gov/pdfs/9013_energy_requirements_for_hydrogen_gas_compression.pdf. [Accessed 31 August 2022].

[29] A. Witkowski, A. Rusin, M. Majkut and a. K. Stolecka., “Comprehensive analysis of hydrogen compression and pipeline transportation from thermodynamics and safety aspects,” *Energy*, vol. 141, pp. 2508-2518, 2017.

[30] Y. Lee, U. Lee and a. K. Kim, “A comparative techno-economic and quantitative risk analysis of hydrogen delivery infrastructure options,” *International Journal of Hydrogen Energy*, vol. 46, no. 27, pp. 14857-14870, 2021.

[31] A. Lahnaoui, C. Wulf, H. Heinrichs and D. Dalmazzone, “Optimizing hydrogen transportation system for mobility via compressed hydrogen trucks.,” *International journal of hydrogen energy*, vol. 44, no. 35, pp. 19302-19312, 2019.

[32] J. Moreno-Blanco, G. Camacho, F. Valladares and a. S. M. Aceves., “The cold high-pressure approach to hydrogen delivery.,” *International Journal of Hydrogen Energy.*, vol. 45, no. 51, pp. 27369-27380, 2020.

[33] A. Lahnaoui, C. Wulf and Didier Dalmazzone, “Optimization of Hydrogen Cost and Transport Technology in France and Germany for Various Production and Demand Scenarios,” *Energies,* vol. 14, no. 744, 2021.

[34] D. Apostolou and a. G. Xydis, “A literature review on hydrogen refuelling stations and infrastructure. Current status and future prospects.,” *Renewable and Sustainable Energy Reviews,* vol. 113, p. 109292, 2019.

[35] J. Mouli-Castillo, H. SR, KiaMouli-Castillo, S. R. Haszeldine, K. Kinsella, M. Wheeldon, a. A. M. K, W. M and M. A, “A quantitative risk assessment of a domestic property connected to a hydrogen distribution network.,” *International Journal of Hydrogen Energy.*, vol. 46, no. 29, pp. 16217-16231, 2021.

[36] J. Mouli-Castillo, G. Orr, J. Thomas, N. Hardy, M. Crowther and M. W. a. A. M. R. Stuart Haszeldine, “A comparative study of odorants for gas escape detection of natural gas and hydrogen.,” *International Journal of Hydrogen Energy,* vol. 46, no. 27, pp. 14881-14893, 2021.

[37] M. Mintz, J. Gillette, A. Elgowainy, M. Paster, M. Ringer, D. Brown and a. J. Li, “Hydrogen delivery scenario analysis model for hydrogen distribution options.,” *Transportation research record,* vol. 1, pp. 114-120, 1983.

[38] AndreasZüttel, “Materials for hydrogen storage,” *Materials today,* vol. 6, no. 9, pp. 24-33, 2003.

Conclusion

The focus of this PhD thesis is the evaluation of low-carbon systems and the transition from fossil fuels to RES. The thesis is divided into five chapters. The first chapter is associated with a method for the estimation of global carbon dioxide mass using remote sensing. The available method of carbon dioxide mass calculation based on observation has not changed since 1983, although new measuring platforms are available, and more data are accessible. The estimated carbon dioxide global mass at the beginning of 2021 is around 3.23×10^{15} kg. The results from 2019 to 2021 are compared to the results of applying Fraser's method to NOAA data. The maximum and the average difference between the proposed method and the results of Fraser's method application on NOAA data were 1.23% and 0.15%, respectively. It is possible to estimate the local carbon dioxide mass by the proposed method considering the calculations, which are done separately for each cell, compatible with the resolution of the OCO2 satellite. The method proposed in the first chapter could be used in decision-making for the design and location of systems for carbon capture and low carbon systems. The main issues regarding remote sensing are related to the availability of data from satellites and passing the quality check. It can be addressed in future studies by the combination of satellites or by using proper algorithms to reproduce missed data. In addition, in future studies, temporal variation of desired location can be investigated to check the carbon dioxide mass changes as a function of time.

In the second chapter, the performance of the first demo plant of an innovative technology, which is called ejectors system, for port entrance sediment management is provided. It is found that the plant was able to reach the desired condition after almost one year of operation (June 2019–April 2020), considering the water depth threshold. The estimated transported sediment volume is around 245 and 750 m^3 considering various sea storm conditions. For future studies, the arrangement and the location of the ejectors can be changed to optimize the demo plant operation. In addition, the number of ejectors can be reduced to decrease the total power consumption and carbon dioxide emissions.

In the third chapter, carbon dioxide emissions of hydrogen production via PEM and alkaline electrolysers are compared. Considering the current grid condition in Australia, the carbon dioxide emission to generate 1 kg of hydrogen in Australia is estimated approximately 30 to 40 kg and 40 to 50 kg, at stack operational level, through PEM and alkaline technologies, respectively. If the current amount of hydrogen which is produced in Australia is produced by PEM technology the emission equivalent is 10.5 to 14 Mt of CO_2, while for alkaline technology it could be 14 to 17.5 Mt of CO_2. It is predicted that, in 2030, the emission in Australia would be 25 to 35 kg of CO_2 emission for 1 kg of hydrogen generation by PEM technology and 30-40 kg for Alkaline technology. The current CO_2 emission to produce 1 kg hydrogen in Italy is around 12 to 15 kg CO_2 and the anticipated emission in 2030 is 5 -10 kg CO_2 using PEM or alkaline technologies. It is found that PEM energy consumption is more sensitive to cell voltage in comparison to current density. It could be due to undesirable reactions or electrolyte impurities that amplify the importance of cell manufacturing and electrolyte resistance. The result of sensitivity analysis regarding energy sources scenarios revealed that there is a possibility to reach around 5 kg and 1-3 kg CO_2 emission in Australia and Italy, respectively, by a complete transition from fossil fuels to RES. For future studies, more detailed sensitivity analysis of PEM and alkaline regarding cell characteristics can be defined, in addition, cell characteristics can be optimized to reduce carbon dioxide emissions.

Considering the higher value of carbon dioxide emission by alkaline technology, in the fourth chapter the LCA is performed on the PEM plant. For this purpose, the environmental impact of nine energy and stack configuration scenarios in Australia, Italy, and the whole world are quantified and compared in this study. For the current situation, it is realized that the main contributor to the environmental impact of hydrogen production is the electricity supply, and other sections' contribution is almost negligible. With the transition from fossil fuels to RES, stack materials become important contributors. It is shown that for the current condition, Australia has the highest and Italy represents the lowest emissions. Considering the possible confirmation of cells according to the literature, by a sensitivity analysis regarding the variation of stack material weight, it is found that iridium, platinum, and Nafion variations are important in the final result. The transition from fossil fuels to RES results in the desired result of several indices such as global warming. Carbon dioxide emission of 1 kg of hydrogen production could reach the range of 1-2.3 kg from around 25 kg of CO_2 emission. The difference between the result of chapter 3 and chapter 4 is related to the impact factor estimation difference of databases. It should be noted that this transition could result in undesirable values, such as mineral resources scarcity. Therefore, the transition from fossil fuels to RES could be a suitable solution for global warming mitigation but the material intensity and their cost become more important in decision-making. It is found that the transition to wind energy could result in undesirable results, thus, a deep investigation is needed for the allocation of RES. The best and worst scenarios in comparison to the SMR method are Sc3 and Sc6, respectively. It is shown that electricity is the main contributor to global warming of hydrogen generation, but it is important to define the materials of stack and BOP with the highest contribution. The materials with the highest carbon dioxide emissions are titanium, iridium, and platinum. The optimization of these materials can be more effective for scenarios related to RES in the future. For future studies, the same approach can be applied to alkaline technology.

In the last chapter, various hydrogen delivery pathways are compared and a guide for pathway choice regarding the demand quantity and delivery distance is provided. Based on the literature, it is found that pipeline delivery has the lowest GHG emission compared to the other two main hydrogen delivery methods. Moreover, the lower emission between the tube trailer and the cryogenic tank can be determined based on the delivery distance. By comparing the hydrogen content of the same volume of carriers it is realized that ammonia can deliver a very low amount of hydrogen while metal hydrides show the best performance. A transport model is proposed in this chapter to optimize the cost of hydrogen delivery. The recommended equation includes the cost of hydrogen production and delivery, carbon tax for hydrogen production, and carbon tax for hydrogen delivery. This model provides the opportunity to define the location and capacity of a new hydrogen plant in the network. In addition, if global warming is considered the only parameter which determines the allocation of hydrogen from each plant to each end-user, the cost can be substituted by the amount of carbon dioxide emission in the proposed model. For future studies, it is recommended to apply the model to a real network for the model evaluation.

In conclusion, it can be seen that there are various ways to reduce carbon dioxide emission reduction, but different factors affect the decision-making about a technology. These factors could be the policies regarding the transition from fossil fuels to RES, the investors, and the social acceptance of new technology. In addition, despite the positive result of this study, there are still more options that should be assessed to check their impact on carbon dioxide emission reduction, such as using other RES, like geothermal and tidal energy, and using other technologies such as anion exchange membrane water electrolyser.